FACULDADE DE ENGENHARIA DA UNIVERSIDADE DO PORTO

Adaptive Ocean Sampling with Modular Robotic Platforms

Nuno Alexandre Lopes Moreira da Cruz

Programa Doutoral em Engenharia Eletrotécnica e de Computadores

April 20, 2016

Adaptive Ocean Sampling with Modular Robotic Platforms

Nuno Alexandre Lopes Moreira da Cruz

Programa Doutoral em Engenharia Eletrotécnica e de Computadores

April 20, 2016

Abstract

Sampling the ocean is a very difficult task, not only requiring people to work in very uncomfortable and stressful conditions, but also because the equipment has to be reliable and robust. Very often, it also requires access to expensive support vessels. Moreover, traditional sampling methods can fail to capture the dynamics of many phenomena, due to insufficient sampling rate in space, in time, or both. There is therefore a great demand for faster, more effective and efficient methods for sampling the marine environment. This thesis proposes an integrated approach to ocean sampling that includes the design and development of a new family of vehicles, the conception of innovative principles of operation and the implementation of the corresponding guidance algorithms.

Part of the proposal is a consistent program for the development of small size AUVs based on modular building blocks. This development relies on modularity both in terms of hardware construction, and also in terms of electronics, software and control. Using these blocks, the MARES AUV has been built, a man-portable, hovering AUV that has been continuously updated and used in the field in many different configurations, since 2007. In 2011, the versatility of the system components has been pushed further with the development of TriMARES, a 75kg, 3-body hybrid AUV/ROV system, which was developed in little over 6 months.

The family of new robotic platforms also includes small size ASVs based on modular components. Many of these building blocks are in fact common to the ones used for the assembly of AUVs, which emphasizes their value and versatility. They have been used to build the Zarco ASV, in 2005, and later to replicate the system to assemble Gama, in 2008. Both vehicles have been extensively used for testing multiple aspects of marine operations and they have undergone a continuous evolution since their first trials.

Finally, the work includes a strategy to use autonomous robotic platforms to efficiently map a class of oceanographic features. The distinctive characteristic of these features is that they have a *boundary*, a transition zone across which there is a much stronger variation in one of the values measured by the vehicle, as compared to the values in the rest of the survey area. Given the limited amount of computational power available on board, the strategy relies on admitting a relatively simple feature model for which the vehicle can estimate relevant parameters in real time using simple calculations, and then use these parameters to define the motion characteristics (and sampling pattern) accordingly. In order to implement this strategy, some algorithms are proposed for detecting the value and location of the maximum gradient of a scalar field traversed by the vehicle, as well as for the generation of motion references, in real time. This strategy was implemented in the vertical plane for one-dimensional feature tracking and also in the horizontal plane, for two-dimensional boundary tracking.

Keywords: Autonomous Underwater Vehicles, Autonomous Surface Vehicles, Ocean Sampling, Ocean Feature Tracking, Thermocline Tracking, Boundary Tracking, Adaptive Sampling.

Resumo

A recolha de dados do oceano é uma tarefa árdua, que requer trabalho em condições desconfortáveis e acesso a equipamento fiável e robusto. Por vezes, envolve também o acesso a navios de apoio, cujo custo de operação é extremamente elevado. Por outro lado, os métodos tradicionais de medição não permitem captar a dinâmica de certos processos oceanográficos, devido a uma insuficiente frequência de amostragem, quer temporal, quer espacial. Existe, assim, uma necessidade premente de novas ferramentas que permitam uma amostragem mais rápida, mais eficaz e mais eficiente. Este trabalho propõe uma abordagem integrada para o problema da amostragem no mar, que inclui o projeto e desenvolvimento de novos veículos robóticos, a conceção de princípios de operação inovadores e a implementação dos respetivos algoritmos a bordo dos veículos.

A proposta assenta num programa integrado para o desenvolvimento de submarinos autónomos de pequenas dimensões baseados em blocos modulares. Neste caso, considera-se a modularidade tanto a nível de construção mecânica, como em termos de sistemas eletrónicos, software e controlo. Com base neste blocos, o submarino autónomo MARES foi construído em 2007 e desde então tem sofrido sucessivas melhorias. Trata-se de um veículo de pequenas dimensões, com capacidade de pairar na coluna de água, e que tem sido utilizado em diversos cenários de operação. Em 2011, a versatilidade dos componentes modulares foi mais uma vez demonstrada com o desenvolvimento do veículo TriMARES, em pouco mais de 6 meses. Neste caso, trata-se de um veículo híbrido, que tanto pode funcionar em modo autónomo como teleoperado, constituído por 3 corpos e com um peso total de 75kg.

A família de plataformas robóticas inclui ainda barcos autónomos, também baseados em componentes modulares. De facto, muitos destes módulos são comuns aos usados nos submarinos autónomos, o que reforça o seu valor e a sua versatilidade. Com base nestes componentes, foram construídos os barcos Zarco e Gama, respetivamente em 2005 e 2008. Ambos têm sido intensamente utilizados em diversos cenários de operação e recebido uma evolução contínua.

Finalmente, o trabalho inclui uma estratégia para a utilização de plataformas robóticas na caraterização eficiente de uma classe de processos oceanográficos. Os processos escolhidos distinguem-se por terem uma região fronteira, onde se verifica uma variação mais acentuada de um dado parâmetro do que no resto da área de pesquisa. Atendendo à limitada capacidade computacional a bordo destas pequenas plataformas, a estratégia consiste em admitir um modelo muito simplificado do processo, para o qual o veículo consegue estimar os respetivos parâmetros em tempo real, com cálculos muito simples. Seguidamente, utiliza esses parâmetros para determinar as caraterísticas de movimento e, como tal, o padrão de amostragem. Para implementar esta estratégia, foram propostos algoritmos para a deteção do valor e da localização do maior gradiente de um campo escalar atravessado por um veículo, assim como para a geração de referências de movimento, em tempo real. Esta estratégia foi implementada para o seguimento de regiões fronteira tanto no plano vertical, numa única dimensão, como no horizontal, em duas dimensões.

Palavras Chave: Submarinos Autónomos, Barcos Autónomos, Amostragem do Oceano, Seguimento de Termoclinas, Seguimento de Fronteiras, Amostragem Adaptativa.

Acknowledgements

First, I would like to thank Aníbal Matos for his informal but effective guidance, particularly at the latest stages of this work. Also for all the projects he has managed and for actively contributing to all the results of my thesis. Without his skills in systems engineering, software engineering, and control, all our autonomous vehicles would be useless electronic dummies.

My subsequent appreciation goes to everyone at the OceanSys team. There is no doubt that it takes the commitment of a dedicated group of people to make things work in robotics, and I couldn't ask for a better team to work with. I would like to acknowledge in particular Bruno Ferreira, who can control anything that moves; João Gonçalves for the excellent work with the acoustics' boards; José Melo for all the sonars and bathymetry; Júlio Ferreira for the early days with MARES, when the lab was really tiny and we were just, well, just a few; Nuno Abreu for software drivers and all the black magic required to make sensors talk to vehicles; Patrícia Ramos for showing us how to use AUVs for measuring pollution; and Rui Almeida for the all the hardware work, particularly during the crazy days of building TriMARES in only a few months. Also all of our technicians and support personnel who oiled the machine and have been a fundamental glue to hold everything together throughout this work and so much more. I am deeply grateful.

The lab people also include visiting researchers. We've had very productive discussions and some fierce but honest arguments, and I have learned a lot with all! I hope they have gained something from their stay, but my feeling is that they have always left so much more than they took. A particular thanks to André Sena, for all his dedication to OceanSys, his underwater robotics skills and for risking traveling to work with whom he had never met before; the Argentinian/Spanish team (Alejandro Rozenfeld, Gerardo Acosta and Sebastian Villar) for their crazy idea of a million sonars in a small vehicle; the Brazilian team from UFJF (Leonardo Honório, André Marcato, Pedro Barbosa and Edimar Oliveira) for hiding so much knowledge behind so relaxed temperaments (and all the Rodízios in Juiz de Fora!); the Italian team (Roberto Petroccia and Daniele Spaccini) for flying from Rome with a bag full of modems to test networking with our vehicles (and eat Francesinhas); Joaquín Aparicio for a great integration in the team and the deep understanding of the underwater environment; João Rendas for convincing me (well, almost) to study information theory; and Jerome Jouffroy for stressing the need (paranoia?) for mathematical demonstrations.

I will never forget my experience in the USA and I want to express my deepest gratitude to Jim Bellingham and Chris von Alt, two of the most brilliant leaders I had the privilege to meet. They truly deserve the success they've achieved and all that is yet to come. This naturally extends to the many lab mates I've had, both at MIT AUV Lab and at the OSL at WHOI. By the end of the nineties, there was a nice competition going on in underwater robotics and I was fortunate to have, not one, but two VIP passes.

At the MIT AUV Lab, I remember my complete ignorance about ocean matters and I've had a great help from my office mates, particularly Scott Willcox, Yanwu Zhang and Justin Manley. Also staying a few months at John Leonard's home helped a lot in understanding things. In my best memories are also the cruises to test underwater docking with the Odyssey IIb, both in Cape

Cod Bay and in Sargasso Sea with *R/V Oceanus* (I still talk about the famous science meetings!). Those were my first cruises and if I had any doubts about my future, it clearly vanished by then.

At WHOI, I had the privilege to be integrated in the team that was developing Remus, and I couldn't ask for a better place to learn about small AUVs. Where else could I find a better team than Tom Austin, Mike Purcell, Ben Allen, Roger Stokey and Ned Forrester? Later, I was again fortunate to be invited to the Leo-15 operations, in Tuckerton, coordinated by another great guy, Scott Glenn, from Rutgers University. It was an integrated effort that I had never seen before and my first contact with a pragmatic AOSN, solving real problems, and away from the pure fun of robotic systems.

I would like to thank my colleagues at FEUP and INESC TEC, in particular for giving such a great push when I felt I was getting too old for this. Also the informal meetings close to *my* coffee machines, with our discussions just about everything, makes this such a terrific place to work. A special thanks to Zé Carlos for the multiple discussions over lunch! I would also like to thank my students, particularly the ones involved in extra-curricular projects or final year dissertations. They ask questions, argue, and raise challenges, but mostly they bring out of the box ideas that exercise the mind and help solving problems.

My gratitude also goes to my Department, both to the former Director, Prof. Pedro Guedes de Oliveira, for relieving me from some of the teaching load to advance part of this work, and lately, Prof. Adriano Carvalho for forbidding me to enroll in further activities before finishing this thesis.

At INESC TEC, I'm thankful to the coordinators of the robotics unit, Eduardo Silva and A. Paulo Moreira, for their full support and for flooding us all with new projects and ideas. I've also had full support from all at the administration, but I'm particularly grateful to Prof. Vladimiro Miranda for his passion about ocean robotics, his support of all our projects, and for convincing me that my PhD is important for this great Institution. I'm a bit afraid of what that means, though.

Much of the work that is described in this thesis has been published before and most of it went through a blind reviewing process. I've had many contributions from these anonymous reviewers, who generously provided valuable suggestions that I gladly incorporated. I am thankful for that even though I do not know who to thank. Other people that I met, particularly in conferences, have also provided very useful ideas for the work conveyed in these pages and for future directions, and I am grateful for it. I would like to point out Yanwu Zhang and Stephanie Petillo for our interesting discussions and *competition* on thermocline tracking algorithms. We should fuse them together, before someone else does it!

I have received very useful comments, corrections and suggestions from colleagues who donated their valuable time to read parts of the manuscript and greatly improved the final result. I am particularly thankful to Aníbal Matos, A. Paulo Moreira and José C. Alves for their help in locating blunders, mistakes and unclear passages. Surely they are not to blame for all that remain.

Over the years I have received financial support from many agencies, either directly or through several R&D Projects. In particular, I would like to acknowledge Fundação para a Ciência e a Tecnologia, that helped me in my first steps as a researcher.

I cannot forget the full time support of my family and friends, throughout all these years. It's so comforting to know there is always a safe harbor nearby.

Finally, my gratitude to my dearest wife and wonderful kids. What more could I ask for?

This has been a very, very long journey and countless times I have anticipated the moment of writing these words. Now it's done and I feel light. Thank you all once again.

Nuno A. Cruz, Nov. 2015

Never discourage anyone who
continually makes progress,
no matter how slow.

Plato (427 BC–347 BC)

Contents

List of Figures

List of Tables

Acronyms

ABE	Autonomous Benthic Explorer
ADCP	Acoustic Doppler Current Profiler
AOSN	Autonomous Ocean Sampling Networks
ASC	Autonomous Surface Craft
ASV	Autonomous Surface Vehicle
AUV	Autonomous Underwater Vehicle
CAD	Computer-Aided Design
CFD	Computational Fluid Dynamics
COTS	Commercial Off-The-Shelf
CTD	Conductivity, Temperature, Depth (sensor)
DGPS	Differential GPS
DOF	Degree of Freedom
GDEM	Generalized Digital Environmental Model
GPS	Global Positioning System
GUI	Graphical User Interface
HAB	Harmful Algal Bloom
IAUV	Intervention Autonomous Underwater Vehicle
IMU	Inertial Measurement Unit
IoUT	Internet of Underwater Things
IEEE	Institute of Electrical and Electronics Engineers
LARS	Launch and Recovery System
LBL	Long Baseline
LOS	Line of Sight
MARES	Modular Autonomous Robot for Environment Sampling
NIB	Navigation and Instrumentation Buoy
NMEA	National Marine Electronics Association
OEM	Original Equipment Manufacturer
REMUS	Remote Environmental Measuring Units
ROS	Robot Operating System
ROV	Remotely Operated Vehicle
SBC	Single Board Computer
SBL	Short Baseline
SIB	Synchronized Intelligent Buoy
SLAM	Simultaneous Localization and Mapping
SONAR	Sound Navigation and Ranging
SWATH	Small Waterplane Area Twin Hull
UAV	Unmanned Aerial Vehicle
UDP	User Datagram Protocol
USBL	Ultra Short Baseline
UUV	Unmanned Untethered/Underwater Vehicle
UWSN	Underwater Wireless Sensor Networks

Chapter 1

Introduction

"Begin at the beginning," the King said gravely, "and go on till you come to the end: then stop."

— Lewis Carroll, *Alice's Adventures in Wonderland (1865)*

The Ocean is unarguably an essential component of the Earth ecosystem. The relevance of the surface water is clear for its interface with the atmosphere, representing a gateway for complex energy exchanges that regulate the climate with global consequences. It is also through this access that the oxygen produced by photosynthesis of microscopic marine plants reaches the air, in levels comparable in importance to the ones produced in rainforests. However, the relevance of the whole Ocean is much more considerable than the topmost layer. It acts as a gigantic regulator of the whole interactions at the surface, with a tremendous capacity of energy storage, and it also contains an enormous amount of natural resources, essential for providing a food source to a great fraction of the world population, and a great variety and quantity of minerals.

Even though there is a global awareness of the importance of the marine environment, very little is known about the complex dynamic processes taking place in the oceans, particularly when it comes to the deepest regions (Ramirez-Llodra et al. (2010)). In fact, considering the full volume of water of the worlds' oceans, it is clear that it remains vastly undersampled. The main reason for this absence of data can be ascribed to the harshness of the marine environment. Operations at sea can be risky both to scientists and equipment, since they are typically carried out in stressful conditions. Not only all the accelerations and rolling can wear the human body and impair wise decisions, but also the exposure of equipment to salt water promotes corrosion and even humid salty air alone can be sufficient to destroy electronic systems. The difficulties augment when it comes to deep water sampling, with the need to lower equipment from very long cables and the requirement to withstand almost unbearable levels of hydrostatic pressure.

This work addresses the development of efficient tools to improve the collection of ocean data. In particular, it addresses the development of robotic systems and their use in the observation of dynamic oceanographic processes. The intention of this chapter is to provide both a preamble to the remainder of the work and also an overview of the thesis, encompassing two parts. The motivation section briefly explains why some dynamic oceanographic processes cannot be sufficiently sampled using traditional methods. It also describes such mature instruments and techniques to highlight their benefits and shortcomings in sampling the relevant parameters, and introduces the potential advantages of using autonomous vehicles as a mechanism to increase the efficiency in the sampling process, particularly in a more general framework of autonomous ocean sampling networks. Finally, the section ends with the problem statement, *i.e.* the fundamental questions that will be addressed in this thesis. The second section provides an overview of the manuscript, identifying the relevant assumptions, the scenarios where the solutions are sought and the intended contributions. Finally, the chapter concludes with a brief summary of the thesis organization.

1.1 Motivation

There is a numerous community of scientists studying multiple aspects of ocean related topics, and many of them embark on scientific cruises to gather valuable data for their research. The requirement for ocean sampling is not restricted to science, with an increasing number of marine facilities being installed at sea, for exploration and exploitation of marine resources, that demand various types of ocean data. However, sampling the oceans is a very difficult task, not only requiring people to work in very uncomfortable and stressful conditions, but also because it requires equipment that has to withstand shock, vibration, temperature extremes, and being submerged in a corrosive media, often under a tremendous hydrostatic pressure. Collecting these data is also a very expensive activity, with the cost of ship time frequently dwarfing the (yet expensive) cost of the equipment. It can also be quite frustrating, particularly when a specific piece of equipment fails under operational stress or when some long-planned cruise has to be shortened or even canceled due to weather conditions. Finally, there are many scenarios where the environment is simply too dangerous to allow any human presence.

Even after passing all operational difficulties to get the raw data, there is often the need for intensive data processing to allow proper interpretation. This cycle may take longer than the timespan of a single cruise, or at least too long to resample the same process. In fact, traditional sampling methods can fail to capture the dynamics of many phenomena taking place in the ocean, due to insufficient sampling rate in space and time. There is therefore a great demand for faster, more effective and efficient methods for sampling the marine environment, that may include innovative uses of available technology and the development of new technology. Marine robotic systems can take a leading role in fulfilling this demand. Recent advances in specific systems, from navigation sensors to low power electronics and more efficient energy storage, have enabled the development of a myriad of new platforms. More, the increase of embedded computational power endows these systems with an on-board intelligence that permits real time interpretation of

data and new paradigms for ocean sampling. These new techniques can further benefit from the use of multiple platforms in cooperation or even in collaboration. Also important, robotic systems can work 24 hours a day in risky environments, with minor deterioration. Therefore, they can truly be useful tools to get more data, more rapidly, more accurately and more efficiently, contributing to get a better picture of oceanographic dynamic processes by improving the space and time sampling density.

In this section, we start by describing a few simple but illustrative examples of oceanographic processes whose dynamic characteristics demand a rapid response. In these cases, traditional sampling methods fail to provide a clear picture of such dynamics. We pass briefly through an overview of the traditional sampling methods and then explore the potential benefits of autonomous robotic systems, both on their own and also integrated in heterogeneous networks of sampling platforms.

1.1.1 Dynamics of Oceanographic Processes

There are many reasons for sampling the ocean, but one fundamental aspect that always has to be taken into consideration is the relevant spatial and temporal variation, and associated scales. This has been recognized ever since man started to depend on the ocean for food, shipping or transportation. Early sailors, for example, wanted to understand the space and time dynamics of the prevailing winds and currents as they influenced the course of the ships.

When sampling the water column for a single parameter, the sampling process can be seen as an estimate of a multidimensional scalar or vector field. For example, a bathymetry map can be seen as a two-dimensional scalar field, where we can define $depth = f(lat, lon)$, if we neglect any time variation, or a three-dimensional field, in a dynamic scenario such as a river estuary. In many situations, we can make very reasonable assumptions about the dynamics of a given process, while in others we may need to increase or confirm that sensitivity by increasing the sampling rate, *i.e.* sampling as densely as possible.

In this work, we are concerned in conceiving new sampling mechanisms to capture data of dynamic processes and there are many examples to illustrate this. For example, the fact that sound waves travel in the underwater environment far better than visible light and other electromagnetic energy has been widely known for a long time, and propagation velocity has been accurately estimated in the early 19th century. It was later realized that acoustic signals behave differently in different places in the ocean, with variations that could be related to environment conditions such as pressure, temperature and salinity. During the second World War, underwater acoustics made great leaps, which allowed for surface ships to detect enemy submarines more easily, and sonar (which stands for SOund NAvigation and Ranging), became a very important instrument for the detection of the submerged enemies. As the use of sonar became more widespread, interesting phenomena started being noticed, such as the fact that sound from surface ships refracted away from submarines if they hid under thermoclines. This, in turn, fomented the study of the characteristics of the sound channel and the relationships between sound speed and other water parameters.

Since then, underwater sound has been extensively used, together with other parameters, for the study of the oceans. Current research in acoustic communications, for example, employ multiple techniques to take advantage of the instantaneous characteristics of the acoustic channel, so that the transmission method can be adapted to maximize throughput (Schneider and Schmidt (2013)).

In case of mapping an ocean front that separates different masses of water, both length and time scales can vary significantly. In the open ocean, it is common to find long term fronts that span tens of kilometers (Pollard and Regier (1992)), while in a coastal environment, fronts can form and disappear within a few minutes and show length scales as small as hundreds of meters (Farmer et al. (1995); Schmidt et al. (1996)).

There are also many examples of ocean plumes from hydrothermal vents, sewage outfalls or other pollution sources, that show a wide range of length and time scales. In the case of a diffusing plume from a pollution source, the associated scales can be very short, as it can span a few hundreds of meters and last for only a few hours (Ramos et al. (2001)). Another example of a rapidly evolving plume is a harmful algal bloom (HAB) episode, a complex phenomenon dependent on light level, nutrient concentrations, and water temperature (Tang et al. (2006); Babin et al. (2008)). These episodes demand a rapid response, not only to assess the exact status of the process, but also to predict its evolution with better accuracy.

All these examples share the requirement for rapid response and fast/dense surveying, preferably reacting to data in real time to better capture the dynamic characteristics of the specific ocean process. An in depth analysis of some of these examples will be carried out in the next chapter.

1.1.2 Traditional Ocean Sampling

There are many instruments for sampling the oceans and some methods developed to optimize their use. It is difficult to draw a line between what are "traditional" systems and sampling techniques, and what is the "state-of-the-art" as far as ocean technology is concerned. In fact, technological evolution has provided for steady and continuous improvements in the last few decades, so that we are regularly being faced with the development and deployment of new products, some of them envisaged a long time ago.

Our idea is not to provide a precise boundary, but solely to present a general overview of some of the well established techniques for ocean sampling and render a qualitative distinction between "traditional" and "state-of-the-art". This is particularly relevant to the non-oceanographic engineer that could otherwise have difficulties in understanding the relevance of the present work in the context of ocean engineering. We include as "traditional" all techniques that have been around for some decades, have already proved to be successful in various domains, and are still in use. We rule out of this group all systems and techniques that have only emerged and/or matured in the last few years and also the new methods that still have to prove to be reliable and useful for sampling the oceans. These reflect the latest worldwide research efforts and, in our opinion, will be the trends for the near future. We include in this former group many forms of Autonomous Vehicles, particularly when operating under the Autonomous Ocean Sampling Networks paradigm, and the

technologies required to make them a reality (the so called "state-of-the-art"). We are particularly interested in a new class of *intelligent* vehicles.

In terms of operation, the division can also be seen in terms of ability of the operator to command the location or trajectory of the sensing platform. In a more traditional approach, a scientist decides the sampling locations and makes sure that the sensors are physically deployed in these locations. Alternatively, the scientist can also use data available from a predefined location. The most advanced systems, instead, can be *programmed* with the trajectory along which to sample and the sampling pattern. They are able to fuse many sources of information, in real time, to approach the destination, typically resulting in more accurate tracks than using human control. Here, for organization purposes, we'll divide the traditional methods into *local sensing*, aggregating the cases where the scientist needs to go to the operation area and use sensors on site, and *remote sensing*, where the scientist can be virtually anywhere in the world and receive data from a remotely located system.

Local Sensing

A natural way to get ocean data from a specific location is to take a sensor and make local measurements. In fact, many ocean parameters can be directly measured using **in-situ sensors** that can be deployed from any ship and store data internally or communicate with a computer for immediate analysis and visualization. This includes typical water parameters measured with a CTD (for Conductivity, Temperature, Detph), or many other characteristics such as turbidity, dissolved oxygen, or pH. A vertical profile can also be obtained just by releasing the right amount of cable, either manually or using a simple winch. In the case of more complex systems, sometimes it is required to deploy complementary parts. For example, when analyzing the characteristics of the acoustic channel, it may be necessary to deploy one or multiple receivers and move the ship to emit sound in different locations. Although the number of parameters that can be measured in-situ is always increasing, in some cases the measurements have to be made in laboratory and require a physical sample of water, of suspended solids, or of the ocean floor. This can be obtained with a sample bottle, a special net (to collect phytoplankton, for example), or a grab/corer to sample the bottom of the ocean.

The list of equipment and methods is vast and their full inventory is beyond the scope of this work. The main intention here is to highlight that getting meaningful scientific data is seldom as simple as it sounds, particularly when trying to measure the dynamics of an oceanographic process. For example, a simple CTD profile has to account for ship motion during the vertical excursion. In a small scale process, an error in the exact location of the sensor and even the offset off the vertical can lead to incorrect conclusions. Also, the velocity of the profile has to be chosen so that the sensor is not sampling water that is dragged along the movement. All these factors may affect the validity of any conclusions, particularly when the water depth is very high, regardless of the sensor accuracy and calibration.

Towed bodies are sensor holding platforms controlled from a ship via an umbilical cord that provides power and communications. An advantage of this arrangement is that all sensor data can be correctly synchronized. They have limited maneuverability and can follow simple trajectories, using deflection surfaces for changing depth and orientation. There are some undulating versions to allow vertical profiling along the way, so they can be seen an extension of the typical deployments from a ship, but providing quasi-synoptic two-dimensional sections of the evolving fields.

The use of **manned submersibles** for ocean exploration has been inspired by the pioneering descents of William Beebe and Otis Barton, who, in 1934, made history with a record dive to 923 meters in a *Bathysphere* off the coast of Bermuda (Beebe (1934)). Their report on direct observation of deep water animals that had never before been seen alive has incited other scientists to embark on similar achievements. The number and variety of vessels increased steadily in the following decades and, in the 1970s, more than 150 manned submersibles had already been manufactured all around the world, with some dives deeper that 1000 meters (High (1971)). In the vast majority of these dives, scientists could only rely on direct observation and video/photo recording of new species. In January 1960, Don Walsh and Jacques Pickard made a tremendous breakthrough by descending to the bottom of the Mariana Trench on board the *Bathyscaphe* "Trieste". This experience was only repeated 52 years later, in March 2012, by the Canadian film director James Cameron, in the submersible "Deepsea Challenger".

Alvin is arguably the most well known manned research submersible used for science, allowing dives down to 6500 meters of depth, with an impressive record of dives in all oceans around the world, since 1964 (Lippsett (2014)). Evolving in parallel during the last years of the cold war, another successful example of a manned submarine is the 6000-meter-rated Russian MIR with countless dives with military and scientific purposes (Sagalevich (2012)).

The idea of personal immersion in the underwater world is very exciting, but also very dangerous. An alternative, safer technology is to use **Remotely Operated Vehicles** (or ROVs) – underwater robotic machines that operate with a physical link with the surface. ROVs for underwater work and exploration have existed for many decades, however it was not until the 1980s that small electric vehicles became technically available and relatively affordable, making it possible to gather important underwater data without complicated logistics. Before then, the complexity and operational cost of these systems precluded their use for oceanographic studies, with the exception for a small number of private companies involved in the oil industry. The main objective was then to replace diver workers in the visual inspection of dangerous locations.

Earlier ROVs were merely a set of remotely controlled thrusters, fixed to a protective frame where camera and lights were also attached to (many decades later, there are still companies selling similar versions). The cable was typically a multiple conductor umbilical, connecting a control console at the surface to a junction box at the vehicle, where dedicated sets of cables were split into individual subsystems. Such a thick cable caused a major impact on dynamics that greatly

complicated control, particularly when operating in strong currents. Therefore, any ROV operator needed special training, even to conduct a simple inspection mission.

With the requirements of operational scenarios becoming more demanding, and the advances in feedback control systems providing effective solutions for basic control problems, some of the operator tasks started being performed autonomously by dedicated systems at the surface (like *auto-depth* or *auto-heading*, for example). Naturally, the minimization of electronic components and the increase in computational power made it possible to move some of the automated control from the surface to the underwater system itself, monitoring more variables and responding faster and more accurately to disturbances. This also reduced the cable requirements to transmitting only power and few communication links that were interpreted by an on-board system, allowing for thinner umbilical cables.

Regardless of all technological advances, the mobility and range of these vehicles is severely constrained by the umbilical, and the drag associated to the frame and the cable prevents high velocities, so their major application is still to perform slow-moving close range operations. With the automation of some tasks, the required training for an ROV operator is less demanding and some operations can be done directly by the specialist, including visual inspection of habitats and collection of physical samples. In larger systems, a dedicated crew of several skilled people is necessary to operate the vehicle's subsystems. The scientist or specialist works in close collaboration with this team to provide indications such as trajectories, orientation, or manipulation requirements, for example. The primary advantage to the use of an ROV is that the operator can have a remote presence for observation, work or intervention in underwater tasks. The physical arrangement also enables the installation of multiple sensors that can be easily synchronized. Since the cable can provide a large amount of power and virtually unlimited energy, the suite of possible actuators is also large and operations are not time constrained. This ability to perform continuous operations yields a significant saving in mission costs, particularly when they are based in large ships.

Remote Sensing

Typically, the term "remote sensing" refers to data collected from satellites, but here we generalize the concept to all the cases where the scientist is not in physical contact with the sensing platform. One of the first methods to make in-situ measurements has been the installation of all sorts of instrumentation in **ships of opportunity**. Typically, these can be fishing vessels, cargo ships, or ferryboats, *i.e.* vessels that routinely/periodically follow a given trajectory. In some of these cases, data can be transmitted in real time, while in others the sensor can log all the information and the scientist needs to wait for the end of the journey to get the data. Naturally, data tends to be highly concentrated along specific trajectories and therefore this can be a vey good method to obtain a time series of data from a specific location. In any case, the main advantage of the method is that the cost of gathering data is very low.

In-situ **observatories** are important tools for monitoring time-variations of oceanic processes (whether periodic or sporadic). Ocean observatories are unmanned systems located at a fixed site,

providing information regarding the seafloor, the water column and/or the surface. They can be simple instrumented moorings installed for a short period (sometimes called "portable observatories") or very complex systems comprising arrays of instrumented buoys and underwater nodes. For a historical perspective on the development of oceanographic buoys, see for example Soreide et al. (2001). Most complex systems try to get the most out of the moored instrumentation by combining a profiling mechanism to a moored based system, such as described in Brown et al. (2001). In some other cases, there can also be a shore component, for example measuring water currents using long range radar from an elevation. Because of installation and retrieval cost, complex systems are usually justified only for long term (multi-year) studies of a particular region. Most of these are installed close to shore, using underwater cables to provide power and communications, therefore allowing data to be available in real time. For installations in remote locations, energy is typically harvested from the environment and data is sometimes transmitted intermittently, in batches, to save on transmission cost by satellite links. In the case of deployments that last more than just a few months, another concern is biofouling of sensors, which can degrade data quality, so a regular maintenance visit is usually required. Just like data from ships of opportunity, the spatial resolution of these observatories is sparse. The main advantages are that the location sites may be defined according to scientific or other interest and there is a virtually continuous time series of data from such specific locations.

Due to their global coverage and sophisticated instrumentation, **environmental satellites** are playing an expanding role in monitoring ocean conditions, namely in sea-surface temperature and chlorophyll concentration. They can be seen as a special case of a remote observatory, with a very large field of view in the horizontal plane. The contributions of satellites are fundamental to measuring variations on time scales ranging from seasonal-interannual to decadal. However, they lack in detail and have poor vertical information. Satellite data has been used fundamentally for the detection of sea surface temperatures and identification of processes that are characterized by temperature data, such as warm core eddies studied more than 40 years ago (Scully-Power et al. (1975)).

Drifters are another example of technology to collect ocean data with global coverage. They are instrumented floats deployed from a support vessel, which then drift horizontally with the local currents for long periods of time. ALACE is an example of an autonomous, subsurface drifter, which surfaces periodically to return profile data using ARGOS satellites (Davis et al. (1992)). These floats have the ability to change its buoyancy and, taking advantage of the increase of water density with depth, they can drift at a preset depth, up to a maximum of 2000 meters. Present **profilers** are similar to the drifters in the ability to change buoyancy, but instead of fixing a certain depth, they use variable buoyancy to move vertically while drifting through the ocean. Davis et al. (2001) describe the profiling version of ALACE and other subsurface floats developed in the late 20^{th} century. By the end of the millennium, the Argo Program was created, as the first implementation of a global array of subsurface sampling platforms. In 2007, Argo reached the initial objective of deploying 3000 profilers and this number has been maintained or even augmented

with the annual deployment of hundreds of additional floats (Roemmich et al. (2009)). Currently, Argo has more than 3800 free-drifting profiling floats around the globe, continuously sampling the oceans and releasing data online[1]. Note, however, that given the nature of the platforms, some parts of the Ocean are oversampled, while others still have spatial gaps.

1.1.3 The Role of Autonomous Vehicles

It is clear that the above mentioned techniques are very useful but not sufficient for the so-called real time oceanography, which requires not only the measurement of spatially distributed and temporal correlated data, but also a rapid response to episodic events, in order to study dynamic ocean processes. Autonomous marine vehicles are robotic systems with the ability to control their trajectory in the marine environment without human intervention, while collecting sensor data. We are aggregating here all the vehicles that can be programmed to make measurements at a given latitude, longitude, and depth. More, these instructions can often be transmitted remotely, without the need of physical contact with the vehicles. There are multiple possible configurations and complementary characteristics of such vehicles that can be exploited to address specific observation challenges, reducing people risk and also ship time and people involvement, therefore reducing operational costs and increasing efficiency in the sampling process.

The use of robotic systems at sea has been increasing remarkably in the last years, with impressive performances in almost all scenarios of marine operations. However, a more widespread adoption of robotic solutions at sea is threatened by the absence of international legislation regarding the navigation of unmanned systems. This is particularly relevant to vehicles that operate at the surface, since the risk of collision is much higher than with vehicles or systems that remain underwater most of the time. Although this subject has been addressed with the early technology demonstrations and the research community has been implementing technology solutions to minimize the risk of collision, a proper legal setting is yet to be defined by the international organizations (van Hooydonk (2014)).

One of the most promising uses of autonomous vessels at sea is to take advantage of the on board computational power to process data in real time and change the sampling pattern according to such data. In fact, regardless of our efforts to sample the oceans more densely, observations will remain expensive and scarce comparing to the needs, therefore we should strive to use the vehicles' intelligence to sample where data can be more useful. The other potential benefit from emerging capabilities comes from the possibility of using multiple vehicles in cooperative missions. These can serve to capture temporally correlated and spatially distributed data or to enable distributed/complementary observation systems.

Robotic Surface Vehicles

Robotic surface vehicles are extremely valuable scientific devices that have been playing a discreet but consistent role in many areas of marine science, by providing an effective and affordable

[1] All data can be accessed through the Argo Program website at http://www.argo.ucsd.edu/

way to sample the ocean. These vehicles are commonly referred to as Autonomous Surface Vehicles (ASVs), Autonomous Surface Craft (ASC), Unmanned Surface Vessels/Vehicles (USVs), or Unmanned Marine Vehicles (UMVs), and they combine the ability to transport a large variety of sensors and actuators with real time, high-bandwidth communications, resulting in advanced systems for tele-presence in the marine environment. The earliest examples were developed in the 1990s, with many more designs proliferating with the new millennium, with main applications for science, bathymetric mapping, and defense. They have also served as preferred demonstration platforms in general marine robotics research. An interesting perspective of the historical development of this technology can be found in Manley (2008).

ASVs navigate at the ocean surface, therefore their ability to probe the water column is rather limited. In situ sensors can be used to measure sea surface data, or winched down to survey deeper layers within reasonable limits. Additionally, there are many sensors that can transported at the sea surface and provide long-range measurements, such as sonars or acoustic current profilers.

The propulsion system consumes a very significant part of the total available power of an ASV, and there have been proposed many options to provide propulsion to ASVs. The most common alternatives are rechargeable batteries, fuel, and energy harvested from the ocean. Rechargeable batteries are typically found in smaller, fully electric vehicles, for operations in coastal or calm inland waters (Vaneck et al. (1996); Curcio et al. (2005); Cruz et al. (2007)). Fully electric ASVs are very easy to control but the limited amount of energy stored on board prevents their use in long range missions.

Fuel propulsion is typically found in larger, faster systems, such as the vehicles developed for military applications. The "USV Masterplan" from the United States Navy dates back to 2007, but describes some examples of these systems particularly suited to meet the Navy's present and foreseen needs. These vehicles are separated in different classes according to size and mission requirements, from the smaller X-Class, up to 3 meters long, to the 11 meter long Fleet-Class (United States Navy (2007)).

Harvesting the propulsion energy from the environment is a way to overcome the limitations in energy storage and transportation. Autonomous Sailboats are a particular class of ASVs that rely on wind to provide propulsion and only need electrical energy for the on-board electronics and rudder/sail adjustments. They are a proven technology for ocean monitoring, sampling and surveillance and they have gained particular attention in the last few years for their unique ability to maintain long term unassisted operations in the sea surface, with a wide range of application scenarios spanning the scientific, civil, and military communities (Cruz and Alves (2008); Rynne and von Ellenrieder (2009)). In particular, the silent nature of sailboat operations yield a great potential in marine surveillance, as well as in the detection and tracking of marine mammals across vast areas of the ocean (Stelzer and Jafarmadar (2012); Silva et al. (2013); Klinck et al. (2015)).

Another example of the effort to achieve a long term ocean presence by harvesting energy from the environment is to take advantage of the energy in the waves. The concept of using the

waves to propel a boat has been proposed a long time ago, with early prototypes reported in the nineteenth century (Ashburton Guardian (1897)). However, it was only very recently that this concept has been adapted to autonomous robotic vehicles. An an example, the Wave Glider uses a set of underwater wings coupled to the surface hull and transforms the vertical wave-induced motion into forward thrust (Hine and McGillivary (2007)). Although this implementation is still very recent, it has already an impressive record of thousands of miles at sea, collecting data in very harsh conditions, with some missions lasting longer than one year.

Autonomous Underwater Vehicles

In the last two decades, some important technological advances together with new ideas for efficient ocean sampling, forested the development of Autonomous Underwater Vehicles (AUVs). These vehicles operate with no physical link with the surface, carrying a set of relevant sensors to characterize the underwater environment, while navigating along a predefined sequence of waypoints. They are designed with hydrodynamic shapes, optimized to be efficient when navigating underwater at velocities up to a few meters per second. Early AUV developments and deployments were engineering responses to sampling demands in challenging environments, such as deep-water hydrothermal vents (Yoerger et al. (1991)) or under Arctic ice-sheets (Deffenbaugh et al. (1993)). By the turn of the millennium, a few companies have emerged as *spin-offs* from academic laboratories, which was a sign of the maturity of such devices and of the great potential ahead. In fact, the emergence of AUVs yielded a big revolution in the access to ocean data, with the capability to measure in all 3D water column. Probably the main disadvantage in the use of any kind of AUV is the difficulty of real time data transmission while the vehicle is in operation, due to the strong attenuation of electromagnetic signals in seawater that impairs high-bandwidth communications at practical distances. In a typical AUV mission, the vehicle is programmed with a sequence of waypoints that have to be visited, with a predefined vertical pattern (fixed or *yo-yo*). During the transit, all sensor data is stored on board for later retrieval, while some of it may be transmitted using low data rate, high-latency acoustic modems. Since GPS signals are blocked by seawater, AUV navigation is also a challenge and has been a hot topic of research since the early developments.

Most of the current work done with AUVs concerns the replacement of traditional techniques for ocean sampling, in order to exploit the physical *autonomy* (i.e. the absence of physical connection with any operator) and mobility to achieve a wide coverage with a minimal setup and operational cost. Although this can yield significant improvements in efficiency, the full capabilities of AUVs are yet to be exploited, by devising new approaches for a more productive utilization of this new tool. One of such approaches is to replace the standard predefined AUV "mission" by an adaptive sampling mission, for which a set of rules are given, but where there is no a priori knowledge of the trajectories that will be followed by the vehicle. Such an approach exploits the on-board computational power to make assumptions about the oceanographic environment and to react to this environment by making decisions about the best sampling strategy to use. By continuously interpreting collected data, this decision can be made autonomously, in real time, so that the

vehicle can use most of the available resources (mainly power) in sampling the ocean in regions of interest.

Gliders are a particular case of AUVs that can also be seen as an evolution of profilers, since they only require power to inflate or deflate a buoyancy engine and toggle between ascending and descending modes. They not only use variable buoyancy to move vertically, but they have also wings and control foils designed to allow steerable gliding, thus providing for some limited control on horizontal propulsion. These vehicles can surface from time to time and fix position via GPS and communicate via appropriate satellite. Nonetheless, the amount of information that can be transmitted is very limited and the scientists need to wait for recovery to get full data. For a long time, there have been suggestions for the harvest of propulsion energy from the environment to allow for very long range operations, and recently Webb Research has developed a heat engine that draws energy from the ocean thermocline. The energy required to change buoyancy results from heat flow from warm surface to cooler deep water, so that the vehicle can cycle thousands of times between the surface and some programmed depth (Webb et al. (2001)).

In summary, the main advantage of gliders is the extended operational range, that can typically reach hundreds or thousands of miles. However, this comes with the inconvenience of a reduced velocity, typically a fraction of 1ms^{-1}, and a very limited power available for sensors.

1.1.4 Autonomous Ocean Sampling Networks

The concept of Autonomous Ocean Sampling Networks (AOSN) emerged with the realization that a single technology could not cope with all the demands of oceanographic exploration. It was first described in Curtin et al. (1993), in a novel approach to provide a framework to encompass a set of cooperative efforts taking place, integrating multiple information sources about the oceans in order to provide a synergistic observation system. Under the AOSN paradigm, a network of both traditional and new ocean sampling assets cooperate to collect data from an area of interest, maximizing the efficiency in the sampling process.

Curtin *et al.* envisaged the installation of moored instrumentation linked to shore via radio or satellite communications, providing oceanographic and atmospheric data in real time. At the same time, a set of small, high-performance vehicles (for example gliders, AUVs and ASVs) would be navigating in the area to provide intensive 4-D data about the region. Long-term deployments would be possible with a set of docking stations – underwater garages with enough power to recharge the vehicles' batteries and also linked to shore, or surface platforms, to allow for mission (re-)programming and data download. The development of underwater acoustic modems would also make it possible to communicate with the vehicles, thus allowing real-time control of the network, rapid assessment and fast response to a particular situation.

The AOSN concept has been suggested more than 20 years ago as a long-term vision and it was followed by many years of development of key enabling components. These included, for example, multiple aspects of organization of the network (Turner et al. (1996)), experimental docking stations (Singh et al. (2001); Stokey et al. (2001a)) or navigation of multiple vehicles

(Singh et al. (1996); Cruz et al. (2001). These concerted efforts lead to the first implementations of true networks of platforms, such as the case of Fiorelli et al. (2006), for example, where a coordinated fleet of underwater gliders was used in an AOSN experiment in Monterey Bay.

Today, autonomous vehicles are seldom used isolated to study a specific region. Instead, they are usually integrated in a larger fleet of complementary assets to provide ocean data.

1.1.5 Problem Statement

This work will focus on the development of tools for the efficient study of dynamic oceanographic processes in scenarios such as described in the AOSN paradigm. In particular, we are interested in developing effective robotic vehicles, rapidly reconfigurable to suite specific sampling needs, and also efficient methods to take advantage of their on-board computational power to increase sampling density.

1.2 Thesis Overview

This work encompasses a subset of interdisciplinary developments, ranging from the more technological solutions to design new vehicles, to the focus on innovative sampling strategies to capture more and better information about specific oceanographic processes. This section provides an overview of the rationale on our strategy to solve the problem stated in the earlier section. Our work is targeted to specific classes of oceanographic processes that may be studied with robotic platforms. We will start by stating the assumptions that justify the forthcoming work, and then a brief description of our approach and application scenarios where we think our strategy can be successfully used. We conclude this chapter with a summary of the anticipated contributions and an overview of the rest of the manuscript.

1.2.1 General Assumptions

In an ideal scenario, an AUV or other robotic system could run an ocean model in real time and close the observation/modeling loop by continuously sampling the ocean. In order to capture more detail, either in space or in time, both the number and velocity of the vehicles could be increased. This is far from reality for a variety of reasons, including the inadequacy of ocean models to show details at the AUV scale, the complexity of such models, and the requirement of much more computational power than is reasonable on board practical vehicles.

Our paradigm is based on the assumption that there are ocean processes that can be represented by simple models with time varying parameters. We are particularly interested in processes characterized by a sharp transition, or a boundary, in a given parameter that can be measured in situ. As an example, one might consider an aerial view of an oil plume at the surface, in which case a simplified model can be the closed contour limiting the plume. In order to track the evolution of the plume, it may suffice to know the temporal evolution of the contour. We will restrict

our study to processes that can be described under this assumption and we will present the corresponding strategies to identify their characteristics by adaptively changing the sampling pattern of the AUV(s).

The same paradigm can be extrapolated for three dimensional analysis. For example, if we want to study the space and time evolution of a plume emanating from a sewage outfall, we may have all the relevant information if we can characterize the space and time evolution of the limiting surface of the plume. This can be done by finding, for each depth, the time variation of the shape of the boundary and the value of the gradient at the boundary. Once again, we are assuming that the overall feature can be represented by a reduced number of parameters. Weather forecasting is a discipline where a similar approach is commonly used, as the forecast for a region is generally established by the study of the position and evolution of atmospheric features: warm and cold fronts and high and low pressure centers. These features govern the prevailing winds, which, in turn, significantly influence the evolution of the features. This loop allows for the forecasting of the weather conditions for a few days and the detection of locations where data can be obtained to correct the model using detailed numerical methods.

Our key idea is to adapt the observation strategy of a given scalar field to the characteristics that are identified as the vehicle(s) move and sample the same field. For this to be possible, it is important that some form of *a priori* knowledge about the process is available, so that the sampling algorithms can be more efficient and the performance of the sampling strategy can be evaluated. Typical variations of the phenomena features, both spatial and temporal, are important, but the quantitative evaluation of the uncertainty of the prior knowledge is of particular importance. If this information leads to an over-estimation of the variability, then it will result in a more extensive sampling than required, decreasing the survey efficiency. On the contrary, an under-estimation will result in under-sampled surveys, therefore likely to miss important features.

In terms of vehicle design, our main assumption is that a rapid response to rapidly evolving processes is better ensured with small, highly maneuverable systems. Naturally, the smaller the vehicles, the simpler the launching and recovery systems and the easier and faster it is to organize a cruise to use them in the field. We also assume that it is preferable to use customized vehicles for particular missions than to try to use a reduced number of designs in many application scenarios. A simple justification for this can be ascribed for example in terms of maneuverability. In some situations, a simple torpedo-shaped AUV with only 3 degrees of freedom may be enough to survey a given area, while in other cases, a more complex version with full 6 degrees of freedom may be required to provide hovering capability. Finally, we assume that even the smallest practical vehicle designs can transport useful sensors, therefore size reduction does not impair oceanographic missions, which is supported by the trend of miniaturization that has been generally followed by sensor manufacturers.

1.2.2 Our Approach

We propose an integrated approach to ocean sampling, that includes the design and development of a new family of vehicles, the conception of innovative principles of operation and the implementation of the corresponding guidance algorithms. We strongly support the validation of all developments by field demonstrations in operational scenarios.

As far as robotic vehicles are concerned, our approach is based in the development of small modular marine vehicles. Smaller vehicles require low operational logistics, therefore they require simpler support ships and they are easier to mobilize in order to respond to a specific event. They are also less expensive to build and maintain, promoting the utilization of multiple units in more risky environments, by reducing the cost of potential losses. Moreover, they are more likely to be adopted by lower budget institutions to support both operations and applied research. Modular vehicles have the potential to be rapidly reconfigured to suite a particular application scenario, although modular assemblies often result in slightly larger systems as compared to complete redesigns.

In terms of vehicle operations, our approach envisages the tracking of features in the ocean in such a way as to understand the evolution of the phenomena. Our features can be seen as represented by a reduced dimension parametric model that captures the main characteristics of the oceanographic process. This parametric model can be seen as a simplified geometric representation and does not need to be the result of an analytical solution or numerical integration of a physical model. In fact, many engineering systems are becoming very complex, which hinders their solution using analytical approaches. Alternatively, new methods are emerging with the use of heuristic approaches that are validated by simulation and then by experimentation. As an example, a closed geometric contour can easily represent a pollution oil plume at the ocean surface, and if we know the evolution of such a curve, we may obtain both qualitative information about the plume, such as shape and potential hazard to a coastal region, and also quantitative information, such as size and rate of growth.

The main goal of our sampling strategy is to spend most of the limited energy making measurements around these features, in order to capture the most relevant information about the ocean process. In other words, the idea is that if we have a finite set of samples, we want to "spend" them in locating the features and not mapping vast regions with little or no information at all. Assuming the same pollution plume described above, using a vehicle to track the boundary would be sufficient to provide many geometric points of the contour and also the concentration of pollutants.

Finally, our approach also encompasses field validation and feedback from the results of field experiments into the developed solutions. This is paramount when designing any new engineering system and particularly relevant when such a system is meant to be operated in an unpredictable, dynamic environment.

1.2.3 Anticipated Scenarios

We anticipate that our approach for ocean sampling can be implemented in many AOSN scenarios. For example, let us assume we have an AOSN installed in a given region, and an AUV is waiting at a docking station for a given event to trigger a survey operation. This event may be the onset of an HAB episode, for example, and it may determined through remote sensing (satellite data, for example), measurements made from the moored instrumentation installed on the docking station, or it may simply be a time driven survey of a permanent process. On a "traditional" approach, the vehicle would leave the docking station and perform a land-mower pattern over a given area, hoping to find relevant information. The size of this area would depend on the water conditions (for example, with stronger currents, it would be expected to have faster motion of the feature) and given the uncertainties involved, the tendency would be to consider oversized areas of survey. The final number of useful data points would be very modest, thus resulting in poor efficiency in resource usage. With our sampling approach, the vehicle can get out of the station, find the relevant feature and follow it for some time. The vast majority of data points are collected in the neighborhood of the feature, providing far more information about the process than the "traditional" approach. On the other hand, the vehicle will travel as far as it is required to keep tracking the feature, so it will not spend energy taking almost-useless measurements. When there is enough information about the process, or the energy level reaches a critical threshold, the vehicle goes back to the docking station, where it recharges batteries, downloads information gathered about the process and waits for new instructions.

Similar scenarios can be anticipated in the case of three dimensional mapping of plumes from hydrothermal vents (for example, performing a periodic survey), from sewage outfalls (it can be a periodic survey, or triggered when the current direction points towards the coast or when there is an increase in the wind speed), from an oil leak close to an oil field (in this case, the triggering event can be the detection of hydrocarbons).

In parallel with this utilization in mapping dynamic processes, we may also extend the concept to more traditional applications, like autonomous bathymetry. In this case, the vehicle may adapt its trajectory in order to maintain a given altitude above bottom, or a given attitude with respect to the bottom slope, in order to maintain a certain level of accuracy.

The extent of anticipated scenarios broadens largely when we consider the coordinated operation of multiple vehicles. These can serve, for example, to capture a more synoptic picture of a plume by sampling simultaneously in multiple boundary locations, or, more importantly, to take advantage of complementary and/or distributed assets among different vehicles. For example, one ASV or AUV scout can be used to detect the edge of an underwater elevation and provide waypoints to a follower AUV that performs a slow, smooth, and continuous close-range inspection.

1.2.4 Thesis Contributions

The aim of this work is to provide various levels of contributions to the problem stated in section 1.1.5, in particular:

- The adoption of an integrated approach to problem solving by carefully taking into account the overall requirements and the limitations of available solutions to identify the main challenges to fulfill such requirements.
- The design and development of a new family of modular robotic marine vehicles, including ASVs and AUVs, that may be easily reconfigured to become efficient and effective tools for specific missions.
- The conception of innovative principles of operation of robotic marine vehicles in the emerging area of real time adaptive sampling, including the development of guidance algorithms for specific classes of dynamic oceanographic processes and the validation of all developments by field demonstrations in operational scenarios.

1.2.5 Thesis Organization

The remainder of this thesis is organized as follows. Chapter 2 provides background information and a state of the art in terms of technology and methods for ocean sampling. Chapter 3 summarizes the current challenges for the development of efficient tools for ocean sampling. Chapters 4 and 5 present our strategy for the development of modular robotic vehicles, AUVs and ASVs, respectively. In chapter 6, we detail the algorithms designed for the implementation of the adaptive sampling strategies, as well as data from field trials. Finally, we conclude in chapter 7 with a summary of the contributions and some perspectives of future work.

Chapter 2

Background and Related Work

The farther backward you can look, the farther forward you are likely to see.

— Sir Winston Churchill (1874–1965)

The main objective of this chapter is to lay the foundations for the research undertaken in the remainder of the thesis. It starts by providing some background information about oceanographic processes that are amenable to be studied by small-size robotic platforms. The focus is not on the physical study of the processes, but mainly on the typical space and time scales of the characteristic scalar fields. The chapter also describes the achievements of other researchers, in a synopsis of the state of the art systems, techniques and paradigms currently employed in ocean sampling, and this is split in two main fractions. The first addresses the autonomous robotic platforms that are available for *intelligent* ocean sampling, either alone or in networks, under the AOSN paradigm. The second describes the specific results that have been achieved in the implementation of adaptive sampling techniques.

2.1 Characterization of Relevant Oceanographic Processes

The ocean is an extremely dynamic environment, with a myriad of interrelated physical and chemical processes taking place continuously, but at varying temporal and spatial scales. This work addresses the efficient use of technology for sampling the ocean, by advancing the state of the art in terms of robotic capabilities, and also by increasing the sampling performance by a proper use of the on-board *intelligence*. As seen in the previous chapter, small robotic vehicles move relatively slowly and current technological constraints still limit the maximum practical range to tens or a few hundreds of kilometers, therefore we are mainly interested in processes with relatively small spatial features. This rules out processes that have been thoroughly studied using basin wide ocean models, like the Gulf Stream, steady circulation, and other large-scale phenomena (Dyke (1996)).

Even the simplest, local models of ocean dynamics require some intensive processing that is not feasible to run in real time in embedded systems of small robotic vehicles. Instead, our approach is based on the assumption that there are ocean processes that can be approximated by simple models with a small number of time varying parameters. It should be pointed out that it is not required that the model is *exact* or mathematically derived from equations with physical meaning. The single requirement is that the model parameters can be identified by the vehicle, in real time, by adapting the sampling pattern. This will allow the vehicle to concentrate measurements in the region of interest and, consequently, to sample the process more frequently.

This section will describe some of these ocean processes. Given the above constraints, candidate processes have small spatial scale and variable degrees of temporal scales, mostly occuring in coastal waters. This is where the dynamics happen faster and in smaller spatial scales, and that is a reason why most observatories are installed in coastal waters (National Research Council et al. (2000)). The main objective of this characterization is to provide typical spatial dimensions, temporal variations and required measurements, so that it will be possible to derive an adequate sampling strategy. It should be stressed that the aim is not to provide a thorough survey of all the possible processes, neither to provide oceanographic explanations of the phenomena. Instead, our effort is towards the identification of the main characteristics of the processes that we propose to sample using our robotic tools. Using a systems engineering perspective, this will provide requirements for our sampling tools that we need to leverage with our capabilities. Therefore, the forthcoming list of processes is not exhaustive, but it is varied enough to justify the development of our technology.

2.1.1 The Thermocline

Temperature and salinity are probably the two most important characteristics of a water mass. Their variation with depth allow the determination of the *T-S relationship*, a characteristic that distinguishes different water masses. In fact, temperature and salinity are practically unaltered in the interior of the ocean if the water does not mix with other water masses, and this is the reason why this relationship is also known in oceanography as *T-S signature* (Sverdrup et al. (1942); Pickard and Emery (1990).

The thermocline is a vertical transition layer in the water column, separating the warm surface layer, or *mixed layer*, from the cold deep water bellow it. The mixed layer, closer to the surface, is the most easily influenced by atmospheric conditions (wind, rain and solar heat), which naturally results in a wide range of values throughout the year. However, the dynamic of the surface waters, due to the wind and wave action, mix the water in such a way that the gradient is small. In the thermocline, typically a relatively thin layer of the water column, the water temperature drops nearly linearly as the depth increases, with a significantly higher gradient as compared to the rest of the profile. Finally, the deep-water layer is the bottommost and less dynamic zone. Water temperature in this layer decreases slowly as depth increases. Figure 2.1 shows an example of a temperature profile measured 2km off the Portuguese coast, in about 40m of water, exhibiting a clear thermocline between 11 and 14 meters of depth.

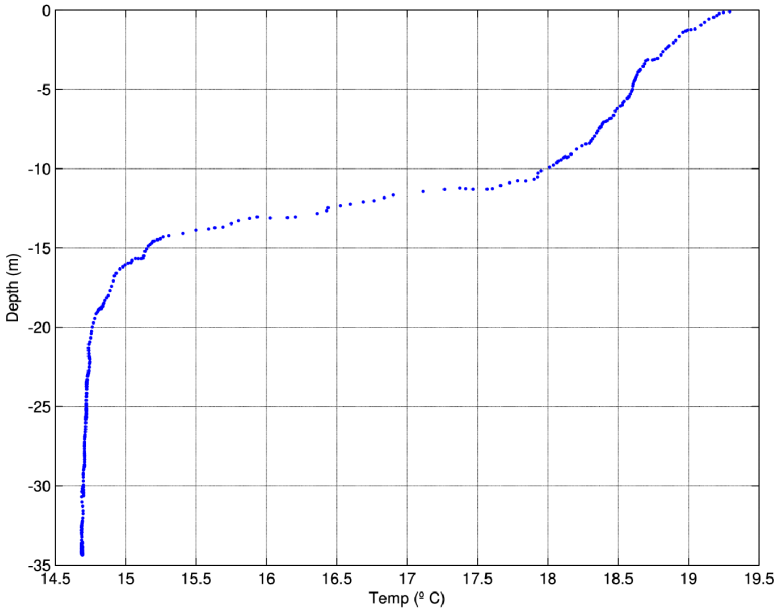

Figure 2.1: Temperature profile measured 2 km off the Portuguese coast, June 2009. The thermocline can be easily identified at about 11-14 meters of depth.

The thermocline is most usually associated to the ocean basins, including both the seasonal occurrences in shallow waters, with very short spatial scales, and the *permanent thermocline* found in all the world's oceans between 100 and 1000 meters of depth (Pickard and Emery (1990)). It is also possible to find seasonal thermoclines in fresh water, particularly in large lakes and dam reservoirs (Johnson et al. (2004)). Figure 2.2 shows the temperature profile in a river reservoir along the year, highlighting the seasonal characteristic of the thermocline.

Relevance of the Thermocline

The characteristics of the permanent thermocline has a strong impact in oceanography, namely in the study of the ocean circulation. This ocean circulation dictates the thermal structure of the ocean, and it has two components: a shallow wind-driven circulation and a deep circulation of temperature and salt. The depth and gradient of the thermocline is related to the static stability of the ocean, the heat transport and diffusivity (Wunsch (2002); Boccaletti et al. (2004)).

The observation of thin layers of phytoplankton has long been associated with seasonal thermocline in lakes and coastal ocean, such as described in Gessner (1948), Derenbach et al. (1979), and Sharples (1999). Its presence, location, characteristics, and variability (both spatial and temporal) can provide valuable information about phytoplankton concentration. This, in turn, affects many other aspects of coastal ecology, like primary production, nutrient concentration or the distribution of fish population.

As far as underwater acoustics are concerned, the temperature profile has also a major effect in underwater sound speed and, consequently, in the propagation of sound waves. Therefore,

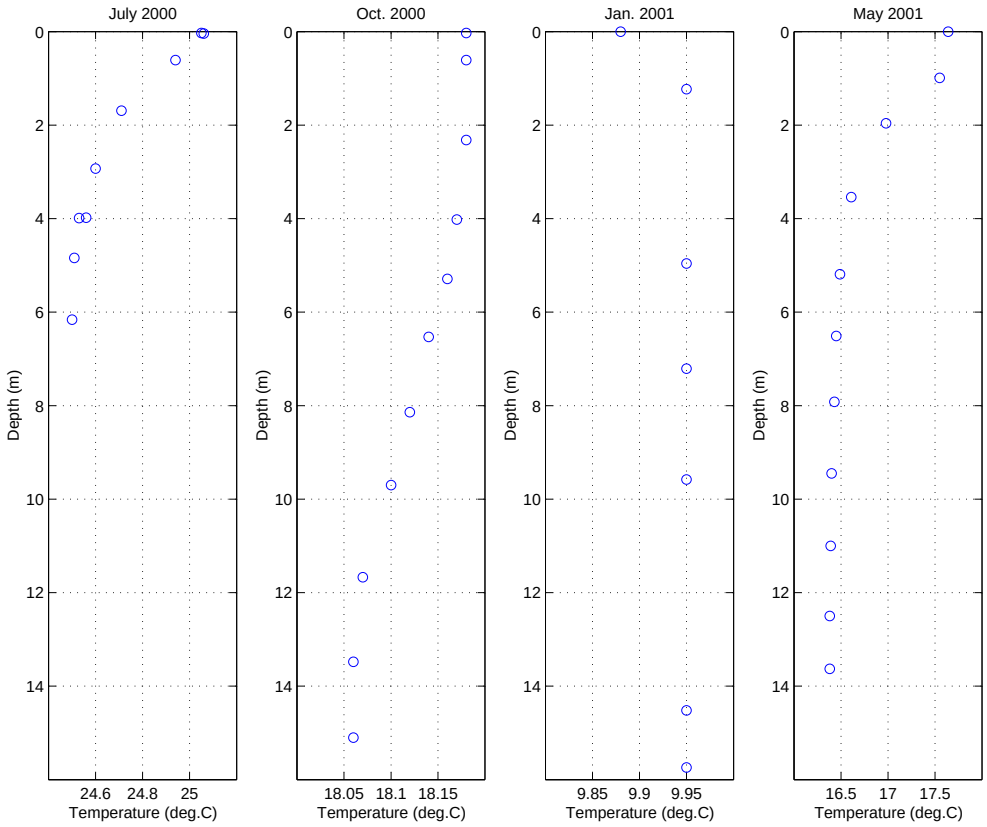

Figure 2.2: Vertical temperature profiles in the Crestuma reservoir of the Douro river, highlighting the summer thermocline. Courtesy Prof. Bordalo e Sá, CIIMAR, Porto.

the location and characteristics of the thermocline can greatly affect the performance of acoustic communication systems and sonar equipment (Urick (1983); Siderius et al. (2007)).

Seawater Temperature Models

Temperature profiles have been collected and systematically stored in databases during the last decades. Typical data sets include position information together with temperature, with a much higher resolution and accuracy in the vertical position than in the horizontal. Teague et al. (1990) lists many examples of oceanographic atlases that collect this information. Given the huge amount of data that exists about the world oceans, there have been several attempts to represent these temperature profiles by simple sets of coefficients. Furthermore, this effort has been helped by the relatively regular *shape* of the profiles, that suggests a parametric representation. It is obvious that any accurate parametric representation of such profiles would allow for a dramatic reduction in data warehousing requirements.

One of the first attempts to provide a simple model to represent the thermocline was suggested in Csanady (1971) to explain the typical shapes of spring and summer temperature profiles in Lake Ontario, Canada. In this case, both the shapes of the thermocline and the characteristic values of the parametric models are derived based on physics of the moving water caused by the warming of the surface coastal water.

The Generalized Digital Environmental Model (GDEM) consists of worldwide temperature and salinity data averaged over time, in specific spatial grids and aggregated in various time scales. GDEM temperature profiles are compressed into coefficients of base functions. These coefficients are obtained through curve fitting algorithms, and consider three different levels of detail. The top-most layer shows more variation and is represented by eight coefficients, the middle layer has seven and the bottom-most part of the profile is represented by a simple quadratic polynomial (Teague et al. (1990)).

Haeger (1995) proposes a simpler intuitive 3-layer piecewise linear gradient model, with a high gradient at the thermocline, and low gradients both above and below. Figure 2.3 shows such a representation, where the three vertical zones can be easily identified. Note that this is a coarse representation of the temperature profile (compare with the measured profile shown in fig. 2.1). However, it results in only six parameters that are able to capture the overall shape.

In Chu et al. (1997) and Chu et al. (1999), similar geometric representations of a layered structure have been used to model the Yellow Sea and the Beaufort/Chukchi Sea temperature profiles, respectively. In Chu et al. (2000), an analogous parametric model was used to infer the subsurface thermal profile from satellite sea surface temperature, based on GDEM data for the South China Sea.

A completely different approach has been described in Babovic and Zhang (2002), where the authors employed Genetic Programming to model the vertical thermal profile based on average historical data from the World Ocean Atlas, concerning the South East Asian Seas. The most accurate relationship was found to be a simple 3^{rd} order polynomial, in which the temperature

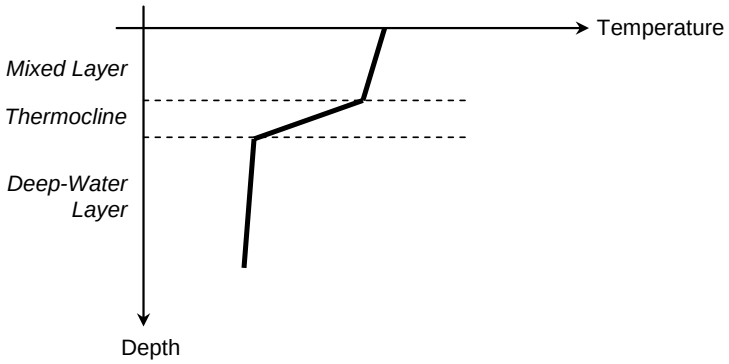

Figure 2.3: Simplified vertical profile of temperature, assuming a 3-layer gradient model as suggested in Haeger (1995).

gradient is related only to the temperature value at the corresponding layer:

$$\frac{dT}{dz} = aT^3 + bT^2 + cT + d \tag{2.1}$$

Note that in this case there is no intuition, neither any physical explanation for equation 2.1, it just emerged as the best approximation to the data set. This means that even though it may be an efficient way to condense the information about the profiles, it lacks some of the information conveyed in the parameters suggested by the geometric representations.

Sampling the Thermocline

The principal tool to obtain a temperature profile is the CTD, an instrument that measures conductivity, temperature and pressure (depth) and allows to compute other indirect parameters of the sea water, such as salinity and density. In a traditional approach, the temperature is sampled locally, with a CTD deployed from a research vessel and getting a profile of the water column in specific locations. Obviously, the water depth, size of ship, characteristics of the sensors and quantity of sampled locations would dictate the spacial and temporal resolution of the process. Alternatively, an undulating tow-yo with a CTD could be applied to increase the velocity and spatial resolution of the sampling. It is also possible to obtain temperature profiles remotely, using for example data from profilers that drift with the currents, or that are installed in ocean observatories.

Lately, AUVs have also been employed to capture the temperature profile, by defining a horizontal trajectory and performing yo-yo control in the vertical plane. The mission parameters are programmed *prior* to the mission and typically, the yo-yos are programmed from the surface to the ocean bottom, or to a reasonable depth to ensure that the thermocline is crossed in every profile. Apart from the CTD, AUVs may also transport other sensors so that thermocline data may be compared with other parameters of interest.

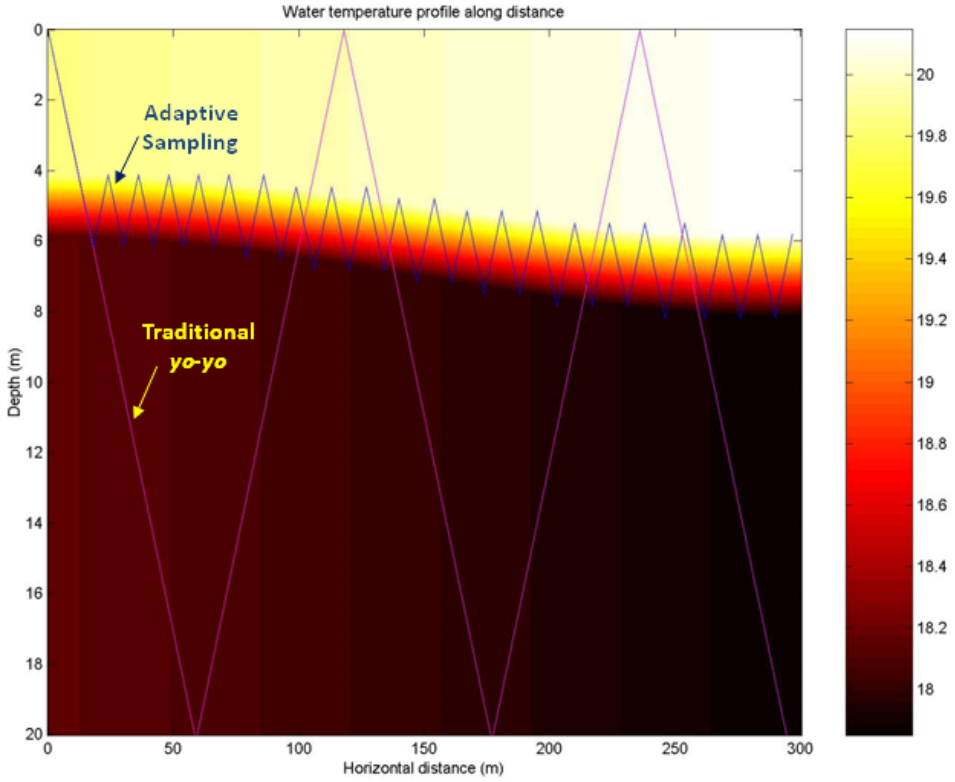

Figure 2.4: Illustration of using an adaptive sampling algorithm to sample the thermocline

If the thermocline is very thin as compared to the vertical range defined for the yo-yo, then the frequency of thermocline crossings will be relatively low. In our approach, we propose to use a simple model for the thermocline, with a reduced set of parameters that can be extracted by simple algorithms, in real time. These parameters should allow the vehicle to change the yo-yo profile dynamically, in order to track closely the thermocline, therefore obtaining much more data in its vicinity. Figure 2.4 provides an illustration of the gain that is anticipated for a case of a thermocline whose characteristics change along the trajectory. In the profile shown in figure 2.1, the implementation of this approach would allow an AUV to avoid diving to the deepest part of the profile.

2.1.2 Ocean Fronts

A front is a boundary that separates masses of water with different properties, including different velocities. A front may be *convergent* or *divergent* depending on the relative motion of the water masses. In convergent fronts, the water masses collide, therefore some of the surface water is dragged down in a down welling process. The opposite happens in divergent fronts, where the spreading causes a depression that brings deeper water towards the surface. In both cases, the boundary layer is relatively thin, sometimes merely a few meters, and naturally dynamics by changing with mixing, currents and tides. Although fronts may span the full water column, they show a large horizontal gradient of water characteristics at the surface. In fact, fronts can be easily

observed in the ocean because of this surface expression, with clear marked *lines* in the boundary, and the name was adopted due to similarities with the atmospheric counterparts.

Different water masses in both sides of a front are identified by their Temperature-Salinity signature, two conservative properties of seawater. In fact, there are no sources or sinks of heat and salt in the interior of the ocean, therefore this signature barely changes as the water mass moves through the deep ocean and only changes with mixing with other masses.

Examples of Fronts

When the wind blows consistently parallel to the coast line, the surface water is transported to the right (in the northern hemisphere) due to wind stress and the rotation of the earth. That surface water is then replaced by the rising of cold, deep water, mixing the whole water column in a process called coastal upwelling. The water that is replaced is not only warmer and lighter than deep water, it is usually depleted of nutrients. Upwelling replaces it by nutrient rich water, which leads to phytoplankton growth. This process is very common in the West Coast of Portugal during the summer months, as a result of the North-South wind. **Coastal upwelling fronts** develop when there is a rapid transition between a stratified mass of water and this mixed coastal water subject to upwelling.

Estuarine fronts, as the name implies, form in estuaries, in the interface between fresh water from a river and the ocean salt water, therefore the spatial scales are in the same order of the estuary's. Naturally, the characteristics of these fronts depend on river transport, ocean currents and tides, so they are very dynamic events, changing in only a few hours. For example, Largier (1992) analyzes tidal intrusion fronts, when dense seawater plunges beneath estuarine water, forming a salt water wedge. O'Donnell (1993) describes two other types of surface estuarine fronts, apart from this tidal intrusion front: tidal mixing fronts and shear fronts.

Garvine (1974) describe the dynamics of **small scale oceanic fronts**, typically boundaries that occur in coastal water. Marmorino et al. (2002) also address small scale oceanic fronts, in this case, when the Gulf Stream collides with shelf water near Cape Hatteras. They report features with spatial scales below 1 km and significant variations in tens of minutes.

Relevance of Fronts

An upwelling event mixes the water column, bringing nutrient rich, cold, deep water to the surface. This leads to phytoplankton growth, which in turn are eaten by larger and larger fish, therefore upwelling has a significant impact on primary production and fisheries. The observation of a front and its characteristics may indicate the presence and dynamics of upwelling. During upwelling, a significant volume of cold water is transported to the surface, affecting the balance of heat transfer with the atmosphere, and so it may also affect local weather.

A convergent front may be a place of accumulation of marine debris, both natural and pollution, when buoyant material is dragged with a colliding water mass, but is not welled down due to excessive buoyancy.

Sampling Fronts

The dynamics of small scale ocean fronts are very difficult to model due to a great number of factors governing its evolution, therefore there are no computer models to simulate the behaviors of fronts (Gottlieb et al. (2012)). One of the factors that has always facilitated the study of fronts is their surface expression, which allows for visual observation, even from remote locations. Given the changes in water velocity at a front, it is also possible to detect the presence and characteristics of fronts due to their reflections of radar signals. For example, Marmorino et al. (2002) use microwave radar from aircraft and in situ video imagery from a research ship to examine small scale horizontal structure of a frontal region, caused by the interaction of the Gulf Stream with and shelf water near Cape Hatteras.

Sampling both water masses from a research ship to measure seawater parameters is a very complex task, due to the slow mobility of the ship as compared to front dynamics. This is an ideal scenario for using autonomous vehicles, programmed to sample the whole water column in the vicinity of the front. For example, Zhang et al. (2012b) proposed an algorithm for autonomous front detection and tracking using an AUV and, in Zhang et al. (2013), report data of its successful implementation in Monterey Bay, CA, USA. For a few days, the long range Tethys AUV detected and tracked an upwelling front by moving across it multiple times. We will discuss this example and other implementations in further detail in section 2.3, when we address the state of the art in adaptive sampling.

2.1.3 Plumes

In the context of this work, we deliberately consider the term “Plume” as a generalization of what is usually separated in the literature as “Plume”, “Jet” and “Buoyant Jet”. The difference between jets and plumes lies in the driving mechanism that causes a relative motion of a fluid in another fluid. In the case of jets, the source has an initial momentum, while a plume can be defined as a source of buoyant flux only, with no initial momentum, therefore plumes are driven only by differences in density. It is also possible to have a combination of both, also called “buoyant jets”, when the initial flow is controlled by momentum but then becomes determined by buoyancy (Roberts (1979)). In all the cases, there is some variable degree of mixing between the two fluids, mainly occurring near the *boundary*, and some energy wasted due to turbulence.

A time averaged plume is smooth, time invariant and fits a Gaussian model with the peak at the source. Using a time averaged gradient, pointing towards the source, it is relatively straightforward to locate the source. However, measurements are made in the instantaneous plume, with irregular, time varying shape due to turbulence. Therefore, instantaneous plumes show high concentrations at significant distances from the source and the gradient does not point towards the source.

Various types of plumes can be seen in the atmosphere and they have been studied in order to establish emergency response and risk assessment dealing with releases of toxic materials, whether accidental or deliberate (*e.g.* a terrorist action). These studies motivated the first efforts to model the behaviors of plumes, later adapted to the water environment, and being in air allowed a simpler

collection of data to confirm the accuracy of the models. For example, Peterson and Lamb (1992) study the relationship between data from a model of an atmospheric plume and measurements of concentration.

Examples of Plumes

Disposal of treated waste water is usually achieved by discharge and dilution into streams, rivers, lakes, estuaries, or the ocean, using **sewage outfalls**. Oceans constitute preferential receiving environments for waste water, as they provide a tremendous assimilation capacity. Sea outfalls are designed to take full advantage of this capacity, but, at the same time, minimizing the effect on the receiving water.

In a typical sea outfall, the effluent is ejected horizontally as round buoyant jets from multiple ports situated in the diffuser, since a submerged horizontal discharge into a cross flowing tidal current provides a 20-50% improvement in the dilution as compared to a corresponding vertical discharge (Lee and Neville-Jones (1987))). Upon entering the receiving water, the initial jets rapidly become plumes, since sewage discharged into the ocean is very buoyant. For a typical multi-port diffuser, the plumes merge with their neighbors, forming the so-called *line plume*, and so the waste field behaves as if it were discharged from a line source Roberts (1979).

Mixing and dilution is very rapid in the region just outside the diffuser ports, since the turbulence generated by the discharge causes the plume to entrain large amounts of ambient water that dilutes the effluent. This first region is called "the near field" or "initial mixing region" and the spatial scales depend on the size of the outfall but can be in the order of hundreds of meters, clearly compatible with the range of even the smallest AUVs. If the water column is stratified, the initial mixing is done with dense ambient water, which reduces the initial plume buoyancy. As the plume rises with less buoyancy into less dense water, it may eventually come to a point in which the average plume density equals that of the surrounding medium. In this case, the plume stops rising and begins spreading laterally (Roberts (1996)).

Hydrothermal vents occur around the world over a wide range of depths, from intertidal to the abyss (Tarasov et al. (2005)). Deep water hydrothermal vents were first observed in 1977, in about 2700 meters of depth at the Galapagos Rift area in the Pacific (Ballard (1977)), and greatly increased the awareness and interest of previously known vents in shallow waters. Hydrothermal vents develop in some areas of volcanic activity, where the tectonic plates are slowly spreading apart creating fissures in the ocean floor. Cold seawater seeps down into these crevices, circulates within hot crust and heats up, rising back to the surface of the ocean floor, rich in newly dissolved minerals. Water gushes out into the almost freezing water due to temperature difference, that can reach hundreds of degrees. In contact with the cold surrounding seawater, some of the dissolved metals precipitate, forming the distinctive smokestacks. Vents are usually clustered in *fields*, with individual vent cavities ranging from a few centimeters to a few meters. Since the first observations, thousands of other vents have been discovered all around the world, usually in deep waters,

and many visits of manned and remotely operated vehicles have witnessed these processes (Chase et al. (1983); Sleep and Morton (1983)).

Apart from the geological phenomena involved, the first observations of deep water hydrothermal vents also showed that they supported a completely new ecosystem, with dense communities of organisms whose nutritional requirements and overall metabolism were perfectly adapted to such extreme environments, where no sunlight penetrates to support photosynthesis (Ballard (1977); Gugliandolo et al. (1999)).

Pollution plumes form another type of process that can occur in the marine environment, with a wide range of possible scales. Pollution plumes are usually the result of an accident, such as a continuous flow of contaminant (for example, a leak in a factory or a ship), or a single release of a pollutant. In reality, most pollution plumes are in fact jets, or buoyant jets, for example if they result from a leak in a pumped oilfield.

Harmful Algae Blooms (HAB) develop when there is a proliferation of some harmful algae in a given region, either at sea or in fresh water. There is still some debate in the scientific community to decide when a algal bloom really becomes *harmful* (Smayda (1997)), a discussion that is clearly beyond the scope of this work. Freshwater blooms are generally accepted as being promoted by an excessive runoff of nutrients, for example from fertilizers (Babin et al. (2008)). Sea water HABs usually occur in coastal waters and sometimes are referred to as "red tides", but there is few consensus about the exact causes. What is consensual is that the causes for HABs are biological rather than physical, or probably both, which means that the dynamics are not governed (only) by physical dilution and dispersion, as with the other plumes. However, we chose to aggregate them together with the other plumes because the *features* than can be perceived are similar and, therefore, may be sampled in a similar way.

Under favorable environmental conditions, these blooms can occur and subside over relatively short time scales, from a few days to a few weeks (Wong et al. (2007)). In terms of spatial spreading, HABs can span anywhere from tens of meters in small lakes or enclosed water to tens of kilometers (Ho and Michalak (2015)).

Relevance of Plumes

There is a variety of reasons to study the different types of ocean plumes, from the purely economic potential, to the impact in coastal management, public health, and science. With a significant percentage of the world population living close to some body of fresh or salt water, it is no surprise that the environmental impact of sewage outfalls has been a major topic of research during the last decades, in the field of wastewater engineering (Metcaff & Eddy, Inc. (1991) provides a comprehensive analysis of all aspects). In fact, in order to avoid adverse environmental impacts, the quality of the treated and dispersed effluent must comply with minimum water quality standards. Naturally, these standards have been improving with the increasing awareness towards environmental issues. The compliance with stricter requirements has been made possible with the new results in treatment technology, together with a better understanding of the dynamic interaction

between the treated effluent and the receiving aquatic environment. Mathematical modeling plays an important role in the analysis of the behavior of the plume emanating from a sewage outfall. Using accurate models that represent the dynamics of the mixing process, it is possible to predict the effects of the discharged effluents in the receiving environment and thus estimate the impacts of such discharges in the surrounding areas. In order to evaluate the accuracy of these models, a large quantity of data is required, not only to capture the space and time dynamics of the plumes, but also to correlate that dynamics with different conditions of the receiving water.

Similarly to the case of sea outfalls, studying the behavior of other pollution plumes is of utmost importance, due to potential impact on the ecosystem and on public health. Recent cases of major environmental accidents at sea (*e.g.* Deepwater Horizon oil platform and Fukushima nuclear plant), have raised public awareness towards the necessity to minimize the risks to the environment, in particular if it affects coastal areas. Part of this effort is required to increase our knowledge about the dynamics of plumes at sea.

HAB episodes are also a major concern for the ecosystem, and even though their effects are typically of short duration, they can cause a great impact in local economy, for example when they affect aquaculture structures. However, a thorough understanding of all the conditions that lead to a HAB episode may provide a great help on prevention or, at least, anticipate its outbreak.

There are many different algae that can cause HABs: some produce toxins that contaminate the ecosystems, potentially causing health problems in humans, while others can reach dense concentrations, causing damage to to marine life due to anoxia. They can also affect tourism and recreation activities, by discoloring the water and producing unpleasant, or even dangerous slimes and odors.

The amount of available data is large and growing, but there is still much research to be done to fully understand all the processes controlling the global increase in HABs, both at sea and in freshwater. This understanding is paramount to allow some conclusions on timing, spatial extent and intensity of a HAB, therefore contributing to a potential prediction of HAB episodes and dynamics, and corresponding anticipation of mitigation measures. Ho and Michalak (2015) provide an in depth analysis of the existing challenges in sampling HABs, particularly in fresh water, and highlights the need to integrate heterogeneous types of observations in future monitoring programs, and to guide modeling efforts.

Hydrothermal vents are a recently discovered phenomena and there are still many open questions that puzzle the scientific community, particularly in what concerns deep water. Earlier observations surprised biologists with the variety of organisms that evolved and thrive around hydrothermal vents, from tiny bacteria that directly feed off the chemicals spewing out from the vents, to giant tube worms, clams, and other ghostly creatures. A lot of observation is still necessary to expand our understanding of this hydrothermal ecosystem, as pointed out in the analysis of Gugliandolo et al. (1999) and Ramirez-Llodra et al. (2010).

Apart from the purely scientific interest, there is also some economic potential in areas around

present and past hydrothermal vents. Not only the commercial exploitation of geothermal resources has been proposed for current vents (Sleep and Morton (1983)), but also the abundance and variety of minerals can be better identified to assess the profitability of extraction, particularly from inactive sites.

Plume Models

The interaction of buoyant jets with the surrounding water is a classic problem in fluid dynamics and has been thoroughly described in the literature (Hirst (1972); Wright (1977). The improvement of computational performance at affordable price allowed the expansion of Computational Fluid Dynamics (CFD), *i.e.*, the utilization of numerical methods to solve complex problems with fluid flows. CORMIX is an example of a specific computer based modeling and expert system to simulate turbulent buoyant jets in fluids, created in the early 90's at the University of Cornell (Doneker and Jirka (1991)). It allows the user to provide input data that affect both the near-field (momentum and buoyancy flux at the difusers, and outfall geometry), and also the far-field, where spreading is mostly governed by the characteristics of the receiving water. The result is a graphical model of the plume, together with various quantitative information. In situations where the pollutant characteristics are known, the study of pollution plumes may be simulated with a similar model, but in this case, the impact in the ecosystem may require the analysis of other parameters. For example, AQUATOX is a user-friendly computer simulation tool to predict the fate of pollutants in an ecosystem, providing time-varying concentrations that can be exported for further analysis (U.S.E.P.A. (2000)).

When looking at an image from a hydrothermal vent, the resemblance with a sewage outfall is evident, which suggests that a similar approach can be applied to simulate these plumes, or even use the same software tools. However, there are many fundamental differences in both processes that impair such adaptation, not only in terms of the fluid, but also in terms of the physical structure. Sewage outfall simulations assume that the number and geometry of the diffusers is known, as well as the density and initial velocity of the treated waste water. As opposed to this, water from hydrothermal vents has an assortment of dissolved minerals that affects density, has an unknown temperature and velocity, and it is flowing from irregular shaped orifices, sometimes in awkward orientations. All this makes hydrothermal plumes much more complex to model than sewage outfalls or pollution plumes, but there has been some recent efforts to advance in this topic, as the example described in Han et al. (2012). Yet, these models will remain very hard to calibrate, since there is very few in situ historical data. Moreover, typical hydrothermal vents occur in deep water, an environment of difficult access and where navigation challenges may also augment uncertainty of position measurements.

In the case of HAB episodes, both the triggering mechanisms and other factors governing its evolution are biological rather than physical, therefore the models have to be completely different. Even though the problem is much more complex than simulating other plumes, there are already some tools for HAB modeling and prediction, such as the works described in Wong et al. (2007) and Sivapragasam et al. (2010).

Sampling Plumes

Plumes may be sampled using local or remote sensing methods. The traditional way to monitor the behavior of a sewage outfall is to take measurements in reference locations around the diffusers and check whether some parameter falls outside the safety range. There are some in situ sensors that may be used as indicators, such as turbidity for example, but usually water is also collected for laboratory analysis of bacteria. In critical locations, a set of distributed sensors may be installed permanently to allow instantaneous evaluation of plume spreading and also to capture long time series for statistical analysis (Petrenko (1997)). There has been some trials with AUVs sampling the region around the diffusers, such as the work described in Ramos et al. (2001), which showed the signature of the low density treated waste water in CTD measurements. Remote sensing may also be used to monitor plumes, particularly when they have a strong surface signature. Typical examples include the use of satellite imagery to track oil spills or HAB episodes.

Sampling the water around hydrothermal vents is a very difficult task, not only when they occur in deep water with difficult access, but also because water temperature can reach hundreds of degrees centigrade (Sleep and Morton (1983)) and there are many dissolved minerals that can damage equipment. Sampling shallow water hydrothermal vents is somewhat easier, since it may be possible to dive to the vicinity to make measurement. For example, Gugliandolo et al. (1999) report the collection of thermal water samples in shallow water vents for analysis of bacteria. Almost all studies of deep water hydrothermal vents rely on visual observation, either directly in manned submersibles like Alvin (Ballard (1977)) or MIR (Sagalevich (2012)), or indirectly using towed cameras or ROVs. After the discovery of the first hydrothermal vents, many efforts have been put to allow the use of assorted sensors in robotic systems. For example, Miller (1989) reports the development of special equipment to take measurements in high temperature hydrothermal vents, while Vuillemin et al. (2009) describe the development and utilization of an in situ chemical analizer, and Komaki et al. (2015) use an Acoustic Doppler Current Profiler (ADCP) and newly developed chemical sensors on underwater vehicles to detect hydrothermal plumes. A totally different approach to sample hydrothermal vents was described in Lupton et al. (1998). In this case, a neutrally buoyant drifter was entrained in a hydrothermal event plume in the Juan the Fuca Ridge for 60 days, while collecting data with a series of on board sensors.

There is a lot of expectation in the use of adaptive sampling techniques to sample diverse types of plumes using autonomous vehicles. In fact, some of the methods tested in thermocline tracking or front tracking can easily be adapted to follow plume boundaries. Mechanisms to take water samples in specific locations of the plume could also be adapted, for example from the work described in Zhang et al. (2009). In general, a robotic marine vehicle may be used to detect and follow the plume boundary and capture relevant information in the vicinity, so that the plume parameters can be correlated with surrounding conditions (*e.g* currents and stratification). An ASV can sample a pollution plume at the surface, after cuing from analysis of satellite imagery or other remote sensing data, and also correlate data with atmospheric conditions. In the case of three dimensional plumes, AUVs may be employed, isolated or in fleets. For example, sewage leaving

the underwater diffusers in a sea outfall tend to rise and disperse, forming a characteristic conical shape profile, with concentration gradients across the boundary decreasing towards the surface. The vehicle(s) can be programmed to follow the boundary at fixed depth intervals, for example as suggested in Petillo et al. (2012).

Another possible use of adaptive sampling algorithms is to find the source of a plume. Farrell et al. (2003), for example, report the use of a Remus AUV with a turbidity meter to find the source of a pollution plume, simulated by Rhodamine dye released at sea. In this case, the algorithm does not assess the impact of the plume in the environment, since the vehicle does not evaluate the spreading of the plume, therefore it could hardly be used in HAB monitoring, for example. However, it is a promising way for finding new hydrothermal vents, or to discover the source of an oil pollution plume. A similar problem was addressed in Pang (2010), investigating the use of AUVs to locate the source of hydrothermal vents, based on guidance by chemical signature.

2.2 Robotic Platforms for Ocean Sampling

Autonomous marine vehicles are robotic systems with the ability to control their trajectory in the marine environment without human intervention, while collecting sensor data. The use of robotic systems at sea has been increasing exponentially in the last years, with impressive performances in almost all scenarios of marine operations, including research, commercial, and military applications. In this section we provide an analysis of the state of the art in marine robotics, particularly in what concerns small, low logistics vehicles, and the application scenarios that are being addressed. With so many different designs and specifications, it is not easy to define a comparison metrics to chose the higher ranking systems. Instead, we will chose an illustrative set of vehicles that represent some of the benchmarking in performance or accomplishments. These platforms are first separated into surface and underwater vehicles, two classes of autonomous systems that were first developed separately, but soon were sharing components, such as power sources, navigation systems, on board computers and mission software. Later, we address the emergent designs of hybrid vehicles, *i.e.* vehicles that can have more than one traditional mode of operation. We end the section with a special attention paid to modular vehicles, a particular class of design that promises high versatility and adaptability, such as will be explored in this work.

2.2.1 Autonomous Surface Vehicles

Robotic marine vehicles that work at the surface are commonly referred to as Autonomous Surface Vehicles (ASVs), Autonomous Surface Craft (ASC), Unmanned Surface Vessels/Vehicles (USVs), or Unmanned Marine Vehicles (UMVs). They can transport a large variety of sensors and elevated antennas to facilitate radio based communications, therefore they can have real time, long range, high-bandwidth communications, resulting in advanced systems for tele-presence in the marine environment.

The earliest known examples of ASVs were developed in the nineties, starting with the early development of **ARTEMIS** and **ACES** at the MIT Sea Grant College Program (Manley (1997)).

These vehicles were mainly platforms for testing navigation and control algorithms, and to perform autonomous bathymetry in very calm waters. Given the general logistic constraints, most of these platforms were relatively small, weighting a few tens of kilos. There was also a trend to use SWATH (for *Small Waterplane Area Twin Hull*) designs to facilitate installation of new subsystems. By the end of the nineties, a few other designs were being demonstrated, starting to address new challenges in cooperation between ASVs, like the work described in Curcio et al. (2005) with a fleet of 4 **SCOUT** ASVs. Later, other vehicles have been employed for cooperation between AUVs and ASVs, such as the case of the European ASIMOV project (Pascoal et al. (2000)) or the work at MIT for cooperative navigation (Fallon et al. (2009)). Many more designs proliferated with the new millennium, with application scenarios in science, bathymetric mapping, and defense. An interesting historical perspective of the early days of this technology can be found both in Caccia (2006) and in Manley (2008). More recently, Dunbabin and Marques (2012) provide a very detailed description of the technology available for monitoring the environment, including ASVs.

After this initial surge of designs and deployments, most of the challenges to develop "robotic boats" have been overcome, with the availability of reasonable embedded computers, affordable navigation systems and rechargeable batteries that could provide power for a few hours of operation. The literature also displayed multiple solutions for the typical problems of navigation, guidance and control. Therefore, the number of new vehicle designs in the literature slowed, and, at the same time, a few companies have emerged with commercial off-the-shelf (COTS) solutions for a number of typical applications, mainly for hydrographic surveys. As far as research was concerned, the trend shifted towards vehicle cooperation and autonomy, with the objective to design very long endurance vehicles, optimizing propulsion systems and harvesting energy from the environment. The following description attempts to provide an overview of the latest achievements in ASV design and operation, both on research and commercial levels.

Research ASVs

In terms of new vehicle designs, the **Sea-RAI** was the first example of a marine marsupial robot team with an ASV that hosts an unmanned aerial vehicle (UAV). The system was developed by the University of South Florida for the inspection of littoral environments. The ASV has a typical SWATH configuration, with two catamaran pontoons supporting a frame with mounting rails for the watertight enclosures. The vehicle is very compact, only 1.8m long, but the weight of the complete system is 170kg, although it can be disassembled for transportation. The vehicle is fully electric, with propulsion provided by two differential trolling motors, reaching a top velocity of 7.7 knots. The UAV takes off from a miniature elevated helipad and communicates with the ASV using a wireless network (Lindemuth et al. (2011)). Recently, UNINOVA, in Portugal, used a similar approach to develop **Riverwatch**, an autonomous system for environmental monitoring in rivers and calm waters. The ASV is longer, a 4.5m long catamaran, and it is particularly suited for detailed inspection of the environment, both above the waterline, with a laser scanner and a multi camera system, and underwater, with a multibeam echosounder. The longer size of

Riverwatch allows for a large ($1.3m^2$) platform for piggybacking the 6-rotor UAV that provides a complementary aerial perception of the environment (Pinto et al. (2014)).

The University of South California has been developing a consistent work in the use of robotic platforms in networks, and ASVs have been taking a special role. Sukhatme et al. (2007) describe a system with ten sensor nodes and one ASV to track space and time patterns of temperature and Chlorophyll in a lake. In this case, the ASV was a modified version of a small RC airboat, with a thermistor, a fluorometer and a six-vial sample collection cartridge. Smith et al. (2010) details an integrated system for the study of the ecosystem of the South California Bight in multiple scales. It was deployed in 2009 and the platforms included static buoys, one AUV and one ASV, a modified version of a commercial Q-Boat from Oceanscience (see below). One of the goals of the system is to detect and understand the dynamics of HAB episodes.

Another example of an ASV working in a sensor network is being developed at the University of Minnesota. Bhadauria et al. (2010) describes a small ASV equipped with an antenna to detect, localize and track a fish with a radio-frequency identification tag. The authors expect to expand the system to use a network of similar ASVs for cooperative localization.

A further example of robotic coordination was recently presented in Paulos et al. (2015), for the case of multiple miniature ASVs with the capability to self organize to assemble large structures.

One of the technologies that has evolved over the last years in **wind propulsion**. Harvesting the propulsion energy from the environment is a way to overcome the limitations in energy storage and transportation. Autonomous Sailboats are a particular class of ASVs that rely on wind to provide propulsion and only need electrical energy for the on-board electronics and rudder/sail adjustments. They are a proven technology for ocean monitoring, sampling and surveillance and they have gained particular attention for their unique ability to maintain long term unassisted operations at the sea surface. In particular, the silent nature of sailboat operation yields a great potential in marine surveillance and detecting and tracking marine mammals across vast areas of the ocean. Stelzer and Jafarmadar (2012) and Klinck et al. (2015) describe the **Roboat** ASV and its use for recording whales in the Baltic Sea. A similar operation was performed with the Portuguese **FASt** ASV, off the coast of Sesimbra, in Portugal (Silva et al. (2013)).

Commercial ASVs

ASV Ltd.[1] is a British company that sells the electric vehicle **C-Cat 2**. C-Cat 2 is a 2.4 meter long SWATH, weighting around 100kg. It can navigate up to 6 hours or 20 nautical miles, with velocities up to 5 knots. The vehicle can be teleoperated or programmed to follow a sequence of waypoints, and carry various types of sonars or an ADCP. The company has a few other designs, including **C-Stat**, a vehicle with hovering capability for up to 4 days, and a diesel electric hybrid power system to provide large power to payload, and **C-Enduro**, a 4.2 meters ASV with a combined solar/wind/diesel energy management system for long term deployments, up to 3 months.

[1] http://www.asvglobal.com/

Liquid Robotics, Inc.[2] manufactures the **Wave Glider**, a platforms that harvests energy from the environment and has the potential for very long term deployments. The Wave Glider uses a set of underwater wings coupled to the surface hull and transforms the vertical wave-induced motion into forward thrust, following a concept first described in Hine and McGillivary (2007). Although this system is still relatively recent, it has already an impressive record of thousands of miles at sea, collecting data in very harsh conditions, with some missions lasting longer than one year. The main drawback of this platform is the reduced velocity, with an average of 1.5 knots.

The MOST (Autonomous Vessels) Ltd. **AutoNaut**[3] is another example of a wave propelled ASV, but using the "wave foil technology", a combination of hull design and additional foils to produce thrust from the wave motion. The vehicle harvests solar energy to power the on board electronics, and carries a methanol fuel cell for additional power if required. It is a scalable mono-hull, with two standard configurations, with 3.5 meters (120kg of weight) or 5 meters (230kg). The endurance of the vehicle is 3 months and the missions are preprogrammed and may be altered using a satellite link. The top velocities are 3 and 4 knots, respectively. Payload capability is 185 liters/40kg for the 3.5m version and 500 liters/130kg for the 5m version.

Teledyne Oceanscience[4] develops the **Z-Boat 1800**, a mono hull electric ASV with 1.8m of length and 30kg of weight. It can navigate up to 2.5 hours, with a maximum velocity of 4 knots. The vehicle is intended for hydrographic surveys, with a payload capability of 20kg, and it can be remotely controlled or programmed to follow waypoints. The company has also the **Q-Boat 1800**, a very similar mechanical design, but intended to transport ADCPs or water quality sensors.

The **Saildrone**, from Saildrone Inc.[5] is an example of a fully autonomous commercial vehicle powered by wind and solar energy. Saildrone has a very high carbon-fiber wing sail, around 6 meters high, and travels at speeds up to 16 knots. The vehicle has a large payload capacity, of over 100kg, and has already been tested with sensors for atmospheric parameters, sea surface temperature, salinity, dissolved oxygen, and fluorescence.

2.2.2 Autonomous Underwater Vehicles

Autonomous Underwater Vehicles are remarkable machines that revolutionized ocean sampling. They can be programmed to navigate through the ocean's interior and make measurements along the way, synchronizing data from multiple ocean sensors and even collecting physical samples. Each measurement is a sample of a three-dimensional field, therefore a dense sampling is require to resolve space and time ambiguity. Either alone or coordinately, they have gone through a tremendous evolution to capture more details about the underwater environment.

In the late eighties and early nineties, the first prototypes required a tremendous effort and ingenious engineering solutions to compensate for the technological limitations in terms of computational power, battery endurance and navigation systems. Although the challenges were immense,

[2] http://www.liquidr.com/
[3] http://www.autonautusv.com/
[4] http://www.oceanscience.com/
[5] http://www.saildrone.com/

these early developments anticipated a bright future and new applications were being envisaged, such as described in Bjerrum (1993). Soon, many of the technological challenges were surpassed and reasonable computational systems, electronic devices and navigation sensors were available at moderate prices. This allowed for the development of AUV subsystems and even complete solutions in the benches of small universities and research groups, and not only in a restrict number of highly specialized research labs, either military or funded by defense. At the same time, battery technology also improved with the demand from consumer electronics and the increase in the efficiency of power control and propulsion systems allowed for longer (therefore more useful) missions. Yuh (2000) provides a very extensive survey on design and control of AUVs during the nineties, when about 30 new AUVs were reported to have been built. These new capabilities also stimulated new potential users and the scenarios of application generalized to include science, civil, and military domains (Bellingham (1997); Wernli (1999); Fletcher (2000); Mindell and Bingham (2001); Doolittle (2003)).

The demonstration of robotic systems in the field is an indisputable proof of concept, but testing at sea is particularly difficult and the logistics requirements augment with the size of the equipment. Therefore, it was no surprise that this widespread development of solutions was also directed towards reduction in logistical requirements. The scope of our work also includes the development of *small* robotic solutions, therefore our survey will be more focused on man portable systems, requiring low logistics. However, we will not bound the extent of the analysis to any particular limiting size or weight. Instead, we will select a few examples of successful designs, although this may also be a subjective issue.

Research Vehicles

Underwater Robotics is a peculiar field of knowledge, bringing together complementary competences in mechanical and electrical engineering, and also in computer science. The initial development of the technology required a significant amount of funding and the commitment of a large, competent, well organized team. Therefore it was no surprise that the most important milestones were done in the most prestigious research laboratories in the world, mostly funded by military agencies. Today, the sources of funding are diverse, including many private companies that already believe in the technology, but there is still the need of a large interdisciplinary team to devise new solutions for complex problems. Thus, most of innovative applications are still being demonstrated by research vehicles.

The **Odyssey** series of AUVs started to be developed in the late eighties, at the Sea Grant AUV Laboratory of the Massachusetts Institute of Technology (MIT), in the USA (Bellingham et al. (1994)). An early demonstration of capabilities and also a remarkable achievement was the navigation under the Arctic, described in Deffenbaugh et al. (1993). Another challenging scenario where the vehicle was successfully demonstrated was the study of ocean frontal dynamics at the Haro Strait, between USA and Canada (Bellingham et al. (1996)). At a later stage, the upgraded version Odyssey IIb (Fig. 2.5) also served to demonstrate the development of multiple

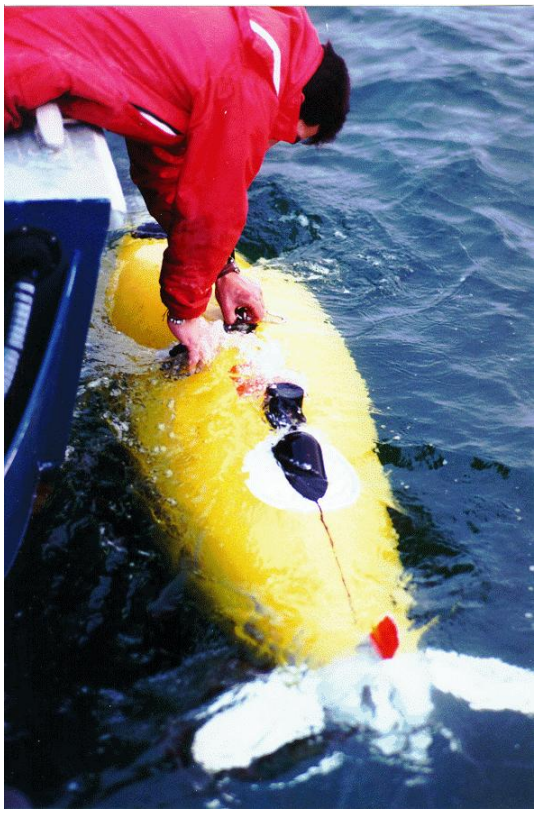

Figure 2.5: Deployment of the OdysseyIIb AUV, Cape Cod bay, November 1996

AUV subsystems, such as navigation techniques (Vaganay et al. (1996)) or underwater docking at sea for battery charging and data transmission (Feezor et al. (2001)). In our understanding, the main reason for the success of the Odyssey vehicles was the range of risky scenarios where it was systematically deployed. Rather than merely replacing old technology, these vehicles were employed in pioneer missions where no other technology had been, and could be, employed.

Part of the technology involved in the development of the Odyssey AUVs has been transferred to the vehicles of Bluefin Robotics Corp. The company was founded in 1997 by a core group of engineers from the MIT AUV Laboratory (Wernli (2000)), although the potential for commercialization of Odyssey had already been proposed a few years before in Altshuler et al. (1995).

Geographically close to the MIT AUV Lab, two other research vehicles were developed in the nineties in two different laboratories of the Woods Hole Oceanographic Institution (WHOI). The **ABE** (for *Autonomous Benthic Explorer*) AUV was specifically designed for the exploration of the benthic habitats, in particular surveying hydrothermal vent areas (Yoerger et al. (1991)). In fact, the vehicle has been particularly dedicated to the study of hydrothermal vent fields around the globe, including for example Chile (German et al. (2010)) and the Kermadec Arc, close to New Zealand (de Ronde et al. (2014)). An interesting account of the milestones of ABE development and operation for the period 1995–2008 can be seen in Yoerger et al. (2009). Unfortunately, the ABE AUV was lost on March 5, 2010, on a research expedition off the coast of Chile, after a remarkable record of 222 dives (Lippsett (2010)). This number alone serves to demonstrate the

enormous success of the design, but it is even more impressive when a great fraction of these dives were performed in deep water, capturing extremely important information about geology and biology of the ecosystems around hydrothermal vents.

A follow-up design of ABE, the **Sentry** AUV was also designed at WHOI, with improved characteristics but also intended for deep water operations. For example, this new vehicle has the ability to hover in the water column, in order to conduct close range surveys. The vehicle has been used all around the world, since the first trials in 2006 (Yoerger et al. (2006)), mainly for deep water operations, from pollution monitoring at the time of the Deepwater Horizon oil spill (Kinsey et al. (2011)), to surveys of hydrothermal vents (de Ronde et al. (2014)).

The **REMUS** (or *Remotely Environmental Monituring Units*) AUV was also developed at WHOI under funding from the Office of Naval Research, and it was the first truly man-portable AUV, weighting less than 40kg (von Alt et al. (1994)). The vehicle was intended only to coastal waters, up to a maximum depth of 100 meters, which allowed a great reduction in size. The vehicle has been extensively used in a wide range of scenarios, including mine hunting in military context (Stokey et al. (2001b)), or pollution monitoring (Ramos et al. (2001)).

One of the new trends in AUV development has been to extend the duration of the missions. For example, the **Tethys** AUV, developed at the Monterey Bay Aquarium Research Institute (MBARI), is a 105 kg propeller-driven vehicle with an impressive range of thousands of kilometers, during months of operation. Hobson et al. (2012) reports a three week deployment covering 1800 km at a speed of 1 m/s, with a suite of payload sensors averaging 5 watt of power consumption.

Another innovation that will surely take a relevant role in the future is the concept of Intervention Autonomous Underwater Vehicles, or IAUVs (Ridao et al. (2014)). The main idea is to integrate some small manipulators in AUVs, so that the vehicles can perform simple intervention tasks without the need of an operator. One of the flagship designs in this respect is the **Girona 500** AUV, developed by the University of Girona, in Spain (Ribas et al. (2011)).

Commercial Vehicles

Following some years of success with the development and deployment of the first AUV prototypes, a few companies have emerged as *spin-offs* from academic laboratories, dedicated to the development and operation of AUVs, which was a sign of the maturity of such devices and of the vision of a great potential ahead. Wernli (2000) provided a perspective of AUV commercialization at the change of the millennium, trying to anticipate the best contenders to succeed in a global market with great potential.

Two of the most successful designs in commercial AUVs were initially developed and used in research institutions during the nineties: the **Odyssey** AUV and the **REMUS** AUV. Probably the main reason for their success and longevity, on top of the engineering aspect, was the multiple number of missions they have performed, in challenging environments, and the corresponding

publication of results in the literature. At the time, these operations required a great dedication by the engineering team that designed them, to support the utilization of such delicate and cumbersome pieces of technology, but also to analyze the performance in the field and receive suggestions for improvements. These operations, and mostly the data they produced, proved that AUVs were no longer science fiction concepts, but were real tools that could be used almost like any other ocean sampling equipment.

In 1997, Bluefin Robotics Corp.[6] was founded by a core group of engineers from the MIT AUV Laboratory, who brought the know-how of the Odyssey vehicles to build a new series of AUVs. Bluefin Robotics Corp. has now a full range of autonomous vehicles, from the smallest Bluefin-9 (1.75m, 60kg) to the largest Bluefin-21 (4.93m, 750kg), with a wide range of sensor possibilities.

The REMUS AUV that was initially developed at WHOI, was licensed to Hydroid, Inc. in 2001, and this company that was later acquired by Kongsberg[7]. There are already hundreds of **REMUS 100** vehicles in operation all around the world, owned by civil and military institutions alike.

A few years before the incorporation of Hydroid, the University of Porto acquired a REMUS vehicle from WHOI, under a special agreement for the development of an underwater research program in Porto. The vehicle was delivered in 1997 and, in the following years, it served as an excellent testbed for the demonstration of subsystems and principles of operation. The first operational missions took place in 1998, in the estuary of the river Minho, in the northern border between Portugal and Spain (figure 2.6). During autonomous missions, typically longer than one hour, the vehicle continuously collected CTD and bathymetric data, while navigating on a LBL network of COTS acoustic transponders (Cruz et al. (1999)).

The vehicle also served to demonstrate the effectiveness and accuracy of LBL navigation systems based on acoustics, such as described in Cruz et al. (2001), both at sea and also in challenging scenarios for acoustics, such as rivers (2.7) and estuaries.

The **Iver2** is one example that did not go through the research institutions path and was directly designed by Oceanserver Inc.[8] in 2005. At the time, the company made a great effort to reduce manufacturing costs, in order to transfer those savings to the customer, and was estimating a shallow water vehicle with a market price of 20k$USD (Anderson and Crowell (2005)). However, one year later, the company was finishing the field testing and announced a revised final price target to be 50k$USD (Crowell (2006)). Even though it was far higher than initial estimated, it still is one of the most affordable commercial AUVs. Apart from the cost of acquisition, another reason for the success of Iver2 is the little requirements in terms of logistics, since the basic version weights only around 20kg. Recently, the company launched **Iver3**, an improved version with larger battery capacity and revised electronics, allowing for 8 hours of operation at a nominal velocity of 2.5 knots (Crowell (2013)).

[6] http://www.bluefinrobotics.com/
[7] http://www.km.kongsberg.com/hydroid
[8] http://www.ocean-server.com/

Figure 2.6: Preparing for launching a REMUS AUV in the Minho estuary, Portugal, summer of 1998.

Figure 2.7: REMUS AUV being launched in the Douro river, May 2000

2.2.3 Hybrid Marine Vehicles

Robotic marine vehicles have been traditionally classified as ROVs, ASVs and AUVs. Some of these have been further divided, for example according to size, degrees of freedom, or type of energy used. However, is some situations, the divisions become blurred, and one of the latest trends in marine robotics has been to take advantage of more than one technology to develop a *hybrid* vehicle. This can be a design decision right from the start of the project, or it can result from an upgrade of an existing product or prototype, to overcome some limitation of the initial concept or to widen the range of application scenarios.

Two examples of vehicles that upgraded from existing versions are the **Wave Glider** and the **Slocum** glider. Both vehicles have original versions that are notably slow and therefore they may have trouble to overcome currents or they may simply be too slow to capture adequate details of dynamic processes. In the case of the Wave Glider, Liquid Robotics has recently released model SV3, a vehicle similar to the standard (SV2), but with an additional propeller to fight currents or simply to speed up the mission. Since the surface part of the vehicle has a solar panel, the excess power available may be used for propulsion with no loss of endurance. In the case of the Slocum glider, the decision was also to add a small thruster with a propeller, although its operation will degrade endurance because the energy available on board is limited. However, this opens up the possibility of operating a glider that can reach a site of interest in its typical mode and then perform a seafloor survey, as any standard AUV.

The **E-Folaga** hybrid vehicle, from Graaltech[9], in Italy, also works as a standard propelled AUV or as a glider, having a complementary propulsion system using a buoyancy engine and a thruster. However, unlike the Slocum glider, the decision of this hybrid propulsion system has been taken in the design phase (Caffaz et al. (2010)).

The **Seaeye Sabertooth** was designed by Saab Seaeye[10] as a hybrid ROV/AUV. The vehicle can hover in the water column, has deep water capability, long excursion range and a six degrees of freedom control system. There are two possible versions, a single hull and a double hull version.

Another new concept that has recently been proposed with dual purpose is the **Submaran**, from Ocean Aero, Inc.[11]. The company promises a vehicle that can work both as an AUV, and as a wind/solar propelled ASV, but it is still in an early phase of prototyping and there are still no published data about field testing.

2.2.4 Modular Marine Robotics

The adoption of modular architectures has been exploited in mature manufacturing processes for a long time, with the realization that such approach yields great benefits in terms of adaptation

[9] http://www.graaltech.it/
[10] http://www.seaeye.com/
[11] http://www.oceanaero.us/

to new demands from customers and also in terms of product variety, *i.e.*, the diversity of solutions that can be manufactured from the same basic components (Ulrich (1995)). To maximize the potential benefits of the modular architecture, such product variety has to be methodically considered during the design phase, by a proper analysis of module characteristics and how they affect overall system performance (Martin and Ishii (2002)). One of the key aspects of a modular design is the specification of the interface between modules. These have to be simple enough to be incorporated in all modules, but also generic enough to allow for product evolution, while ensuring backward compatibility, if possible. Naturally, all this extra burden during the design phase can affect significantly the development cost and, most importantly, can have a strong impact in the time to market.

Another direct consequence of the development of modular physical devices is the waste of space associated with the interfaces, as compared to a unique custom solution that can have optimized dimensions. Logically, this impact is less important in larger systems, or, in general, in the cases where versatility and ability to evolve is more significant than miniaturization.

In the marine environment, an early example of modularity was employed for the design of the Makakai manned submersible, as described in Murphy (1971). One of the design goals of the 2-person vehicle was precisely to be modular so that different subsystems could be tested without major impact in the rest of the system.

The development of specific payload modules has also been a priority for military purposes to allow the installation in different vehicles. For example, Schnoor (2003) reports the development of vehicle packages to be installed either in ASVs or in AUVs, for mine countermeasures. For this to be possible, both systems need to accept a specific type of *modules*.

As far as full vehicles are concerned, there are many examples of research ASVs that have a relatively modular architecture, in the sense that it is relatively easy to install, or swap, specific modules, something that is common in research laboratories. For example Caccia et al. (2011) describe the installation of a payload module for marine security applications in the Charlie ASV, taking advantage of the modular architecture of the system. The scenario is very different when it comes to commercial ASVs, which are typically closed systems, for which the integration of additional payload has to be done at the factory. One notable exception is the case of the **WAM-V** series of ASVs, from Marine Advanced Research, Inc.[12], which are good examples of commercial modular vehicles. The company has many options of standardized units that can be easily assembled, disassembled or individually replaced. The company offers a choice of different hulls to assemble the vehicle, starting with a 12 feet long (3.6m) version, and there are also modular engine pods for alternative propulsion systems. The company has developed the concept of "Wave Adaptive Modular Vessel", in which the center platform remains stable even when the hull moves with the waves.

There are some other cases of modular designs in Autonomous Underwater Vehicles. For example, Smith et al. (2001) reported the design of the Morpheus AUV at the Florida Atlantic

[12] http://www.wam-v.com/

University. Some of the design goals of the vehicle were to be portable by one or two people, to operate in coastal waters and to allow the rearranging of the modules without rewiring or opening the pressure vessels. The result was a propeller driven platform with interchangeable modules manufactured from injection molded plastic pressure vessels. The initial tests of the prototype were done in 2000, for shallow water mine countermeasures and, in 2002, Hobson et al. (2002) reported the integration of a hovering module for Morpheus, including some initial sea trials. Unfortunately there were no further reports of any advances of the system, neither of any other operations.

One other case of modular design is the Starfish AUV, developed at the Acoustic Research Laboratory of the National University of Singapore. The basic configuration is a torpedo-shaped propelled AUV, with 1.7m of length and 20cm of diameter. Along the diameter, additional sections with 20cm of diameter may be included to incorporate different payload sensors (Sangekar et al. (2008)). Apart from the more common hardware and software modules, Shuzhe et al. (2011) also propose a methodology to develop modularized hydrodynamic models, so that the vehicle control system may be easily adapted to account for the installed modules.

In terms of commercial AUVs, a good example of modularity is the Gavia AUV, originally developed by Hafmynd ehf, in Iceland. The company was acquired by Teledyne in 2010 and is now Teledyne Gavia ehf.[13]. Gavia AUVs are assembled from a set of interchangeable modules with 20cm of diameter, that include battery, navigation or payload sensors. They result in very compact systems for a wide range of surveys. The suite of available sensors has been continuously expanding, to accommodate newer systems or functions, such as described in Hiller et al. (2012).

Due to the extra physical space required for module interfacing, it is more common to find modular designs in larger vehicles, such as the case of the AUVs from Bluefin Robotics[14], for example. Bluefin AUVs are assembled from multiple pressure vessels surrounded by a flooded fairing, and similarly to the Gavia AUVs, their subsystems may be swapped in the field. The modularity has also been explored to the development of additional modules for integration in the portfolio of available options (Taylor and Wilby (2011)).

2.3 Adaptive Sampling in the Ocean

The idea of using autonomous vehicles for adaptive sampling in the ocean is a natural evolution of what is already common with human intervention. The adaptive sampling paradigm can be implemented in several different ways, with increasing complexity. At a basic level, a human analysis of environmental data to (re)program an AUV mission can be seen as one simple example of "adaptive sampling". Alternatively, an AUV mission can be designed to monitor a specific area according to data processed from previous missions, so that sampling may be more exhaustive in certain regions of interest. As an example, in Ramos et al. (2001), the AUV mission was

[13] http://www.teledynegavia.com/
[14] http://www.bluefinrobotics.com/

programmed according to the result of a dispersion model, fed with data collected in the field by an oceanographic vessel.

A related issue is the determination of the optimal placement of sensors for observing a given process, and this has been a topic of research for many years. For example, Anton et al. (1971) addressed the identification of ocean pollution plumes and the determination of the best placement of sensors to monitor them. At the time, the authors were interested in the placement of fixed sensors, assuming a Gaussian plume, and used some concepts that were later included under the broader scope of information theory. Zhang and Sukhatme (2007) use a similar approach to guide an ASV to reconstruct a scalar field that is being simultaneously sampled by a set of fixed sensor nodes. The algorithm computes the path for the ASV taking into consideration the constraint that the robot has limited energy.

In an AOSN scenario, it is frequent to see *adaptive sampling* identified as the ability to *plan* new missions according to data arriving in real-time from a variety of sources (such as satellite data, CODAR seasondes or meteorological sensors). Schofield et al. (2002), for example, report the study of an upwelling event along the coast of New Jersey using AUVs and research vessels that were waiting for a triggering event. These platforms started their operations when there was an increase in the turbidity of the water column, as detected by complementary remote sensors.

In this work, we consider a step further in this approach, by transferring this adaptive sampling ability to the vehicle that is making the measurements, in a concept also known as "Real time adaptive sampling". The objective is to improve the efficiency in the sampling process, by concentrating the measurements in a region of interest identified according to the local characteristics of the scalar field being measured by the vehicle. This has been proposed some time ago in the literature, for example in Consi et al. (1994); Burian et al. (1996); Willcox et al. (2001). Such an approach exploits the on-board computational power to make assumptions about the oceanographic environment and to react to this environment by making decisions about the best sampling strategy to use. By continuously interpreting collected data, this decision can be made in real time so that the vehicle can use most of the available resources (mainly power) in sampling the ocean in regions of interest.

2.3.1 Autonomous Tracking of Dynamic Ocean Features

As described earlier, we are interested in ocean processes that exhibit a boundary region, that we consider to be the feature of interest. More, we consider that the vehicle makes pointwise measurements, and that it has to move through the scalar field to detect the feature. Therefore, the following examples refer to the cases where the vehicle has to extract relevant information from data that is streaming, and decide the best trajectory to keep tracking of the feature.

Tracking Thermoclines

Some of the earliest experiments describing adaptive sampling of thermoclines using AUVs were not fully autonomous, as they involved different levels of human intervention to define thresh-

olds. Woithe and Kremer (2009) proposed a thermocline tracking algorithm for a Slocum glider in which the vehicle would toggle between ascending and descending modes whenever thermocline layer was detected. This detection was based on a consecutive number of values above thresholds in depth and temperature, but these thresholds were fixed throughout the mission. They have validated the algorithm in simulation, but it failed to suceed in a real mission. Wang et al. (2009) based their thermocline detection algorithm in the profile of the sound speed. In this case they programmed an Odyssey III AUV to stay within a vertical layer where the gradient exceeds a given threshold. This threshold was calculated daily based on a forecasting model. Finally, Cazenave et al. (2011) developed a method for thermocline tracking based on a yo-yo motion between two predefined temperature values. These lower and upper temperature bounds were defined by visually analyzing a preliminary vertical profile. Even though the algorithm was successfully applied with the Dorado AUV in Monterey Bay, it was not fully autonomous.

Regarding autonomous implementation, two other algorithms were demonstrated at the time of our own implementation, very similar to ours. Zhang et al. (2010) proposed a method in which the vehicle identified the peak of the vertical gradient during a profile and the corresponding layer. In the following profile, the vehicle would define the yo-yo as a fixed depth range around the depth of the peak gradient. The advantage of this method is that it results in a constant vertical span of the yo-yo, however it may fail to capture sudden changes in thermocline depth, such as happens in dynamic environments. This algorithm was initially tested by post-processing data from a previous mission with the Dorado AUV. Later, it was implemented in the Tethys AUV and validated in Monterey Bay, as reported in Zhang et al. (2012a).

Petillo et al. (2010) also proposed an autonomous thermocline tracking algorithm for an AUV. In this case, the vehicle performs a preliminary deep profile to calculate the average vertical gradient of temperature. Then, the thermocline layer is defined as the layer where the gradient exceeds such average and this defines the range of the yo-yo. The algorithm also considers a periodic reset to the values by performing full profiles. The advantage of this method is the ability to reset the values to ensure a correct tracking even if the thermocline changes. The main disadvantage is that the full profile average will be biased if the vertical excursion is too deep, resulting in large vehicle yo-yo's.

Tracking Ocean Fronts

An ocean front is the boundary between two water masses and may exhibit very small scale variations. This is an ideal scenario for using autonomous vehicles, that can be programmed to detect the front location and measure the water parameters close to it.

In an early experiment described in Eickstedt et al. (2007), an ASV was used with a winched CTD to adaptively detect the thermal gradient in Monterey Bay. The ASV performed a zigzag pattern for a predetermined distance in order to compute the direction of the thermal gradient and would then sample another zigzag pattern in that direction. The system was relatively slow due

to mechanical constraints associated to the winch, but those could easily be avoided by using an AUV instead.

Zhang et al. (2012b) proposed an algorithm for autonomous coastal front detection and tracking using an AUV and, in Zhang et al. (2013), report data of its successful implementation in the long range Tethys AUV, while tracking an upwelling front for several days in Monterey Bay, CA, USA. In order to detect a front, the vehicle performs yo-yo's and determines whether the water is stratified (open water) or not (upwelled water), depending on the magnitude of the maximum vertical difference in a profile.

Gottlieb et al. (2012) address the same problem and follow a similar approach, proposing a momentum function to aggregate the vertical differences along distance. Although they show promising results from testing the algorithm in archived data, they did not demonstrate it in any real time tracking mission.

Smith et al. (2014) designed a method to sample and track an ocean front assuming that it can be represented by a continuous line in 2 dimensions. They further assume that the optimal sampling of the front is carried out by repeatedly crossing through the frontal boundary, and they propose to use the algorithm described in Zhang et al. (2012b) to detect the frontal point during the crossing. The algorithm is based on a zigzag pattern along the front, expanding or contracting the periodicity of the zigzags to accommodate changes in curvature, resulting in a similar effect to our own two-dimensional boundary crossing (as described later). However, they did not demonstrate it in a real front tracking mission.

Tracking Plume Boundaries

Cannell et al. (2006) used a single ASV to autonomously track the surface boundary of a thermal plume, generated by the outflow of the cooling water from a nuclear power plant. They use a combination of temperature, salinity, dissolved oxygen, and flow magnitude to compute a plume indicator function to detect the boundary crossings.

Camilli et al. (2010) used the Sentry AUV to sample the underwater plume from an oil leak in the Gulf of Mexico. They used an iterative approach, where the vehicle carried a mass spectrometer and made transects across the plume. The trajectory was then reconfigured according to preliminary analysis of data. In one of the surveys carried out in zigzags, each segment reported elevated values of hydrocarbons from its mass spectrometer. Although this was not a case of autonomous boundary tracking, it is clearly a scenario where such implementation seems to be possible using the hydrocarbon signature to detect the boundary crossings.

Petillo and Schmidt (2012) propose the adaptation of methods for front tracking to the boundary of plumes, assuming that the problem of tracking a 3-dimensional plume can be divided into multiple tracking of 2-dimensional boundaries. In order to optimize the sampling, they propose to distribute multiple AUVs along the boundary and combine partial data to reconstruct the full boundary.

2.3.2 Reactive Marine Robotics

The concept of adaptive sampling is far from being limited to the ocean environment, and there are many fields of knowledge where similar methods have been applied and can serve for inspiration or maybe adapted for implementation in underwater robotic systems. Some examples from the interpretation of animal behavior in nature may serve as inspiration to build innovative sampling methods. For example, bio-mimetic robotic plume tracking algorithms based on olfactory sensing (for homing, foraging and mate seeking). Consi et al. (1994) proposed algorithms for AUV guidance to mimic the behavior of lobsters, while Belanger and Willis (1998) analyzed the way moths track odors and propose some algorithms for robotic systems to find plume sources. Harvey et al. (2008) also discuss different methods to find the source of a plume, all using insect inspired algorithms.

Naeem et al. (2007) review possible approaches to the problem of chemical plume tracing with autonomous vehicles (whether water-borne or not), using isolated vehicles or swarms.

Some of these and other forms of reactive behaviors have already been implemented with success in AUVs, particularly for the case of finding the sources of chemical plumes, most of them trying to mimic the real animal behavior in odor source localization. Typical steps involve a two stage algorithm: sense the chemical and sense or estimate the environment (fluid velocity); and generate speed/direction commands to guide the vehicle towards the odor source. Farrell et al. (2003) and Pang and Farrell (2006) report the use of a REMUS AUV with a turbidity meter to find an underwater chemical plume and to trace it to its source, using also aditional information about the environment (water velocity). A similar problem was addressed in Pang (2010), investigating the use of AUVs to locate the source of hydrothermal vents, based on guidance by chemical signature.

Bachmayer and Leonard (2002) also address the problem of gradient descent, but instead of a single vehicle, they take advantage of the coordinated operation of vehicle networks.

Note that the plume source detection is out of the scope of this work, since we are interested in boundary tracking problems. Although the identification of the source location does not provide an indication of its boundary, we include these examples here as they can serve as inspiration or they may be used in complement.

There are other interesting applications in marine robotics that may be adapted to the problem at hand. For example, Bennett and Leonard (2000) present a technique for adaptively tracking bathymetric contours using an AUV with a single altimeter sonar. Barat and Rendas (2003) propose an algorithm to track the boundary between different benthic habitats, based on a segmentation technique of the returns from a profiling sonar

2.4 Discussion

This chapter provided some reference work related to the main objective of this thesis, that is to contribute to increase the efficiency in the process of ocean sampling. Our approach for ocean

sampling is based on the development of innovative, modular robotic solutions and, at the same time, on the utilization of the technology using new methods. These methods rely on the paradigm of adaptive sampling, a concept that exploits the on board computational power to process sensor data, in real time, and guide the vehicle so that it can capture more information about the process.

One of our assumptions is that some dynamic oceanographic processes may be represented by features that evolve in time, in space and time scales compatible with the velocity and range of small size vehicles. The first part of this background information was dedicated to the identification of some of these processes and their main characteristics. One of the target for our sampling strategy is the thermocline, a very important ocean process that is well understood in large scale, but still lacks sampling in the small scale. Another class of processes that can described by a well defined boundary are fronts, that can be as small as a few hundred meters (in some estuarine fronts). Finally, we also characterize many types of plumes, where the extent can be seen as a three dimensional limiting surface.

The second part of the chapter was dedicated to the state of the art in ocean sampling technology, including some of the milestones in the development and operation of robotic solutions in the marine environment. We concluded the chapter with an overview of the specific efforts that have been made under the paradigm of adaptive sampling, in particular the cases where the authors seek solutions for some of the ocean processes that we have considered.

The above mentioned tasks conclude a preliminary, but extremely important stage of the work, that is the clear definition of the scope and the understanding of the current available tools. The limitations of these tools and the absence of solutions for other open problems dictate the requirements for new developments and the challenges they encompass. This is the main objective of the next chapter.

Chapter 3

Challenges in the Problem Domains

The greatest challenge to any thinker is stating the problem in a way that will allow a solution.
— Bertrand Russell (1872–1970)

Despite some remarkable achievements in technological integration and overall performance, robotic marine vehicles are relatively complex systems with their own limitations. In order to improve efficiency, some of these limitations can be minimized, maybe sacrificing some other aspect, but it is difficult to devise a simple figure of merit for a fair comparison that takes into account all possible parameters. As a simple example, acquisition cost is always a factor to take into account, but when one reads through the main features of new AUVs being built, there is always a claim that the new vehicle will be "low-cost", be it a few thousands of dollars worth of equipment to a few millions of dollars. In fact, this characteristic is typically more highlighted than many performance figures, but when comparing the initial cost of acquisition with the accumulated operational cost, it is easy to conclude that an improve in performance can easily payoff in the not-so-long term.

There are certain key requirements to increase the efficiency in the use of robotic systems to sample the ocean, but the available technology imposes limits on achievable goals. On the other hand, current sampling methodologies do not fully explore the potential of emerging assets, such as the processing capabilities of current autonomous intelligent vehicles. In this chapter, we perform a joint analysis of the main requirements together with the current state of the art, in order to identify the main challenges that the marine robotics community is facing to design new assets for ocean sampling or to improve the capabilities of the available platforms. Our belief is that this thesis provides a contribution towards overcoming some of these challenges.

3.1 Technological Challenges

It is obvious that current and near-future technology impose serious constraints on the type of missions that can be performed with robotic marine vehicles. In this section, we provide an insight into the most critical technological pieces for robotic-based sampling systems. These are challenges that need to be addressed to maximize the impact on mission performance and sampling efficiency. Given our assumptions described above, we will concentrate on challenges associated with the development and operation of small AUVs and ASVs. Naturally, most of the challenges are associated with AUVs, not only because of their potential and increasing role as ocean sampling platforms, but also because they require an additional level of protection against the environment as compared to ASVs, and, above all, because the difficulties in communications greatly increase the operational jeopardy.

3.1.1 Vehicle Components and Constraints

An autonomous marine vehicle is a relatively complex system whose overall performance is affected by the individual performance of all interacting subsystems, and also by the internal mechanisms used to incorporate the contributions from these subsystems. When operating multiple vehicles, either similar or heterogeneous, the overall performance of the sampling system is further affected by inter-vehicle interactions.

Energy Considerations

Autonomous robotic vehicles operate with no physical link with any control station, therefore they have to carry enough energy for the mission, or harvest it from the environment. Obviously, if the vehicle has no means to capture energy from the environment, the amount of energy stored at the start of a mission dictates the maximum range the vehicle can travel before recharging. In any case, the power management system is one of the most important components of these vehicles and it should report an accurate value to a mission supervisor. If the available energy reaches a critical level (for example if the vehicle spends too much energy fighting a current), then it may have to abort the mission and proceed to a safe location, or simply emerge in the case of an AUV. Such a decision may be difficult to make, particularly if the accuracy of the available energy is poor, and a conservative approach results in a reduction of the effective range of vehicle operation. In case of a vehicle that is harvesting energy from the environment, the power management system is much more complex, since it has to incorporate the uncertainty in the forecast of the energy that can be captured.

In terms of energy storage, the vast majority of small-size autonomous vehicles curently use rechargeable Li-Ion batteries, a technology that was not mature enough to power the early AUVs in the nineties (Bradley et al. (2001)). Lithium-based batteries have high energy density and a long life and they have emerged as the preferred power sources for the consumer electronics market. They are also being adopted for energy storage systems in renewable energy plants, as

well as power systems for electric vehicles, therefore they will surely maintain or even expand their leading role in autonomous vehicles (Scrosati and Garche (2010)). Obviously, the maximum energy that can me transported in an AUV or ASV is dictated by volume and weight available on-board. Currently, the maximum energy density found in commercial batteries is around 200 Wh/kg and this number has been increasing relatively slowly in the last decade.

For a long time, there have been proposals of other power sources for autonomous vehicles. For example, fuel cells have been proposed to provide energy for long endurance vehicles (Tamura et al. (2000)) and seawater batteries also had the potential for long-term deployments (Wilcock and Kauffman (1997)), however a series of practical difficulties obstructed their adoption. In fact, in the case of autonomous marine vehicles, there are specific requirements that batteries have to meet. Batteries are placed in sealed containers, where ventilation is usually feeble or absent, which impedes any technology with outgassing. Temperature may also be a risk, since the containers also obstruct thermal transfer. This means that even working in relatively constant temperatures (particularly underwater), the batteries may be subject to heating generated by components installed in the same container. For example, an interesting finding reported in Waldmann et al. (2014) indicates that aging rates of Li-Ion batteries increase with decreasing temperature below 25^{o}C and increase with increasing temperature above 25^{o}C.

As for future technologies, the challenge is to significantly increase energy densities, ideally by an order of magnitude, so that the mission endurance can take a giant leap. In fact, energy densities above 2000 Wh/kg have alredy been proposed, based on evolution of available lithium batteries (Scrosati and Garche (2010)), which could result in a smooth transition from existing devices. Such a dramatic improvement could result directly in a tremendous gain in sampling efficiency with minor changes in vehicle design. Smaller vehicles could easily be deployed for days instead of hours; larger vehicles could equally extend their range, but, additionally, they could also integrate larger power demanding devices, taking advantage of their ability to deliver higher power to subsystems than their smaller counterparts.

On Board Electronics

All marine systems need electronics to be placed in sealed containers, to avoid ingress of water or salty humid air. In the case of AUVs, further protection is required for the water pressure and, as the intended pressure increases, so does wall thickness and weight. Space is typically a scarce resource and miniaturization has been the key to squeeze some more electronics systems into sealed enclosures. However, the main limitation to size reduction in electronics comes with the need to dissipate energy, which, in turn, results from inefficient electronics. Therefore, an important challenge to advance the state of the art in autonomous vehicles is to proceed the quest for low-power, more efficient electronic systems. Note also that all energy wasted in on-board electronics is dissipated as heat. Not only this is a useless energy expenditure that results in a direct loss of vehicle endurance, but it can also cause additional problems by increasing the temperature inside the sealed housing.

An autonomous vehicle is typically commanded by a master computer, usually in the form of an embedded PC that works on its own or in a distributed system. Small, low power computer systems have been around for a long time, with the expanding market of embedded systems steadily driving technological improvements. Recently, the advances in computational power on small systems have been tremendous and there has been an escalation in the available alternatives of very low cost single board computers (SBCs). They are gradually gaining importance as secondary processors but may soon take grander roles, at least for research level applications. As with other electronics, reductions in size and power consumption are main concerns, but also an increase in interfacing options to allow the installation of a larger number of sensors and actuators.

With the new envisaged capabilities for autonomous systems, there has been a shift in priorities with respect to the role of the main computer. Early concerns for autonomous vehicles were simply to be able to cope with hardware interfacing, on a bottom layer, to navigation and control, on a higher level, and all this was commanded by a mission management system. Various alternative architectures were proposed in the early days of AUV development (Bellingham et al. (1990)), but the focus has shifted when the first implementations were successful. Now, the emerging "intelligent" algorithms are again demanding a substantial increase in computational power, that is expected to cope with real time processing of data from oceanographic sensors, feature extraction from video images and, eventually, running ocean models in real time.

Payload Sensors

There is absolutely no point in using advanced platforms for ocean sampling if they do not carry capable sensors. Fortunately, the range of sensors and transducers that accurately convert physical, chemical, or biological properties into measurable electrical signals is large and expanding. Oceanographic sensors have a long tradition of using low power electronics for long term deployments and vehicle integration will continue to benefit from this. Unfortunately, some of the available sensors have a low update rate, that can be either to save power or to output a more precise measurement by averaging multiple samples. Whenever installing sensors in a moving platform, the time constant is an important factor, which is seldom the case when the same sensor is installed in a buoy. So, one requirement that is often disregarded is that sensors need to be fast, along with accurate and precise. Note that precision is particularly relevant when sensor data is used for real time control.

In terms of physical integration, sensors need to be compact and low power, like any other electronic system, but they should also be lightweight to minimize integration impact on autonomous vehicles, particularly in AUVs. Another aspect that is important for systems' integrators is the availability of many versions of the same sensor. Some manufacturers already offer different form factors (from "OEM versions" to a set of housings for specific pressure ratings), different output options (serial or analogue), and different voltage requirements. In many cases, sensors can also be programmed to produce some indirect calculations, with variable output rate. Usually data is transmitted to the on board computer that stores it with a time stamp. When the sensor has internal

memory to save data, it is important to synchronize the sensors' clock with the computer's, so that data from different sources may be correlated.

As far as challenges are concerned, some of the available sensors will soon have some increased processing capability, reducing the burden on the receiving devices. These include, for example, cameras or sonars with automatic feature detection, or 3D/stereo cameras with automatic distance calculation. There are also multiple efforts to enlarge the suite of available in situ sensors, by converting typical laboratory equipment into standalone devices, including nutrient analyzers and mass-spectrometers. Finally, sensor manufacturers can also partner with vehicle developers to design and implement distributed sensors that benefit from the ability of robotic devices to operate coordinately, obtaining distributed and correlated data for immediate or post processing.

Communications

The AOSN paradigm envisages heterogeneous vehicles cooperatively collecting data, together with moored devices, and all them communicating using acoustic or radio signals. By definition, missions with autonomous vehicles are meant to be performed without interference from an operator. Ideally, however, there should be real time telemetry to a mission supervisor that could take an early action in case of some misbehavior. In the case of buoys and ASVs, that can easily be guaranteed, since there are multiple options for real time, high bandwidth radio based communications that ensure global coverage. More, there are also solutions to provide networking to these nodes, so that all devices can be accessed seamlessly, independently of the operator location. In terms of AUVs operations, the same level of interaction is simply not possible. The only viable option for communications in practical ranges is using acoustic modems, but they provide a very low data rate, with a high latency, and have a particularly poor performance in coastal/shallow waters. Furthermore, existing solutions are typically meant for point to point communications and networking with these devices is still very immature. There is, therefore, a strong demand for robust long range underwater communication devices, that ensure both point to point and networking capabilities.

AOSN operations have other communication requirements that need to be addressed by the research community, maybe using solutions that have long been neglected. For example, it is known that radio frequencies are greatly attenuated in seawater, therefore hindering this technology for long range underwater communications. However, when an AUV approaches a docking station, or when it is navigating in formation with other AUVs, they can all exchange information using short-range radio communications. A similar reasoning may apply to optical communications, that may well be a viable option for operations in clear, dark waters, ensuring high bandwidth, even though it may only be at modest ranges.

Motion Primitives

As far as mission organization and programming is concerned, each mission is typically organized as a sequence of maneuvers or tasks. Sometimes there is a set of elemental tasks and some complex

maneuvers that use the elemental tasks as building blocks. Typical missions are defined according to geographical coordinates, sometimes including also time constraints, but the most common task is a straight line trajectory between two predefined waypoints, following some vertical pattern. Many robotic vehicles use proprietary maneuver syntax, either because they evolved from purely research projects, or simply to protect intellectual property. There is a lack of normalization of maneuvers and mission syntax and even though the Robot Operating System (ROS) attempts to pursue this goal, there is a lot of work to be done in terms of mission script standardization.

The new paradigms of ocean sampling require additional types of maneuvers that include, for example, autonomous feature tracking or autonomous docking. The integration of these maneuvers into the standard suite may also require additional mechanisms to ensure proper termination, or adequate fault handling. The challenge gets even more complex when it comes to the coordinated operation of multiple vehicles, requiring fixed or adaptive spatial formation of the fleet.

Navigation and Control

The main task of the navigation system of an autonomous vehicle is to estimate its position in real time. This serves for the control system to make necessary corrections in trajectory, and, at the same time, it allows sensor data to be spatially tagged. At the surface, GPS signals are usually sufficient to provide a position estimate, and, if necessary, accuracy can be improved with differential GPS (DGPS) or even with inertial sensors. Underwater, GPS signals are not available, so other solutions have to be employed to allow the computation of vehicle position. One of the possibilities is to fuse together data from multiple sensors, using an extended Kalman Filter, or other data fusion algorithm. Pressure sensors, digital compasses, IMUs, accelerometers, gyroscopes, and Doppler velocity meters, are typical sensors readily available for integration. However, these data alone produce an estimate with an error that grows in time due to continuous integration of biases, so it requires an external aid to provide an absolute measure and avoid divergence. This is usually ensured with acoustic transponders, in a variety of techniques such as Long Baseline (LBL), Short Baseline (SBL), or Ultra Short Baseline (USBL). Other methods have also been proposed, such as SLAM (for *Simultaneous Localization and Mapping*) using sonar data, but it requires bottom features that are often absent in open sea. Both Bingham (2009) and Tan et al. (2011) present very good surveys on common underwater navigation techniques and associated challenges, that are still up to date. The main challenges for the navigation system is to be able to provide an accurate estimate of location, in a timely manner so as to allow closed loop control and geographic tagging of data. Ideally, this should be done without external aids, and with the widest possible coverage.

In the case of adaptive sampling missions, the vehicle trajectory may be dictated by ocean data that is streaming in from the sensors and processed in real time. In this case, there is no *a priori* knowledge about the possible locations of the vehicle, so it is difficult to use a standard network of acoustic beacons. For these scenarios, there is a need to increase significantly the range of current transponders, or otherwise to devise innovative methods to ensure accurate navigation. Simultaneously, it is important that the safety of the vehicle is not disregarded during an adaptive

sampling mission, and a possibility is to implement a supervisory procedure that prevents the vehicle from leaving a safe area, for example a region with good acoustic coverage from the transponders.

Navigation of underwater vehicles can be more challenging when multiple platforms are operating simultaneously. Traditional navigation based on exchange of acoustic signals may be difficult to implement due to cluttering in the acoustic channel. At the same time, it may be required that each vehicle has also a good estimate of the position of all the others in the fleet. Some techniques have already been proposed to solve this problem, for example using synchronized beacons that transmit periodic signals (Almeida et al. (2010)) or algorithms based on time differences (Bellingham et al. (1992); Cruz et al. (2001)), but they have yet to be demonstrated in the field for a significant number of vehicles.

The design of control systems for marine vehicles is still a complex and challenging task, although it has been a very active topic of research for many decades and the literature abounds (Fossen (1995); Whaite and Ferrie (1997); Abril et al. (1997); Prestero (2001)). Most control techniques rely on the existence of an accurate dynamic model of the vehicle, but the preparation and execution of missions for parameter identification is very resource consuming, so the existing models are usually derived from empirical formulas, therefore very inaccurate. This is particularly relevant in the cases where the physical configuration of the vehicles change frequently, by adding different sensor packages, for example. Furthermore, motion is usually allowed in several degrees of freedom and there is some coupling among them, but the control designers often neglect such coupling and considers a decoupled model for simplicity. All these effects combine to produce unwanted disturbances in the behavior of the vehicle, degrading control performance. Even when the models are reasonably accurate, there is often some difficulty with the definition of a performance index. Among other things, this index has to reflect the tradeoffs between trajectory smoothness, tracking accuracy and control effort (energy), and all can be equally important. However, in terms of control, the main challenge concerns the emergent use of AUVs in small manipulation tasks, where the vehicle is supposed to hover at a specific location while using a robotic arm to grab an object or perform some other operation. Another demanding scenario is underwater docking, where the AUV needs to approach the docking station with very high accuracy.

3.1.2 Mission Support Systems

An operation with one or multiple robotic vehicles also poses some technological challenges in what concerns external systems that support the mission. They include not only the software tools to allow mission preparation and supervision but also all physical devices that need to be in operation.

Mission Specification, Simulation, Supervision and Playback

A mission of an autonomous vehicle is typically organized as a sequence of maneuvers. In the simplest case, this can be specified in a text file, with a set of waypoints, and possibly some

velocity (and depth settings for AUVs). In reality, however, there are many additional parameters that need to be set at the time of mission specification, therefore resulting in a set of files with instructions and/or parameters. Current mission programming tools include GUIs (*Graphical User Interfaces*) that provide a friendly interface to program waypoints and different mission/maneuver settings. With traditional maneuvers based on geographical waypoints, the same interface provides an overview of the mission that appeases the programmer. In the case of new sampling strategies based on feature tracking, for example, it is not trivial to define and to show the mission in a graphical way. There is, therefore, some effort required to simplify this mission specification, reducing the number of mission files and scripts that are sometimes obscure and need to be defined by the vehicle specialist. Ideally, most of the mission should be specified and programmed by the scientist, with minimal intervention from the vehicle specialist. All these requirements are emphasized for the case of missions using multiple heterogeneous assets.

Simulation has long been a great help in evaluating different algorithms for vehicle control. Usually the simulator requires the same dynamic model of the vehicle as the on board controllers, and this can easily be done when simulating motion in geographic coordinates, since the models are defined in terms of physical equations of motion with respect to inertial or body fixed coordinates. When trying to simulate one or more vehicles in an adaptive sampling mission, the simulator also requires an accurate model of the environment. There are many models of the ocean, in many scales, but typically they do not have the relevant scale to mimic the real environment that the vehicle finds. It is therefore a challenge to incorporate such models in vehicle simulators, so that they produce realistic data that allow an effective assessment of mission performance. On a related topic, there are also simulators of communication networks that are being independently developed by the communications community, to support multiple vehicle operations. Such simulators need to be incorporated into an integrated simulation tool, so that all aspects of a multiple vehicle operation can be truthfully validated through simulation before being tried in the field.

There is always some risk in the operation of autonomous robotic vehicles, but this risk is hugely stressed in the case of AUVs, In fact, there are so many things that can go wrong with the operation of a complex system in a harsh environment, that it is virtually impossible to consider all scenarios. One can only expect to minimize the risks by using reliable equipment and through careful mission planning. All vehicle operators gain valuable experience through successes and failures, but almost all publish their successes and just a few share their failures (Stokey et al. (1999) provides an interesting account of failures in AUV operations). One of the ways to minimize the risk of operation is to have tracking mechanisms that allow some degree of supervision. In fact, when an AUV is deployed for a day of operation off a support vessel, there is a feeling of anxiety that only fades when the mission evolves and there is some feedback indicating the correct behavior of the vehicle.

Given the difficulties in communicating underwater, mechanisms for external tracking of an AUV are usually based on acoustic signals that produce a position estimate every few (sometimes

tens of) seconds, at a receiving station. This info is then compared against the programmed mission to confirm that the vehicle is moving as planned. Normally this processing is done by a human supervisor that has some intuition about typical errors and outliers, and mentally filters the incoming information. There is some effort required to automate this information processing, particularly as mission durations become longer and/or with multiple vehicles working at the same time. A particular challenge is the case of adaptive sampling missions, since there is no preplanned trajectory to match and alternative methods have to be devised to confirm the correct execution of a mission. This may require the use of complementary vehicles that serve as moving receivers and information gateways.

At the end of the mission, another important role of the support software is to concentrate all the sources of information stored on board. Part of this data is downloaded to deliver to the scientists, while specific engineering information is analyzed separately, but all of them have to be synchronized by a global mission timekeeper. If multiple systems operate during the same mission, this synchronization should embrace all the individual clocks. In this case, the support software should be able to playback the mission, incorporating all the sources of information.

Communication Networks

Every autonomous marine system has at least one communication device that is used to report data and receive commands. Given the availability of many commercial solutions for radio communications at affordable prices, there are usually multiple systems installed, to provide redundancy or to be used in specific circumstances. In the case of AUVs, underwater communications are ensured with slow data rate acoustic modems, while radio solutions are common for when the vehicle surfaces. Satellite communications are adopted in the case of remote observatories, and they are common to all meso-scale platforms, such as gliders (Eriksen et al. (2001); Sherman et al. (2001); Webb et al. (2001)). When integrating multiple platforms for operations in a given region, following the AOSN concept, each of these platforms is a node that needs to be assessed, both from a supervisory location, but maybe also from the other platforms. These nodes may have different communication devices, some of them may be moving, and some may be temporarily out of contact, such as it is often the case with AUVs.

The integrated operation of multiple assets requires the support of a communications network that has to be dynamically reconfigurable, *i.e.* it has to adapt in real time to the behavior of the links and physical positions of the nodes. Part of this behavior is already common in wireless radio networks, but in the marine environment the most demanding aspect will come from the low data rate and high latency nature of both acoustic modems or satellite links. The goal is for the communications network to be adaptive according to the instantaneous conditions of the acoustic channel and to the capabilities of the moving nodes. To overcome any potential losses of connectivity due to the location of the network nodes, additional nodes (moving or moored) may se strategically placed in the operation area to behave like repeaters or access points. In particular, some of the nodes may have to move to increase the overall throughput, while, at the

same time, the network routing will deal with the transmission conditions between the available nodes to ensure a proper transmission of information.

Recently, the paradigm of Underwater Wireless Sensor Networks (UWSNs) promises to provide internet connectivity to underwater systems, following the concept of Internet of Underwater Things (IoUT) (Domingo (2012)). However, much research has yet to be done before marine assets can communicate seamlessly, as land based systems already do.

Logistics

In a typical survey in open sea, launch and recovery of a vehicle from a support ship are probably the most stressing moments of the mission, particularly in harsher sea state conditions. Vehicle handling is usually more complex for larger and heavier vehicles, however recovery at sea is a complicated task even for the smallest AUVs, since it often requires human operators close to the water. For safety reasons, these operations typically occur only up to sea state 4. There have been some developments of specific Launch and Recovery Systems (LARS) for large AUVs, which are mechanical devices designed to facilitate these tasks. However, these systems are still limited to a maximum of sea state 5 (Rauch et al. (2008); Hayashi et al. (2013)) and some more work needs to be done to allow recovery in higher sea states, therefore increasing the window of opportunities for vehicle deployment.

Docking Stations

Docking stations are generally seen as underwater garages for AUVs to recharge their batteries. In an AOSN scenario, these are fundamental for extended deployments and they can be placed in any part of the water column. Providing power to a docking station is a critical issue, particularly in a remote location. The easiest option is to use primary batteries, and this has been the solution used in early successful demonstrations (Singh et al. (2001); Stokey et al. (2001a)) but currently other options are being employed, using renewable energy. In any case, many years after these initial trials, there are no operational docking stations for AUVs, probably due to technological or operational complications. One of the main difficulties that still needs to be solved robustly is the docking maneuver. Many AUVs have propellers and fins, which means they have a minimum cruising velocity, so they require a very accurate approach to avoid hitting the docking station and causing damages to both. Another mechanical problem that may arise in long term deployments is biofouling, that can impair a correct system operation. Finally, installing docking stations in deep water is a complex task that may be difficult to pay off. An alternative can be the development of docking stations based on mobile devices, such as tanker ASVs, that avoid the need for moorings, but require a good coordination during rendez-vous. A similar approach could be followed to support launch and recovery in high sea states.

Even though all the examples of docking stations has been proposed for AUVs, they may also have a relevant role in the long term use of ASVs. A surface docking station may be an ideal

resting place where ASVs can charge their batteries, upload large quantities of information, wait for ideal weather conditions, or simply hold station while waiting for further instructions.

3.2 Methodologies

In the previous section, we have identified some of the technical aspects that are limiting the development of more efficient autonomous marine robots and we have provided some ideas to overcome such challenges. However, building the so called "intelligent" vehicles is not a guarantee of efficiency, if it is not matched with proper methods to use these technologies. In this section, we provide an overview of the pending challenges in new methods for utilization of marine robotic technology, that require solutions beyond what is now the state of the art.

3.2.1 Sampling Challenges

In order to sample a dynamic scalar field with a moving platform, it is important not only to transport the relevant sensor, but also to avoid aliasing, both in time and in space. Both sensor errors and aliasing may contribute to erroneous conclusions about the dynamics of the process. When a moving platform is used to sample a scalar field, we can see it as moving in a four dimensional space, and there may be an ambiguity in space and time variation. For example, if a single vehicle is moving along a boundary of a pollution plume, it will be possible to detect local gradients and pollutant concentration, however it will not be possible to know if the boundary locations are static or dynamic. Velocity of survey is more important as the processes evolve more rapidly, so if the plume changes shape or location it is important to travel rapidly along the boundary. In summary, whenever a synoptic view is required, as is often the case, it is important that the velocity of data collection is high, but also that the spatial coverage is high. The main challenge here is to find the correct balance between both space and time sampling, taking into account some a priori information about the dynamics of the process, the velocity constraints of the moving platform, and the characteristics of the sensors. Part of these problems may be solved by adequately considering multiple sampling platforms to resolve some of the space and time ambiguity. Although this can add more complexity to mission design, it can follow the ground earlier paved by Willcox et al. (2001) and Zhang et al. (2001).

3.2.2 Ocean Modeling

The computational effort required to model ocean processes is enormous and primarily intended to the study of processes with global impact, such as global warming, circulation patterns or the "El-niño" phenomenon. Traditionally, the observation/modeling loop has been closed with global observation platforms, such as environmental satellites or networks of roaming buoys. Nonetheless the major importance of these models, there is also a strong demand to develop fine-resolution ocean models, that may help in several areas, ranging from aquaculture to search and rescue operations or coastal management. At the same time, such small-scale models may show details that

can be observed with small, highly maneuverable platforms that are already available, which may therefore contribute with groundtruth data for calibration of these models. Similarly, data assimilation is now easily available with high performance, affordable computers that are able to process such data in near real time. Apparently, the fine scale models could be obtained simply by scaling down the existing basin wide models. However, the existing global ocean models disregard specific small-scale interactions and assume large-scale approximations that simply cannot be scaled down, otherwise failing to represent the physical processes involved.

A very important challenge for the modeling community is therefore to focus on small scale models of local ocean processes. It is unlikely that those models may run in small vehicles in real time, but simpler approximations may be used to guide these vehicles into obtaining relevant data to feed the models. Some very simple approximations of ocean features can be made inspired by geometric modeling. For example, this can be done by assuming a time-varying virtual line separating two bodies of water, and using logistic regression to infer the position of the sample. In logistic regression, a variable is binary, *i.e.* the decision needs to be made whether a sample belongs to one of only two categories, and in oceanography there are many processes that fall into this category, for example being inside/outside of a plume, or above/below the thermocline.

Probably the hardest challenge in ocean modeling will be to couple multi-scale modeling efforts, for example using large scale models to provide boundary conditions for small scale models. If such an integration is performed, the result will clearly encompass the best of both approaches, but that requires a close cooperation between modelers and observers. In fact, there has been a traditional distinction between modelers and observers, each relying on his own view of the problem. With the development of faster sampling platforms and trying to close the loop more rapidly, these views have to be considered simultaneously, working cooperatively so that the modeling/observation loop is closed more efficiently. Modelers need to understand the capabilities and limitations of the platforms and measuring methods, and technology developers need to comprehend better the demands for data assimilation.

3.2.3 Adaptive Sampling

Although the concept of adaptive sampling is very intuitive and appealing, the first implementations are relatively recent and modest. One of the reasons for this slow progress is the absence of truthful models that relate the motion of a vehicle with the variation of the scalar field. Without this relationship, there is the need to develop heuristic approaches that require long and exhaustive validation. Take for example a seemingly simple problem of navigating a vehicle along a bathymetric line. If there is no information about bottom roughness, it may be quite difficult to design a stable controller for such a vehicle. Note the difference from this example to the case of navigating at a fixed depth, where the model that relates an AUV depth with actuation of thrusters and fins can be determined from physics. As an ultimate goal in adaptive sampling, an autonomous vehicle, or collectively a fleet, need to have an internal model of the dynamic oceanographic process whose

parameters were unknown. The vehicle(s) have then to move in order to identify the relevant parameters, in real time, and then use the model to provide feedback laws that allow values of the scalar field to be used as motion references.

When trying to develop adaptive sampling algorithms, it is important to start by modeling the ocean process in such a way as to allow the implementation of such mechanisms. This will highlight the parameters that need to be identified and allow the implementation of guidance or control laws to identify them. It is also important to define the conditions for successful detection, considering the trade-off between accuracy and efficiency (time and energy consumption). These conditions and algorithms can include some early concepts planned for mission planning that may now be used on line. For example, (Singh (1995)) considered the case of entropy of sonar measurements to design AUV missions and a similar approach can now be employed to maximize the information about a given ocean process.

Safety has to be a major concern whenever too much *autonomy* is put into a vehicle computer. In a standard mission programming, many safety aspects are implicitly ensured by the way the operator defines the sequence of maneuvers. However, in an autonomous system such safety precautions can not be taken for granted, and particular attention has to be payed to ensure the integrity of the systems involved. One important aspect to attain this is to define conservative conditions of failure and to design the proper action to recover from them. Defining metrics for evaluation of algorithms can serve also this safety purpose, if it is computed iteratively and available during the mission. In this case, it may be possible for a supervisory process to monitor this figure of merit and take any action if it lowers below a preset threshold. Extended simulation is another way to detect potential problems, but here the challenge comes from the difficulty in modeling the oceanographic process with realistic data, as described earlier.

Another challenge that may affect safety is related to navigation and tracking. If the AUV(s) use acoustic systems for navigation and tracking, the transponder coverage has to include all the region the vehicles are likely to visit during the search/follow process, which may require dynamic positioning of the beacons, or limit the operation area. It is also worth mentioning that the mission management system has to deal with the fact that new "commands" are generated throughout the mission. This may prevent a thorough preliminary validation of the mission plan by simulation.

Some of the challenges in adaptive sampling are related to signal processing. For example, when looking at a full temperature profile such as the examples shown in section 2.1.1, one can visually identify the thermoclines and envisage an online algorithm to extract the 3 associated regions: mixed (surface) layer, thermocline region and deep layer. This seemingly simple task is facilitated by the *long* low gradient regions, both above and below the thermocline. In many real vertical profiles, however, these regions may not be present at all, or they may be very difficult to detect by an human observer, due to a number of reasons, such as small gradients, small spans, multiple inflections, etc.

Furthermore, in many examples, the boundary of an ocean feature is defined by the maximum gradient of a scalar. Therefore, an autonomous vehicle has to navigate along a trajectory and

detect, in real time, the value and location of the maximum gradient of the scalar field that is being measured along that trajectory. The challenge is to detect that peak as early as possible, avoiding the need to navigate regions with low gradients, but a peak can only be detected if the value decreases after having reached a maximum. Therefore, the vehicle has to detect, as early as possible, a significant decrease in the gradient, meaning that the peak has already passed. A difficult problem in detecting the gradient is then to estimate the derivatives of the scalar field along the track from a limited number of previous values of data points and decide if those derivatives are sufficient to conclude that the maximum gradient has already been passed and there is no need to proceed further. More, it is quite likely that this data is updated several times per second, possibly showing small scale variations, it may not be uniformly distributed and, surely, it may have errors.

3.2.4 Operation of Multiple Vehicles

As described in the previous chapter, there have been several cases of operation of multiple vehicles in different scenarios, but typically coordination is ensured by mission programming. Each vehicle has a specific role assigned in the overall goal of the operation and each mission is programmed in such a way that the vehicles take distributed measurements synchronously. For this type of coordination, there are specific technological challenges associated with the simultaneous operation of multiple assets, mainly related to navigation and logistics, and these were described earlier in this chapter. For *cooperative* missions, however, the platforms need to adapt their behavior depending on each other, therefore requiring exchange of information. So there is a need to consider cooperative missions in a framework that also takes into account communication needs, since some collaborative tasks may not be performed at all if a minimum communication throughput is not guaranteed.

When working in cooperation, multiple assets can be viewed as autonomous platforms that follow a certain protocol in order to fulfill a given goal. The main challenge is to define the protocol that leads to such an efficient mapping and to have the mechanisms to ensure that the protocol is feasible given the constraints of the available assets. There are also many open challenges in job allocation based on characteristics of the different assets, and, in particular, in defining metrics to assess the adequacy of an asset to a particular task. This allocation problem complicates further if we extend the concept from fixed to dynamic role assignment, in which the above mentioned adequacy changes over time.

3.3 Discussion

Although a tremendous effort has been recently dedicated to the development of marine robotic technology, particularly in the case of AUVs, there are still many open challenges that need to be addressed to allow a more widespread and efficient utilization in real scenarios. The intention of this chapter was to provide a perspective on some of these challenges, but it was deliberately focused on the engineering side of small, portable vehicles, following the same approach as in

previous chapters. The analysis was centered on technological aspects and methods of using the technology, in some areas where our background allows us to better provide contributions.

The remainder of this thesis attempts to provide a contribution to solving some of the challenges identified in this chapter. Naturally, such a contribution is just a minor fraction of all the effort that is required to produce a global leap in the use of marine robotic vehicles. Therefore, there are still many exciting opportunities for research and development to overcome the identified challenges, as well as others that will surely emerge in the coming years. More, it is clear that the full challenges span many areas of expertise and the work ahead is enormous, but fortunately there is a worldwide, prolific community that has been working towards the same goal, and we can foresee a bright future for marine robotics. In fact, solving a good fraction of these challenges in the near future will ensure that robotic marine vehicles will play an increasing role in ocean data collection and contribute to a broader understanding of the ocean dynamics.

It should be noted, however, that there are some additional threats and challenges that may impose serious obstacles to the widespread use of robotic systems in real marine scenarios. One of these challenges is to perform a thorough analysis of the impact from the simultaneous operation of robotic platforms together with humans or manned systems (either coordinated, cooperative, or totally independent). Probably the most relevant threat is the absence of regulation of robotic activities at sea with the clarification of corresponding legal issues. These fall out of the scope of this work but surely need to be addressed to avoid unwanted hindrances to the general acceptance of this technology.

Chapter 4

Modular Underwater Vehicles

If you can dream it, you can do it.

— Walt Disney (1901–1966)

The utilization of underwater robotic systems to assess multiple aspects of the ocean has increased tremendously in the last decade. A great fraction of these operations have been taking advantage of the versatility of commercially available systems, which is certainly a good option in terms of cost effectiveness for a great variety of applications. On the other hand, as the users get more demanding, certain scenarios require solutions for which specific configurations would be more effective and/or more efficient. However, this encompasses a great deal of customization effort, typically done at the factory, with the corresponding increase in delivery time and cost. Such inconveniences can be minimized by following a modular architecture in the development of these systems, so that versatility is no longer achieved from the same *rigid* vehicle with multiple uses, but, instead, it comes from a vehicle with multiple possible configurations, each one targeted for a specific application scenario.

In this chapter, we describe a consistent program for the development of small size AUVs based on modular building blocks. Our approach relies on modularity both in terms of hardware construction, and also in terms of electronics, software and control. Using these blocks, we have first built the MARES AUV (Cruz and Matos (2008)), a hovering AUV that has been continuously updated and used in the field in many different configurations, since 2007. In 2011, the versatility of the system components has been pushed further with the development of TriMARES (Cruz et al. (2011)), a 75kg, 3-body hybrid AUV/ROV system, which was developed in little over 6 months. Both TriMARES and a version of MARES have already been exported to Brazil, suggesting that our concept has some commercial potential that may be exploited in the near future.

The remainder of the chapter is organized as follows. We start by expressing, in section 4.1, the main requirements that we've identified for a new approach in the design of underwater robotic vehicles. Section 4.2 describes the building blocks that are the basis of these vehicles and the way

they can be interconnected to achieve a variety of configurations: mechanical components, on-board electronic systems, software organization and control strategies. Then, sections 4.3 and 4.4 present the examples of two different vehicles assembled from the existing blocks (MARES and TriMARES), and some operational results. Finally, we conclude the chapter with a discussion on the main achievements of our modular approach and some hints on how this modularity may be further exploited to assemble other configurations in the near future.

4.1 Design Requirements

The design of an Autonomous Underwater Vehicle is a relatively complex task and it is paramount to start by identifying the most critical requirements for the envisaged missions, both in terms of software flexibility and hardware performance, including depth rating and other mechanical constraints, payload sensors that may be integrated, motion degrees of freedom, and battery endurance. The development of a specific AUV is governed by a combination of these requirements, but also taking into account possible constraints in fabrication, assembly and operational logistics. In our case, we started an R&D program for the development of a new type of AUV in 2006, following 10 years of experience in the customization and utilization of small AUVs in the field for environmental missions (Matos et al. (1999); Ramos et al. (2001)). This experience contributed to the identification of critical subsystems, sensitive components, and typical failure modes. At the same time, it was also possible to recognize that seemingly irrelevant design choices can have a strong impact on operational logistics, therefore affecting the ability to carry out frequent field deployments.

From a thorough analysis of all these issues, we have produced some guidelines and overall characteristics that this new generation AUV should possess. As far as operational scenarios were concerned, the main idea was to conceive platforms for field validation of scientific developments and, at the same time, to be able to carry out environmental sampling in coastal waters. Ideally, the systems should be upgradeable to address operations in more demanding scenarios. Given our limited access to deployment facilities and operational logistics, our first priority was then to develop small, man-portable systems, requiring low operational logistics. In fact, the decision on vehicle dimensions can be seen both as a requirement or an outcome of other requirements. On one hand, smaller AUVs are easier to launch, recover and handle with no special equipment, resulting in a tremendous simplification in logistics. This results in the ability to obtain faster experimental feedback, which is paramount to the development and validation of new algorithms, something that we were seeking. On the other hand, large AUVs can carry more energy and have more alternatives regarding sensor integration. Fortunately, there is already a wide variety of sensors for *in-situ* measurements, with reduced size and power consumption and it is expected that this miniaturization trend will continue in the future.

Since the main purpose of the vehicle was to be employed for field validation of scientific developments and to carry out environmental sampling in coastal waters, our initial target for depth

rating was 100 meters. This relatively modest figure yields some simplifications in the choice of materials and dimensions for the mechanical construction of the physical building blocks.

In terms of physical assembly, another requirement was that our vehicles should have a highly modular construction, in the sense that it should be very easy to reconfigure (swapping or adding sensors, for example) and at the same time allowing for the development of subsystems in separate. This fostered the idea of the creation of relatively simple blocks that could be combined together to form specific AUVs. Naturally, cost is also an important factor, and we were interested not only in diminishing development costs, but also in minimizing maintenance and operational costs. This reduction can be achieved by a modular approach in the overall design and also by the reduction in the size and weight, not only of the vehicle, but also of the necessary mission support equipment. It should be noted that this concept of modularity was not restricted to the physical aspect of the AUV system, as we have expanded the notion of modularity to the other aspects of AUV development, such as electrical sub-systems, software components and motion controllers. In fact, our ultimate goal was to be able to rapidly reconfigure all the components of an AUV to respond to a specific demand and/or mission scenario.

4.2 Modular Building Blocks

4.2.1 Mechanical

Probably the most obvious aspect of the modularity of our building blocks comes from the design of the hull sections. In order to assemble AUVs from modular components and achieve an overall smooth profile, the blocks have matching edges and constant cross sections. In our case, we have chosen to design modules with 200mm of outer diameter. This dimension is a good tradeoff between a small enough size to result in a manageable vehicle and a large enough size to accommodate electronics in dry compartments and to support a wide range of wet sensors. Furthermore, there are several options of materials to be machined with this dimension, from several types of plastics to most common metals, available off the shelf in rods, in plates, or in tubes. In fact, we've taken advantage of this range of options to produce parts in several different materials: most of them were machined from polyacetal copolymer (POM-C), with some others in aluminum, stainless steel and fiberglass. Polyacetal is a high performance polymer, with a high degree of rigidity and mechanical strength that makes it an excellent weight-saving metal replacement, as it has approximately half the density of aluminum and one sixth of stainless steel (1.4 vs. 2.7 vs 8.0, respectively). The yield strength is the stress at which deformation is no longer elastic and becomes plastic, and POM-C has even a slightly better figure than aluminum (65 vs. 55). In addition to the weight reduction, the use of plastics completely avoids corrosion, which is critical in the marine environment. There are many types of plastics readily available, at reasonable prices, in different sizes and shapes, but compared to more common plastics like nylon or other polyamides, POM-C absorbs very little moisture, which means that the parts have very good dimensional stability in water. It is also very easy to machine, presenting no particular health hazards, and in fact many

Table 4.1: Relevant mechanical properties of materials for AUV parts. Note that values may change slightly depending on manufacturer.

Material Property (units)	**A4 (AISI 316) St. Steel**	**6061 Aluminum**	**POM-C**
Density (kg.m^{-3})	7.99x10^3	2.70x10^3	1.41x10^3
Young's Modulus (GPa)	190	69	2.7
Yield Strength (MPa)	205	55	65
Elongation at Break (%)	50	25	30

of the parts were machined in house, while others were ordered in local machine shops. Table 4.1 shows some physical properties of POM-C as compared to 6061 aluminum and A4 (or AISI 316) stainless steel, two examples of materials commonly used for machining AUV parts, including pressure housings. Although most of the characteristics of POM-C do naturally differ from the metals', we can even take advantage of seemingly worst figures (for example the Young's modulus denotes a low stiffness), to produce parts with very good resilience and ability to recover shape after impact.

All mechanical parts were designed using a 3D CAD software. The ability to have a CAD model of all the parts is essential to progress with the overall design and virtually assemble different components before actually fabricating them. It is also fundamental to prepare the integration of new components while waiting for part delivery, which can take a very long time for many underwater equipment. Fortunately, many vendors of these equipment provide precise 3D models of their systems that can be integrated into the other designs, resulting in a very realistic and accurate representation of the assembly. Furthermore, the software produces very accurate physical data (weight, centers of mass and buoyancy, etc.) about the components, that are critical to the estimation of the parameters of the dynamical model and to the design of motion controllers.

The modules were designed with a matching, repeatable, male/female coupling system, following a *sectional* modular architecture, which means that each section can be attached to each other in any order, extending the coupling system (see Ulrich (1995) for different types of modularity). They are fixed in place by radial set screws, equally distributed along the perimeter to enable rotation of each module in steps of 90 degrees. The repeatability of the coupling patterns helps to minimize the number of different parts and tools to assemble the blocks together. It is also helpful in terms of fabrication in computer controlled machines, since it is translated into repeated operations, saving valuable programming time. Our basic modules are divided in three different classes: pressure housings, wet extensions and end sections.

4.2.1.1 Pressure Housings

Pressure housings are sealed compartments designed to withstand hydrostatic pressure. Inside, all electronic systems can be installed as in any other standard enclosure at atmospheric pressure. Given our choice of 200mm diameter modules, our pressure housings are sealed cylinders with

the constraint of having an outer diameter of 200mm. Typically, an AUV has a single dry compartment, and the length is chosen to accommodate all computer systems, electronic boards and battery packs, while ensuring a specific pressure rating. For a given material, this pressure rating depends on the ratio between the length of the cylindrical tube and the thickness of the wall, therefore, we have to specify the inner diameter to ensure the proper thickness. A pressure housing is probably the most vital component to ensure the integrity of an AUV and therefore it is paramount to minimize the risks of failure or its consequences. If the housing crushes under pressure, all electronics will be ruined and the vehicle will sink due to the significant loss of buoyancy. The easiest way to avoid this is to over rate the design specification to account for small cracks and scratches, material fatigue and imperfections in the machining process.

Cylindrical housings are very common in oceanographic systems and the types of failure under pressure have been widely studied (see, for example, Sharp (1981); Roark and Young (1989)). Using a conservative approach, we've chosen a thickness of 12.5mm to achieve a depth rating of 200m for a tube up to 600mm long (*i.e.* a safety margin of 100% for the intended 100m of maximum depth of operation).

Note that this dry compartment is usually the main source of vehicle buoyancy, while the flooded sections are typically denser than water. Since the overall vehicle should have approximately zero weight in water, it is possible to extend the length of the pressure housing to account for additional heavy devices that may need to be installed. Naturally, such an extension has to be analyzed properly, as it reduces the depth rating of the hull. For example, the volume of water displaced by a 600mm long cylinder and diameter $d_{out} = 200$mm is about 18.9dm^3 (or 18.9 liters). Using a wall thickness of 12.5mm, a POM-C cylinder of these dimensions weights 61N, therefore resulting in a net buoyancy of 124N, or about 207N per meter.

Both ends of the cylinders are terminated with flat end caps, attached to the cylinders using radial set screws. Flat end caps are a very common sealing solution for cylinders with electronics, as they are easy to machine, and provide a good surface to install connector bulkheads and sealed penetrators. In our case, we have designed the end caps with 9 bore holes pre-drilled for standard underwater bulkheads or penetrators with 7/16"' thread, an industry standard for miniature circular bulkheads. We have also designed dummy plugs that are installed in any unused holes to guarantee sealing. To avoid any risks to the integrity of the pressure housing, there are no holes or protuberances in the cylinder, and all connections to the internal electronics are done through the end caps.

The possibility of a broken seal is a major concern in the design of a pressure housing. If this happens, the best chance of saving the vehicle and electronics is to detect it early, avoid the deployment or recover the vehicle as soon as possible. There are many possible causes of leaks, some occurring during vehicle maintenance and/or assembly and others during operation. We have addressed these possibilities by a mix of mechanical preventive considerations and safety mechanisms.

Figure 4.1: Three o-rings ensure redundancy in sealing of the pressure housings.

O-rings provide very inexpensive and effective seals, but they have to be seated on smooth surfaces, as any scratch can become a path for water ingress. In our end caps, we have designed 3 o-ring grooves, providing redundant sealing and alternatives for assembly if one of the surfaces gets scratched (figure 4.1). We have also designed a vent/vacuum port in one of the end caps, which is simply a small closeable port. This port is open during battery charging, to exhaust any gas build up, and also when the end caps are installed, to provide an escape route for the air inside the cylinder. Upon the installation of the end caps, a vacuum pump can be connected to this port to test all the seals. The procedure is very simple, just requiring a reduction of the internal pressure to detect if the seals are able to hold it for some time. If there is any broken seal, it will be signaled by an increase in the internal pressure towards atmospheric pressure. Otherwise, the test is concluded successfully, the internal pressure goes back to atmospheric pressure and the port is sealed with a small plug. Note this procedure should be performed immediately before deployment.

In the event of a leak occurring during an autonomous operation, the chances of saving the vehicle and the electronics depend directly on the response time, and it is paramount to detect any water ingress as early as possible. In order to do it, we have installed 2 water detectors in the lowest part of the dry compartment, close to the end caps. They have small sponges to absorb small quantities of water, therefore promoting the detection from any droplets passing by and, at the same time, delaying possible damages in electronics. Another source of liquid water inside the hull is condensation and to prevent it we use small silica bags to absorb any moisture that may had entered before sealing.

In a mono-hull design, especially with a relatively small diameter, it is important to lower the center of mass to separate it from the center of buoyancy and increase roll and pitch stability (note that the center of buoyancy only depends on the submerged volume, therefore is not affected by the arrangement of the dry components). For this reason, the batteries are typically located at the bottom, while the rest of the electronics occupy the top part of the available volume. Inside the cylinder, a longitudinal frame eases the task of installing electronic boards and batteries. The frame is assembled using three COTS aluminum structural profiles, with a 20x20mm square section, and weighting approximately 4N per meter. There are many accessories for these profiles that provide

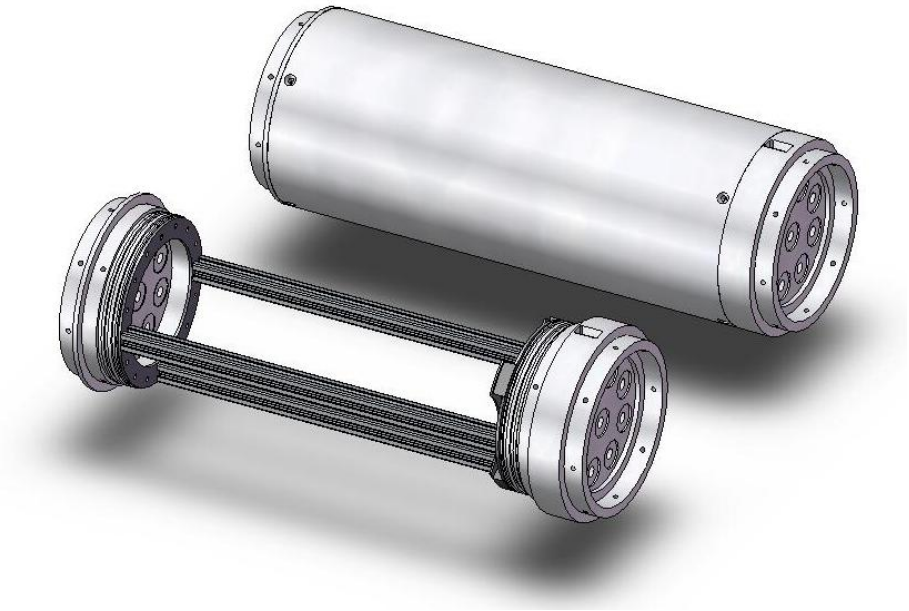

Figure 4.2: 3D models of dry compartments, showing the internal frame for the installation of electronic boards and batteries. Both end caps have bore holes for bulkhead installation and male terminations to accept other modules.

multiple options for mechanical attachments and cable routing.

The internal frame is typically attached to one of the end caps. In order to close the hull, the frame slides inside the cylinder and then the other end cap is attached, sealing the pressure housing. After assembly, both extremities of a pressure housing have exactly the same mechanical termination – a male protuberance with equally spaced threads along the perimeter. This means that the orientation of the pressure housing can be reversed without any significant impact on the rest of the vehicle. The full vehicle can be assembled by attaching extension modules to both ends, including sensors and actuators (fig. 4.2).

4.2.1.2 Wet Extensions

There are two typical ways to mount sensors and actuators in an AUV. One is to use fully waterproof systems with underwater connectors to provide power and communications. The other is to have a hole in the pressure housing and install the sensor flushed, requiring only to seal this interface. In our approach, all sensors and actuators in direct contact with water have to be fully waterproof, in order to limit the damage in the event of a mechanical break (due to a collision, for example). These devices are held in position along the AUV by wet extensions – an assortment of water flooded cylindrical rings. These sections share the common 200mm outer diameter constraint of the whole AUV, and they propagate the mechanical interface, by having a male termination at one end and a female termination at the other. Therefore, they can be stacked, interchanged, rotated, or attached directly to the dry compartments, resulting in a great variety of possible combinations.

Figure 4.3: Examples of water flooded extensions used mainly to hold sensors and actuators in the hull.

Since the wet extensions are flooded, there are not very stringent requirements in terms of materials to be used for producing such modules. The main requirements are mechanical stiffness to hold the whole structure together and dimension stability in water (*e.g.* minimal water absorption) to ensure proper terminations and mechanical compatibility. Once again, POM-C provides a good compromise of characteristics and it's been used extensively for the majority of wet extensions. Typically, the modules are machined from a COTS tube, with radial cavities to hold the physical devices in place.

A wet extension can be machined for holding a single underwater device, maximizing modularity, or it can be machined for a combination of devices, reducing dimensions. In our case, we tend to combine devices in the same extension whenever they are present in the same vehicle configuration. For example, most AUV configurations require an acoustic transducer for navigation, an altimeter for measuring height above bottom and a strobe light for safety, therefore we combine these in a single extension. Until now, several modules have been designed and machined (see fig. 4.3), ensuring a great variety of functions:

- Through-hull thrusters for vertical or lateral motion;
- Communication devices, such as radio modems or Wi-Fi, when the vehicle is at the surface;
- Navigation devices, such as GPS receivers and acoustic transducers;
- Scientific payload, including various types of sensors (cameras, echo sounders, CTD or optical sensors);

- Mechanical reinforcement rings, for example to provide lifting points;
- Simple hollow sections to provide additional flotation, when filled with syntactic foam.

All wet extensions machined from POM-C have an internal diameter of 160mm. Once these extensions are stacked together, all cabling to/from the underwater devices pass through the middle cavity to connect to the corresponding end caps of the pressure housing. The 2cm wall thickness provides a sufficient depth for the threads in the male termination and also a sufficient wall for holding the wet devices in place. However, such an internal diameter results in relatively heavy rings. For each meter, the net weight (in fresh water) can be easily computed as:

$$W_w = \frac{\pi}{4}\left(d_{out}^2 - d_{in}^2\right)\left(\rho_{POM} - \rho_{H_2O}\right)g = \frac{\pi}{4}\left(0.2^2 - 0.16^2\right)\left(1410 - 1000\right)9.8 = 45\text{N} \qquad (4.1)$$

where d_{out} and d_{in} are the external and internal diameters of the rings, and ρ_{POM} and ρ_{H_2O} are the densities of POM-C and fresh water, respectively.

4.2.1.3 End Sections

As the name suggests, the end sections are specially designed modules to provide both the bow and the stern of an AUV. They are water flooded sections, with a ellipsoidal shape, providing a basic hydrodynamic mechanism to reduce motion drag. Since they provide the final terminations to both stacks initiated at the main pressure hull, they only have a female mechanical interface.

The tail sections can support multiple configurations of propulsion thrusters, that can be re-arranged depending on power requirement and maneuverability. The thrusters are physically attached to a small ring, where the final ellipsoid is also fixed. In most cases, the nose sections are also simple skins just to ensure a laminar flow around the overall hull, while, in some exceptions, they can be used to install special sensors (for example, forward looking sonars). Figure 4.4 provides some examples of these end sections.

Since these sections have a revolution shape, they can easily be machined in a typical machine shop. However, this operation requires the removal of about 95% of material to achieve a relatively thin and light skin from an original solid rod, which makes the machining operation quite expensive, both in terms of material and labor cost. Therefore, we have taken advantage of the same overall shape of both ends to design a single mold for producing fiberglass end sections, with a significant save in manufacturing cost. Naturally, the same mold can be reused to produce sections based on different materials, like carbon fiber or Kevlar®.

4.2.1.4 Crossbeams

A simple vehicle arrangement can be assembled as a mono-hull, with a few wet extensions stacked on both sides of a pressure housing, and terminated with a nose cone and a tail section. However, for some applications it may be required to have a multi-hull system, by mechanically connecting

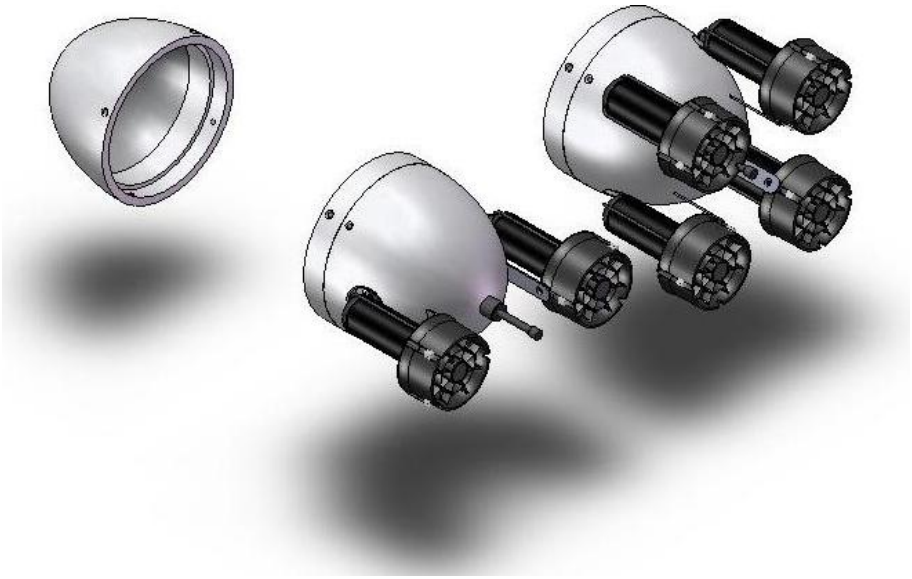

Figure 4.4: Examples of end sections, showing a simple nose cone and different types of horizontal thruster assemblies. Note the connector in the middle of the thrusters, used to charge the batteries once the vehicle is recovered.

multiple of these simpler bodies. We have considered two options for the relative position of the main revolution axes of these bodies and we have designed two types of crossbeams to assemble them: a *straight* crossbeam, used to assemble bodies in the same horizontal or vertical plane; and a *diagonal* crossbeam, used to assemble bodies that have both a vertical and a horizontal offset. With only these two types of crossbeams, it is possible to assemble many configurations of multiple-bodies vehicles, as can be seen in the examples of figure 4.5.

In a typical multi-hull configuration, there is a need for interconnection cables between the main bodies, and the crossbeams are a natural routing path for these cables. At the same time, any crossbeams connecting cylindrical bodies are naturally seen as *handles* to lift the whole vehicle, even though they might be fragile. For these reasons, the crossbeams have been designed with relatively large dimensions and a groove to accommodate the underwater cables. This facilitates routing and helps protecting the cables from scratches and entanglement, while reducing overall motion drag.

One of the reasons for designing a multi-hull system is to enlarge the vehicle footprint with a small increase in overall weight. Such an enlargement may be required, for example, to install large sensors that do not fit within the diameter of the tubes. The crossbeams are natural places to attach such sensors, either directly or by designing mechanical adapters to support them.

4.2.1.5 Other Mechanical Components

Apart from these major modules, some other mechanical parts are needed to assemble an AUV, such as small pieces to attach sensors, batteries or electronic boards. Whenever possible, we try to

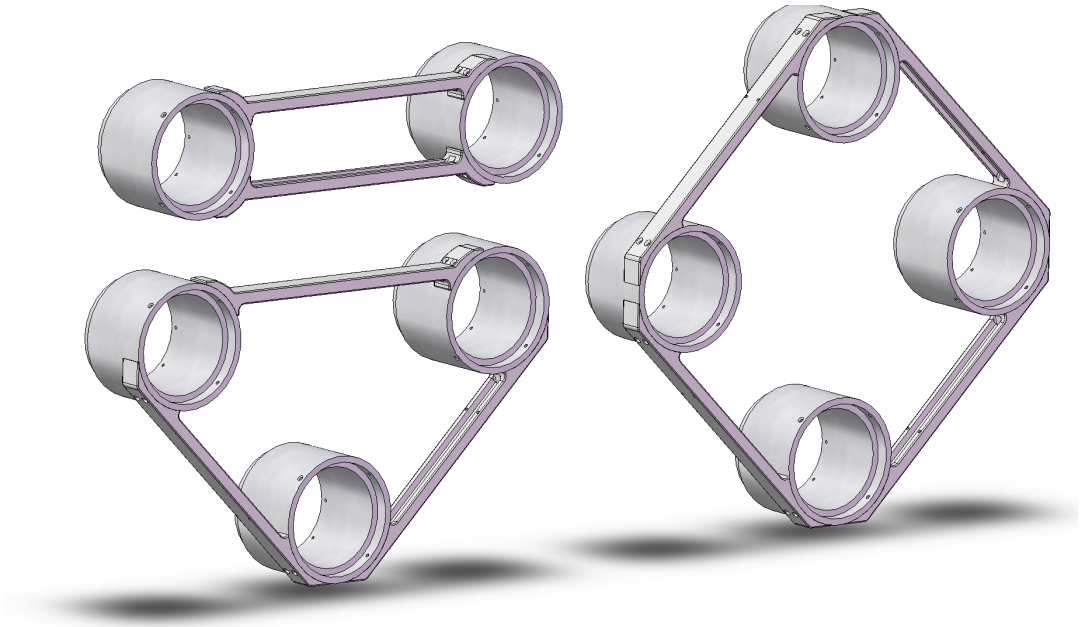

Figure 4.5: Illustration of possible configurations of multi-hull systems using only *straight* and *diagonal* crossbeams. Note the inner grooves for cable routing.

use COTS parts, but in some occasions we've had to manufacture then from a variety of materials, or printed in ABS plastic, directly from the CAD software using a 3-D printer.

Finally, one final set of mechanical parts that is fundamental to assemble an AUV concerns the adjustment of weight and buoyancy. The easiest way to increase weight and adjust pitch and roll is to use lead parts either in dry or flooded sections of the vehicle. These are available off the shelf in a great variety of sizes, from small fishing weights to large diving belts. However, most of the times it is necessary to reduce overall weight, or to compensate it by increasing buoyancy. This can be achieved by inserting flotation modules inside flooded sections, usually close to the heaviest components, in order to keep each module as close to neutrally buoyant as possible.

There are several companies offering syntactic foams in large blocks that can be machined to the required shapes. These foams are specially made materials that withstand pressure without changing dimensions, with a density lower than the water's. There are different formulations for these materials, depending on depth (*i.e.* pressure) rating and, naturally, the deeper they need to go, the denser the material gets. In our case, we are using a foam with a Hydraulic Crush Point of 30 Bar and a density of 200kgm^{-3}, able to withstand a maximum operational depth of 190m. We can use a disc of this material to fill part of the internal cavity of a POM-C ring, resulting in a maximum flotation, per meter, of

$$B_w = \frac{\pi}{4} d_{synt}^2 \left(\rho_{H_2O} - \rho_{synt}\right) g = \frac{\pi}{4} 0.16^2 \left(1000 - 200\right) 9.8 = 157\text{N} \tag{4.2}$$

Figure 4.6: Example of a disc of syntactic material inserted around the electrical connectors of an endcap. The flotation material fills the voids around the bulkheads and do not perturb connector mating.

where d_{synt} is the maximum diameter of the flotation disc, and ρ_{H_2O} and ρ_{synt} are the densities of fresh water and the flotation material, respectively.

As a standard procedure, we always fill the voids around the electrical connectors with a disc of syntactic material, to compensate for the large weight of the end caps. The same applies to the thruster section, typically one of the heaviest of an AUV, where a flotation block fills the voids inside the ellipsoidal skin. Figure 4.6 shows an example of a disc of syntactic material inserted around the electrical connectors of an endcap.

4.2.2 Electronics

The core of an AUV electrical system relies on a power management module and a computational system with many interfaces. In terms of electrical connections, there is a large set of separate boards with specific functions, interconnected by board to board cables, instead of coupling multiple boards into a single *motherboard*. This slightly complicates the assembly by cluttering the limited space with cables, but simplifies debugging and, above all, greatly facilitates any upgrades or reconfigurations.

The power management subsystem deals with the conversion, distribution and monitoring of energy to all electrical devices, following a simple architecture as depicted in figure 4.7). The rechargeable batteries are installed inside the pressure housing, together with the corresponding monitoring boards to measure charge and discharge rates, as well as charge level, and communicate them to the main CPU using a serial interface. The battery voltage is converted to an adequate level for the thrusters and several low-voltage levels required for the on-board devices, and distributed as power buses protected by fuses. When the vehicle is on deck, batteries can be recharged without opening the housing, just by connecting a power supply to a connector located in the tail section. Although it has not been implemented yet, the system is also prepared for the possibility of charging at an underwater docking station.

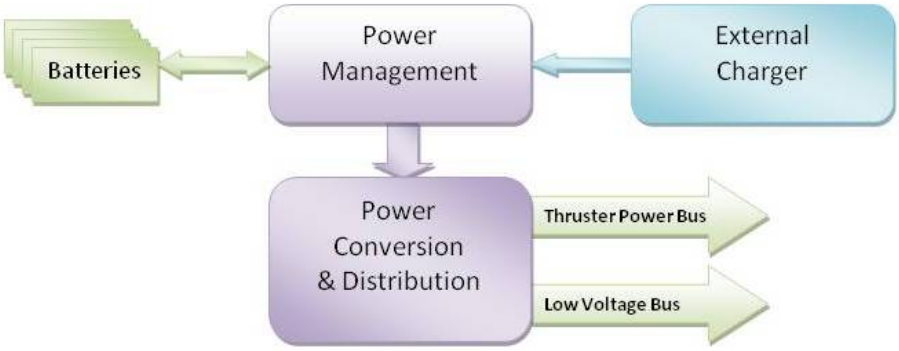

Figure 4.7: Overview of on-board power management.

There are several technologies currently available for rechargeable batteries, and several specialized vendors providing off the shelf solutions, both for batteries, and for power monitoring and conversion boards. We've assembled different configurations, mainly based on Li-Ion technology, with energy from 400Wh to 800Wh, always following the same architecture. Whenever an alteration is necessary, to make an upgrade in terms of energy or power capability or to replace any defective battery, all other subsystems and interconnections remain unchanged.

Our on-board computational systems are based on PC-104 stacks, an inherently modular architecture with a multitude of COTS solutions. PC-104 is a well established architecture, widely used in industry, with many vendors continuously releasing new solutions while supporting old designs. A typical system is composed by a power supply board, a main processor board, and additional boards to interface with peripherals, such as health monitoring systems, actuation devices, and navigation and payload sensors. A flash disk is used to store both the on-board software and also the data collected during operations.

There are many electrical subsystems on-board an AUV, that are connected to the computational system and require some form of power supply. Therefore, there are usually two cables dedicated to each subsystem – one that carries power at the required voltage level(s) and another that is used for data exchange with the proper interface port (USB, RS232, RS485, TTL-serial). If the system is located outside the pressure housing, these two cables are fused together into a single connector bulkhead, so that the external device can be connected using a single underwater cable.

Our typical approach to on board electronics is to adopt COTS subsystems, since there are many vendors offering robust solutions for OEM devices that we install inside the pressure housing, for example embedded PC boards, battery management systems, and inertial sensors. However, in the case of subsystems that need to withstand pressure (because they need to be installed outside the pressure housing), the options are greatly reduced and the price increases dramatically. In many situations, such subsystems do not exist at all, or their specifications do not comply with

Figure 4.8: A combined GPS receiver and Wi-Fi *pen* for surface localization and communication, assembled from OEM electronic boards enclosed in polyurethane and reinforced with fiberglass.

our requirements, therefore we need to develop custom solutions. In some of these cases, our customization is simply a mechanical protection of an OEM electronic device to withstand pressure and avoid water ingress. This includes, for example, devices for radio communications (including Wi-Fi *pens*) and GPS receivers, that are extremely useful when a vehicle is at the surface. Our procedure is to use underwater cables for the electrical connections, and to enclose these devices with epoxy resin or polyurethane resistant to salt water and then cover it with a fiberglass skin. Figure 4.8 shows an example of a combined GPS receiver and Wi-Fi *pen* enclosed in water resistant polyurethane and reinforced with fiberglass.

In other cases, the custom solution may include simple electronics to be installed inside the pressure housing (for example, leak sensors to detect water ingress) or a combination of electronics that are installed in the pressure housing with an external component that has to withstand pressure. One example is the strobe light, where a ring of ultra bright LED's is placed on the top part of the hull to facilitate searching and provide basic visual information about the status of the vehicle, while the driving electronics interfaces with the main CPU is placed inside the pressure housing. This separation minimizes the size and complexity of the external component and facilitates improvements, providing another example of the modularity of the whole system.

Finally, a special case concerns the acoustic navigation system, where all electronics were developed to provide the ability to transmit and detect arbitrary signals. Although there are some commercial solutions for acoustic ranging, they are extremely expensive and with limited capabilities. On the other hand, we have been developing our own acoustic transmitters and receivers for over 15 years (Cruz et al. (2001)), that provide us a great flexibility of use, both as basic blocks for standard navigation and also as research opportunities in related domains as underwater communications. These boards are located inside the pressure housing and interface with a T257 acoustic transducer, from Neptune Sonar Ltd., located in the vehicle hull. This on board system is complemented by a set of acoustic beacons previously deployed in the operation area, whose position is known to the AUV navigation software (see appendix A for details on these beacons and the

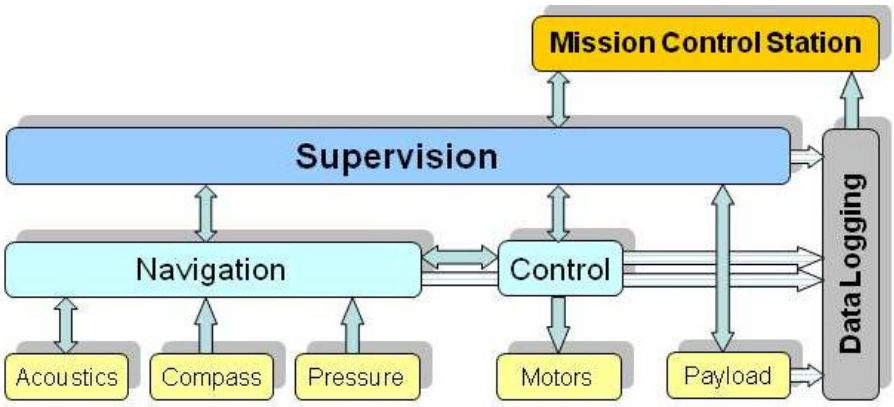

Figure 4.9: Overview of on-board software architecture, with a hierarchical organization. The bottom modules represent the interface with the physical devices while the upper modules represent increasing data fusion and processing.

whole acoustic system).

4.2.3 On-board Software

The fundamental task of the on-board software of an autonomous mobile vehicle is to manage the execution of a *mission*, here defined as a set of maneuvers. For each of these maneuvers, the vehicle needs to estimate its position based on a set of navigation sensors, and issue commands to the actuators based on some control algorithms. In parallel, the on-board software may also have to deal with incoming data from the payload sensors, that may require some sort of pre-processing before being logged.

In our implementation, each on-board software suite is composed by a set of independent modules (CPU *processes*) that exchange data using a message passing mechanism based on User Datagram Protocol (UDP) (Cruz and Matos (2008); Matos and Cruz (2009)). These modules are hierarchically organized, with the hardware interface modules at the lowest level (Fig. 4.9). On top of those, two modules - navigation and control - are responsible to provide in real time the position and attitude estimates of the vehicle and to implement the control laws that ensure the adequate behavior of the vehicle, respectively. At the top level, a supervision module is always monitoring the vehicle behavior, scheduling appropriate maneuvers according to a mission plan or to an external command, and taking emergency behavior when required.

Hardware interface modules act as an abstraction layer. Sensory data provided by these modules is transmitted using standard data formats, thus insulating the navigation subsystem from the individual characteristics of the specific devices present in a given configuration of the system. Besides the definition of the data provided by a particular sensor (such as yaw angle, or surge velocity, for example), additional information about the measurements are also taken into account, namely the update rate and a characterization of the measurement error, as well as information related to the relative location and orientation of the sensing device. This makes the whole system

highly modular, greatly simplifying the replacement or the inclusion of a new sensor. When that occurs, besides including the corresponding interface module in the on-board computer, it is only required to include in a configuration file the major characteristics of the measurements provided by the sensor, as described above.

The navigation module, based in an extended Kalman filter as described in Cruz and Matos (2008), is prepared to process different measurements - GPS positions at the surface, range measurements to acoustic beacons located in the operation area, velocity data with respect to the water column or to the sea bottom provided by a Doppler velocity logger or any other sensor, accelerations and angular velocities provided by a inertial system, depth data from a pressure cell, or attitude related data from a magnetic compass. The filter internal structure depends on the current sensor package of the vehicle and is automatically defined from the characteristics of the different sensors.

On the other hand, actuation data transmitted from the control to the hardware interface modules is defined in terms of the forces that each thruster or control surface should produce. This creates a uniform interface between the control module and the low level modules contributing to the independence of the control subsystem with respect to the actuators hardware. Similarly to the case of a new sensor, the inclusion of an actuator in the system (for example, a thruster or a control surface) requires not only the inclusion of the appropriate interface module in the on-board computer but also the standard characterization of the actuator in a proper configuration file. This characterization comprises the location and orientation on the actuator in the vehicle, the limits of actuation, the dependence of the actuation with the velocity of the vehicle and also its maximum update rate and a characterization of the actuation error. These characteristics are then used to the control subsystem to perform thrust allocation and define at each moment the required force from each thruster of control surface. A specific actuation package might impose constraints on the mobility of the vehicle that might turn certain elementary maneuvers unfeasible. Although it is possible to automatically determine the set of feasible forces and torques, and from it evaluate in real time the feasibility of a given elementary maneuver, no automatic process to perform this task in currently implemented in the on-board software. Instead, the set of feasible maneuvers in defined manually for each specific configuration of this class of AUVs, with just an automatic validation by the on-board software.

In terms of payload sensors, there is a *device driver* associated with each sensor that needs interfacing with the on-board software. Typically, such a driver manages the requests for new data, if needed, and may perform some filtering on data before logging into disk, according to settings maintained in a sensor configuration file.

All the on-board software was developed in C++ and runs on Linux kernels, although it should be straightforward to run on different operating systems. These modules have already been combined in multiple vehicles and with numerous configurations (sometimes even in the same operation) with minimum overhead.

4.2.4 Modeling and Control

The AUV control literature is vast and implements numerous control methods to minimize some *cost function* (distance to target, distance to trajectory, etc.). In the same way as for the software architecture and the mechanical design, our intention was that the controllers of the vehicles were modular, in the sense that they could be switched on or off, or swapped by another, during a mission or between missions.

Our control layer is composed of two main *sub-blocks* that include dynamics and kinematics stabilization. The idea of the kinematic stabilization is to abstract from the dynamics and facilitate the derivation of the control law. Anyway, this control layer is based on the current *state* of the vehicle and produces outputs to feed the actuators, therefore it is easy to replace by a different strategy.

When compared to linear controllers, nonlinear controllers for underwater vehicles generally provide superior performances for a broader range of operation. Most of these require a quite precise model of the vehicle dynamics in order to generate the proper thrust and possibly fin angle commands and hence create smooth and precise trajectories. Sliding mode controllers admit larger model errors but at the expense of more *abrupt* control with natural consequences on trajectories, power consumption, and mechanical stress of components. Our current approach implements a Lyapounov direct method at the inner loop level. Roughly speaking, this nonlinear control method feedforwards the external forces acting on the vehicle body and simultaneously compensates for errors on the velocity. Feedforward is obtained by means of estimation of forces acting on the vehicle as it is not feasible to measure them in real time. Such an estimation can use inertial measurements like linear/angular velocities and accelerations. The design of specific controllers for the vehicles is beyond the scope of this work, and has been thoroughly described in other manuscripts (Ferreira et al. (2010, 2011, 2012b,a)).

We have considered a *basic* set of behaviors, or elemental maneuvers, that can handle most of the trajectory needs in typical missions, therefore we have designed a generic control system so that each robotic platform is able to perform the following:

- **Line-following** – The vehicle tracks a line, while keeping a certain velocity, that can be varying in time;
- **Circle-following** – Given a point and a radius, the vehicle tracks the respective circumference;
- **Target tracking (station-keeping)** – The vehicle tracks a (possibly time-varying) point and remains stationary;

In addition to these behaviors and to reinforce the modularity of the control layer, the controllable degrees-of-freedom (DOF) can be commanded by any external entity. A composition of pose and/or velocity references can be set externally, thus allowing to create complex motions without efforts on dynamics control developments. The several controllers intrinsically decouple

the several controllable DOFs. Furthermore, the references can be expressed in both the inertial reference frame or the body-fixed one.

Using the above mentioned behaviors, any type of complex trajectory can be followed by setting a coherent sequence of instructions. This can be set either by using a static mission script or by instructing the vehicles on-the-fly via a communication link. From the robotics point of view, the maneuvers can be seen as a set of feasible tasks.

The general model of an underwater vehicle is a second order, six-dimensional equation that relates the applied forces and moments with the angular and linear velocities. Inspired by the notation in Ferreira et al. (2012a) (see also Fossen (1995)), the general kinematics and dynamics expressions are respectively given by

$$\dot{\eta} = J(\eta)\nu, \tag{4.3}$$

$$\dot{\nu} = A(\Theta,\nu)\nu + g(\Theta,\eta) + \tau(\Theta), \tag{4.4}$$

where $\eta \in \mathbb{R}^6$ is the pose vector, $\nu \in \mathbb{R}^6$ is the velocity vector, $J \in \mathbb{R}^{6\times6}$ is a matrix that maps the linear and angular velocities expressed in the body-fixed frame into the earth-fixed, inertial referential frame. The matrix $A \in \mathbb{R}^{6\times6}$ results from the hydrodynamic forces applied on the body of the vehicle when it is moving at a velocity ν. The term $A(\cdot,\cdot)\nu$ constitute the effect of added mass, Coriolis, centripetal and viscous damping forces and moments. The vector $g \in \mathbb{R}^6$ includes the effects of the restoring forces and moments. The actuation force and moments are given in the vector $\tau \in \mathbb{R}^6$, expressed in the body-fixed frame.

Note that the model is parameterized by a set of parameters $\Theta \in \{\Theta_{AUV_1}, ..., \Theta_{AUV_n}\}$ that are specific of each vehicle. This means that the expressions for the control laws can be exactly the same for the velocity stabilization. The only concern in implementation is related with the selection of the corresponding set of parameters Θ, which we believe is an important feature to achieve rapidly reconfigurable systems. Moreover, this allows saving a large amount of time when porting the source control code into a new vehicle. Notwithstanding, a strong effort is required for the derivation of the hydrodynamics coefficient with enough accuracy so that the model is precise enough to allow the desired control performance.

Hydrodynamics coefficient can be obtained either by CFD software, empirical and semi-empirical formulas, or experimental testing. The determination using the first method implies intensive simulation of the vehicle dynamics using simulated particles of water colliding with the vehicle body. The hydrodynamics coefficients can therefore be determined by assessing the forces, the velocities and the accelerations. The derivation of the coefficients based on formulas remains a valid alternative where an extensive calculus exercise has to be carried out to obtain the final model (Prestero (2001)). Both CFD and formula-based models are affected by errors due to very complex dynamic water simulation in the former, and approximations and observation-based formulas in the later. Experiments can provide very precise coefficients but imply the use of specialized tools and sensors such as the ones used in tow tanks (Prestero (2001)), and they are usually very expensive.

The MARES and TriMARES hydrodynamics coefficients were derived based on empirical and semi-empirical formulas found in Prestero (2001); Faltinsen (2005); White (2002); Hoerner (1965). See Ferreira et al. (2010) and Ferreira et al. (2012b) for the complete list of coefficients. Since both vehicles have the same planes of symmetries, the parameter sets Θ_M and Θ_T have the same number of hydrodynamic coefficients. In order to determine these coefficients, we've considered a set of modules that includes ellipsoidal noses and tails, cylinders and motors. The protuberances are the antennas, the acoustic transducer, the altimeter and the strobe light. All these are characterized by their dimensions and their positions in a body-fixed frame. It should be noted that whenever a change on the configuration is made, the model may have to be re-determined, even under a simple swap of modules. It is very likely that such a change may alter the position of the centers of gravity (CG) and/or buoyancy (CB), even if the length or the positions of the protuberance have not changed, which implies a considerable effort on computation. Hence, we have implemented a program that accepts the length of the vehicle, the positions and the dimensions of the protuberances (including the motors), the through-hull dimensions and positions, the CG and CB positions as arguments. Therefore, the determination of the hydrodynamic coefficients for any configuration using the modules (of any length) and the protuberances considered is only subject to the definition of a relatively small set of parameters.

4.3 The MARES AUV

MARES, or *Modular Autonomous Robot for Environment Sampling* (fig. 4.10), is a 1.5m long Autonomous Underwater Vehicle (AUV), designed and built by the Ocean Systems Group, at the University of Porto. The MARES AUV has been conceived following a long experience in the customization and utilization of various small AUVs, which has provided the essential know-how to build a modular open system, incorporating design innovations, and at a small fraction of the cost of a commercial solution. Like all other AUV systems, MARES can be programmed to follow predefined trajectories, while collecting relevant data with the on-board sensors, up to a depth of 100 meters. However, unlike similar-sized systems, MARES has no control surfaces (*fins*) to control pitch and heading. Instead, two vertical thrusters allow for purely vertical motion in the water column and the horizontal propulsion is also provided by two thrusters, resulting in a vehicle that has no minimum forward velocity.

In this section, we describe how the MARES AUV was fully assembled from the modular building blocks described in the previous section. In fact, both the modularity concept and the vehicle assembly evolved in parallel when we started our AUV program. The vehicle is fully functional and is being routinely used in operational missions since late 2007 (Cruz and Matos (2008); Matos and Cruz (2009)). The major application areas include pollution monitoring, scientific data collection, sonar mapping, underwater video imaging or mine detection. This wide range of applications requires a great variety of configurations, demonstrating the versatility of our approach. In 2012, a custom order has been requested by a Brazilian R&D group to INESC

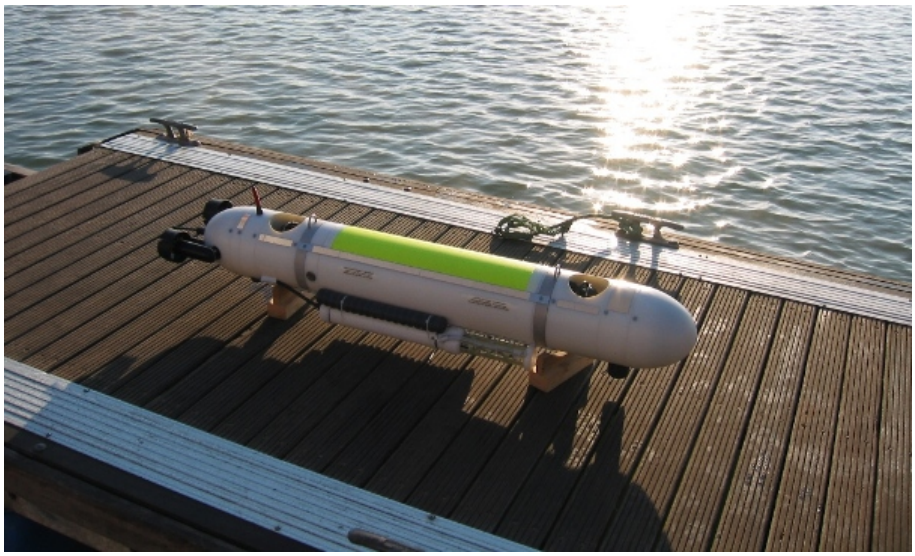

Figure 4.10: The MARES AUV with an externally mounted CTD, ready for the first ocean deployment off the Portuguese coast, November 2007.

TEC, for the delivery of a MARES AUV to conduct experiments in navigation and control, and it was shipped in May 2013.

4.3.1 Vehicle Requirements

MARES is a small size, torpedo-shaped AUV, developed in 2007 (Cruz and Matos (2008)), and the main drive for its design was to develop an open architecture system to carry out research activities in underwater robotics. In particular, we were interested in environmental sampling in coastal waters, and so we settled on a 100 meter depth rating. In terms of energy requirement, there is currently a wide variety of sensors for *in-situ* measurements, with reduced size and power consumption. At the same time, battery capacities are getting higher, in smaller packages, and there is a great pressure to proceed further in this direction, to power all sorts of mobile devices. There are also other emerging technologies for electrical power supply (fuel cells, for example). We then decided to start by relaxing the battery endurance requirement to a few hours, with the belief that in the near future some of these technologies will allow for a considerable increase in energy densities.

Mission performance was also considered, and this resulted in a variety of other requirements. In terms of mobility, for example, our approach somehow diverges from the vast majority of similar-sized solution, where the main emphasis is given towards increasing vehicle velocity. In our case, we are also (maybe more) concerned with the ability to operate in confined spaces, at slow speeds down to $0 ms^{-1}$ if necessary. Thus, one of the key requirements regarding motion performance was the possibility of hovering in the water column, which is a feature seldom seen in small vehicles.

Table 4.2: Summary of MARES AUV characteristics, with physical dimensions corresponding to the vehicle first demonstrated at sea in November 2007 (figure 4.10).

Length	1.5 m
Diameter	20 cm
Weight in air	320 N
Depth rating	100 m
Propulsion	2 horizontal + 2 vertical thrusters
Horizontal velocity	0–2 ms^{-1}, variable
Vertical velocity	0–0.5 ms^{-1}, variable
Energy	Li-Ion batteries, 600 Wh
Autonomy/Range	about 14 hrs / 50 km @ 1ms^{-1}
Scientific payload	CTD, fluorometer, turbidity, bathymetry, video with light, sidescan sonar

Regarding mission programming, the vehicle should be able to follow predetermined trajectories, in simple lawnmower and/or *yo-yo* patterns, but the software architecture should also allow for unconventional control and guidance schemes, based on real time processing of information from payload sensors. These requirements should be mapped into a comprehensive library of elementary maneuvers, using a simple mission programming environment and a user friendly interfacing with the vehicle and with all mission support equipment. This ability to incorporate alternative control and guidance schemes was another reason (together with hovering capability) for developing our own robotic solutions, given the strict set of behaviors/commands allowed by typical commercial vehicles.

Finally, but surely not the least important, overall system safety should be ensured. This includes vehicle tracking capability during the missions, as well as redundant tracking and recovery procedures at the end. Note that our concern is not restricted to the physical assets that we deploy, but also to the valuable data they convey at the end of a mission.

MARES configuration can change significantly according to the application scenario, so that it is difficult to define what is a *standard* configuration. In table 4.2 we summarize the main characteristics of the AUV, with the physical dimensions referring to the version that was first demonstrated at sea in November 2007, as can be seen in the photo of figure 4.10.

4.3.2 Mechanical Assembly

MARES was assembled with the mechanical building blocks described in the previous section and all the vehicle design was available in CAD before actually producing or ordering the first parts (fig. 4.11), which was useful to start estimating many physical parameters of the vehicle at an early phase of the project. A few small parts were machined in aluminium and others in stainless steel, but the majority was machined out of polyacetal copolymer (POM-C) rods and tubes, in a local machine shop.

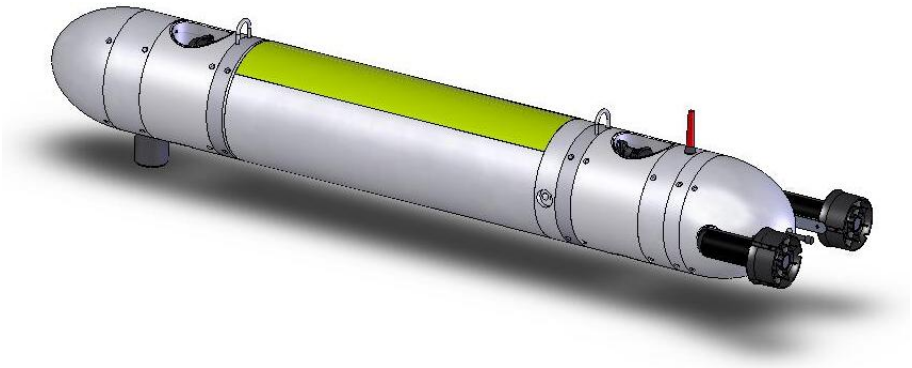

Figure 4.11: A 3D CAD model of the first version of MARES, designed in 2006 and operational since November 2007.

The vehicle hull evolves around a central watertight cylinder, where all electronic boards are installed, with the battery packs located at the bottom to lower the center of mass. Each end cap has 9 holes to accommodate standard bulkhead connectors and at the moment there are still several unused, sealed with dummy plugs. To simplify the design, this is the only watertight enclosure and therefore all other equipment has to be waterproof. The other polyacetal sections are designed to carry wet sensors and thrusters and they are fully interchangeable. This allows for very easy sensor swapping and/or repositioning, or even to test different configurations of thrusters.

The overall vehicle shape resembles that of a torpedo, with ellipsoids both at the nose cone and at the tail. This configuration is very simple to construct and allows for the vehicle length to be easily extended, as compared to other hull shapes without constant cross-sections. The central cylinder provides most of the vehicle flotation and it is also possible to increase its length, for example if more batteries are needed.

In order to minimize the power required to change depth, the vehicle weight in water should be zero. In practice, however, it is usually kept slightly negative for safety reasons. Whenever necessary, syntactic foam is machined and inserted in wet compartments to compensate for any new board or device that is installed.

Typical small-size AUVs use vertical and horizontal fins to adjust heading and pitch, but this requires a minimum forward velocity for the control surfaces to be effective (Anderson and Crowell (2005); von Alt et al. (1994)). On MARES, four independent COTS thrusters provide attitude control both in the horizontal and in the vertical plane. Two horizontal thrusters located at the tail control both forward velocity and rotation in the horizontal plane, while another set of thrusters, in the vertical direction, control vertical velocity and pitch angle. This arrangement permits operations in very confined areas, with virtually independent horizontal and vertical motion at velocities starting at 0 ms^{-1}. This is one of MARES innovations, as it cannot be seen in any AUV of similar size and weight. Furthermore, the modularity of the system allows the integration of other thrusters, for example to provide full control of the lateral motion.

It should be stressed that fins are usually more efficient for diving than thrusters, but with

simple fins it is not possible to control pitch angle independently of depth. In mission scenarios where bottom tracking is important, such as sonar or video acquisition, a fin controlled AUV will pitch up and down to follow the terrain, affecting data quality. On the contrary, MARES AUV can control **both** pitch angle and depth independently, being able to maintain data quality even if the terrain has significant slopes.

Another advantage of using thrusters is that all moving parts can be fully shrouded and there are no fins protruding from the hull, which minimizes the risk of mechanical failure in operation or breakdown during handling and transportation. In the end, we deliberately traded some of the efficiency with increased maneuverability and robustness.

4.3.3 Energy, Power, and Endurance

In MARES, all energy is stored in rechargeable Li-Ion battery packs, manufactured by Inspired Energy Inc., in the USA. Currently, there is a total amount of 600 Wh (or 2.16×10^6 J), at a nominal voltage of 14.4 V. Battery power is directly available to the motor controllers and, through a set of voltage converters and fuse-protected distribution boards, to the rest of the on-board electronics. These batteries can be swapped when discharged, or recharged inside the vehicle, with a full recharge taking a maximum of 3 hours. Given the limited amount of energy stored on-board, it is very important to use it wisely and efficiently. Most of the power required by an AUV is usually spent in propulsion, with a relatively small amount permanently needed for the on-board electronics, and so, battery endurance greatly depends on vehicle velocity, both in the horizontal and in the vertical plane. As far as energy management is concerned, it is important to design the missions with some safety margin, to account for practical limitations. For example, vehicle missions do not start immediately after power up and so some energy will be spent during mission setup and vehicle diagnostics. More, at the end of the mission, there should be some amount of energy left to ensure localization before vehicle recovery. Finally, it should also be noticed that batteries will degrade in time and their nominal capacities are based on discharged patterns that are not matched in practice, especially after some aging.

Horizontal Motion

If we only consider the horizontal motion, then the horizontal thrusters have to provide enough power to balance the steady state drag force acting on the submerged body. This force is proportional to the square of the horizontal velocity (or *surge*), u, and it is given by:

$$F_d = \frac{1}{2}\rho C_d A u^2 = K_{du} u^2 \tag{4.5}$$

where ρ is the density of the water (about 1000 kg/m^3), C_d is the drag coefficient (depending on the shape of the AUV), and A is the projected area.

Table 4.3: Dynamic parameters of the MARES AUV

Symbol	Value	Description
E_t	2.16×10^6 J	Available energy
P_h	15 W	Hotel load
η	0.15	Propulsion efficiency
K_{du}	4 kg m^{-1}	Drag constant (horizontal)
K_{dw}	200 kg m^{-1}	Drag constant (vertical)
d	4.5×10^{-3} m	C_B/C_G separation
b	0.85 m	Vertical thrusters separation

If we assume that the thrusters have an overall efficiency of η, then the energy required to move the AUV over a horizontal distance R_h is given by:

$$E_m = \frac{F_d}{\eta} R_h = \frac{K_{du}}{\eta} u^2 R_h \tag{4.6}$$

Consider that all the other on-board subsystems need an average power (typically called *hotel load*) of P_h. In this case, the total energy draw from the batteries, when the AUV travels a horizontal distance R_h with average velocity u, can be calculated as:

$$E_t = P_h \frac{R_h}{u} + \frac{K_{du}}{\eta} u^2 R_h = \left(\frac{P_h}{u} + \frac{K_{du}}{\eta} u^2 \right) R_h \tag{4.7}$$

This expression can be rewritten so that we can estimate the maximum horizontal range of the AUV, depending on the velocity, u:

$$R_h = \frac{E_t}{\frac{P_h}{u} + \frac{K_{du}}{\eta} u^2} \tag{4.8}$$

We can therefore estimate the optimal velocity, that is, the velocity that yields a maximum horizontal distance traveled, by taking the derivative of the above expression, with respect to the velocity, u:

$$\frac{dR_h}{du_{opt}} = 0 \Rightarrow u_{opt} = \left(\frac{P_h \eta}{2K_{du}} \right)^{\frac{1}{3}} \tag{4.9}$$

In order to estimate the quantities described in these equations for the case of MARES, we can use the set of parameters summarized in table 4.3. The hydrodynamic parameters were calculated following the approach in Prestero (2001) and using some typical values found in Hoerner (1965).

Using the parameters of table 4.3 in equation 4.9 results in an *optimal* velocity of $u_{opt} = 0.66 \text{ms}^{-1}$ for the MARES AUV. If we replace this value in the expression 4.8, we can then estimate the maximum horizontal range to be $R_{h_{max}} = 63$km, corresponding to a mission lasting over 26 hours. Surely, there are many scenarios in which this *optimal* velocity may be too slow, for example if there is a need to perform a faster survey to capture a dynamic ocean feature. In other

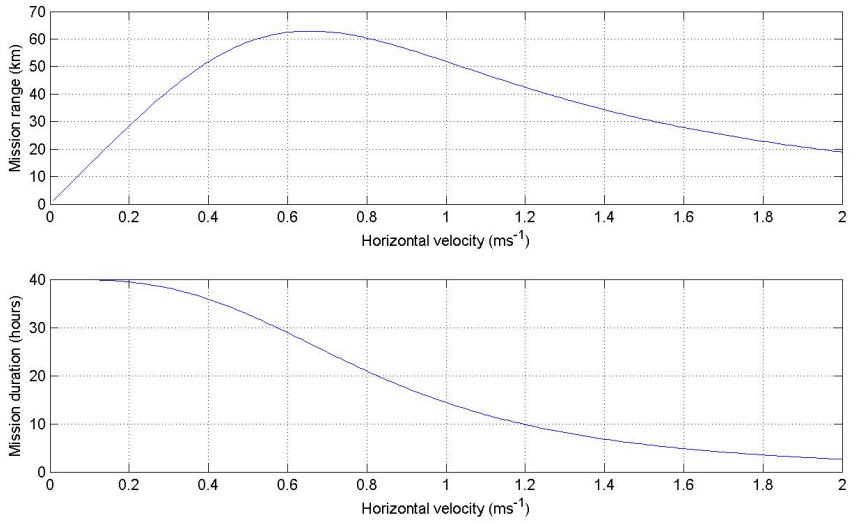

Figure 4.12: Autonomy of the MARES AUV as a function of horizontal velocity.

missions, the requirements may impose slower surveys, for example if mapping the seabed with a sonar. In any case, a deviation from this *optimal* value will reduce the maximum range, as can be seen in fig. 4.12. Note, however, that the peak of the curve is relatively flat, and a wide span of horizontal velocities, from 0.4 to 1ms^{-1}, result in more that 50km of range.

Once again, it should be noticed that these values are estimates that may be affected by practical limitations. For example, even in purely *horizontal missions*, the vertical thrusters need to be used to provide a steady state downward force to compensate for a slight vehicle buoyancy usually adopted for safety reasons. Naturally, they also need to be used by the on-board controllers to compensate for any disturbances in pitch and depth. All this actuation requires power and will degrade the estimation of maximum range.

Coupled Horizontal and Vertical Motion

Coupling horizontal and vertical motion is very typical in oceanographic missions, with data being gathered in *yo-yo* patterns to capture 3D snapshots of scalar fields. Since most of oceanographic data shows greater variations in the vertical plane as compared to the horizontal plane, it is usually necessary to travel more in the horizontal plane than in the vertical, therefore the horizontal component of the velocity is typically higher than the vertical.

MARES has two independent vertical thrusters, located away from the center of mass (fig. 4.11), that provide the capability to control both pitch and vertical velocity. With this setting, there are two possibilities of producing a trajectory with inclination α_t. The first option is to assume a zero pitch angle and provide both horizontal velocity (surge) and common-mode vertical velocity (heave) as inidicated in figure 4.13. This mode of operation may be very useful whenever it is important to keep track of the bottom, for example during sonar or video mapping in constant

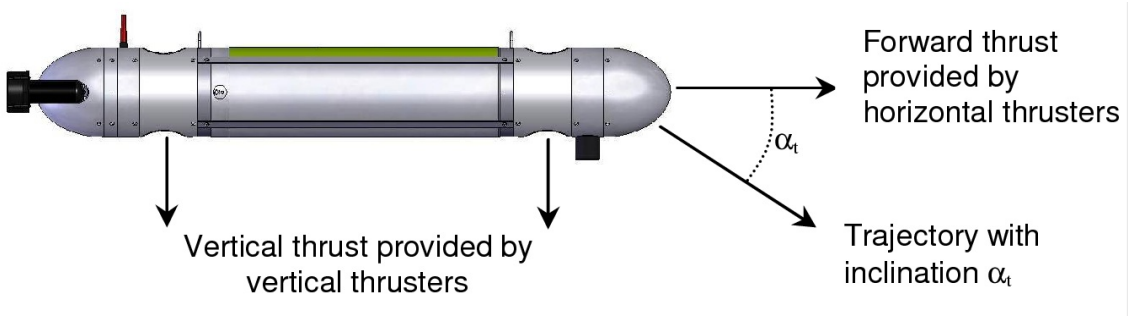

Figure 4.13: Coupled horizontal and vertical motion with zero pitch angle.

altitude above the sea floor (in *bottom following*). In this case, the steady attitude in pitch allows for the acquisition of very *smooth* data.

In order to evaluate the mission endurance in this configuration, we assume, for simplification, that there are two separate drag forces that can be considered independently: one horizontal, similar to the case of pure horizontal motion mentioned above, and an additional vertical component, that has to be balanced by the vertical thrusters.

The drag coefficient for the vertical motion of an AUV, K_{dw}, is much higher than the above K_{du} due to the significant projected area (in the case of MARES, $K_{dw} \approx 200$, as indicated in table 4.3). If we assume that the vehicle will be moving at a constant vertical velocity, w, then the vertical thrusters will have to balance a constant drag force of $F_{dw} = K_{dw} w^2$.

To ensure an inclination α_t, the vertical component of the velocity has to be $w = u\tan(\alpha_t)$ and the distance traveled in the vertical plane is given by $R_v = R_h \tan(\alpha_t)$, where R_h is the horizontal distance. The total energy required for motion is now given by the combination of the fractions for horizontal and vertical motion, given by

$$E_m = \frac{K_{du}}{\eta} u^2 R_h + \frac{K_{dw}}{\eta} w^2 R_h \tan(\alpha_t) = \frac{K_{du} + K_{dw} \tan^3(\alpha_t)}{\eta} u^2 R_h \tag{4.10}$$

Comparing with equation 4.6 above, the result of including a vertical motion can be seen as the same of increasing the drag coefficient. The new equivalent drag is now $K_d = K_{du} + K_{dw} \tan^3(\alpha_t)$. Figure 4.14 shows the variation in horizontal range, when there is a vertical component of the velocity, for values of trajectory inclination α_t between 0° and 30°. We assume for simplicity that the vehicle is neutrally buoyant, which means that all vertical thrust is used to change the inclination of the trajectory. Note that the AUV cannot travel simultaneously with large velocities and steep trajectory inclination, due to the saturation in the vertical component of the velocity. This is the reason for the incomplete lines in the graphs of figure 4.14.

The analysis of the plots of figure 4.14 shows that for relatively small angles of the trajectory ($\alpha_t < 15°$), the deterioration of the maximum range is not very high (<20%), but as the angle of the trajectory increases, this maximum range occurs for smaller horizontal velocities. For example, the plots indicate that the vehicle can perform vertical *yo-yo*'s with an inclination of 15° during

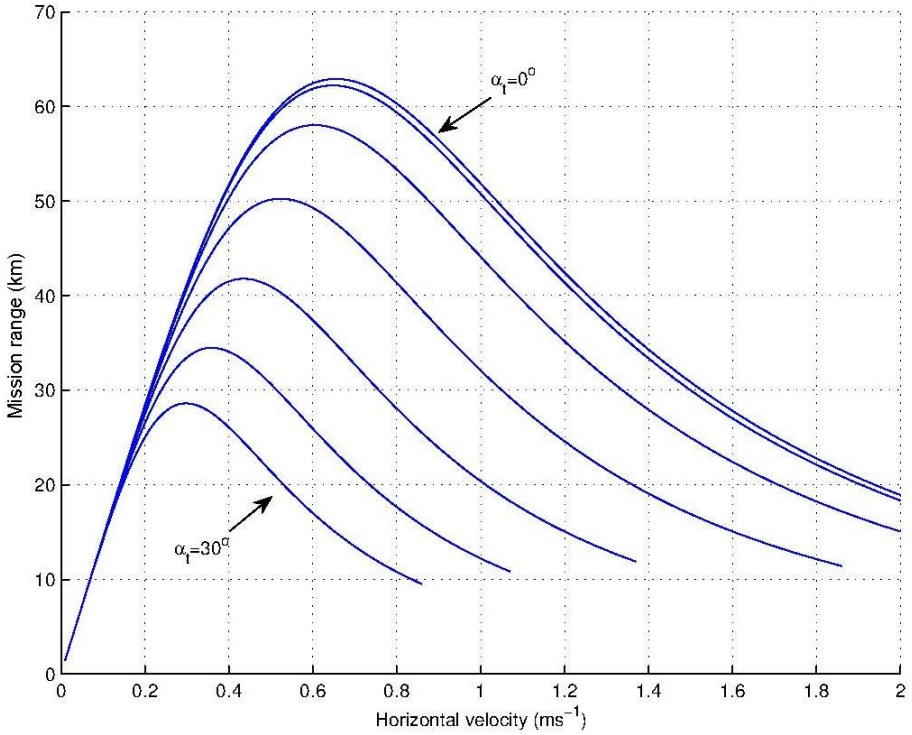

Figure 4.14: Horizontal range of the MARES AUV as a function of the horizontal velocity, assuming zero pitch and trajectory inclination α_t between 0° and 30°, in 5° intervals.

approximately 50km, at a horizontal velocity of 0.5ms$^{\cdot 1}$. If the angle increases to 30°, then the range is less than 30km and has to be done at only 0.3ms^{-1}. This deterioration is natural since the trajectory is dictated by the ratio between surge and heave, and the power required to provide motion is much higher in the vertical plane than in the horizontal, due to drag.

In the above analysis we assumed that both vertical thrusters contributed to the vertical component of the velocity, *i.e.* the AUV had only *common mode* actuation and the resulting vehicle pitch was zero, even though the longitudinal trajectory had an inclination α_t. A second option in terms of vertical motion is to use a *differential mode* of the vertical thrusters to provide a torque and therefore achieving a steady state pitch angle, α_t. The horizontal thrusters will then push the AUV forward (in the longitudinal direction), resulting in the same spatial trajectory as above, but this time with a pitch angle different from zero, aligned with the trajectory (figure 4.15).

In this mode of operation, the horizontal velocity, u_h, is the projection of the longitudinal velocity (surge), u, into the horizontal plane:

$$u_h = u\cos(\alpha_t) \tag{4.11}$$

As far as energy is concerned, we still need to overcome the drag associated with surge, but now the energy required to maintain a steady state pitch angle has also to be accounted for. A neutrally buoyant underwater body with weight $W = mg$ and a separation of d between center of

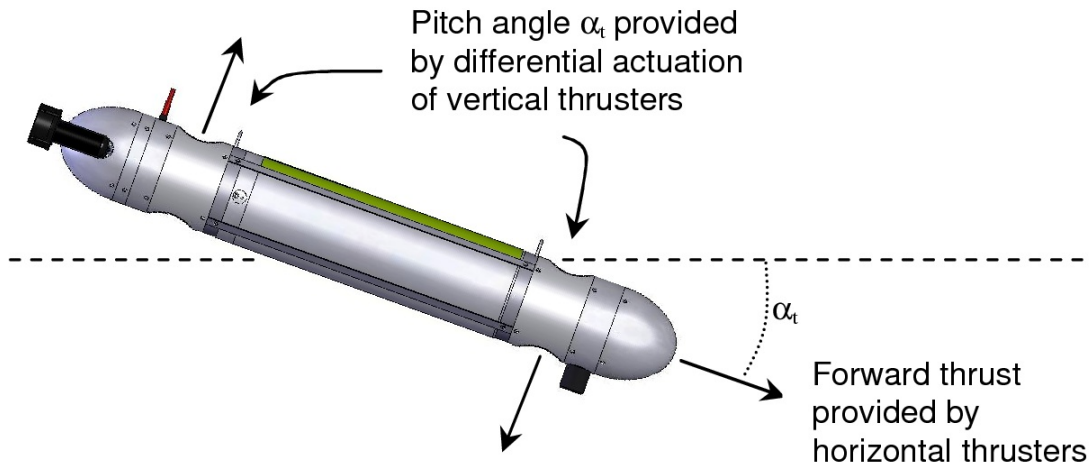

Figure 4.15: Coupled horizontal and vertical motion controlling the pitch angle aligned with the intended trajectory.

buoyancy and center of mass, will have a righting moment if pitching at an angle α_t, given by $M = Wd\sin(\alpha_t)$. Therefore, to maintain this steady state pitch angle α_t, the vertical thrusters have to balance this moment, and so

$$F_T b = M = Wd\sin(\alpha_t) \tag{4.12}$$

where F_T is the force of each vertical thruster and b is the separation between thrusters. Note that we assume for simplicity that the vertical thrusters are symmetrical with respect to the center of mass, and we also assume that thrusters behave equally working in forward or reverse modes, which is not entirely accurate. However, some of these asymmetries can be compensated in software, by using proper calibration curves, and this analysis can be easily expanded to accommodate the exact characteristics of the propulsion system.

In MARES, the electrical power required to provide a force F_T in each thruster can be approximated by

$$P_T \approx k_T F_T \tag{4.13}$$

with k_T estimated from experimental results to be $k_T \approx 5$.

So, we can derive the power required to achieve a steady state pitch angle of α_t as

$$P_T = 2k_T \frac{Wd}{b}\sin(\alpha_t) \tag{4.14}$$

If we wish to analyse the energy expenditure with respect to *horizontal range*, then we have to consider all the energy spent on a mission with average horizontal velocity u_h:

$$E_t = 2k_T \frac{Wd}{b}\sin(\alpha_t)\frac{R_h}{u_h} + P_h \frac{R_h}{u_h} + \frac{K_{du}}{\eta\cos^2(\alpha_t)} u_h^2 R_h \tag{4.15}$$

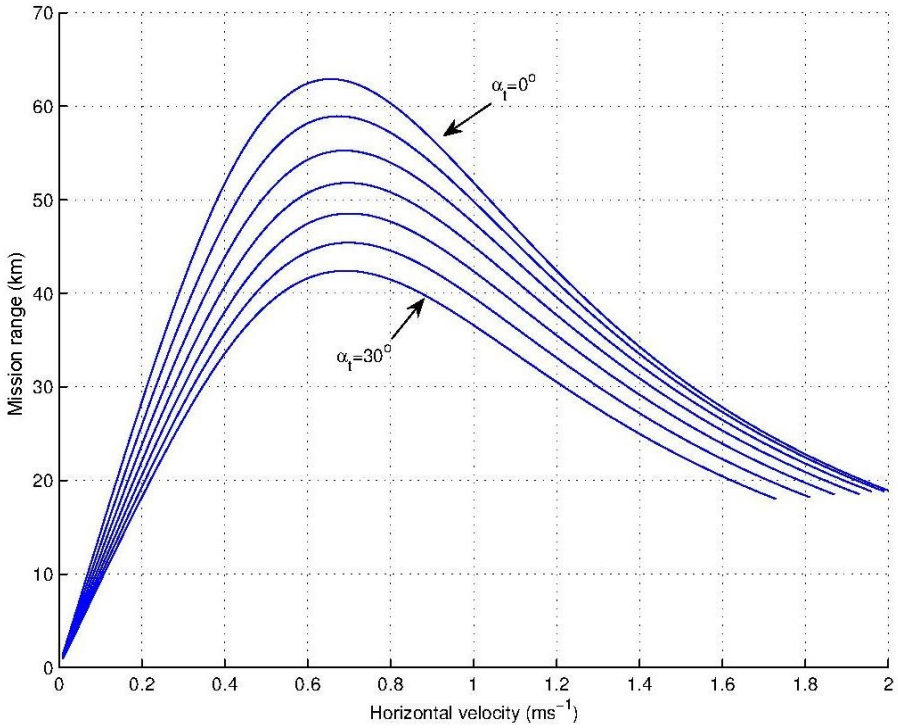

Figure 4.16: Horizontal range of the MARES AUV as a function of the horizontal velocity, assuming that the pitch angle is aligned with the trajectory inclination α_t, between 0° and 30°, in 5° intervals.

or

$$E_t = \left(\frac{2\,k_T \frac{Wd}{b} \sin(\alpha_t) + P_h}{u_h} + \frac{K_{du}}{\eta \cos^2(\alpha_t)} u_h^2 \right) R_h \tag{4.16}$$

This means that the horizontal range can be directly estimated as:

$$R_h = \frac{E_t}{\frac{2\,k_T \frac{Wd}{b} \sin(\alpha_t) + P_h}{u_h} + \frac{K_{du}}{\eta \cos^2(\alpha_t)} u_h^2} \tag{4.17}$$

Comparing equation 4.17 with 4.8, we can verify that the effect of a steady state pitch angle is the same as increasing the vehicle hotel load, and that the horizontal velocity is now a projection of the velocity vector into the horizontal plane. Figure 4.16 shows the variation in horizontal range, for values of AUV/trajectory inclination α_t between 0° and 30°. Note that MARES longitudinal velocity is limited by the power in the stern thrusters to 2 ms^{-1} and, therefore, the increase in trajectory inclination reduces the maximum horizontal component of the velocity, u_h. Once again, this shows up as incomplete lines in the graphs of figure 4.16. The separation of the plots in figure 4.16 is dictated by the amount of power required to change the pitch, which is directly related to the righting moment and inversely related to the separation between the vertical thrusters.

From the comparison between figures 4.16 and 4.14 it is possible to observe that the best mechanism to provide a spatial inclination in the trajectory (for example, to follow a *yo-yo* pattern)

depends on the angle of inclination that is required and also on the velocity of the survey. If the only requirement is the inclination angle of the trajectory, then the AUV is more efficient with a zero-pitch for small trajectory inclinations. If there is also any requirement in terms of minimum velocity to reduce survey time, then the AUV should adopt the same pitch as the desired trajectory for higher velocities. Note that MARES has a relatively small separation between the center of buoyancy and the center of mass (only 4.5 milimeters) and a large separation between the vertical thrusters. This results in a very small power required for the vertical thrusters to change pitch angle. If this separation increases (which is good for motion stability), then the effort required to overcome the righting moment will also increase and the most efficient way to descend will be with zero pitch. Naturally that the above figures and conclusions should be used as tools to design AUV missions, but they may change if the vehicle configuration is altered, for example with the addition of new sensors or actuators.

4.3.4 Scientific Payload

The market for low-power, small-sized instruments for *in-situ* measurements has been growing exponentially in the recent years, with a great demand from an expanding number of autonomous systems, such as oceanographic buoys, AUVs, ROVs or gliders. Therefore, even though MARES is a a very compact AUV, there is already a wide variety of available sensors that can be integrated. The modularity of the vehicle allows for a simple integration of different payload sensors, involving three sub-tasks: mechanical installation, electronics interfacing and software development.

Mechanically, a new sensor may be installed in a dedicated or shared section of the hull, particularly if it is relatively small. Alternatively, it can be externally attached to the vehicle body, since there are many fixing points available. In any case, it is important to verify the weight of the sensor (and of the hull adapter) in the water, to compensate with extra flotation if necessary. Naturally, the overall vehicle trim has also to be adjusted, particularly in the case of bulky or heavy payloads. Figure 4.17 shows two examples of sensors installed on MARES. On the left, a custom hull section was machined to integrate an ECO-Puck Triplet sensor, from WetLabs, measuring scattering and fluorescence (Chlorophyll and CDOM), in the same polyacetal *slice* as the acoustic transducer used for navigation. Note that this section is free flooded and there is much room to insert flotation material to compensate the weight of the sensors. On the right, it is shown a detail of a Fastcat 49 CTD, from SeaBird Electronics, attached to the side of the hull. This arrangement ensures that the water flows easily around the sensor and therefore minimizes the risk of artificially smoothing the measurements of the water characteristics.

Most of the payload sensors transported by the AUV need energy and a communications link with the on-board computer to exchange data and configuration parameters. MARES has several spare connectors on both end caps of the main electronics compartment that can be wired to provide power and communicate with these sensors. At the same time, the computational system has spare communication ports, easily configurable according to the payload specs.

As far as software is concerned, the integration of a new payload sensor requires the development of a dedicated software module, known as a *device driver*. Device drivers establish a

Figure 4.17: Some examples of integration of scientific payload sensors. Top left: a wet extension designed for an ECO-Puck triplet optical sensor, measuring turbidity and fluorescence; top right: detail of figure 4.10 showing an externally mounted CTD; bottom: MARES configured with a sidescan sonar and a small side-looking camera.

communication link between the sensor and the on-board software core, allowing for the configuration of the sensor as well as data logging.

Naturally, these integration tasks are only required the first time the sensor is tested and the integration has to be validated in field trials. After that, the full sensor set (sensor, flotation, electronics and software modules) join the pool of available sensors and can easily be included as payload whenever necessary.

The integration of a payload sensor has a direct impact on the mission duration, as it will require some electrical power to operate that will be provided by the on-board batteries. Admitting that the sensor requires an average power P_s, this amount will add to the existing hotel load, P_h, resulting in an equivalent hotel load $P'_h = P_h + P_s$. Recalling equations 4.8 and 4.9, the optimal velocity will now increase to:

$$u'_{opt} = \left(\frac{P'_h \eta}{2K_{du}} \right)^{\frac{1}{3}} \tag{4.18}$$

while the maximum range will decrease to:

$$R'_{h_{max}} = \frac{E_t}{\frac{P'_h}{u'_{opt}} + \frac{K_{du}}{\eta} u'^{2}_{opt}} \tag{4.19}$$

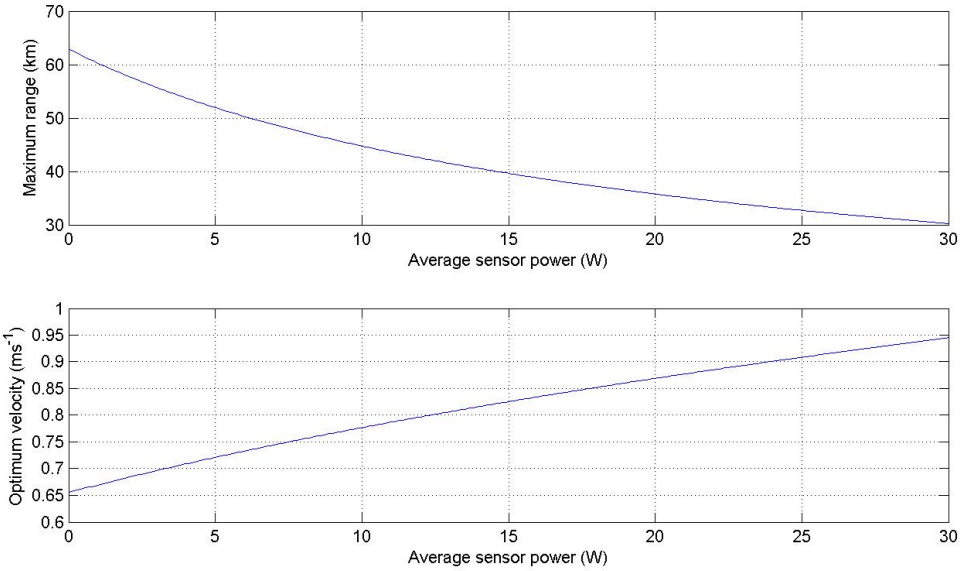

Figure 4.18: Impact of the integration of a payload sensor in overall mission range and optimum velocity.

Figure 4.18 shows the impact of a payload sensor (requiring 0 to 30 watt of power), in the total mission range and optimum velocity of MARES.

4.3.5 Computational System and On-board Software

The on-board computational system of MARES is based on a PC-104 stack (fig. 4.19), with a power supply board, the main processor, and additional boards to interface with peripherals, such as health monitoring systems, actuation devices, and navigation and payload sensors. A solid-state disk is used to store the on-board software and all information collected during operations, logging both internal (battery voltage, device status, etc.) and payload data.

The on-board software was developed in C++, runs on a Linux kernel and is composed by a set of independent processes. In this way, not only the system modularity and robustness are increased but also its debugging and recovery from unexpected events is much simpler. The communication between the modules relies on the exchange of messages using UDP, which allows data exchanges with reduced processing overhead, as recommended in this kind of applications.

The interface with the navigation hardware is managed by dedicated processes that provide an abstraction layer and isolate the data from the physical devices that produce it, as depicted in figure 4.9. A navigation module estimates the vehicle state in real time and the mission dispatcher executes the mission plan, which is essentially a list of predefined maneuvers read from a mission script. These maneuvers can include special cases of real-time adaptive sampling, in which data from the payload sensors can be interpreted by an external program and provide inputs to the on-board controllers. A black box data logging system registers all data related to the vehicle motion on the flash disk, as well as all payload data, according to the specifications indicated in a

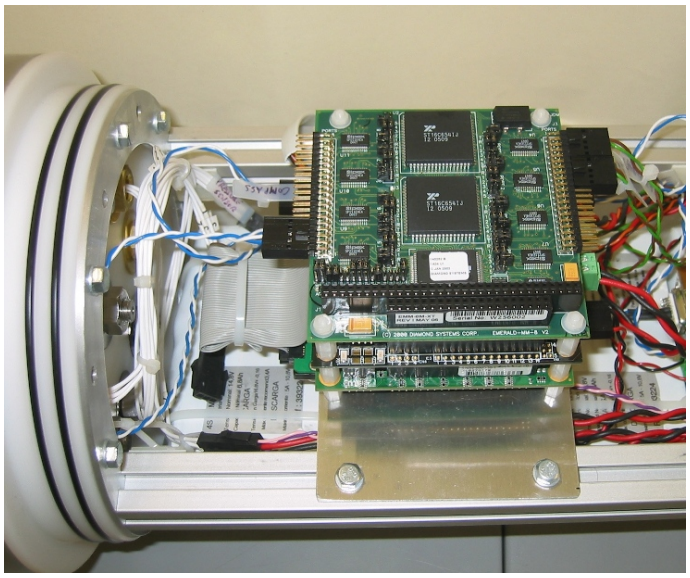

Figure 4.19: PC-104 stack in the internal frame of MARES.

configuration file. Payload sensors and subsystems are also controlled by dedicated modules. In general, these modules interact with the supervision module, for configuration and communication with the control station, and also with the data logger.

A supervision module continuously monitors the behavior of the vehicle and aborts the autonomous operation if safety margins are exceeded or other unexpected event occurs. This module also establishes a communication link with the mission control station when the vehicle is on deck or at the surface.

Navigation and Control

To estimate the position in real time, the vehicle carries an absolute pressure sensor from Keller, a COTS inertial measuring unit with a compass and inclination sensors, from X-Sense, and an acoustic system for long baseline (LBL) position estimation. This acoustic system is the third generation of multi frequency Rx/Tx boards, developed by the Ocean Systems Group, following some excellent results with earlier versions (Cruz et al. (2001)). It is complemented by a set of acoustic beacons previously deployed in the operation area, whose position is known to the AUV navigation software (see appendix A for details on these beacons). Vehicle depth is directly given by the pressure sensor, while the horizontal position is estimated by a Kalman filter that fuses dead reckoning with triangulation data between the AUV and the acoustic beacons (Matos et al. (1999)). This navigation package assures real time accuracies of about 1 cm in the vertical plane and below 1 meter in the horizontal. Furthermore, all navigation data used by the vehicle is stored in the flash disk and is processed at the end of each mission by a smoothing algorithm to improve the accuracy of the estimation of the vehicle's position (Matos et al. (2003)).

The AUV control system is organized into four basic and independent controllers: velocity, heading, pitch and depth. The outputs of the first two controllers are combined to obtain the actuation for the horizontal thrusters, while the outputs of the others provide the actuation for the vertical thrusters. Each controller can operate either in closed or open loop mode. The inputs for all controllers are provided by the guidance systems and depend on the actual maneuver that the vehicle is executing.

A typical AUV mission is a set of elemental maneuvers that the vehicle is expected to complete in sequence. Each maneuver prescribes the behavior of each of the four basic controllers (therefore defining the vehicle motion). It also defines the condition for completion, and a timeout for safety reasons. The basic maneuvers of the MARES AUV include going to a waypoint, with several possible adjustments on trajectory and velocities, and virtual anchoring at a given position (*i.e.* hovering).

The possibility of independently defining each basic controller allows for very different vehicle behaviors, making the operation of MARES very flexible. For example, a pure vertical motion can be easily obtained by a virtual anchoring with a reference in vertical velocity, and a closed loop pitch with zero reference and zero surge command; a combined vertical and horizontal motion can be achieved with a combination of surge and heave. Furthermore, each basic controller is already prepared to accept inputs defined by external processes. This allows for the implementation of unconventional guidance strategies, such as the case as adaptive sampling algorithms described later.

4.3.6 Mission Planning and Supervision

Typical Operation

MARES is very compact and lightweight (32kg), making it easy to transport, deploy and recover from the water by one or two persons. Depending on the application scenario, it can be deployed from the shore or from a small support vessel. If necessary, a line can easily be attached to the lifting points at the top of the hull for launching and recovering from a larger vessel.

A typical MARES mission requires the deployment of at least two LBL multi-channel acoustic navigation beacons in the operation area (with acoustic ranges in the order of 2-3 km). The vehicle on-board navigation system requires an accurate position of the acoustic beacons, since it estimates its own position by triangulation of the acoustic ranges to both beacons. In fact, having only two ranges results in an ambiguous estimation, since there are two possible solutions, symmetric with respect to the *baseline* – the imaginary line linking both beacons. In practice, we resolve this ambiguity by always keeping the AUV in the same side of this *baseline*. In our own typical missions, the acoustic beacons are installed on Navigation and Instrumentation Buoys (NIBs) (figure A.1), that are anchored in the operation area. In coastal water operations, we have been mooring NIBs in up to 40 meters of water, but as the depth increases, so does the slack of the anchor line and, consequently, there may be a significant change in the true position of the beacons during a mission. We have addressed this issue in two ways; first, the NIBs have a GPS

receiver and a logging system that stores all positions (and time) for post mission correction of the vehicle data. This does not prevent the on-board navigation of the AUV to make erroneous estimates of the position and produce incorrect trajectories, but serves to compute the *true* geographic location where data was taken. Luckily, usually both NIBs are affected by the same local effects (current and wind-induced drag), which means that the real trajectory shows only a small offset as compared to the programmed course. The other way to overcome the drift of the beacons during a mission, especially in deeper waters, is to install them on surface vehicles behaving as virtual moorings, or deliberately moving to form establish a mobile acoustic network, such as we've demonstrated in Matos and Cruz (2005); Santos et al. (2008). Both the NIBs and the acoustic system are detailed in appendix A.

Mission Control Station

The mission script describes the sequence of maneuvers that the vehicle is supposed to perform and it is mainly a sequence of waypoints, together with the required depth and control modes for each segment of the mission. Both the mission script and the beacon location are transmitted to the vehicle by radio, either using the Wi-Fi link if the vehicle is close to the operator, or using the long range VHF radio modem. This is supported by the mission control station – a laptop computer connected to MARES and NIBs via a communications hub. Before the mission is launched, there is a set of pre-mission procedures that are performed to double check that all subsystems are operating as expected: radio signals are ok, buoys are transmitting and receiving data, GPS is functioning, AUV pressure sensor is calibrated, AUV batteries are good, etc. Although these are very simple procedures, it may be quite distressing following them at sea in rough conditions, which is customary in the Atlantic coast. For this reason, we've developed an automatic interface to help mission planning and pre-mission check at sea, described in Abreu et al. (2010).

During the execution of the mission, the control station continuously receives radio data from the navigation beacons, relative to their own position and to the acoustic signals being exchanged with the AUV. This data is used to track the vehicle position in real time and it is a good indication that the vehicle is navigating as planned (figure 4.20). To increase operation safety, the laptop interface can also transmit simple special *commands* to the AUV (such as "Abort", for example) that are sent using the acoustic channel and the NIBs as gateways. All this data is stored in the NIBs and, redundantly, in the laptop for mission post-processing. This is particularly relevant in the case of *long* missions, where the beacons position can have significant changes due to currents and/or winds.

At the end of the mission, the vehicle returns to the surface and starts transmitting its own position estimate by radio. This position is obtained by the on-board acoustic navigation system and also from the small GPS receiver located a few centimeters above the hull. All this information is redundant, since it usually confirms the estimate provided by the real time tracking mechanism, but it is important to ensure that MARES (and all data) is safely recovered by the support vessel.

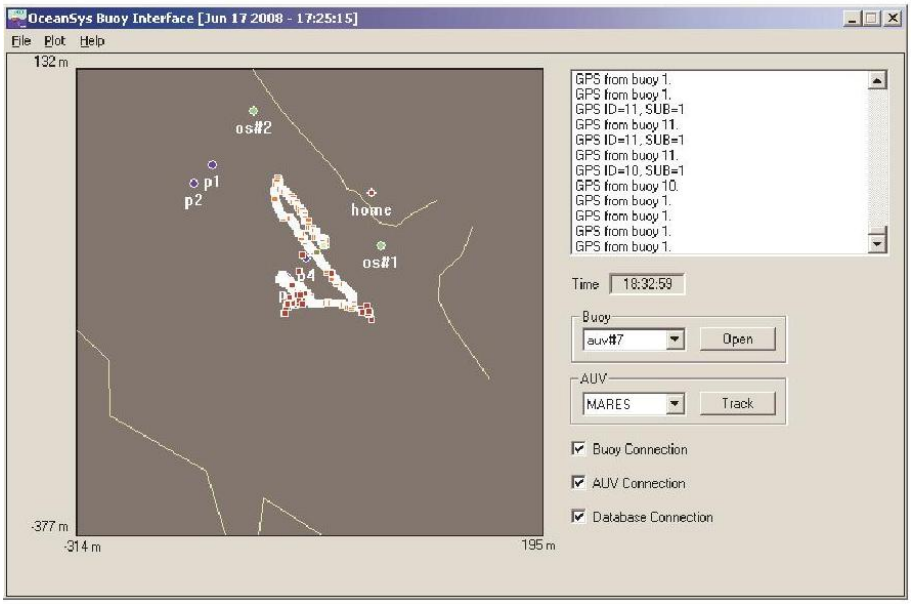

Figure 4.20: Graphical interface at the Mission Control Station showing external tracking of the AUV during a mission.

After the completion of the mission, the control station is also used to download the data collected by AUV and to make a preliminary analysis of the mission results. Navigation information from the buoys is fused together with information stored in the on-board logging system to improve the accuracy of the location of the vehicle during the mission using the smoothing algorithms described in Matos et al. (2003). Furthermore, sensor data, collected either by the vehicle or by the navigation buoys, can be reviewed with the help of playback software to assess vehicle performance and detect undesirable events that might otherwise have been overlooked. This data can also be converted to standard formats for later processing, using Matlab® or other software tools.

4.3.7 MARES Mission Examples

The first water tests with the vehicle started with a simple hull, as soon as we had enough machined parts to build the main watertight cylinder and install the basic electronics and thrusters, in the autumn of 2006. These tests were conducted in a local pool and were useful to validate the integrity of the system, adjust buoyancy and trim, and test simple maneuvers. When we approached the functional version, we moved the test scenario to a reservoir in the Douro river, with a maximum depth of 20 meters, about 30 minutes drive from our lab. We could then proceed with the calibration and validation of the remaining subsystems, such as acoustic navigation, until we had a fully functional AUV in the summer of 2007.

MARES was first demonstrated at sea in November of 2007. This demonstration mission took place in the neighborhood of a sewage outfall located 2 km off the Portuguese coast at Foz

Figure 4.21: MARES starting a mission off the Portuguese coast, November 2007.

do Arelho (figure 4.21). MARES was equipped with a Seabird Fastcat 49 CTD and collected 16 samples/second of CTD data for about one hour. Navigation was based on a LBL acoustic network, with two NIBs being deployed about 600 meters apart. During the mission, the buoys transmitted vehicle location data to a small support vessel anchored in the vicinity, so that the AUV trajectory could be followed in real time. At the end, the vehicle surfaced at the pre-programmed location and immediately started transmitting its own position by radio.

Upon vehicle recovery, CTD data was analyzed to infer the location and shape of the sewage plume, close to the diffuser. Figure 4.22 shows a salinity map produced from CTD data, and although the salinity signature was very weak, it was also very consistent, and a partial plume showed up close to the surface, as predicted by preliminary simulation. This demonstrated the potential for detecting minute anomalies with the on-board CTD, which was the main objective for this mission at sea. It also served as an operational preparation for a long term monitoring plan that started in 2008, under a project with Águas de Portugal (a public company managing water supply and wastewater treatment).

Since these earlier missions, MARES has been extensively used as a platform to collect ocean data in multiple R&D projects, and also as a testbed to support applied research in underwater robotics, such as described in chapter 6 to demonstrate the implementation of adaptive sampling strategies.

4.4 The TriMARES Hybrid AUV/ROV

TriMARES (fig. 4.23) is a 3-body unmanned underwater vehicle with significant payload capability, including high quality video and sonar. It was built using the AUV building blocks de-

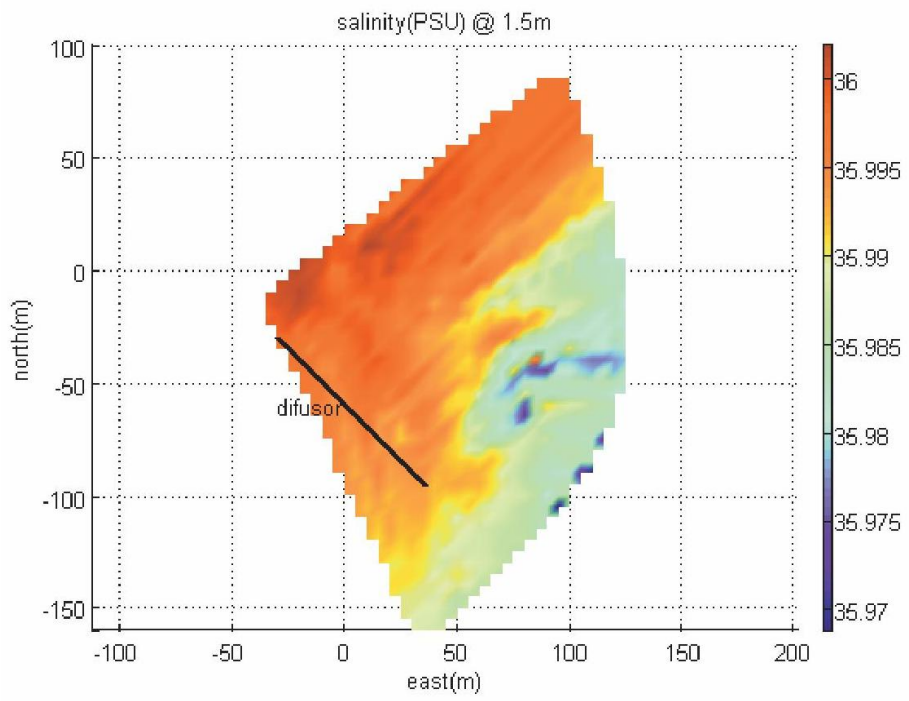

Figure 4.22: Salinity map close to the sewage outfall diffuser, produced with MARES data, November 2007.

scribed earlier, to fulfill the requirements of a Brazilian consortium, interested in a specific system for which there was no commercial solution. The overall physical arrangement ensures motion smoothness for improved quality in payload and positioning data. TriMARES motion is provided by seven independent thrusters, with no control surfaces, resulting in the ability to hover in the water column, to navigate close to the bottom, or to perform close-up inspections of underwater structures. TriMARES is a hybrid vehicle, since it may be programmed for autonomous missions as a standard AUV or, alternatively, it can be operated as an improved ROV with a cable attached for realtime data transmission. In this section, we discuss the design aspects and the development of the TriMARES AUV/ ROV: we start by describing the main requirements at the beginning of the project, we detail the solutions adopted for the main subsystems, and, finally, we present some experimental data from the first in-water trials.

4.4.1 Main Requirements

For the successful design of any complex systems, it is paramount to start by clearly identifying the most critical requirements. When we first started our program for the development of AUVs, we have identified a few cases of operational scenarios, typical maneuvers, logistics constraints and other requirements for the use of our AUVs, primarily as scientific platforms. These specifications dictated most of the design choices, as described earlier.

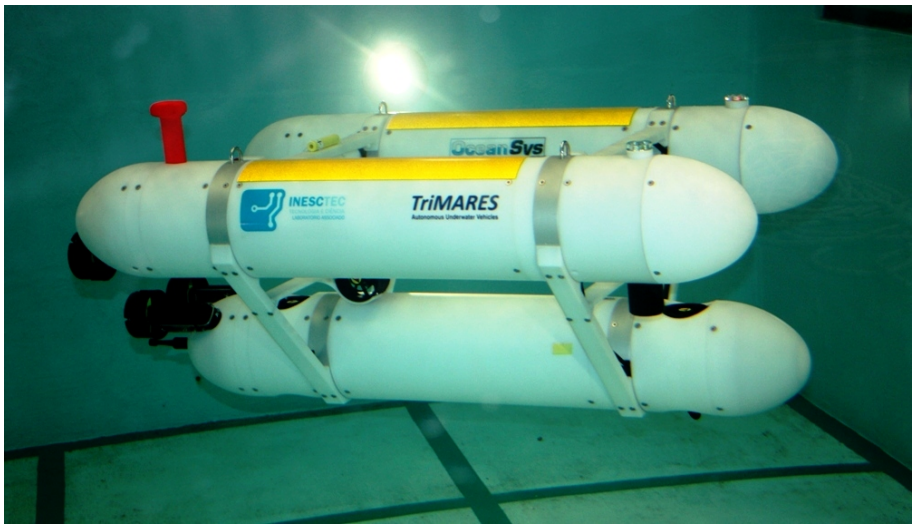

Figure 4.23: The TriMARES hybrid AUV/ROV during the first water trials in Porto, Portugal, June 2011.

There are many companies providing off-the-shelf remotely operated vehicles (ROVs) and a few other exploiting the market of AUVs. However, the demand of robotic systems for underwater operations is so wide that there are many scenarios for which the commercial solutions are not adequate and a custom solution has to be sought. The robotics unit at INESC Porto develops custom solutions for specific engineering challenges, and it was contacted in 2010 by a Brazilian consortium to provide an unmanned robotic system for the inspection of a large dam in Brazil and for the periodic monitoring of the dam reservoir. Their idea was to take advantage of the modularity of MARES to include specific sensors and operating modes, according to a set of requirements summarized in table 4.4.

These requirements pointed towards a solution with two complementary vehicles: an ROV to perform the inspection tasks, and an AUV (similar to MARES) to conduct long surveys of the dam reservoir. The modularity of MARES was appealing for the consortium, as they had little experience in underwater robotics and saw the benefits of having simple shapes, few different parts and an easily reconfigurable/upgradeable system. Moreover, since the system was meant for operations in a remote location with few support personnel, it was much more attractive to have a single vehicle to operate and, above all, to maintain.

Our main concern with the first analysis of the requirement was to map them, as much as possible, into engineering constraints, such as maximum and minimum weight and dimensions, degrees of freedom, propulsion power, computational power and navigation sensors. Ideally, this should result in a list of existing modules to be included, and a list of others that needed to be changed or newly developed. It was clear from this analysis that a MARES version would not comply with these requirements, mainly due to the size and power consumption of the required payload sensors, but also because of the prerequisites in terms of maneuverability and stability of

Table 4.4: Main requirements for the hybrid AUV/ROV, specified by the Brazilian contractor.

Operational Scenarios	Depth rating $\geq$ 100 meters Autonomy $\geq$ 10 hours Autonomous or teleoperated
Physical Constraints	Weight in air less than 100kg Compact, fitting in a small van
Maneuverability	5 DOF (surge, sway, heave, yaw, pitch) Hovering capability Forward velocity of at least 1m/s
Navigation Performance	Absolute position error below 2 meters
Payload Sensors	Prepared for sonar, video and still camera, water quality sensors

the platform for data acquisition.

We started preparing an alternative solution for a hybrid AUV/ROV, having in mind the concept of modularity, to speed up the development phase and also to reduce maintenance and operational costs, which are absolutely critical when the end user is not the developer. As far as operational aspects were concerned, one of the challenges in the design was that the vehicle should be able to work either as a *standard* AUV, for reservoir monitoring, or to have a cable enabling high throughput data transmission, during inspections. This ROV-like operation should also be supported by hidden autonomous behaviors to help a non-specialist pilot, like auto-depth, auto-heading, etc.

After a few months of discussions with the contractor to evaluate and decide possible design trade-offs, the contract with INESC Porto was signed in the summer of 2010, and it included the delivery of one hybrid vehicle to the Brazilian consortium in little over 6 months, followed by local training and support after shipment. We've also established a partnership with a Brazilian research institution – Universidade Federal de Juiz de Fora – for the use and development of the monitoring system during a second stage of the project, that included the integration of the payload sensors. Although the configuration of TriMARES can change by the inclusion/replacement of specific modules, the characteristics of the vehicle that was shipped to Brazil are summarized in table 4.5, and will be detailed below.

4.4.2 Mechanical Structure

The design of the physical structure of TriMARES was based on the mechanical building blocks described earlier and used for assembling the MARES AUV (Cruz and Matos (2008)). MARES

Table 4.5: TriMARES main characteristics, as of July 2011.

Length	1.3 m
Overall width	80 cm
Overall height	50 cm
Weight in air	75 kg
Depth rating	100 m
Propulsion	4 longitudinal thrusters 2 vertical thrusters 1 lateral thruster
Horizontal velocity	0–1.5 m/s, variable
Energy	Li-Ion batteries, 800 Wh
Autonomy/Range	about 10 hrs / 40 km

is a compact mono-hull AUV, with a configuration that is extremely useful for a wide range of application scenarios, but it was clear that this project required a larger vehicle, to accommodate more energy and large sensors, and also to ensure a more stable platform during inspections. At this point we had two main options as far as the hull was concerned, either to scale it up to a larger diameter, or to maintain the same modules and design a multiple body vehicle. We've opted for this second option, to reuse many of the sections that we had designed for MARES and, this way, speeding up the overall project. In fact, this option allowed us to provide schematics of the overall vehicle to the consortium at a very early stage of the development (figures 4.24 to 4.27), receiving feedback and incorporating any relevant adjustments. This also allowed us an early visualization and validation of the full system, long before the actual parts were available. As far as fabrication was concerned, the simplest/smallest parts were machined in house, while larger and more precise parts (like o-ring grooves and watertight containers) were ordered from a local machine shop.

As it is clear from figures 4.24 to 4.27, the TriMARES' mechanical arrangement highlights our modular approach, with three similar bodies linked by a light mechanical structure of crossbeams, which also serve as cable ducting and protection. Each body is built around a 200mm diameter, 500mm long watertight cylinder, with an internal frame to hold batteries, computers and other electronics. This arrangement provides much space for electronics and payload, while still ensuring good hydrodynamics and reduced weight, and it was inspired by a similar configuration that has been developed more than 20 years ago: the ABE vehicle at the woods Hole Oceanographic Institution (Yoerger et al. (1991)). Recently, there have been a few more examples of multiple hull designs, but most of them with much larger weight and dimensions as compared to what we had planned for TriMARES (Kondo et al. (2001); Shea et al. (2010); Ribas et al. (2011)).

The interface between the electronics inside the pressure housings and the external subsystems is done through the end caps, each having 9 holes to accommodate industry standard bulkhead

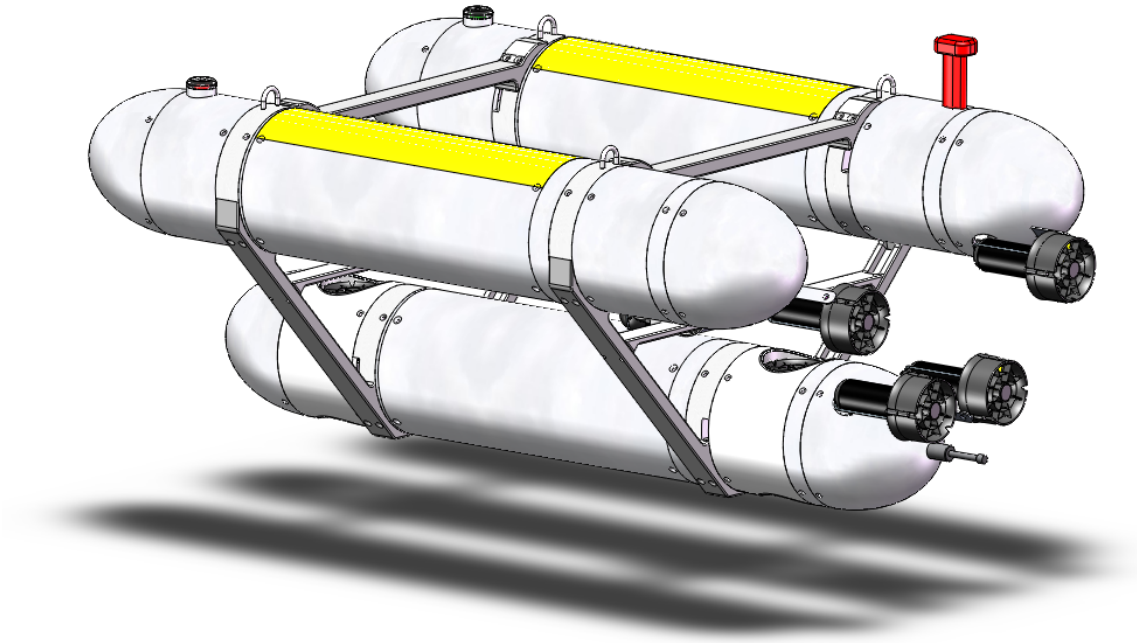

Figure 4.24: TriMARES 3D CAD model.

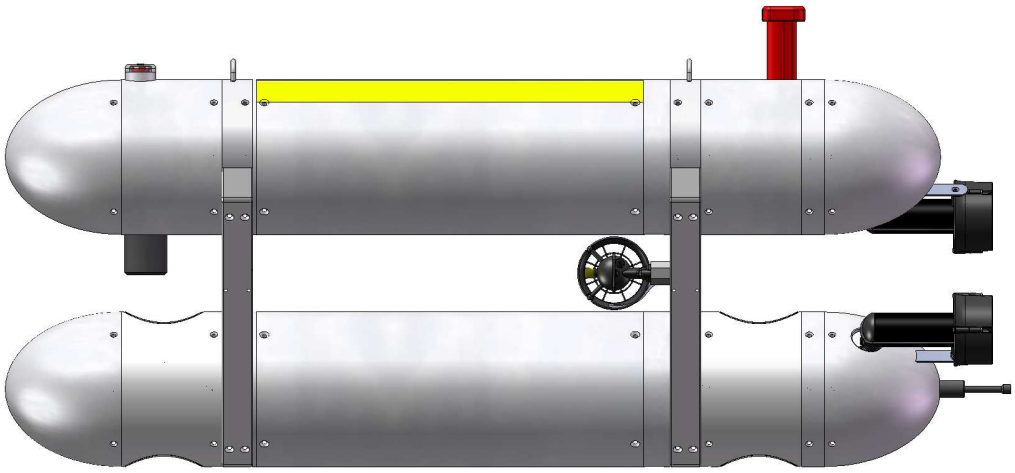

Figure 4.25: Port view of TriMARES model. Note that the cylinders allow enough spacing for the flow of the lateral thruster. Note also that the forward thrusters are aligned in two horizontal planes, to facilitate pitch control during transit. The crossbeams provide a possible structure to attach sensors.

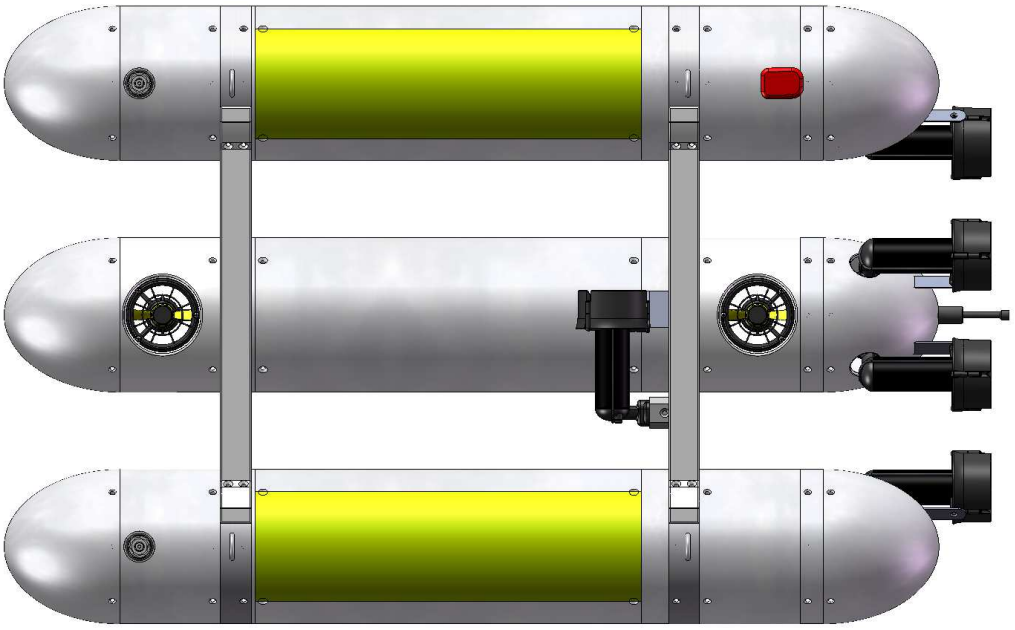

Figure 4.26: Top view of TriMARES model. Note that the cylinders allow enough spacing for the flow of the vertical thrusters. Note also that the forward thrusters are equally spaced, to facilitate heading control during transit. The horizontal crossbeams may be used to manually lift the vehicle and provide a possible structure to attach sensors.

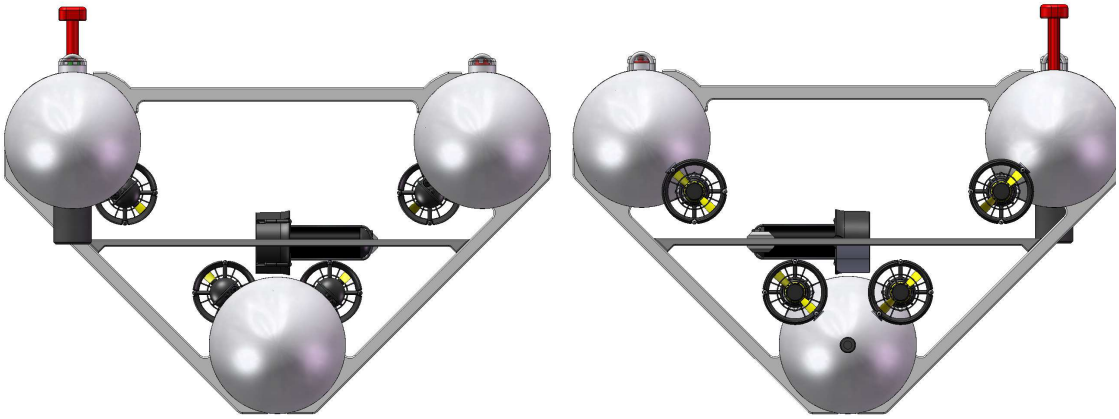

Figure 4.27: Bow and stern views of TriMARES model. The crossbeams form a shell around the vehicle to protect it against collisions with the bottom or any lateral structure. Note the alignment of the rear thrusters in two planes, as well as the position of the lateral thruster propeller, to facilitate sway control.

connectors. Each cylinder has also a vent plug that can be removed to avoid gas build up during battery charge, and where a vacuum pump may be connected to confirm sealing. Both the cylinders and end caps were machined from polyacetal copolymer (POM-C) and designed to withstand 200 meters of hydrostatic pressure, which ensures a 100% safety margin over the specifications.

Attached to the end caps, a set of anodized aluminum rings is used to provide lifting points and to hold the crossbeams connecting the three bodies, forming a triangular prismatic shape with 800mm of overall width and 500mm of height. Due to the risk of hitting the bottom or any lateral structure during inspections, there was a particular care to ensure that there were no sensitive parts of the vehicle protruding from this envelope, as can be seen in the views of figure 4.27. The separation in three individual bodies is not only physical but also functional, and both the number of bodies and their relative positions have been chosen according to this. The rechargeable batteries and the power management system are the heaviest part of the vehicle electronics and are located in the bottom cylinder, to lower the center of mass and increase the separation with the center of buoyancy (therefore improving motion stability). The top-starboard cylinder holds the main computer, the navigation sensors and the main communication devices. Finally, the payload system is located in the top-port cylinder, with all interfaces for the payload sensors and a second computer to provide realtime processing of sensor information. This separation ensures that the installation of additional sensors by the partner institutions only requires alterations of the top-port body, which simplifies any reconfiguration and also facilitates debugging in case of any malfunctioning subsystem.

All other sections were built with flooded stackable rings as in the case of MARES, also in POM-C, with the same outside diameter (200mm), therefore ensuring a continuous profile. They are designed to carry wet sensors and thrusters and, since they all have common mechanical interfaces, they are fully interchangeable. This allows for very easy sensor swapping and/or repositioning, or even to test different configurations of thrusters. Finally, each body terminates with ellipsoid-shaped ends, both at the nose cone and at the tail. These are used as a thin shell to reduce vehicle drag and were manufactured in fiberglass from a mold to reduce fabrication cost.

In order to minimize the power required to change depth, the vehicle weight in water should be zero, i.e., the dry weight should equal the weight of the displaced volume of water. In practice, however, it is usually kept slightly buoyant for safety reasons. A set of syntactic foam parts, with a density of 200kg/m^3, were machined from a large block and inserted in wet compartments to ensure the trimming of the final solution. Extra buoyancy modules and corresponding ballast weights were included to compensate for any new board or device that is installed in the future.

4.4.3 Propulsion

The vehicle required not only a great number of thrusters to ensure maneuverability (5 degrees of freedom), but also enough power to overcome the relatively large drag. Even though the power requirements are clearly higher for the forward direction to ensure a useful velocity during reservoir surveys, we decided to use the same thruster model for all directions, to minimize the number of

different parts. From our previous experience with MARES and other projects, we have selected a set of small off-the-shelf thrusters from Seabotix Inc., USA, based on brushless DC motors. Each provides a nominal thrust of 35N, with possible transients up to 45N.

One of the requirements for this project was for the vehicle to be able to hover in the water column, in order to approach the bottom of the reservoir and to enable close-range inspection of the underwater features. The vehicle is inherently stable in pitch and roll due to the large separation between the center of mass and the center of buoyancy, provided by the three body arrangement. However, the pitch control can be helpful during the mission, to provide a straight trajectory between two waypoints at different depths, or to simulate/compensate a tilt motion of the camera. In order to achieve this, TriMARES has two through-hull vertical thrusters, located in the bottom body. Since they are aligned with a vertical symmetry plane, they can be used to control both heave and pitch independently, with minor influence on the other degrees of freedom. In figure 4.26 it is possible to see that the flow through these thrusters is not directly obstructed by the vehicle structure.

Horizontal propulsion and heading are controlled by four independent thrusters located at the stern, one at the rear end of each of the top bodies, and two in the lower body, as can be seen in figures 4.24 and 4.27. With each thruster providing a nominal force of 35N, this arrangement enables much more power than required to move the vehicle at 1 meter per second, as desired. In any case, this ensures some degree of redundancy, and allows for a proper operations even in the case of a fault, following the approach in Ferreira et al. (2011). Furthermore, we can take advantage of their location in different vertical layers to provide a different mechanism of thruster allocation to provide pitch control together with surge control.

Finally, a single lateral thruster was also installed to control sway motion. This thruster is located close to the center of mass so that the effect in the other degrees of freedom is minimized. Once again, the position of the cylinders was calculated to ensure that the flow through this thruster is not directly obstructed by the vehicle structure, as can be seen in figure 4.25.

4.4.4 Energy and Power Management

Vehicle energy is provided by rechargeable Li-Ion batteries located in the lower cylinder, with a total energy of 800Wh. Depending on vehicle velocity and payload requirements, these batteries can last up to 10 hours, corresponding to about 40km. In the same cylinder, the vehicle is fitted with an intelligent power management system which is capable of handling all aspects of battery charging and system powering (see figure 4.28 for an internal view of the lower cylinder). In addition, this power management system provides fully configurable power protections as well as overall battery health status report, via an RS232 connection with the main on-board computer. This allows to continuously monitor parameters like power flow, power balance and individual battery temperature.

The overall power distribution scheme can be seen in the diagram of figure 4.29. Raw battery power is split in the lower cylinder into a 500W DC/DC converter and a power distribution board.

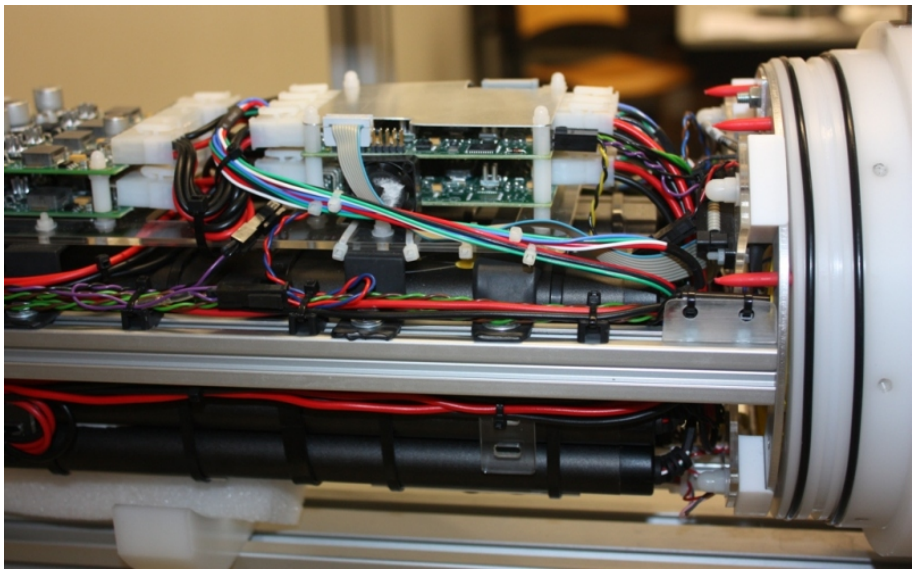

Figure 4.28: Internal view of TriMARES lower cylinder, with 8 batteries of 100Wh below the frame and the power management boards above it.

The DC/DC converter is used to step up the battery voltage level (with a nominal value of 14.4 V) into the 28 Volts needed for the thrusters. After conversion, this higher voltage bus feeds a thruster power distribution board, fitted with individual resettable current protections, where all the thrusters are connected. The power distribution board switches raw battery power for the two upper cylinders and it is also fitted with individual resettable over current protections. The power is carried to the upper cylinders through underwater cables hidden within the mechanical frame bars. When entering each of the top cylinders, a DC/DC converter steps the voltage to the levels required by the various equipment.

To charge the vehicle, a custom 320W DC power supply was developed, based on a commercial power supply that was fitted with specially designed resettable power protections along with an underwater power cable compatible with the vehicle. With this power source, the batteries can be fully charged inside the vehicle in approximately 3 hours. The power management system is capable of simultaneously charging the batteries and supplying power to the vehicle electronics, which allows for immediate downloading and processing of data after mission completion, even in the case that the batteries are completely depleted.

In order to prevent accidental gas accumulation during battery charge, and following the recommendation of the battery manufacturer, the charging procedure is not allowed without ventilation of the lower cylinder. This can be done by opening a small vent cap located in the top of the housing. This vent cap has an embedded magnet that is detected by the charge monitoring board, so that detects both the absence of the cap through a magnetic switch and the presence of an external charger. If the conditions are fulfilled, the charge is allowed, otherwise it isn't and an acoustic warning is emitted.

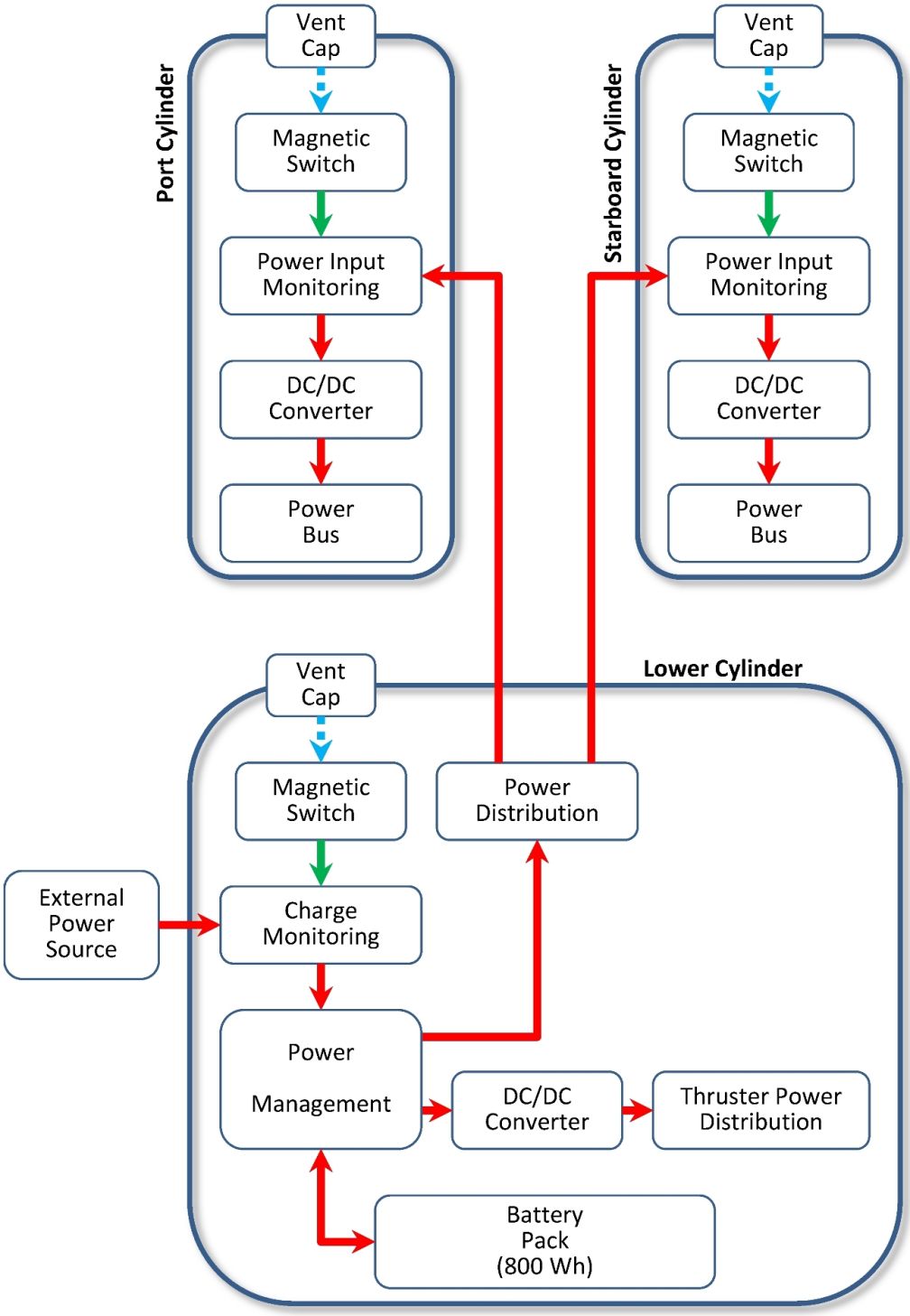

Figure 4.29: Power distribution in TriMARES cylinders.

4.4.5 Computational Systems and On-board Software

TriMARES computational system is composed by two independent computers. The main computer is located in the starboard cylinder and is based on a PC-104 stack, with a power supply board, a main processor board (with AMD Geode LX800 processor at 500 MHz), and additional boards to interface with health monitoring systems, actuation devices, navigation sensors, and communication systems. The on board software runs on a Linux kernel and both the operating system and the on board software are stored in a solid state disk, to avoid the risk of damage due to shock and vibration, if a hard disk were used. TriMARES software is composed by a set of independent processes to increase software robustness and modularity, following an architecture similar to the one employed for the MARES AUV (Matos and Cruz (2009)), as depicted in figure 4.9. The low level processes make the interface with the hardware providing an abstraction layer. On top of them, several other processes take care of specific tasks: position estimation, feedback control, autonomous mission execution, interface for external operation, vehicle supervision and health monitoring, and data logging. Interprocess communication relies on UDP messages and the main feedback control loops run at 10 Hz, with an overall CPU load less than 20%.

The second computational system, located in the top-port body, deals with payload sensors and communicates with the main computer through an ethernet connection. It is also based on a PC-104 stack, with a frame grabber to digitize the video from the camera, and it has enough space to integrate the electronics for the sonar transducers, as can be seen in the picture of figure 4.30. This secondary system can be fully programmed by system users for payload interfacing, processing, and logging, without affecting the normal operation of the modules running in the main computer. This way, the system architecture is kept open without jeopardizing robustness. It should be noted, however, that the secondary system can take control of the vehicle by sending appropriate commands to the external operation interface running on the main computer. This possibility is essential for the execution of adaptive sampling missions, *i.e.* missions in which the trajectory is dictated in real time, according to data processed from the payload sensors.

The communication network of TriMARES is depicted in figure 4.31. When at surface, the vehicle can communicate with a shore station using the Wi-Fi link directly connected to the main computer. Internally, an ethernet switch is connected to both computers and also to an ethernet connector at the tail of the top-port cylinder. A specially configured network bridge running on the main computer assures a transparent connection between the secondary computer and the shore station through the Wi-Fi link. The switch is also connected to an ethernet optic transceiver to enable communication with the vehicle through a fiber optic umbilical, in ROV operation. For long range radio communications at the surface, the system can use a UHF radio modem, and, if necessary, it may support an acoustic system for underwater communication. In both cases, the link is directly established with the main computer.

The fiber optic connection was not part of the original specifications, so in order to operate the original vehicle as an ROV, an underwater ethernet cable was used, connected to the stern of

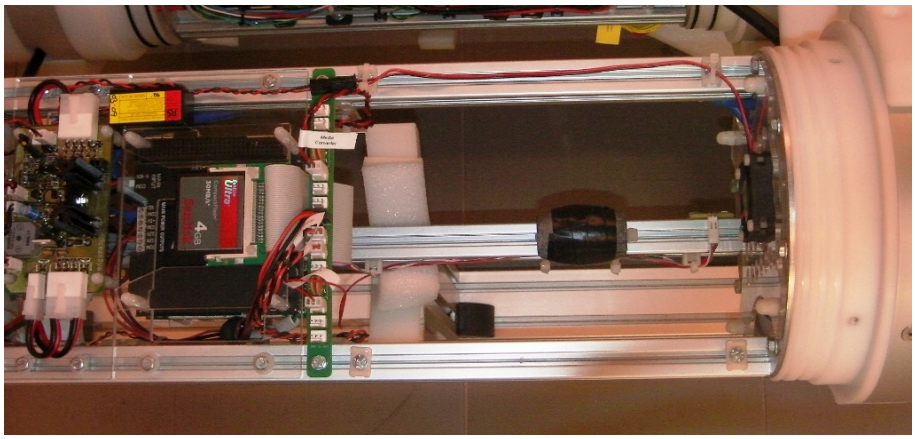

Figure 4.30: Internal view of TriMARES top-port cylinder, with a PC-104 computer and enough room to accommodate payload electronics. The lead attached to the frame is simulating the weight of the electronics, so that when it is replaced by the electronics does not affect the overall balance of the vehicle.

the top-port cylinder. This cable was relatively thick (about 10mm) and therefore made some impact in the hydrodynamics, so the consortium asked for a fiber optic umbilical and corresponding connectors. Note that in contrast to traditional ROVs that need a thick cable to provide power, TriMARES has internal batteries, so the cable is only required for communications. We've decided to order a custom version of an XtremeLight cable, from Falmat Inc., USA. We've asked for the cable to be reinforced with Aramid fiber to withstand 200kg and therefore be able to hold TriMARES, if necessary. This cable was also jacketed in a fluorescent polyurethane foam to become neutrally buoyant in fresh water and reduce the risk of entanglement during operations. Even with these extra layers, the final diameter was only 2.9mm, which results in a minimum impact during inspection operations. The cable was sent to Birns Inc., USA, to have a Millenium 3F connector installed (the other end had a standard SC fiber connector) and we've attached a cable gripper from Scorpion Oceanics Ltd., UK, as a strain relief.

4.4.6 Navigation and Control

In order to obtain geo-referenced positions, the navigation module relies on a LBL acoustic network with at least two moored beacons for determination of the vehicle horizontal coordinates, and a very accurate pressure transmitter, from Keller AG, Germany, to estimate depth. The vehicle also carries an integrated set of 3D accelerometers, rate gyros and magnetometers (an OEM MTi-100, from Xsense, Netherlands) for estimation of global attitude (roll, pitch, and yaw). To surpass the low update rate of the LBL range measurements (typical full update cycles last more than 3 seconds) an online interpolation mechanism based on an extended Kalman filter is employed. This process runs at 10 Hz and fuses acoustic range measurements with thruster RPM, vehicle attitude and depth, and other inertial data, to produce real time estimates of the vehicle position. Raw

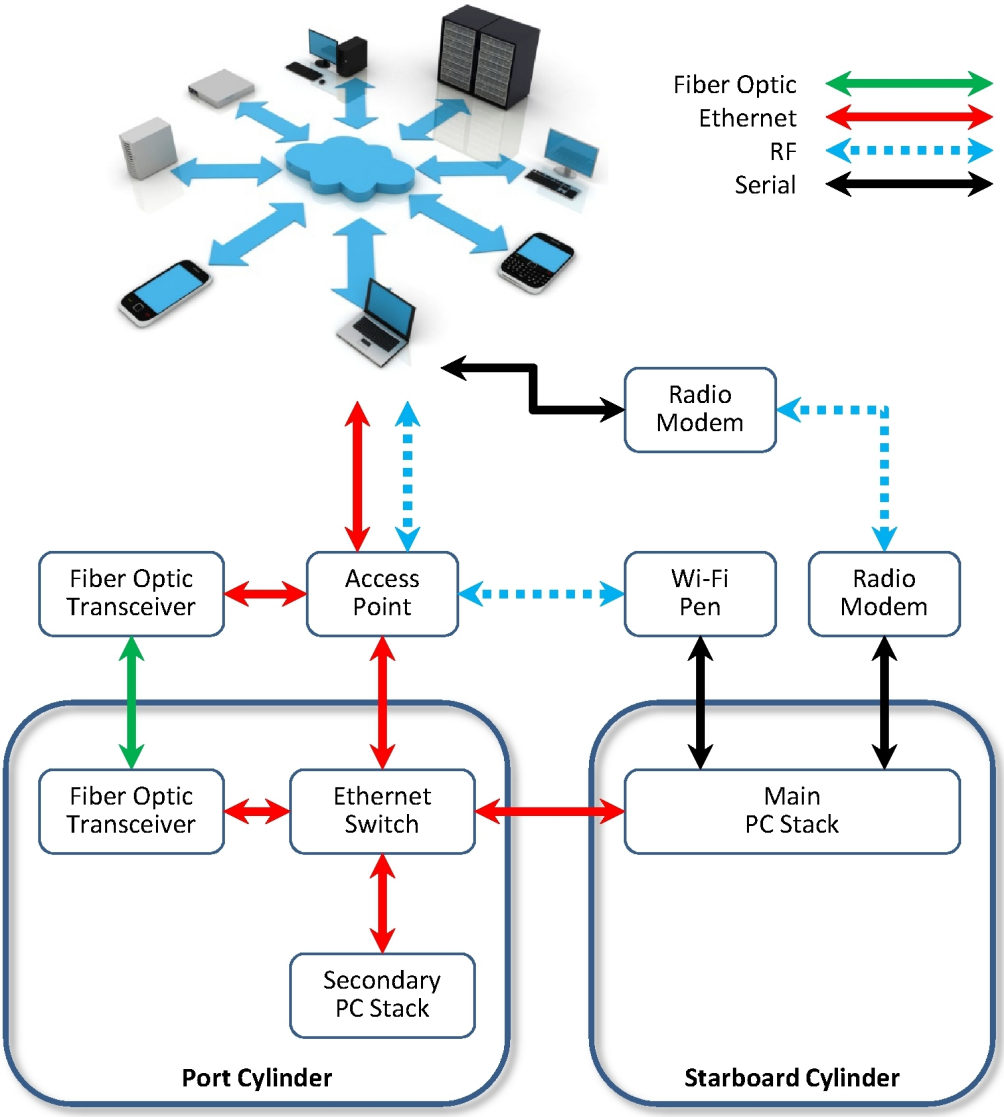

Figure 4.31: TriMARES communications network.

sensor data is logged to allow for post mission accuracy enhancement by smoothing algorithms such as described in Matos et al. (2003).

The control system was designed so that the controllable DOFs (surge, sway, heave, pitch and yaw) can be controlled independently either by setting position or velocity references. Such method allows for controlling the horizontal position or surge velocity independently of the depth, pitch or yaw, yielding greater flexibility and versatility of the TriMARES motion. Based on non-linear control tools, the elementary motions are truly decoupled by compensating the strong cross-relations found in this type of mechanical shape. This characteristic allows the end-user to perform any type of composed motion without having to be concerned with the low-level control nor the intrinsic complex dynamics. To illustrate the idea, suppose that we are interested in performing an elaborated trajectory in the horizontal plane which may involve position and velocity – typical trajectory tracking, for instance. However, the depth must remain constant over the operation and the pitch must be different from zero (e.g., nose pointing toward the seafloor). Such task is made possible by setting the depth and pitch references constant, while the rest of the DOF references remain available and ultimately set by an external entity (naturally, this type of motion is particularly interesting for ROV mode operation).

The specification of position or velocity references can be given in different referential frames, so we consider two possibilities for each of the DOFs: an inertial, earth-fixed reference frame, and a body-fixed reference frame. The control laws were derived in order to meet some essential requirements:

- Ability to move according to position references given in the earth-fixed frame.
- Possibility of setting velocity references in the earth-fixed frame.
- Capability of accepting velocity references in the body-fixed frame.

The task of deriving control laws that satisfy such requirements is not trivial and becomes more complex when the motion along the different axes is intended to be decoupled, since the controllers have to automatically compensate for the hydrodynamic coupling effects. The design and implementation of these controllers is beyond the scope of this work, and is being developed following our previous work with other vehicles, described in Ferreira et al. (2010, 2011). Our approach makes use of the nonlinear control theory, implementing the backstepping method (Khalil (1996)) to achieve robust and accurate control. The performance of this method is strongly related to the mathematical model of the hydrodynamics. Therefore, most of the tests performed with TriMARES before shipping were dedicated to the estimation of a reasonably accurate 6 DOFs model to be integrated in the control law, and were thoroughly described in Ferreira et al. (2012b).

4.4.7 Payload

TriMARES was designed to accommodate a high resolution video and photographic camera, a bathymetric sonar, and a water quality sensor package. However, the modularity of the vehicle

allows for different other payload sensors that can be carried within dedicated sections of the hull or externally attached to the vehicle frame. In both top bodies of TriMARES, the sections closest to the lifting aluminum rings are almost empty, apart from a few cables passing inside, so these sections can be easily drilled to install any sensor, preferably flush with the hull. Similarly, all three noses can be adapted to install new sensors or actuators. Such integration involves not only the mechanical aspects, but also the necessary interfacing in terms of electronics and software, so such a new device needs to be connected to one of the spare bulkheads in the end caps and the proper wiring has to be made to provide power and communications. In case of necessity, extra flotation modules may also be included to trim the overall vehicle and maintain neutral buoyancy.

4.4.8 Vehicle Operation and Safety

TriMARES is relatively compact, weighting approximately 75kg. The deployment and recovery can be made by a support vessel, preferably with a small crane, or the vehicle may be launched from an access ramp and towed to the operation area.

A typical TriMARES mission requires the deployment of at least two LBL acoustic navigation beacons to provide absolute geo-location of measurements during dives (Almeida et al. (2010)). The configuration of the vehicle and the navigation network, as well as the mission programming, are made with the aid of a graphical interface running on a laptop computer. A wireless network links the laptop, the navigation beacons and the vehicle while it is at the surface, using a combination of Wi-Fi and UHF radio communications, to ensure high bandwidth and long ranges. During the execution of an AUV mission, the graphical interface also receives data from the navigation beacons allowing for the real time tracking of the vehicle position. To increase operation safety, the laptop interface can also send simple special commands to the AUV using the acoustic navigation network. In the case of operation as an observation ROV, those navigation beacons may not be necessary if the operator is observing a structure in a known location. Naturally, during such a teleoperation, the vehicle is connected to the control station via a communication cable, so there is much more information available in real time.

The on-board power consumption is always monitored by the main CPU and there are several levels of protection against over current. On a first level, the thruster driver receives a periodic status report from each thruster indicating a proper behavior. Next, the on-board software ensures that the motion controllers never provide thruster commands that exceed the limits of the thrusters and of the underwater cables and connectors. Finally, the thruster allocation is also performed in such a way as to avoid exceeding the total amount of power provided by the DC/DC converters. In parallel with this, and as a backup plan for a software failure or a short circuit, all the power outputs are protected by fuses.

Apart from these preventive measures, there is also a supervision module that continuously checks the inner status of the vehicle: battery energy left, internal temperature, and water ingress using leak detectors installed in the bottom of all cylinders. When the vehicle is powered, a pair of LED lights flashes at the top of the hull, to facilitate visual tracking. Finally, the vehicle

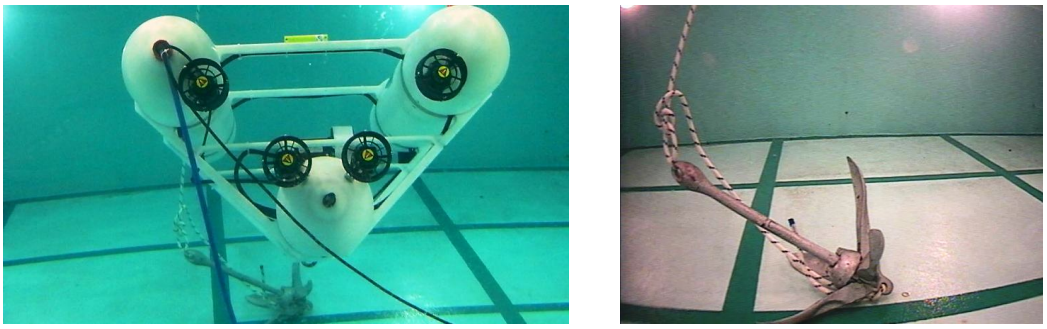

Figure 4.32: TriMARES looking down in ROV mode. Left: vehicle atitude; right: image from on-board camera.

transports a continuous pinger EMT-1-2, from Sonotronics Inc., USA, a self powered device that is completely independent from all on-board software and power, and transmits a periodic acoustic pulse for about 18 months.

4.4.9 In-Water Trials

The first water tests with the vehicle were carried out in a 5mx5m test tank, in our own facilities (figure 4.23). Given that the vehicle has hovering capability, even such a small tank is enough to perform many initial tests, from the validation of the main subsystems and ballasting, at the very beginning, to depth control and programming of simple maneuvers and missions. This kind of tank is also perfect for the first trials as an ROV, since it is possible to assess, at the same time, the behavior of the vehicle (through the inspection windows) and the data being produced by the sensors, in particular video. Figures 4.32 and 4.33 show snapshots of the videos[1] recorded during tests with TriMARES in ROV mode, in June 2011.

When we approached the functional version, we moved the test scenario to a reservoir in the Douro river, with a maximum depth of 15 meters (fig. 4.34). This scenario was chosen not only because it is close to our lab, but also because it is a scaled down version of the final application scenario for TriMARES, in Brazil. During these tests, we have trained the launch and recovery

[1] Some videos of these trials can be seen on Youtube channel *OceanSysGroup*

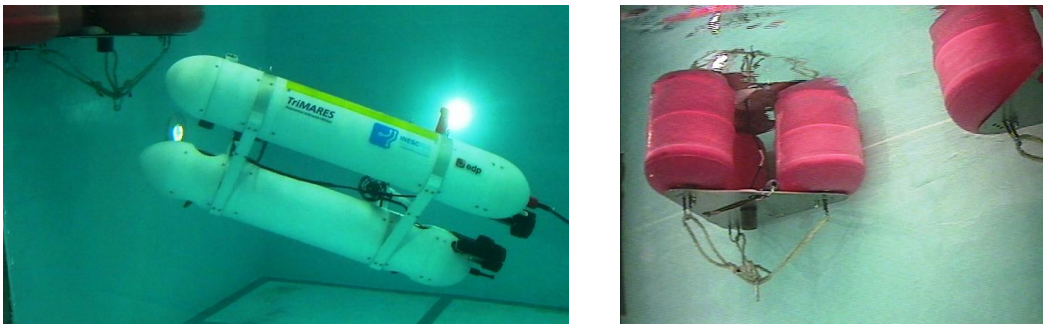

Figure 4.33: TriMARES looking up in ROV mode. Left: vehicle atitude; right: image from on-board camera.

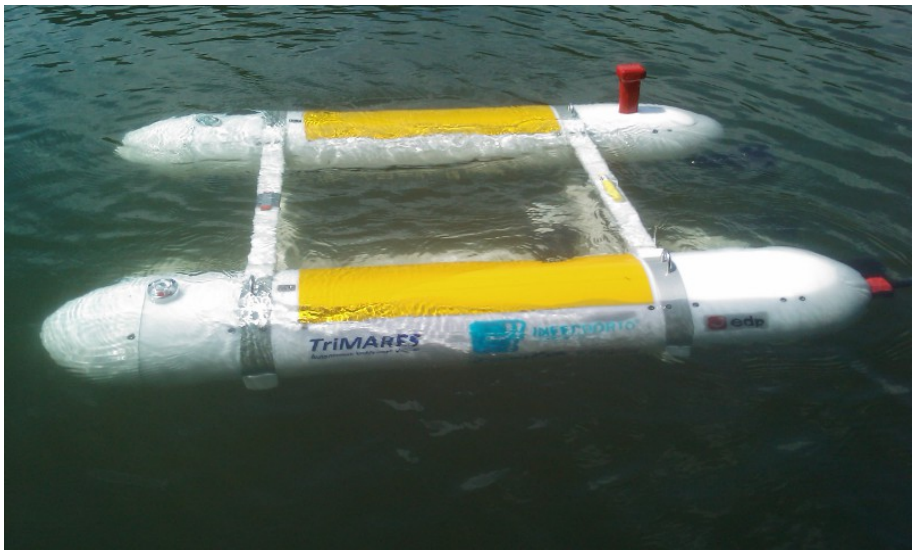

Figure 4.34: TriMARES ready for testing in Douro river reservoir, June 2011.

procedure and we have also tested the performance of the combined GPS/Wi-Fi antenna located at the stern of the starboard cylinder (see figure 4.34). Even with a small height above the surface of the water, it was possible to maintain a Wi-Fi connection more than 200 meters away, using a sector antenna at the control station, and the vehicle would get a GPS update only a few seconds after emerging. Finally, we've installed an acoustic navigation system to track the vehicle during these simple missions and also to test the emergency "'abort"' command, sent acoustically by a navigation buoy deployed in the operation area.

Finally, we have programmed the vehicle to carry out a few simple missions, like following a sequence of waypoints, or hovering at a certain depth. These missions were useful to validate the mission control software and also to tune the hydrodynamic model of the vehicle, in order to improve the performance of the controllers. These models are commonly difficult to derive due to their intrinsic complexity and large number of parameters. Moreover, hydrodynamics literature mainly relies on semi-empirical formulas to derive those parameters and some characteristics such as roughness may be difficult to assess (Fossen (1995); White (2002)). Several experiments were therefore carried out to infer about the overall model as well as validating the control law which strongly depends on it, as described in Ferreira et al. (2012b).

Figure 4.35 shows an example of the performance of depth and pitch control during a dive to a depth of 5 meters. The vehicle starts descending to a depth of 2 meters at approximately $t = 530$s, changes depth reference to 5 meters at $t = 560$s, and switches off the vertical controllers at $t = 650$s. Note the negligible steady state oscillation in depth when the vehicle stabilizes at 5 meters (the amplitude of the oscillation is below 2 centimeters), demonstrating the robustness and the accuracy of the control approach. Such capability is particularly interesting for inspection tasks, such as video recording, and it may even be explored for intervention operations. The small overshoot when the vertical reference changes (about 20cm) can be further reduced, if required,

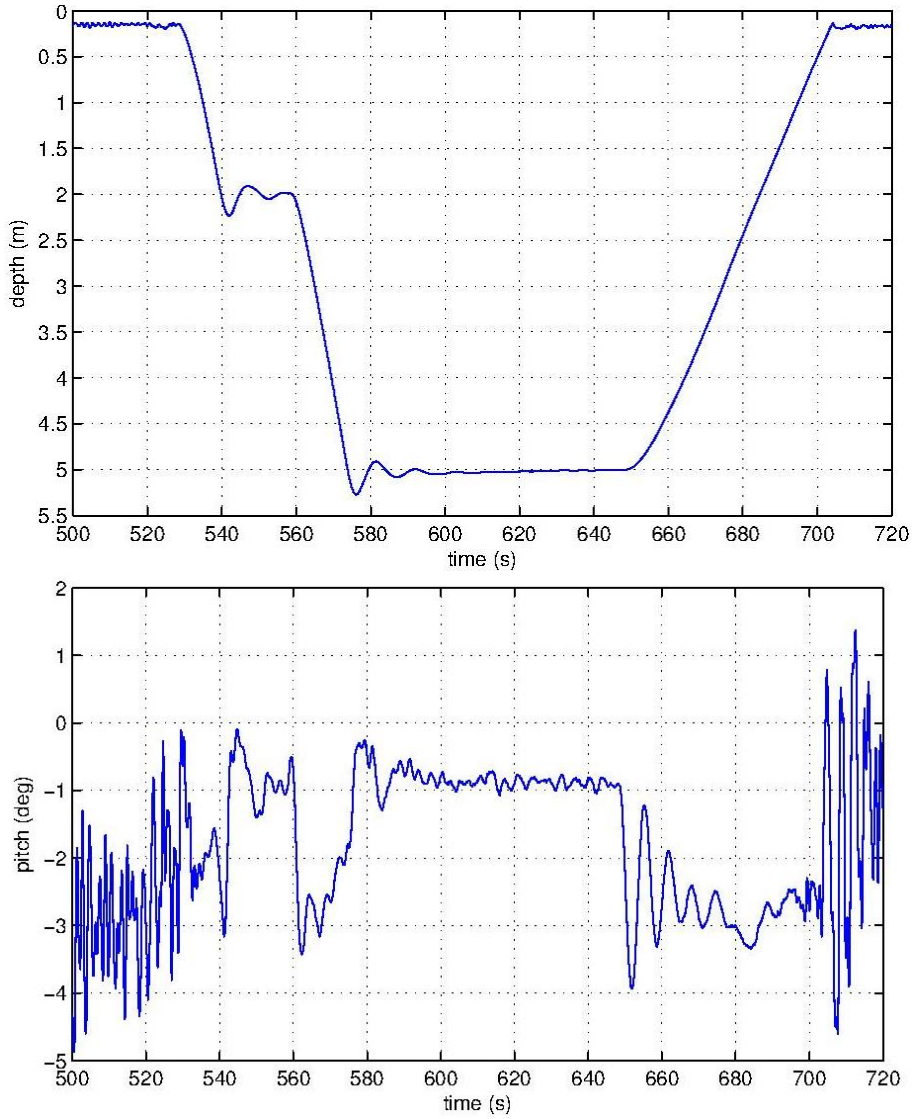

Figure 4.35: Depth and pitch control of TriMARES during a two-stage dive, June 2011. The vehicle was commanded to dive to a depth of 2 meters at $t = 530$s and to a depth of 5 meters at $t = 560$s. The controller was switched off at $t = 650$s.

by a different tuning of the vertical controllers. Although the pitch angle is always small, it is clear the influence of the surface and the natural damping after the controllers were switched off.

After the confirmation of the acceptance tests, the vehicle was shipped to Universidade Federal de Juiz de Fora, Brazil, in July 2011, where the payload sensors were integrated. In September 2011, some of the earlier tests were repeated in a local pool (figure 4.36) during a pre-scheduled training phase that lasted 2 weeks.

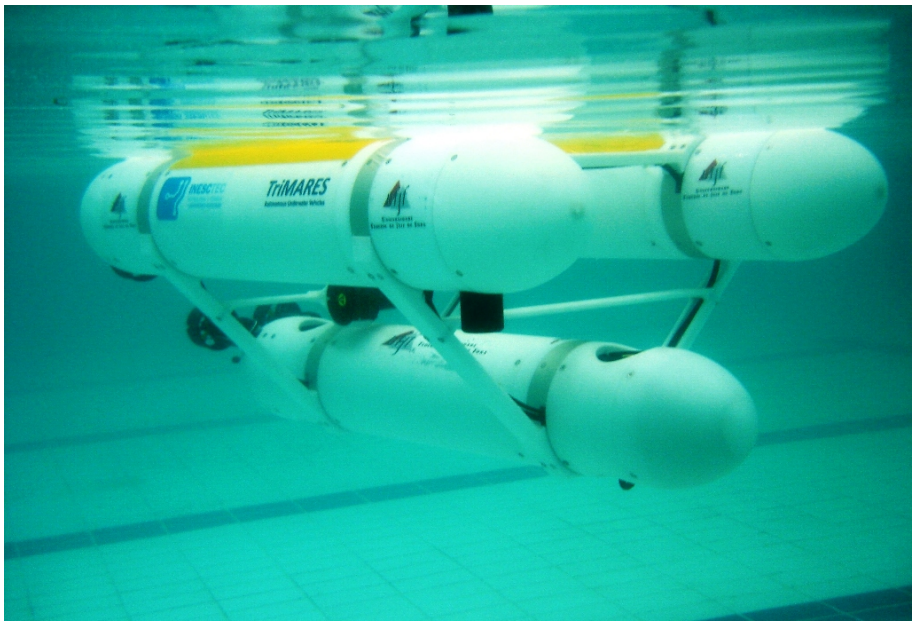

Figure 4.36: The TriMARES hybrid AUV/ROV during water trials at the Federal University of Juiz de Fora, Brazil, September 2011.

4.5 Discussion

This chapter described a consistent program for the development of small size AUVs based on modular building blocks. In this case, modularity encompasses both physical parts and also software and control systems. These modules can be rearranged, replaced or individually redesigned to yield a great variety of AUV configurations in a relatively short time. Moreover, given that the development of AUVs requires a coordinated, interdisciplinary work, this modularity ensures a continuous evolution of possible features, without compromising the overall reliability of the proven solutions.

One of most obvious aspects of our modular approach comes from the physical sections of the AUVs and the way they can be integrated, removed or swapped with a minimum impact in the overall configuration. Actually, the absence of a reliable physical device is still a major hindrance in many laboratories to proceed with validation of scientific developments in an operational scenario. In our approach, there is a single sensitive part – the pressure housing – and all the other parts are very easy to manufacture. Since they do not have any seals, they are very forgiving in terms of dimensions and can easily be machined in almost any material, or even be printed using a 3D printer.

Using a set of modular building blocks, we have first built the MARES AUV, back in 2007, a hovering AUV that has been continuously updated and used in the field in many different configurations. The success of the first demonstration mission at sea proved that the initial requirements and the design decisions contributed to the development of an operational vehicle that can be effectively used in real application scenarios. Overall, the mechanical design has proved to be quite

robust, as the vehicle has been transported for field tests in the trunk of a car tens of times with no mechanical failures.

One of the major advantages of the MARES AUV, when compared with other AUVs of similar size, is the ability to control independently the motion in the vertical and in the horizontal planes. This allows for some new primitives of motion, such as commanding the vehicle to be completely motionless in the water column (for example, waiting for some triggering event). To our knowledge, MARES was the first man-portable hovering AUV and also the first truly modular vehicle of its class. It has already incorporated a great variety of payload sensors and it has supported a great number of scientific research, providing valuable field data to validate theoretical results. For all these reasons, we believe that the MARES AUV is a privileged tool to test new algorithms and sampling strategies in the ocean, especially when it encompasses innovative motion primitives and control strategies (see, for example, Ferreira et al. (2012a)).

In 2011, after a demand from a Brazilian consortium, the versatility of the system components has gone through a great test – to develop a much larger vehicle to provide extra payload capability, including high quality video, multiple sonars, and water quality sensors. The result was the development of TriMARES, a 75kg, 3-body system hybrid vehicle, with the ability to operate as a standard untethered AUV or as an ROV, using an underwater ethernet cable or a very thin fiber optic cable to provide real time communications. The first in-water trials of TriMARES started only 6 months after the final user requirements were discussed. This was only possible due to the earlier experience with other vehicles, with a well planned project, and keeping a tight control of the progress of the project, particularly in what concerned orders of critical components. But, above all, this was enabled be the reutilization of many designs already existing during the evolution of MARES. The successful accomplishment of the trials demonstrates that the engineering requirements were met and the reutilization of the available modules contributed to the development of an operational vehicle adequate for the planned tasks. More, the system is being used by a different research group, in a different continent, and so a lot of effort has been put into documentation and knowledge transfer. To our knowledge, it was the first AUV exported from Portugal.

In 2012, we received another order, this time directly from Universidade Federal de Juiz de Fora, Brazil, who wanted to have a vehicle to proceed their own research and development program in underwater robotics, when TriMARES was finally shipped to the final destination, in Tocantins. This vehicle was a smaller version of MARES, and was shipped to UFJF in 2013, where it has been serving for research with the robotics group of Prof. Leonardo Honório (figure 4.37). Although the commercialization of these vehicles was not an objective when we started the program, these successful examples serve to demonstrate the usefulness of our solutions.

As for future developments, we think that the versatility of the modular building blocks may be further exploited, to result in a greater variety of vehicles, to address specific scenarios. A 2-body vehicle is a natural extrapolation of the work described in this chapter. Other modules can easily be designed to integrate new sensors or actuators, for example to provide control fins to a torpedo AUV. At the same time, the redesign of particular blocks may enlarge the range of

Figure 4.37: TriMARES and MARES in UFJF, Brazil, July 2014. Note that TriMARES fits the trunk of a small van, as required in the initial contract (photos courtesy Prof. Leonardo Honório, UFJF).

potential application scenarios. For example, a redesign of the dry compartment to withstand very high pressures may be used in a deep water AUV, without changes in the other modules.

Finally, with the development of automated vision processing, together with increased navigation accuracy, we are planning to extend the TriMARES features, not only to be able to work as an advanced inspection platform, but also to include some light intervention capability.

Chapter 5

Modular Marine Surface Vehicles

When the solution is simple, God is answering.

— Albert Einstein (1879–1955)

Robotic surface vehicles have been playing a discreet but consistent role in the marine environment, in areas as diverse as coastal oceanography, surveillance, atmospheric studies, or search and rescue operations. These vehicles are commonly referred to as Autonomous Surface Vehicles (or *ASV*s), and they combine the ability to transport a large variety of sensors and actuators with real time, high-bandwidth communications, resulting in advanced systems for tele-presence in the ocean. Even thought they can only move at the surface, the availability of long range sensors (such as ADCPs or sidescan sonars, for example) allows them to probe deeper than the very top layer of the ocean.

In our perspective, robotic surface vehicles are extremely valuable scientific devices, not only because they provide an effective way to sample the ocean (being a critical asset under the AOSN paradigm), but also because they can be used with great efficiency to validate many AUV subsystems and algorithms before actually being incorporated into underwater vehicles. Furthermore, they can also be used to facilitate logistics during AUV operations, for example acting as virtual buoys to provide navigation beacons, either fixed or moving. All these tests can take advantage of the real time communications with ASVs to obtain a quick feedback on system performance, accelerating mission analysis and yielding a tremendous improvement in terms of development effort. As an added benefit, data can be easily tagged in space and time using GPS and, very importantly, without any of the risks associated with AUV operations.

In this chapter, we describe a program for the development of small size ASVs based on modular components. Many of these building blocks are in fact common to the ones used for the assembly of AUVs, described in the previous chapter, which emphasizes their value and versatility. Once again, our concept of modularity includes as many subsystems as possible, both in terms of hardware construction, but also in terms of electronics, software and control. These building

blocks have been used to build the Zarco ASV, in 2005, and later to replicate the system to assemble Gama, in 2008. Both vehicles have been extensively used for testing multiple aspects of marine operations and they have undergone a continuous evolution since their first trials.

The remainder of the chapter is organized as follows. We begin by conveying, in section 5.1, our main requirements for the design of robotic surface vehicles. We proceed, in section 5.2, with the description of the most important building blocks that are the basis of these vehicles, both from the mechanical perspective, but also in terms of electronics and software. Section 5.3 presents the evolution of two similar ASVs assembled from these existing blocks (Zarco and Gama), and some operational results. Finally, we conclude the chapter with a discussion on the main achievements of our modular approach and some hints on possible future evolution.

5.1 Design Requirements

In order to establish the requirements for the development of ASVs involved in a long term program for marine operations, it is paramount to identify the critical aspects associated to their planned operations, following a systems engineering approach. In our perspective, there are 3 main roles that ASVs can play in ocean engineering:

1. Independent platforms to carry scientific instruments, taking advantage of their mobility, precise localization and real time communication capability to capture and transmit ocean data. Usually, these data are autonomously gathered at predefined locations, following a pre-programmed sequence of waypoints. However, given the existence of real time communications with the platform, the operator can also take control of the motion using a joystick or other input device.

2. Demonstration platforms for validation of different algorithms, namely on navigation and control. In fact, modeling of ASV hydrodynamics can be more complex than AUV's due to the interaction with wind and waves, and, therefore, they can provide excellent opportunities to explore more audacious control methods. The relatively *slow* dynamics of marine robotic systems and the prospect of having a permanent radio link with the platform for an emergency remote take-over reduces the stress associated with validation in the field.

3. Components of a multiple vehicle system to cooperatively sample the ocean. This cooperation can take many shapes, either in the form of a team of similar ASVs, for example capturing complementary data, to the case of heterogeneous vehicles, including ASVs and AUVs, in some form of collaboration. This includes, for example, being used as virtual moorings to replace navigation buoys in deep water areas where it is not easy to moor acoustic beacons.

Similarly to the case of AUV development, our decision on vehicle dimensions was strongly influenced by our concerns on logistics. The demonstration of solutions in field experiments is a key aspect in our strategy for the development of robotic solutions, therefore we've tried to reduce

the size of the platforms as much as possible to facilitate transport and deployment. Naturally, this limits the scenarios for possible utilization to calm waters, and also limits the amount of transportable payload. However, the impact of this guideline in ASV development is much weaker than in the case of AUVs, since it is much easier to take advantage of a modular development to strengthen the mechanical structure, should the need arise to operate in rougher environments.

Another guideline for the development of the ASVs was the ability to be replicated and reconfigured at a minimum cost and effort, fostering the possibility of multiple vehicle operations. Reducing the size of the vehicles also helps in this respect, as well as choosing off-the-shelf components whenever possible.

In terms of vehicle performance, our requirements were simply to be able to overcome modest currents and to allow for a few hours of operation (naturally depending on velocity), so we've set some indicative numbers of a maximum velocity above 1 ms^{-1} and maximum range above 10km.

5.2 Main ASV Components

As a particular class of robotic systems, Autonomous Surface Vehicles share the typical subsystems of other mobile platforms, with some particular characteristics associated with the specific environment where they operate. This section describes our approach to the development of the main ASV building blocks, separated into four subsections. First, the physical structure that has to enclose all electronics and support the external sensors and actuators, with a special attention to the fact that they have to operate in a very harsh environment. Second, the propulsion system, that ensures the required mobility. Then, the electrical components, including the computational system, the interface electronics and power management system. Finally, the on board software that deals with all aspects of the operation of the vehicles, either via remote control, or in autonomous mode of operation.

5.2.1 Mechanical Structure

In terms of conceptual design, our approach for the mechanical blocks to assemble ASVs differs from the architecture we use for AUVs. As discussed in section 4.2.1, specific requirements for AUV construction justify a *Sectional* architecture, while in the case of ASVs, we think that there is advantage in adopting a *Bus* modular architecture. This type of modularity is characterized by a main part with a common interface for the connection of all other parts (see Ulrich (1995) for different types of modularity).

In our case, the backbone of an ASV is built using a structural frame, that can be assembled from COTS aluminum profiles and interconnecting accessories. This frame allows the installation of multiple subsystems, either directly attached using standard accessories or inside proper enclosures. It is reinforced in the aft section to hold the thrusters and, if necessary, it can be easily reinforced further with extra profiles and/or enlarged to accommodate more payload. Moreover, the structural frame provides a railing system such that the relative position of all other subsystems can be simply adjusted with a minimum set of tools.

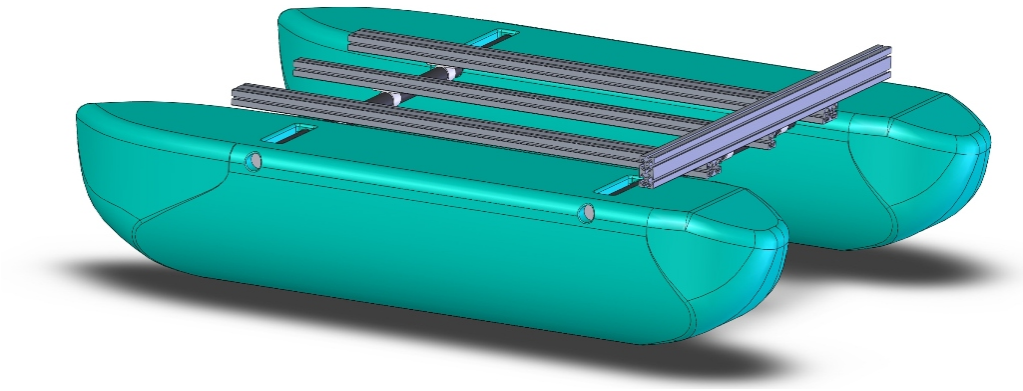

Figure 5.1: CAD representation of an ASV structural frame attached to two floating pontoons, forming a simple catamaran.

The structural frame has to be fixed to the floating platform, either a mono hull or a multiple hull arrangement. For our planned operations, platform stability is quite important, so a configuration like a catamaran is preferable for being more stable. This can easily be achieved by attaching a pair of floating pontoons to the mechanical structure. These pontoons can be adapted from some commercial model, or they can be custom ordered. In any case, the main idea is that they can be easily decoupled for transportation or replaced for different requirements in terms of operation. Figure 5.1 represents a basic configuration of such a catamaran.

Apart from specific sensors and actuators that need to be in direct contact with water, all other devices are installed above the waterline, *i.e.*, above the structural frame, to minimize drag in water and to reduce the risk of water damage. Anyway, since the ASVs operate in permanent contact with water, it is fundamental that all devices are waterproof, since there is always the possibility of capsizing, of the ASV being washed over by a large wave or the wake of another boat, or simply to allow operations in rainy days. However, the amount of pressure that any subsystem is subject to in an ASV is much less than in AUVs, so we have a constraint that all equipment has to be rated at least IP67 (up to one meter of submersion).

The market for *nautic* equipment (IP67 or better) is much larger than the market for *underwater* equipment (from tens or hundreds of meters of depth, to full-ocean depth). Therefore, some of the electronic systems for ASVs can be ordered with enough protection against the elements, at reasonable prices. However, a significant fraction of the on board electronic components need to be enclosed in watertight containers, either to reduce the individual cost of the component or simply to increase the pool of options. Fortunately, the motion drag of the volume above the waterline is much less significant than the submerged part, and so the size and the shape of the watertight enclosures are not critical. This means that we can take advantage of the many options of IP67 enclosures for extreme environments, and use COTS enclosures to hold all these electronic systems. More, with the mechanical structure as described above, the only requirement is that the enclosures have some adaptation frame to allow them to be placed along the longitudinal rail. In our case, we've chosen a series of IP67 polycarbonate enclosures from Fibox, available in a variety

of sizes, and with detachable lateral glands for the installation of electrical connectors.

Finally, the main structural frame can also be used to support other sub-frames. On top of it, an elevated bridge can be attached to provide a higher point of observation, useful for the installation of cameras, airborne sonars and other sensors. Below, an underwater payload tray can be be used to transport waterborne sensors, like sonars or water quality sensors. By using the right accessories, these sub-frames can easily be detached for transportation and quickly reinstalled at the operation site.

5.2.2 Propulsion

There are several options to provide propulsion to an ASV, both in terms of technology involved and also in terms of configuration. Our default choice was a configuration with differential drive, to achieve a solution closely related to our main AUV design (described in the previous chapter). The exact solution was a combination of price, availability, and simplicity of control. Once again, we took advantage of the market for nautical equipment and we've modified COTS trolling motors, so that the actuation handle was removed and replaced by a junction box that receives a PWM command from a motor driver. These thruster are relatively inexpensive, available of the shelf (from several manufacturers) in a variety of power levels, and there are also many off-the-shelf solutions of electronic boards to control them from a computer. Moreover, they are ready to be attached to the stern of a small boat and they can be folded close to the structure for transportation. Figure 5.2 shows one possible configuration of thrusters mounted in a simple structural frame with an underwater sensor tray and a couple of waterproof enclosures. Both the enclosures and the flotation pontoons can be easily detached to facilitate transportation, while the thrusters can also be folded along the frame to reduce the overall bounding box. The enclosures can be positioned anywhere along the frame, to trim the vehicle pitch angle or to allow enough space for an additional payload enclosure. The height of the underwater sensor tray may also be adjusted.

Apart from this default configuration, it is relatively easy to test different options (like using a single thruster and a servo to control direction) or different technologies (for example taking advantage of wind propulsion), with minimum impact on the rest of the system.

5.2.3 Electronics

As far as electrical systems are concerned, our design includes the separation in three main modules: energy, main electronics, and an optional payload module, as can be seen in figure 5.3. Since ASVs maneuver with no physical link with the operator and they require electrical energy to power all on-board systems, they need to transport some sort of energy on board, and/or to capture it from the environment. In our case, we consider rechargeable batteries to store electrical energy and we prepare the system to be able to capture further energy from the environment, typically using solar panels or wind generators, even if this requires the lengthening of the mechanical structure. In the case of our ASVs, our main requirement is that the batteries are able to deliver a few hundred watts to power the electrical thrusters. Usually, the overall weight and volume are

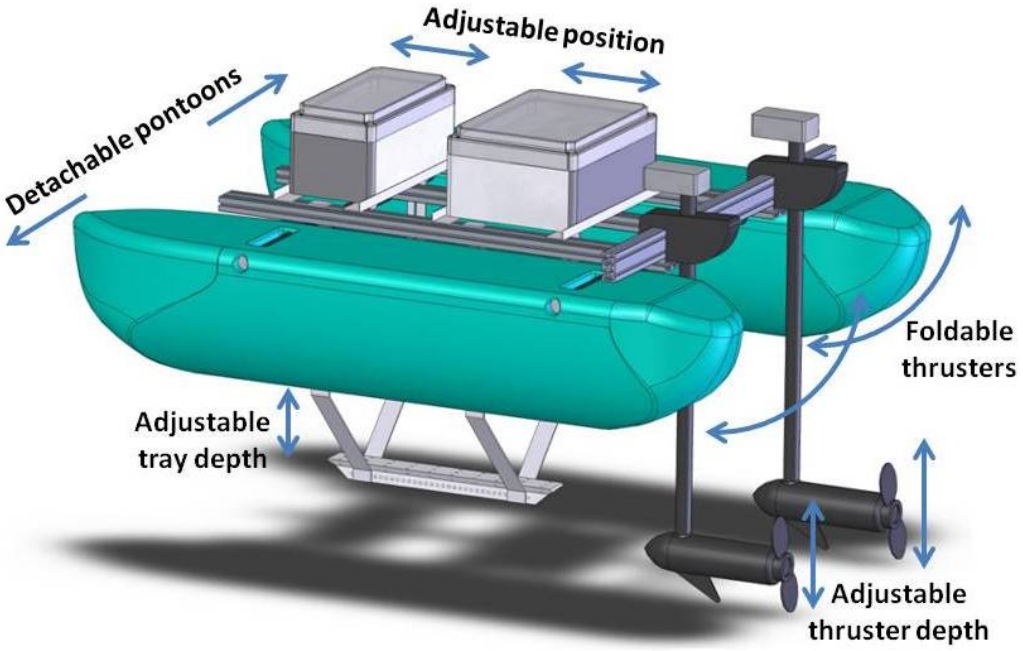

Figure 5.2: CAD representation of an ASV structural frame attached to two floating pontoons, in a catamaran configuration with two rear thrusters, two watertight enclosures, and an underwater sensor tray.

not very critical, therefore our typical choice is to use relatively common deep-cycle Lead-acid batteries, readily available in many sizes and discharge capabilities. Also, their nominal voltage is 12V, which is a convenient value to power the on-board electronics, either directly or using simple converters.

In our typical configuration, the energy module is physically separated from the main electronics module, each with its own watertight enclosure that seats on the aluminum frame. This separation has two main advantages as compared to a single enclosure: first, it is very easy to swap the energy module by a new one when the batteries are exhausted and, second, if there is the need for a continuous long mission, it is possible to use an improved version of the energy module, based on technologies with better power to volume ratios.

The main electronics module encloses the master on-board computer that takes care of mission management, navigation and control, as well as all interfacing electronics. Although all our initial systems were based on industrial boards using the PC-104 standard, there are now low cost alternatives that can be employed for this master PC. For example, recent single board computers like Raspberry Pi or Beagle Bone offer extremely low cost solutions with very reasonable computational performance and modest power consumption. They also have interfacing boards (or *shields*) to expand the connectivity with all sorts of peripherals. In fact, we have four types of interfacing boards: power distribution, communications, sensors, and actuators. The power distribution system is based on a PCB with multiple output voltage levels in a bus of header connectors, where all other subsystems can get power. Some of these subsystems are communication devices, like a

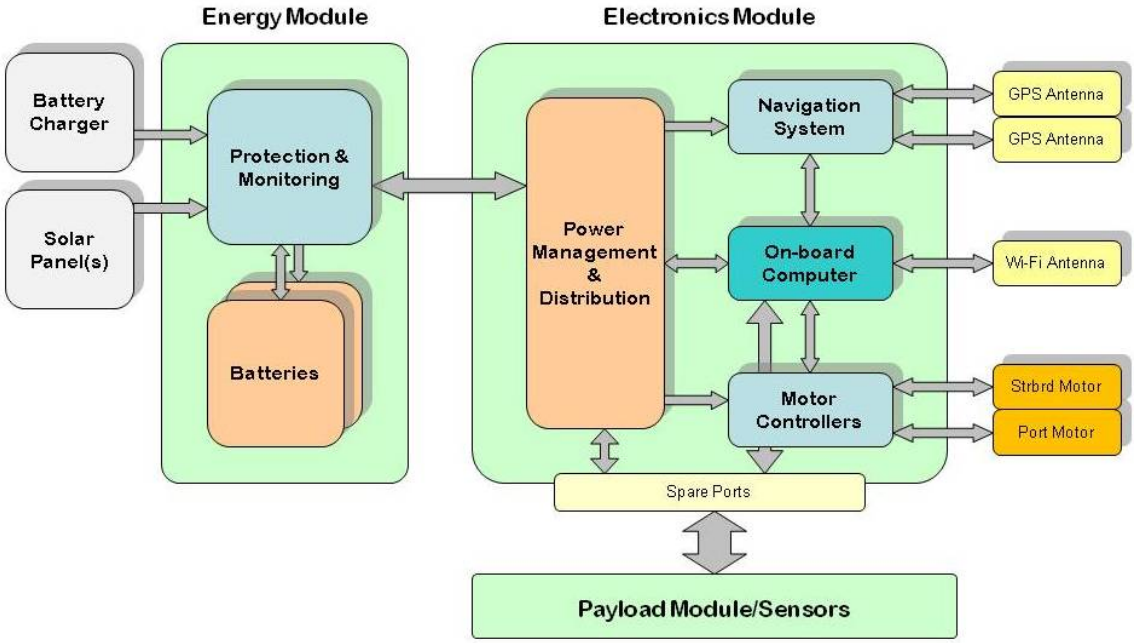

Figure 5.3: Schematic of the distribution of the ASV electronics.

Wi-Fi router and Ethernet switch that is installed on board. Sensors are connected to the main PC, either directly or via specific electronic boards. In the case of actuators, they require dedicated motor controllers, and we have been using different versions of motor controllers from RoboteQ.

The navigation system is a major component of any autonomous system and its main task is to compute the vehicle location in real time. Fortunately, the typical outdoors application with a clear view of the sky makes the GPS a natural choice for the main navigation sensor for ASVs, providing an absolute position with bounded error, while the orientation can be easily provided by a digital compass. In many situations, the 3–5m accuracy of a single low-cost GPS receiver is enough, while, in others, it may be necessary to reduce uncertainty with a more accurate DGPS system, or to fuse such information with data from inertial devices using relatively conventional techniques such as the Kalman Filter.

Since ASVs operate at the surface, it is possible to benefit from all commercial communication solutions based on radio transmission. This includes short range line-of-sight (LOS), high data rate provided by standard Wi-Fi connectivity, to long range RS232 radio modems. In more remote locations, there are also commercial solutions to take advantage of the cellular phone network or using satellite connections like Iridium.

In order to provide electrical connections between enclosures and to the external components, we use IP68 Bulgin Bucanneer bulkheads in the lateral enclosure glands and the corresponding in-line connectors for the interconnecting cables. These connectors were chosen, not only for their robustness and for the availability off the shelf, but also because they have replaceable contact inserts that are available in a variety of patterns, sizes and pin counts, according to the type of contact and current rating.

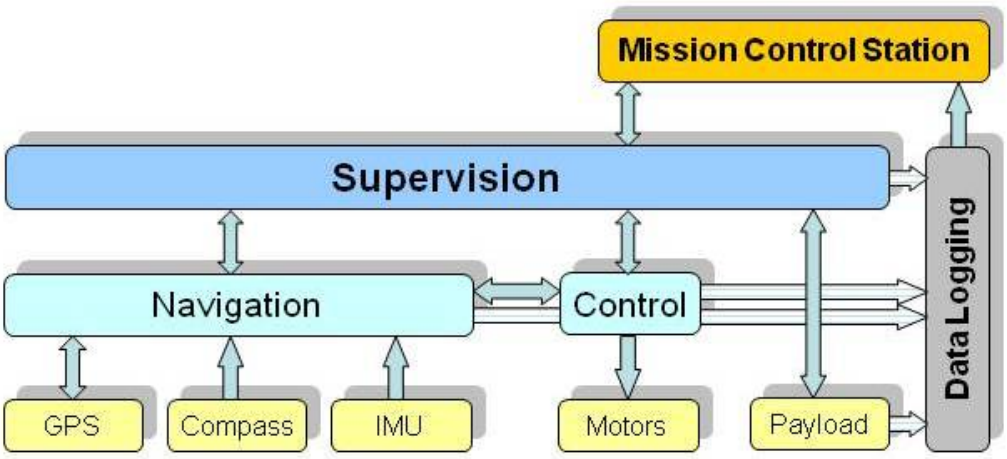

Figure 5.4: Overview of ASV software architecture

The optional payload module communicates with the main electronics module to receive power (switched) and communicate with the on-board computers and to the world via the Wi-Fi router. Apart from the master computer, we can easily incorporate other slave processors, which are typically included to dedicated data processing. In the past we have tested many different configurations for slave processors: Raspberry Pi have been used for image processing and obstacle avoidance, sonar processing has been done with a FitPC, acoustic communication using modems connected to a Gumstix. In reality, given the Ethernet connection ensured by the on-board Wi-Fi, the main PC can even receive information in real time from a remote PC.

5.2.4 On-Board Software

The on-board software is always one of the key aspects of an autonomous mobile system, since it has to manage all incoming data from the sensors (both navigation and payload) and produce the proper actuation *commands*. Our software architecture for the ASVs, depicted in figure 5.4, is very similar to the architecture implemented for AUVs, as shown in figure 4.9 of the previous chapter.

In fact, the software is composed by a set of modules, many of which are exact copies of the modules used for AUVs, such as the case of the hardware interface modules at the lowest level of the hierarchical structure. At at intermediate level lie the navigation and control modules, which are responsible for the real time estimation of the vehicle state and for the real time computation of the vehicle actuation, respectively. At the top level resides the supervision module. Besides being responsible for the communication with the shore station, either executing remote commands or sending back relevant data, it monitors the vehicle behavior and deals with unexpected events. A black box data logging system registers all data related to the vehicle motion on a Flash disk connected to the CPU board. This system can also be used to register payload data.

The navigation module is responsible to compute in real time the state of the vehicle (position, attitude and linear and angular velocities). Similarly to the case of AUVs, this estimation is

performed by an extended Kalman filter based algorithm (Gelb (1996)) that can be configured to incorporate data from different sets of sensors and subsystems. In both cases, a digital compass and an IMU provide orientation angles and accelerations. The main difference with respect to the navigation module of AUVs is that, in the case of ASVs, the GPS signal is usually available and it is used to provide absolute positioning with a bounded error. Given the slow nature of our electric ASVs and the comparatively high data rate of current low-cost COTS GPS receivers, even a low-cost, low performance IMU is sufficient to ensure an accurate localization of the ASV.

The control module is responsible to compute in real time the motor actuation according to the mission that the vehicle must perform. For that purpose, the control system implements a series of control loops according to the actual maneuvers and the error with respect to the active references. At each control cycle, the control system computes the vehicle actuation, tests the completion of the current maneuver and starts a new maneuver, if the completion conditions are met. For control purposes, it is sometimes advantageous to decompose the port and starboard thrusters actuation in common and differential modes, according to

$$F_{port} = \frac{F_{common} + F_{diff}}{2} \tag{5.1}$$

$$F_{starboard} = \frac{F_{common} - F_{diff}}{2} \tag{5.2}$$

since, in this way, the linear and angular motions of the vehicle can be decoupled. When manually operated, both the common and differential mode commands are obtained from the joystick attached to the control station. When in autonomous mode, they are computed by the local control system with a typical update rate of 10 Hz.

5.3 Zarco and Gama ASVs

At the initial stage of the development of our program, and following the requirements identified in section 5.1, our priority was to role number one, *i.e.* to assemble a platform that could be used to transport scientific instruments for remote sensing. In particular, we were interested in experimenting various types of sonar systems, taking advantage of a stable platform with accurate positioning. In order to ensure autonomous operations, it is paramount to develop a series of control algorithms, like trajectory tracking. Naturally, having a physical platform to validate them in the field is a great help, so we've immediately focused also on role number two, *i.e.* to have a demonstration platform for validation of navigation and control algorithms.

Zarco was the first prototype built for this purpose, a small size (1.5 m long) catamaran assembled in 2005 (Cruz et al. (2007)). It can be seen in figure 5.5 in its basic configuration, weighting about 500N, and with a maximum buoyancy of another 500N, therefore easily accommodating a few kilos of extra payload. Even though some of the internal components have changed since the earlier operations, the architecture has been maintained and the evolution has been smooth, ensuring a continuous availability for field testing. In fact, one of the great benefits of the physical

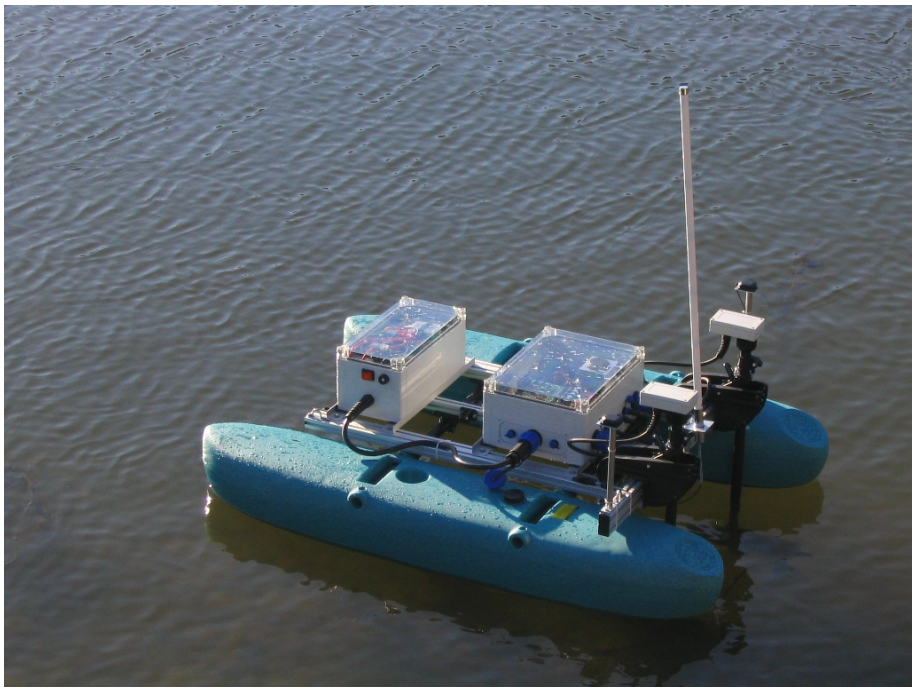

Figure 5.5: Zarco ASV initial tests in the Douro river, December 2005.

arrangement is that in can be easily transported in a simple car and deployed from a small ramp or pontoon, not requiring a crane or any other handling equipment. In terms of general specifications, Zarco is electrically powered from rechargeable batteries and can operate at speeds up to 3 knots, during a few hours. It carries an on-board computer responsible for the execution of autonomous or remotely controlled missions, for the real time interface with all peripherals and for the storage of collected payload data. A Wi-Fi link connects Zarco to a shore station, allowing for the remote control of the boat and the supervision of its autonomous operation.

Following a couple of years of utilization with only minor improvements, we've realized that the platform could be easily replicated to address role number three, *i.e.*, to have more than one ASV for coordination missions. Gama was then built in 2008, using the same architecture of Zarco, and being very small they could be easily transported together to demonstrate coordination in ponds and calm waters. At the same time, the MARES AUV was also operational, therefore allowing for missions with a network of heterogeneous vehicles. In the following sections, we will detail some of the ASV subsystems and their evolution in the last years.

5.3.1 Mechanical Structure and Propulsion

Zarco was assembled using the hardware architecture described earlier, following a highly modular approach. The mechanical structure is based on COTS anodized aluminum elements from Bosch Rexroth, with 30x30mm and 60x30mm cross sections, forming a rigid frame where all other mechanical parts are attached. In fact, this type of structure allows two different ways of interfacing: by clamping around it or by using special insert nuts. In the longitudinal direction, a railing system

separated by 460mm, allows a continuous adjustment of the position of the watertight enclosures, or other components. This type of profiles is very popular in industrial environments, as they are available off the shelf in many sizes, they are easily cut to the required length and there are many accessories to suite all sorts of industry needs.

The mechanical structure attaches to a couple of lateral pontoons by a set of snap buttons, resulting in a catamaran arrangement. In the original version, we've chosen a pair of rugged commercial pontoons from Hobie Cat, USA, the *Hobie Float Cat 60*, that are still being used. These pontoons are intended for personal fishing in class 1 waters, therefore they are suitable for our envisaged scenarios. They are made of molded polyethylene, with a length of 60 inches (around 1.5 meters) and a total net buoyancy of around 1000N. Although they are no longer produced by the company, they can easily be replaced for similar size floating devices, with the corresponding attachments to the main mechanical frame.

Typical propulsion is provided by two independent electrical thrusters located at the rear of the mechanical structure. In our case, we use thrusters based on standard trolling motors from Minn Kota, the Endura 30, typically used in small boats, that provide a maximum thrust exceeding 250N. The commercial version comes with a corrosion-free *indestructible* composite shaft that flexes on impact, and a telescoping handle to control thrust and direction. In Zarco, we've fixed two of these thrusters to provide differential drive and we've removed this handle and replaced it by a watertight junction box to gain access the motor windings and getting direct control from the on-board computer, through a motor controller board.

For transportation, the pontoons are detached from the rigid frame and a lever-lock bracket allows the shafts of the thrusters to change into a horizontal position, aligned with the rest of the frame. All mechanical structure can thus be transported in the trunk of a car and since no tools are required to reassemble it, Zarco is ready to operate within a few minutes upon arrival at the mission site.

Gama structure is exactly the same as Zarco's and in fact all parts are interchangeable. The modular nature of the design allows for an easy rearrangement of subsystems, the replacement of parts or the inclusion of add-ons. As an example, in the summer of 2014, we have assembled a longer frame with longer flotation pontoons, so that we could have enough room to accommodate wingsails for propulsion and a solar panel for charging the batteries. Apart from this mechanical change, all other subsystems were reused from Zarco original assembly. Figure 5.6 shows a picture of Zarco being operated with a wing sail at the Alfeite Naval Base, near Lisbon, in July 2014.

5.3.2 Electrical Components

As far as electrical systems are concerned, a typical configuration has two separate modules, each on its own watertight enclosure that seats on the aluminum frame: an energy module and an electronics module. In the energy module (figure 5.7), there is a set of deep-cycle lead-acid batteries, a technology commonly used in electrical wheelchairs and golf carts. These batteries have modest power to volume (and weight) ratio but they are available of the shelf at very reasonable prices, as opposed to other technologies, such as Nickel-metal hydride or Lithium-Ion. In the case of

Figure 5.6: Zarco ASV with a longer mechanical structure supporting a wingsail, Alfeite Naval Base, Portugal, July 2014.

Zarco, the total energy available on board is 624Wh (2 batteries, each with nominal 26Ah at 12V). Similar to all other autonomous robotic systems, the ASV autonomy is greatly dependent on the payload installed on board and the velocity profile required for the mission, but it is usually in the order of 6 to 8 hours of operation. In the case that longer missions are required, a spare energy module can easily be swapped in the field, in a very short time. Since the time required to fully recharge the batteries is about 5 hours, it is virtually possible to have indefinite missions with two sets of energy modules. The batteries may be recharged without opening the enclosure, since any gas accumulation will be released to the environment via a vent plug. The energy module also holds electronic protection circuits, with voltage and current monitoring, and the main switch that commands the power to the on-board electronics.

Alternatively, if there is the need for a continuous long mission or if the mission profile requires a significant amount of continuous power (high velocity profile or power hungry payload), it is possible to redesign the energy module, replacing the batteries by other models based on technologies with better power to volume ratios.

The main electronics module contains the master computer that runs the on-board software, some electronic boards for the navigation sensors and other interface boards. The watertight enclosure has several spare connectors in the lateral glands to provide energy and communications with payload sensors and allow for future upgrades. Some of these connectors are pre-wired with 12V and RS232 communication signals, forming a standard interface with COTS NMEA devices,

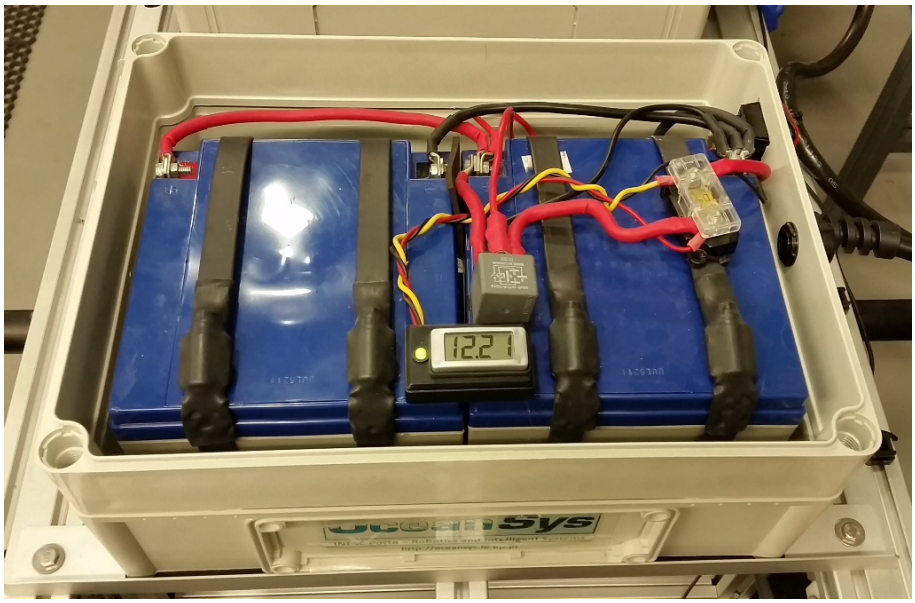

Figure 5.7: Zarco energy module seating on the aluminum frame.

for example meteorological sensors.

Although the specific model has evolved from the first version of Zarco, the master computer is still based on PC-104 technology, with a basic stack formed by a power supply board, the CPU board (with some interface ports) and an additional communications board with 8 serial ports. Given the nature of the PC-104 architecture, it is extremely easy to add other boards to this stack to expand this basic configuration. Figure 5.8 shows an internal view of an electronics module, with the PC-104 stack on the left-hand side. The internal software runs on a Linux distribution and is stored in a solid state memory, to avoid data corruption due to vibration.

Internal to this electronics module, a power distribution board provides multiple header connectors with the various switched voltage levels available, as well as direct access to battery voltage. All other subsystems get power from this bus, with all lines protected by resettable fuses.

One of the most important devices on the electronics module is the motor controller, a board that receives commands from the main computer, via a serial port, and conveys the requested amount of power to the thrusters. Each of our Minn Kota thrusters has a brushed DC motor that can take a maximum current of 30A and it is wise to use a board with a safety margin over this value to account for current spikes and possible degradation due to heating. There are many vendors offering controllers for brushed DC motors, specially for low voltage levels, therefore there is no need to develop specific boards. In our case, we have been using model AX3500 from RoboteQ for a long time, a single board that can switch two channels, up to a maximum continuous current of 40A (with 60A peaks).

Given the typical operation scenario (outdoors with a clear view of the sky) the Zarco navigation system is based on GPS. We have used boards from many vendors, but currently we are using L1+L2 Novatel boards with an external antenna. The orientation is provided by an Oceanserver compass (that also provides inclination) and fused together with data from an X-Sense MTi IMU

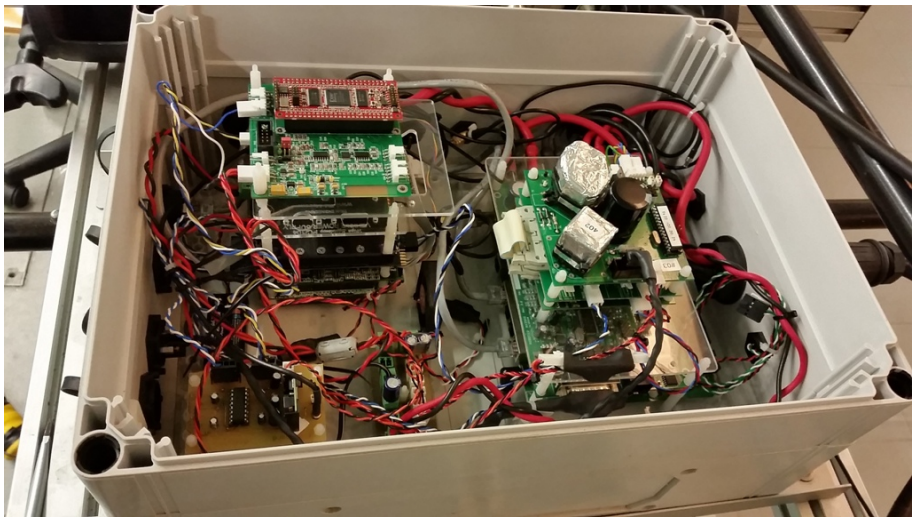

Figure 5.8: Zarco electronics module, with the PC-104 stack on the left-hand side.

to yield the state estimation in real time.

As far as communication hardware is concerned, we have several solutions implemented. A Linksys WRT54G Wi-Fi router is installed on-board, providing an access point from which a remote PC can connect to the master PC. To increase range, a high gain (12dBi) outdoors antenna is placed in the stern of the ASV. The Wi-Fi router has also 4 Ethernet ports, so that other on-board systems can communicate with the master PC using an Ethernet cable. Most of devices, however, have different connectivity and we have a USB hub and a total of 10 RS232/RS485 serial ports that we configure with the proper settings for the connecting device.

5.3.3 Payload Capability

For an ASV to be effective as a platform to gather ocean information, it is important to know the capability to carry extra payload. This capability refers to the mechanical aspects of the integration on board (weight and volume), but also in terms of electrical connections, *i.e.* power and communications. The net buoyancy of Zarco, with the standard 1.5m long pontoons, is about 500N, therefore it can easily accommodate a few kilos of extra payload with minor impact on the structure and the hydrodynamic characteristics. Also, the catamaran configuration is very stable in terms of pitch and roll, providing an ideal arrangement to transport sensors with stringent requirements in attitude (like sonar or video).

Physically, there are many options for the installation of payload sensors along the frame, attached to the thrusters, or on an elevated bridge. However, most of the relevant parameters that need to be measured require sensors that have to be in direct contact with water and these are typically installed in the underwater tray, a 50cm long piece of acetal with multiple holes to provide attachment points. By using a very thin frame for the structure holding this tray to the ASV structure, the changes in the hydrodynamic characteristics of the ASV are mostly dependent

Figure 5.9: Sidescan sonar installed in the underwater sensor tray, shown here elevated to the minimum depth.

on the shape of the integrated sensor. Figure 5.9 shows the example of an Imagenex Sportscan sidescan sonar mounted in the underwater tray.

In some situations, an ASV can be used as a simple transportation system for payload sensors that have a self recording capability and even their own batteries, which means they can store their own information (to be retrieved at the end of the mission). However, in most operations, it is important to capture sensor data in real time with the on-board computer, not only to synchronize the acquisition time, but also to allow real time processing, either on board or, via the Wi-Fi router, on another network device. This communication link can also be used to control the sensor configuration in real time.

The simplest payload sensors only need power to be provided and deliver data in real time using a communication channel. These only require an electrical cable connected directly to the main electronics module, so that these data can reach the master PC, where it is logged with the correct time stamp and possibility distributed to other processes. In some other cases, a sensor may require some specific electronic board for signal conditioning or other processing. This board can be included in the free space of the electronics module, or, preferably, it can be installed in a separate payload enclosure. Even in the relatively short frame of the original Zarco design, there is physical space for an extra enclosure in the aluminum frame, with maximum base dimensions of 500x300mm. Naturally, this can be increased by extending some of the aluminum elements of the frame. Figure 5.10 shows an example of an extra payload interface module installed on board,

Figure 5.10: Zarco ASV with an extra payload module attached to the mechanical frame.

to hold the electronics that interface with a synthetic aperture sonar (Silva et al. (2007a)).

5.3.4 Modeling and Control

One of the roles envisaged for ASVs (described in section 5.1) is to be a demonstration platform for validation of different algorithms, like motion control in the marine environment. In our case, the Zarco configuration as described is a suitable platform to perform such field testing. Nonetheless, one of the benefits of having an ASV is to perform autonomous missions and such *autonomy* is only possible if the vehicle can perform at least a few basic maneuvers without any intervention from an operator. In order to implement controllers for such maneuvers, we've followed a classic approach based on the dynamic model of the vehicle motion.

The derivation of dynamic models for waterborne vehicles usually follows the general approach presented in Fossen (1995) to obtain a 6 degrees-of-freedom (DoF) model of a partially submerged body. This approach is based on the laws of classical mechanics and can take into account the different kinds of forces and torques that act on a body or a set of bodies. In this work we considered a simplification of such general model by taking into account the vehicle symmetries and assuming that the vehicle moves horizontally with zero pitch and roll angles. This assumption is justified with the mechanical arrangement in a catamaran configuration, which results in a very stable platform. Furthermore, we neglected both high order damping terms and hydrodynamic cross relations between the remaining modes (surge, sway and yaw). We also assumed that the body fixed frame is located at the center of mass of the vehicle. Following these lines, we arrived

at a 3 DoF model described by the following equations:

$$m(\dot{u} - vr) = X_{\dot{u}}\dot{u} + X_u u + X_{u|u|}u|u| + X_{ww} + X_{act} \tag{5.3}$$

$$m(\dot{v} - ur) = Y_{\dot{v}}\dot{v} + Y_v v + Y_{v|v|}v|v| + Y_{ww} \tag{5.4}$$

$$I_z\dot{r} = N_{\dot{r}}\dot{r} + N_r r + N_{r|r|}r|r| + N_{ww} + N_{act} \tag{5.5}$$

where m is the vehicle mass and I_z the inertia of the vehicle; u and v are the surge and sway components of the vehicle velocity with respect to the water and r is the yaw rate; $X_{\dot{u}}, Y_{\dot{v}}, N_{\dot{r}}$ are the added mass in surge, sway and yaw, respectively; $X_{u|u|}, Y_{v|v|}, N_{r|r|}$ are the drag coefficients in surge, sway and yaw; X_{ww}, Y_{ww}, N_{ww} are the disturbances caused by the wind and the waves.

In the above equations, X_{act} and N_{act} are the inputs provided by the thrusters. Note that our ASVs only have two actuators, and therefore they are underactuated systems in the horizontal plane. If we assume that these thrusters are aligned with the mechanical frame and at the same distance (d_{thr}) from the forward axis, then the actuation is related to the port and starboard thrust (F_{port}, $F_{starboard}$):

$$X_{act} = F_{port} + F_{starboard} \tag{5.6}$$

$$N_{act} = (F_{port} - F_{starboard}) \cdot d_{thr} \tag{5.7}$$

Finally, we can obtain both the coordinates of the center of mass (x and y) and the vehicle yaw (φ) in an Earth fixed reference frame, using the kinematic relations:

$$\dot{x} = u\cos(\varphi) - v\sin(\varphi) + c_x \tag{5.8}$$

$$\dot{y} = u\sin(\varphi) + v\cos(\varphi) + c_y \tag{5.9}$$

$$\dot{\varphi} = r \tag{5.10}$$

where c_x and c_y are the north and east components of the water current.

This hydrodynamic model is an important step to analyze the behavior of the ASVs, given a specific actuation combination (forces from the thrusters) and for certain environmental conditions (current and wind-induced currents). This can be done using a direct analysis of the equations or with a simulation package like Simulink. This model also serves to design specific controllers for the basic vehicle maneuvers, such as the line tracking algorithm. Since most of the vehicle missions can be described as motion along rectilinear trajectories, this is one of the most important controllers for an ASV.

The development of specific controllers is beyond the scope of this work, but one example of a simple line tracking controller was developed in Cruz et al. (2007), using a separation in two modes: a common mode (F_{common}) to control the linear vehicle velocity (along the trajectory) and a differential mode (F_{diff}) to provide corrections according to the trajectory error. The common mode can be defined *a priori*, resulting in an open loop velocity control, or it can be the output of a velocity feedback control. For most applications, it is advantageous to use open loop velocity

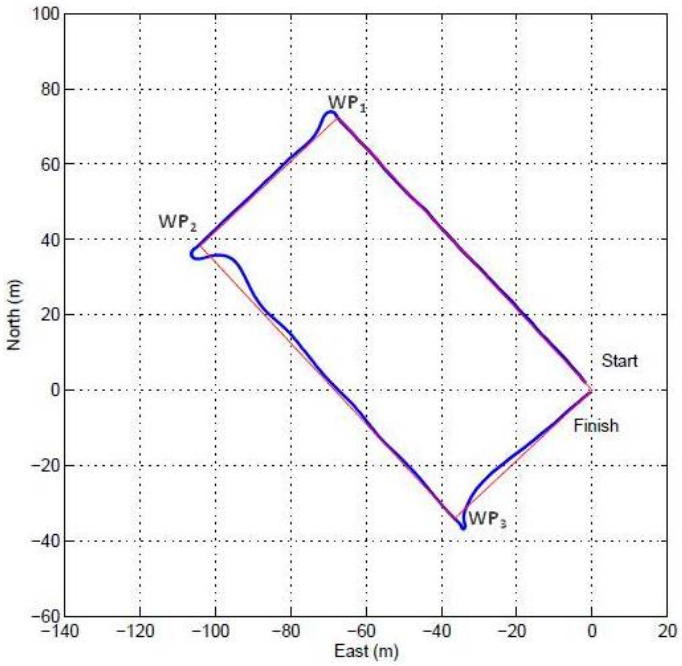

Figure 5.11: Example of line tracking performance of the Zarco ASV, visiting a sequence of waypoints.

control, since it results in smoother vehicle motion and power consumption. When driving the vehicle towards a given line, the most important quantities to take into account are the off-track error (d) and the heading error (β). The goal of the line tracking algorithm is to drive d to zero. Usually, due to water currents, wind, minor misalignment of thrusters and small asymmetries of the vehicle hull, it is not possible to drive both d and β to zero at the same time. This line tracking algorithm is based on a two stage controller: at the outer level, a heading reference is generated, based on the direction of the tracked line and also on the off-track error. At the inner level, a heading controller is responsible to the determination of the differential control of the vehicle:

$$\varphi_{ref} = \varphi_0 - \arctan(k_d d + k_l l) \tag{5.11}$$

$$F_{diff} = k_\varphi (\varphi_{ref} - \varphi) - K_r r \tag{5.12}$$

where φ_0 is the heading of the trajectory, $r = \dot{\varphi}$ and $\dot{l} = d$. The controller parameters k_d, k_l, k_φ and k_r were chosen to balance the tradeoffs between line tracking performance, power consumption, and motion smoothness. One example of a simple mission can be seen in the plot of figure 5.11, where Zarco was used to visit a sequence of waypoints, WP_1 to WP_3 in a 100m x 50m rectangular area.

5.3.5 Vehicle Operation and Safety

In their original configuration, both Zarco and Gama are relatively compact and lightweight, which means that they can be easily deployed from an access ramp or a harbor pontoon. Given their

small size and relatively high center of mass, they are only intended to operate in calm waters, typically in sea state 0 or 1, and maximum sea state 2 (0.5 m wave height). In terms of application scenarios, this includes coastal areas, sheltered locations, and lakes or other large reservoirs. The longer version of the pontoons, with 2.5 meters of length, provides a more stable platform, but require some more complicated logistics for deployment, typically done with a small crane.

Each ASV is self sufficient in terms of navigation and the minimum setup to start operations is a laptop computer that briefly connects to the on board Wi-Fi router to diagnose internal subsystems and start an autonomous mission. In a typical operation, however, there is a permanent link between the ASVs and the console running on the control station, to send commands and receive data in real time. The console is used to plot the vehicles' positions in real time and also to monitor the most relevant on-board parameters. It may also be used to switch an on-board device, to launch or stop a process, or to send special commands to sensors. Such link is based on Wi-Fi, guaranteeing a wide band connection, although at relatively modest ranges. In our case, a high gain omnidirectional antenna on-board and a sectorial or directional antenna on shore, ensures a permanent link up to 2km of range. As a safety measure, we typical use a communications watchdog that stops a vehicles in case the communications drop out for a long period of time. In a more demanding scenario, this control station may be slightly more complex: a reference station may be installed to provide differential GPS corrections, a set of antennas/masts/amplifiers may be needed to extend the coverage of the Wi-Fi link, and multiple computers can be receiving data in real time for distributed processing.

There are many alternatives to operate these ASVs, from fully manual control to fully autonomous mode. In some scenarios, particularly when we are testing specific sensors or other devices, we maintain a direct link with the corresponding software driver and we can use a standard joystick connected to the console to drive the vehicle. This is particularly helpful when the vehicle is within visual range, or when it is very close to a structure. In some other cases, we can use the console to send a specific reference to a given vehicle while we are evaluating some parameter, for example, instructing Gama to hold position at a given location and sending Zarco to a waypoint while we measure ranges using some acoustic ranging device. In most operational missions, however, the vehicles operate in an autonomous mode. The autonomous operation is based on the sequential execution of a set of elementary maneuvers stored in a mission file. Missions are defined in text files which are transferred to the vehicle and processed by its control system. A typical mission file is composed of two main parts. The first contains the definition of points in the area of operation which are relevant to the mission. These points can be defined either in absolute coordinates or relative to other defined points. The second part of the file contains the list of maneuvers that the vehicle must execute. One of the most important maneuvers is *LineTo*, implementing a rectilinear trajectory control at a constant velocity to a destination point, as described earlier. The start point of each maneuver is implicitly defined as the last point of the previous one and an *EarlyEnd* parameter defines the distance from the final point at which the current maneuver is considered completed.

In a particular case of autonomous missions, the on-board vehicle controllers can receive direct

references from other processes. This was implemented so that the mission maneuvers can be defined in real time, taking into account data that is being processed, allowing the implementation of adaptive sampling techniques.

5.3.6 In-Water Trials

The first trials with the Zarco ASV were dedicated to the identification of the hydrodynamic model of the vehicle and the validation of the first motion controllers (Cruz et al. (2007); Matos and Cruz (2008)). These tests were firstly conducted in a large tank, but since the potential hazards associated with its operation are very limited, we soon started operations in the Crestuma reservoir of the Douro river. Almost immediately, Zarco started being used as a sensor carrying platform, and the vehicle motion stability was providential to support the demonstration of an interferometric synthetic aperture sonar (Silva et al. (2007a,b, 2009)). Given the limited logistics associated with its operation, we were able to perform these missions all year round.

Further to these earlier tests, both ASVs have been used extensively as demonstration platforms for testing multiple sensors in the field, taking advantage of the ability to provide real time communications with the mission supervisor to provide a real time feed of sensor data for immediate evaluation of performance (Pinto et al. (2009)). These vehicles have also been used to validate various types of algorithms, including obstacle avoidance (Pinto et al. (2013)), cooperative localization of an acoustic source Ferreira et al. (2012c, 2013), and two dimensional adaptive sampling (Cruz and Matos (2014)), both in river reservoirs and in coastal waters (fig. 5.12).

Both ASVs have also played a crucial role in a long term program for coordinated operation of marine vehicles, with several examples of coordination between heterogeneous vehicles. These include missions with minimum information exchange (Matos and Cruz (2007); Santos et al. (2008)) and also using acoustic communications to evaluate the performance of assorted vehicles (ASVs and AUVs) in acoustic networks, such as the work described in Cruz et al. (2012, 2013a,b), and Ferreira (2014). Figure 5.13 shows an example of Zarco and Gama being used for one of these missions in the Douro river, in the summer of 2014.

5.4 Discussion

This chapter described an ongoing program for the development of small size ASVs. These vehicles have their own potential as preferred tools for sampling the marine environment in certain scenarios, but they particularly relevant to support an integrated program of robotic solutions for marine operations. Not only they can be used to complement the sampling patterns of underwater vehicles, they can also be effective tools to demonstrate specific systems and techniques in two dimensions before being transposed to AUVs. Contrary to AUV development, the availability of high-bandwidth, real time communications accelerates the development phase dramatically.

Similarly to the case of AUV design presented in the previous chapter, our effort has been focused on the development of modular building blocks to foster reconfigurability and versatility.

Figure 5.12: Zarco ASV being recovered after a sidescan survey off the coast of Sesimbra, summer 2013.

Figure 5.13: Zarco (closest) and Gama (farthest) in a cooperative mission in the Douro river, summer 2014.

In this case, we use a very simple architecture to yield extremely versatile platforms that have already accumulated hundreds of hours of operation in reservoirs and coastal waters. In the case of ASV design, we opted for the main structure to use COTS aluminum profiles, a common solution employed in industry to build rapidly reconfigurable assemblies, and with a vast number of accessories. Our mechanical design follows mostly a *bus* modular architecture, in the sense that most of the components can be attached along the main railing system.

The largest components can be detached and reattached to the main structure very rapidly, with a minimum set of tools, which means that the vehicles can be transported in separate blocks and reassemble at the operation site in just a few minutes. This feature is also very important to facilitate debugging, since all system electronics can move from the bench to the vehicle structure in just a few minutes. In fact, the replacement of a single module has great benefits during development, since it allows multiple threads of separate development, while still having a fully functional version ready for operation. Although there have been many developments in the vehicles during these years, both the integration of new subsystems and the improvements of specific modules have benefited from system modularity to ensure a minimum impact on system readiness to operate. The current version of both vehicles seamlessly integrates new designs with original modules. The modularity of the vehicles also extends to the on-board software and control systems. In fact, many of the device drivers are exactly the same as in the AUVs, and the controllers are developed using similar hydrodynamic equations, with the relevant changes in parameters.

This module separation is also very useful during operations. For example, a depleted battery pack can be swapped by a fresh one in a few minutes from a pontoon, with the vehicle still in the water. In practice, however, the recombination of modules can result in a difficult traceability, since it may be difficult to identify what exactly defines Zarco and Gama, but we minimize this issue by maintaining a log with the modules and systems used on each mission.

Zarco, the first ASV built with these modules, has been in operation since 2005, and a second vehicle, Gama, has been assembled in 2008 to support cooperative missions. Cooperation has included not only the coordination of similar platforms, but also the utilization of heterogeneous vehicles (ASVs and AUVs) for specific applications. These vehicles have been used in a variety of scenarios, both in Portugal and abroad, and they have been paramount to provide field data to validate scientific developments in many areas of marine research. This has been translated into tens of manuscripts, including scientific papers, thesis, and technical reports, corroborating their value as an effective tool for marine sampling.

As for future developments, we anticipate that these platforms will maintain their importance as effective tools for operations in the marine environment. On their own, their role as preliminary testbed for sensors and subsystems will facilitate the demonstration of innovative ocean sensors, the investigation of energy harvesting solutions (fostering a long-sought permanent presence in the ocean), or the assessment of audacious control schemes. However, their main role will be as part of a large network of heterogeneous vehicles and other monitoring systems, where the surface component is a crucial part of the puzzle. The modularity of our design will facilitate

these upcoming improvements and therefore we foresee that the evolution of our vehicles will be able to cope with future challenges.

Chapter 6

Adaptive Sampling of Ocean Features

The real problem is not whether machines think but whether men do.

— B. F. Skinner (1904–1990)

The concept of *adaptive sampling* in the ocean has been suggested as a way to increase the efficiency in the use of autonomous robotic platforms for the characterization of oceanographic processes. Instead of performing the standard extensive surveys, the main proposal was to change, or *adapt*, the mission profile (trajectory, velocity, etc.) in real time, in order to better capture some characteristics of the processes. In our case, we are addressing a particular case of adaptive sampling, in which the vehicle needs to keep track of some feature in order to concentrate measurements in a region of interest with respect to that same feature. In order to achieve this, the vehicle has to decide, in real time, the trajectory and the sampling pattern, according to the environmental data being sampled and processed. There are many ocean processes that may be efficiently mapped using this *adaptive sampling* paradigm, particularly if they are characterized by sharp transitions or boundaries in a particular scalar field, as described in chapter 2.1. In most of these cases, the relevant information about the process are the characteristics of the boundary layer itself, or some other parameters in the region close to the boundary. For example, if an AUV is deployed to survey the evolution of a pollution plume, it may be more efficient to follow the contour than to sample the whole region. Therefore, it is important that the vehicles can detect the transition zone and navigate with respect to it. The mapping efficiency is further accentuated if the processes show high spatial and temporal variations, since the vehicle trajectory can result in a much denser sampling of the process, as compared to a standard broad survey.

In this chapter, we describe a strategy to use autonomous robotic platforms, such as the ones described in the previous chapters, to efficiently map a class of oceanographic features. The distinctive characteristic of these features is that they have a *boundary*, a transition zone across which there is a much stronger variation in one of the values measured by the vehicle, as compared

to the values in the rest of the survey area. Given the limited amount of computational power available on board, our strategy relies on admitting a relatively simple feature model for which the vehicle can estimate relevant parameters in real time using simple calculations, and then use these parameters to define the motion characteristics (and sampling pattern) accordingly. In order to implement this strategy, we've developed a few algorithms for detecting the value and location of the maximum gradient of a scalar field traversed by the vehicle, as well as for the generation of motion references, in real time. We implement this strategy in the vertical plane for one-dimensional feature tracking and also in the horizontal plane, for 2D boundary tracking.

The remainder of the chapter is organized as follows. We start by describing, in section 6.1, the algorithms required to implement our strategy for *adaptive sampling*, including mechanisms to evaluate the performance of the algorithms in real time. In section 6.2 we provide the details of an implementation of this strategy, in which the MARES AUV was able to process CTD data, in real time, and change depth in order to maintain the vehicle in the vicinity of the thermocline. Then, in section 6.3 we extend the same paradigm to the two-dimensional case of tracking a horizontal boundary, illustrated with data from the Zarco ASV being used to detect and track the steepest location of a navigation channel. Finally, we conclude the chapter with a discussion on the main achievements of our approach and also with some hints on how it can be extended further to provide three dimensional tracking of ocean features.

6.1 Algorithms for Feature Tracking

Our first assumption for feature tracking is that the scalar field Φ has a transition zone, along which the gradient is *significantly* higher than in the rest of the area. As described earlier, this is a typical characteristic of many oceanographic phenomena, like fronts or plume boundaries. We also assume that there is some *a priori* information about the phenomena being studied, or that there is the possibility of gathering that information in a preliminary survey, and process these data before the start of the autonomous tracking phase. For example, if the mission objective is to track the boundary of a pollution plume, there may be some indication of the likely location of the plume boundary and maybe about the concentration levels of the pollutants.

In terms of vehicle behavior, the tracking algorithm does not provide low-level control laws to command the actuators directly. Instead, it only provides references to vehicle controllers, like waypoints, velocities and depth references, that are assumed to be available in a wide range of vehicles. Finally, we assume that the vehicle can take only local measurements of Φ, therefore in order to find the maximum gradient, the vehicle needs to cross the transition zone, moving from the region where the scalar field has *high* values (the HIGH region, to be defined later) to the region with *low* values (the LOW region), and vice-versa. A simplified view of an expected transect of such a scalar field can be seen in figure 6.1.

Our strategy for autonomous tracking of a given feature starts with an initial tuning of parameters based on preliminary information about the feature. For example, we may know in advance that typical thermoclines in a given region have a gradient of about $0.5^{o}/\mathrm{m}$ and occur at depths of

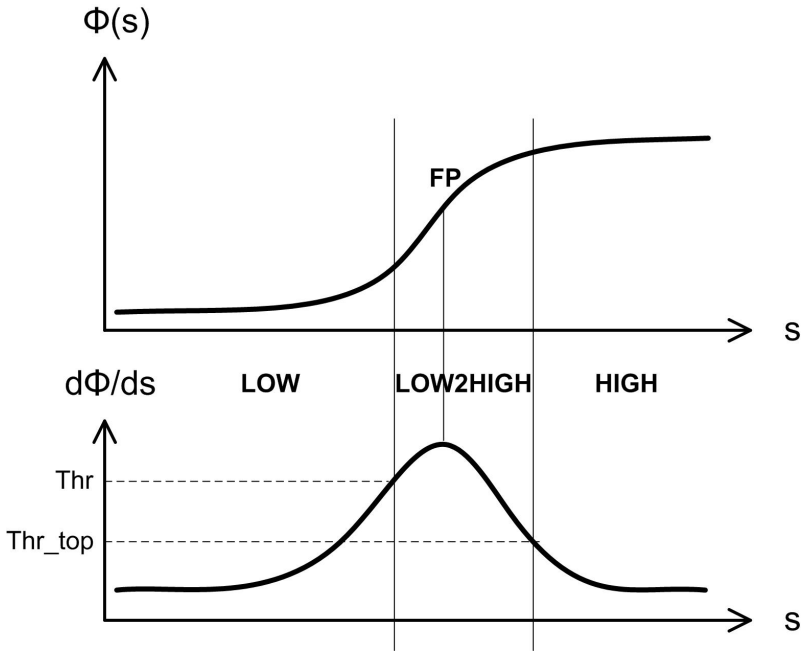

Figure 6.1: A simplified model of a transect of a scalar field, passing from a region with *low* values to a region with *high* values. Below, the derivative along the same trajectory, with the frontal point located at the maximum derivative.

20 to 50 meters. This will serve both to initialize the tracking algorithms and to set some safety parameters (for example, a maximum vertical span for searching the thermocline). Usually this initial tuning depends on nearly-static conditions, like local bathymetry or statistical values, so that it can be processed offline in the laboratory. In other cases, it may depend on specific local/temporal conditions, which means it has to be done in the field, as close as possible to the time of the tracking mission.

Following the initial settings, the vehicle is located close to the boundary region and the main strategy for feature tracking is to ensure a continuous sequence of boundary crossings. Mainly, the vehicle has to process data in real time to detect a boundary crossing, extract its most relevant characteristics, and navigate to a new waypoint in order to keep tracking autonomously. As far as navigation and control are concerned, the vehicle controllers can be set as in any standard georeferrenced mission, with the single difference that the motion references are not known at the beginning of the mission. Instead, they are generated online as the mission evolves.

In summary, the implementation of this strategy for feature tracking can be described by the following cycle:

1. **Real-Time Peak Gradient Detection** – The vehicle navigates following a standard reference, until a strong transition in gradient is detected, or until the vehicle reaches a safety limit

2. **Data Extraction** – The transect/profile is analysed to determine the location and value of the maximum gradient and other relevant information

3. **Guidance** – Generate a new set of references for the vehicle controllers, adjust the parameters of the algorithms, and go back to step 1.

This cyclic operation is ensured with a combination of algorithms for gradient threshold detection, parameter estimation, and vehicle guidance, that will be detailed in the next sections. During the tracking phase, the performance of these algorithms is also evaluated in real time, so that the mission management system can take the most relevant actions in case of inadequate behavior.

6.1.1 Identification of the Maximum Gradient from a Full Profile

The first algorithm that we've developed concerns the automatic identification of the maximum gradient from a full profile obtained by sampling a scalar field Φ along a trajectory s. The main objective of this algorithm is to provide quantitative information about this generic profile $\Phi(s)$, namely the value and location of the maximum gradient, and the amplitude of the transition zone. While the maximum gradient is an exact, unambiguous concept, the *amplitude of the transition zone* has to be defined under some quantitative criteria, for example, when the gradient is above a certain threshold. Naturally, this quantitative definition is not meant to convey any physical property of the scalar field but solely to allow comparison between profiles.

In some scenarios, this algorithm may be used offline to process historical or statistical data and provide the initial tuning of the adaptive sampling parameters. In this case, it can be run multiple times, and the results may be validated by a human operator, sometimes incorporating qualitative information that is difficult to accommodate in an automated process. In these cases, there are few time constraints, which means that the algorithms may me very complex and time consuming. In many other situations, however, it is important that the same algorithm may run online, fully autonomously, based on data just retrieved by a moving vehicle. This is particularly relevant whenever the parameters depend on dynamic local conditions, and therefore our priority was to develop expedited ways to compute the most important characteristics of the gradient using a simple computational (or embedded) system. At the same time, if the data of the scalar field is logged, it is also possible to refine the data offline, after the mission, using more complex mechanisms.

In theory, the estimation of the gradient from a set of samples can be obtained by using discrete methods applied to the samples of the signal at known positions, such as the central-difference formula:

$$f'(x) \approx \frac{f(x+h) - f(x-h)}{2h} \tag{6.1}$$

Ideally, the derivative of the signal is the limit of the above fraction, as the sampling interval h goes to zero. However, in a real profile, there are many possible sources of error that affect both the data values and the estimation of the position/time when it was taken, and in any data set corrupted by noise, a numerical differentiation will increase the impact of noise dramatically, particularly as

the sampling interval h is reduced. Therefore, the estimation of the derivative cannot be done by a simple numerical differentiation of the data values. Instead, it should be performed in such a way as to ensure some insensitivity with respect to the above mentioned sources of error.

There are numerous methods in the literature to address the estimation of the gradient of a signal from a series of samples. However, they require advanced operational calculus techniques that are difficult to implement on-board an autonomous vehicle. One of the most promising cases of simplicity in calculation is based on algebraic differentiation, where the derivative is estimated by simple integrations of the signal. Even though this increases the signal-to-noise ratio, the resulting estimates of the gradient still suffer from errors in the measurements, particularly in the cases of low gradients (Jouffroy and Reger (2006)).

In our implementation, we take advantage of the simplicity of polynomial fitting, together with its ability to filter out small scale variations, in a two stage procedure. Given a set of data samples (X,Y), the least squares polynomial approximation provides the coefficients of a polynomial that minimizes the sum of the squared errors between measured data and approximation, when Y is assumed to be a polynomial function of X. This means that a first order least squares approximation provides the coefficients for the straight line $y = ax + b$, that best describes the linear relationship between X and Y. Therefore, a simple way to estimate the mean gradient of a sequence is to compute the slope a of the linear fit of the same sequence:

$$a = \frac{n\sum_{j=1}^{n} X_j Y_j - \sum_{j=1}^{n} X_j \sum_{j=1}^{n} Y_j}{n\sum_{j=1}^{n} X_j^2 - \left(\sum_{j=1}^{n} X_j\right)^2} \tag{6.2}$$

where n is the total number of samples.

For a full profile, a good estimate of its derivative is the slope of the first order polynomial fit of a consecutive number of data points. So the equation above may be extended to calculate the slope from a number of N consecutive samples at position i:

$$a(i) = \frac{N\sum_{j=i\text{-}N+1}^{i} X_j Y_j - \sum_{j=i\text{-}N+1}^{i} X_j \sum_{j=i\text{-}N+1}^{i} Y_j}{N\sum_{j=i\text{-}N+1}^{i} X_j^2 - \left(\sum_{j=i\text{-}N+1}^{i} X_j\right)^2} \tag{6.3}$$

If we extend the above calculation to the whole profile, we get all the values of $a(i)$ that correspond to the estimation of the gradient at position $i - N/2$ (note that the computation is done at position i taking into account the previous N samples). Therefore the first estimation of the location of the maximum gradient is given by:

$x_{mg} = X(i_{mg})$ where $i_{mg} = \underset{i}{\text{argmax}}\,|a(i)| - N/2$

Naturally, this estimation may be very sensitive to numerical errors, particularly when we consider a relatively small set of samples and the region of gradient is relatively large. To limit

this impact in a real implementation, we tend to oversample the scalar field and average out the data at equal intervals. Note that a large number of samples corresponds to a smooth variation, hiding any smaller scale gradients but with a better location in the overall peak area, while a small number of samples is more sensitive to errors in sensor data or positioning.

For illustration, consider the vertical profile of seawater temperature acquired by the MARES AUV in June 2009, off the Portuguese coast, displayed in the top of figure 6.2. The vehicle had a SeaBird CTD installed and captured data at 16Hz, which was then binned in bins of 0.33 meters. The plot clearly shows a thermocline between 11 and 14 meters. For the second plot, we've used equation 6.3 with $N = 3$, corresponding to a linear interpolation spanning one meter, and we highlight the points where the absolute value of the gradient exceeds 30% of the maximum. For the other plots, we've increased the number of samples to 6, 12 and 24, respectively, and repeat the analysis. As expected, the gradient gets smoother as the number of samples increases, but the identified peak remains relatively constant, between 11 and 12 meters.

This example shows that it is possible to locate the region of maximum gradient with a simple algorithm applied to a full profile. For an automated procedure, we can refine this to make sure that the detection matches some predefined criteria and classify the profile accordingly. One possibility that we address is the algebraic location of the maximum when we assume a *smooth* variation of the profile. In fact, if we try to approximate a real profile by the simplified model of the transition, as shown in figure 6.1, we should see the region close to the peak gradient as a negative parabola, for which it is easy to compute the maximum algebraically. In order to do this, we fit a third order polynomial to the data points located in the region of high gradient, and then derive the position and value of the maximum derivative, following a very simple procedure:

1. Find positions x_{min} and x_{max} around x_{mg} such that $x \in [x_{min}, x_{max}] \Rightarrow a(x + N/2) > grad_{min}$. Typically, the value of the threshold, $grad_{min}$, is configured as a percentage of the maximum gradient.

2. Fit a third order polynomial $y_3(x) = ax^3 + bx^2 + cx + d$ to data points (X,Y) for which $X \in [x_{min}, x_{max}]$. The sign of a should be positive if we have a HIGH to LOW transition, such as the case of figure 6.2, or negative, if the transition is from LOW to HIGH, such as the simplified model of figure 6.1.

3. The location of the maximum gradient can be obtained at: $\frac{d^2 y_3}{d_x{}^2} = 0 \Longrightarrow x_{mg2} = -\frac{b}{3a}$. Naturally, if $x_{mg2} \notin [x_{min}, x_{max}]$, it means that the profile does not contain the maximum derivative.

4. The maximum gradient can be estimated as $MG = y_3(x_{mg2}) = c - \frac{b^2}{3a}$. This value is typically compared to a threshold to ensure that a true/meaningful transition has been detected.

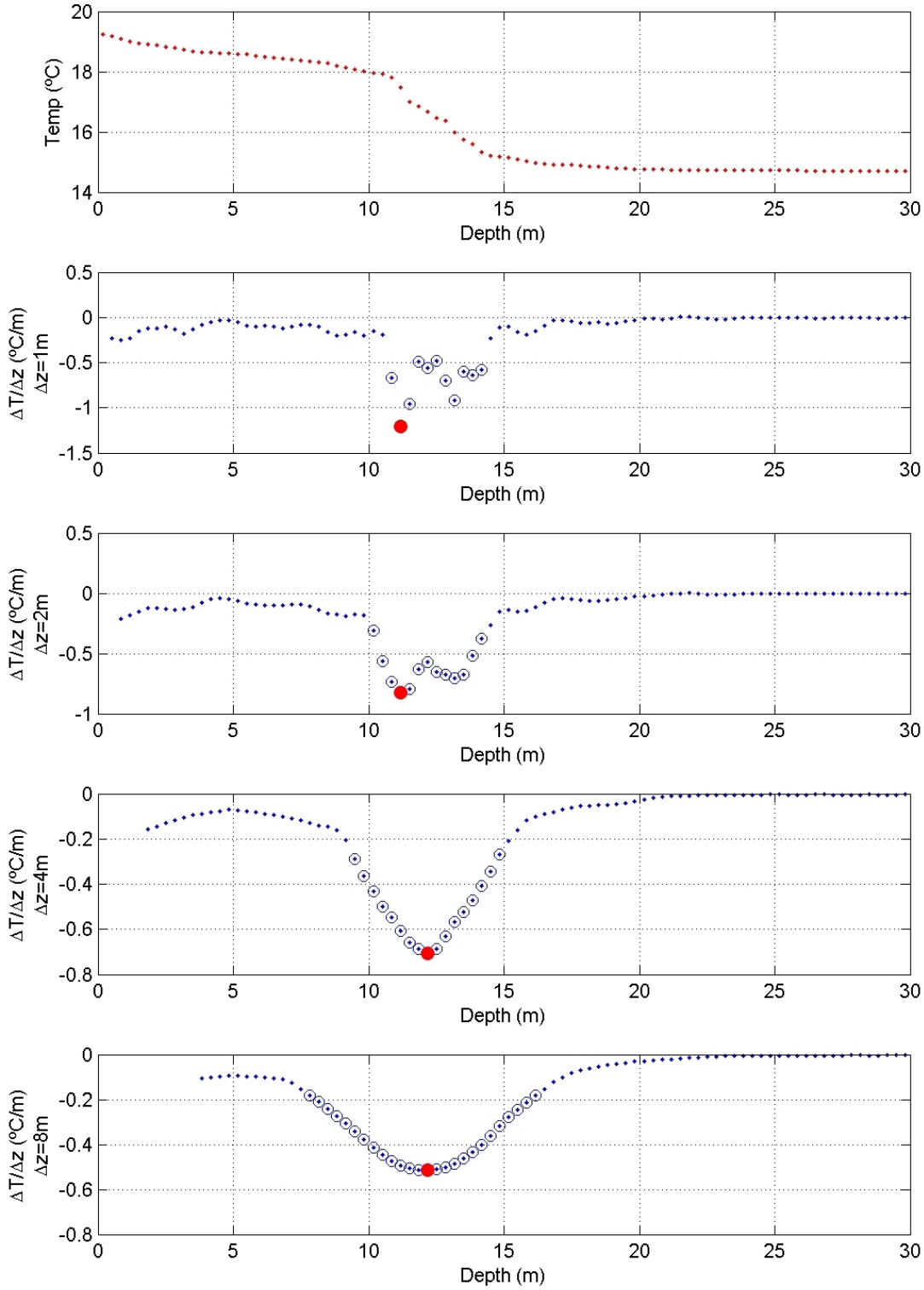

Figure 6.2: Example of peak gradient detection on a full temperature profile acquired by the MARES AUV, June 2009 (top plot, with temperature data binned in 0.33 meter bins). The gradient is estimated as the slope of a linear interpolation of a sequence of samples, corresponding to a vertical span Δz. In this example, the number of samples increases from 3 ($\Delta z = 1$m, second plot) to 24 ($\Delta z = 8$m, last plot). The red dot represents the maximum value of the gradient.

6.1.2 Online Identification of the Maximum Gradient

The online identification of a maximum gradient requires a different algorithm than the above, since we are interested in detecting the crossing of the maximum gradient as soon as it happens, *i.e.* without the full profile being available. In fact, when the vehicle is moving through a transition zone, it has only a partial view of the profile, therefore it may be difficult to decide whether the maximum gradient has already passed or if it has to proceed further. Another difficulty in detecting the maximum $\frac{d\Phi}{ds}$ comes from the non-uniform nature of points s for which data is available, since even with a sensor producing data at a constant rate, the mapping into $s(t)$ depends on the vehicle dynamics.

Our general principle to detect the maximum gradient along a trajectory requires in practice two detections. First, the vehicle has to detect a gradient above a given threshold, indicating it has entered a region with a significant derivative. However, it will proceed its trajectory until the gradient falls to a level below another threshold, typically a fraction of the highest. During this phase, the vehicle keeps updating the maximum gradient and its corresponding location. In the following sections we will detail the practical implementation of this mechanism in the addressed scenarios.

In order to estimate the gradient along the trajectory, we start by clustering the values into bins, as soon as they are available, and then we work on binned data to avoid any distortion produced by non-uniform distribution of data. We employ three alternatives to compute the gradient, depending on the available computational power and the nature of the data. The first is to use the algorithm described above, based on the slope of a moving linear fit, using only the partial profile. This provides results comparable to the full profile, but it requires a great computational power, since the algorithm has to run for every new data point. Note that in some scenarios, data location depends on vehicle dynamics and localization error, which means that a data sample can affect data from earlier bins.

In many cases, data points are available sequentially, maybe even periodically (with equal Δs) as a vehicle is crossing the scalar field. In these cases, a simpler version of the moving linear fit can be used, by taking advantage of an iterative version of the slope of the last samples.

Finally, an online method requiring reduced computational power may be employed, based on finite differences of binned data. In order to implement this, it is necessary to maintain and update an array of gradients starting at the beginning of the profile. For each new data point, only the derivatives (or differences, to be more accurate) affected by this data are updated. These derivatives are estimated by the differences of the averaged bin values. In order to prevent biases in the average values of s, we consider the average of both $\Phi(s)$ and s that lie within a specific bin, as compared to considering an average $\Phi(s)$ in the middle of the s bin. This is particularly relevant if we increase the size of the bins, because as the vehicle moves through the scalar field, the first few samples within a bin are biased towards the bin boundary.

Even with the clustering of data into bins, there may exist some false detections of gradients estimated using finite differences, particularly if we consider a single bin at a time. In order

to avoid these false detections, we need a consecutive number of differences, above or below a threshold, to confirm the change of state. Note that if we increase the number of confirmations required to validate a low gradient, the main consequence will be for the vehicle to proceed further into the *flat* regions of the profile, with a minor impact on performance. On the contrary, if we increase the number of confirmations required for the high gradients, we may not be able to detect a very thin transition zone.

In any of these techniques, the value and location of the gradient can be simply found by the maximum of the array. Alternatively, all the values of the profile may be used with the algorithm described in section 6.1.1 to analyze the full profile.

6.1.3 Guidance and Navigation

The main objective of the guidance algorithm during feature tracking is to make sure that the boundary is crossed, while the vehicle advances along some predefined trajectory. This algorithm does not control the vehicle in real time, in the sense that it is not directly closing the loop between sensors as actuators. Instead, it provides references to the on-board controllers, to ensure that the vehicle describes trajectories during which it extracts profiles of the scalar field. The details of the implementation depend on the exact mission (as described in the next sections), but there are common characteristics. Probably the most important characteristics of the guidance algorithm is to ensure that the algorithm proceeds even if the maximum gradient is not detected online in that profile.

The guidance mechanisms have to take into account some safety measures, for example to ensure that the vehicle does not go outside a safe operation area. At the same time, it is important that the measurements of the scalar field (and naturally gradients) can be correctly geo-referenced. It is therefore required that the vehicle navigation system is able to estimate the position in a global reference. On the other hand, while it may be possible to anticipate the maneuvers of the vehicle, the exact trajectory may be impossible to predict. This means that these missions should be performed with a tracking system in operation, so that a human mission supervisor can follow the location of the vehicle.

6.1.4 Real Time Evaluation of Performance

In all implementations, special attention has been paid to the definition of online performance metrics of the algorithms. Typically, a few simple numbers are computed in real time, describing the ability to detect the transition zones and some of the main characteristics (like amplitude or location). It is important that these metrics are forwarded in real time to the mission supervisor, to make decisions in the event of a poor performance. On a first level, this supervisor can be an on-board program that compares the performance against a given benchmark. If the vehicle can communicate with a control station, this supervision can be reinforced by a human operator.

6.2 Autonomous Tracking of a Vertical Gradient

The first scenario that we will consider is the characterization of a thermocline in a given region. By *characterization*, we mean to gather enough data to compute the maximum temperature gradient and the vertical location of such region. In a traditional way, an AUV would perform a sequence of *yo-yo* profiles, from the surface to an offset above the bottom (or to a maximum depth), gathering temperature data for post processing. The number and frequency of thermocline crossings would depend on the overall vertical span of the programmed profiles. Using our adaptive sampling approach, we can process data in real time and maintain the vehicle in the vicinity of the thermocline, therefore increasing dramatically the frequency of crossings and capturing much more information about the process. This is an example of a tracking maneuver that is done in a single dimension (the vertical), therefore it only requires an algorithm to change the references in that dimension.

6.2.1 Real Time Thermocline Tracking

Our implementation of the thermocline tracking maneuver can be seen as a special case of a *yo-yo*, for which the limits of the vertical extent may be redefined in real time. This maneuver requires a set of default values for depth limits, which can be defined with respect to the surface or the bottom. In case the thermocline is not detected, the vertical motion of the AUV reverts to a standard *yo-yo* between those values.

In a real time implementation, a specific process runs in the on-board computer, identifying the thermocline, filtering temperature data and fitting a gradient search algorithm. The thermocline layer is detected when the vertical temperature gradient exceeds a given threshold. The vehicle will proceed the same direction of vertical motion until the algorithm detects a *significant decrease* in the gradient, as compared to the current *maximum*. At this depth, the vertical profile is reversed and the algorithm restarts in the other direction. In the absence of a positive identification of the thermocline in either direction, then the vehicle will continue the vertical motion until the prespecified limit is reached (either the surface or the maximum depth), as in a standard *yo-yo* motion. All thresholds are dynamic and depend on the gradient information acquired on previous profiles, so that the AUV can be used to track a time- or space-varying thermocline while moving along a pre-defined *lat-lon* trajectory. In order to achieve this, we assume a 3-layer piecewise linear model, similar to the one proposed by Haeger Haeger (1995), with a high gradient at the thermocline, and low gradients both above and below.

The MARES AUV has 4 independent controllers for 4 degrees of freedom, and the vehicle is able to control the vertical velocity, from zero (*i.e. hovering*) to a maximum value around 40cm/s. This means that the vehicle can implement this algorithm to track the vertical thermocline at a single *lat-lon* location, or while following a completely independent *horizontal* trajectory. In most other AUVs, however, the vertical motion is obtained using horizontal fins or deflectors, in which case the vertical motion requires a minimum value for the horizontal velocity. In any case, the same principles described here can be implemented as a particular case of the *yo-yo* maneuver.

Tracking the thermocline

The specific algorithm implemented for thermocline tracking can be described by the state machine represented in figure 6.3. Note that the darker arrows represent the transitions that are expected during a normal tracking maneuver. These transitions will cycle the state machine through the most relevant states, that represent the relative vertical position of the vehicle with respect to the thermocline:

- TOP - The vehicle is located above the thermocline.
- TC2BOT - The AUV is within the region of the thermocline, on a downward vertical motion.
- BOTTOM - The vehicle is located below the thermocline.
- TC2TOP - The AUV is within the region of the thermocline, on an upward vertical motion.

The process usually starts when the vehicle is at the surface, so the first state is set to TOP. On entering this state, the depth reference is set to Z_{max}, which means the AUV will try to dive in the water column. The vehicle will then evaluate the vertical temperature gradient and compare it with a given threshold, Thr_tc. When this threshold is exceeded, the vehicle will assume the thermocline has been detected on the downward motion, entering the TC2BOT state. This can be seen as the *upper limit* of the thermocline region and then the vehicle will try to detect the *lower limit* of this region, by diving deeper. Therefore, the vertical direction will remain the same as before, with $Z_{ref} = Z_{max}$. At this state (TC2BOT), the gradient search algorithm will try to find if the level decreases below another threshold, Thr_bot. Note that this low gradient level has to be searched only for depths greater than the depth of the maximum gradient. In order to confirm the *lower limit* of the thermocline and avoid (early) false detections, an additional test is performed, verifying that the vertical span is large enough, *i.e.* if $z - Z_{tc} > Z_{span.bot}$, where z is the current depth, Z_{tc} is the depth of the maximum gradient and $Z_{span.bot}$ his an optional parameter set by the user. When both these conditions are met, the vehicle enters the BOTTOM state.

Note from the state machine of fig. 6.3 that the BOTTOM state is also reached if $z \geq Z_{max}$. This is a safety mechanism to ensure that the maximum depth the AUV will be limited to Z_{max}, even if the algorithm is not able to positively *find* the thermocline. More, this condition contributes to a performance index, since it signals a failure in the detection algorithm.

When the vehicle enters the BOTTOM state, the thermocline characteristics are extracted from the previous vertical profile (in particular, the maximum gradient and the thermocline limits) and this information is used to adapt the thresholds for the thermocline detection during the next vertical profile. At this state, the depth reference changes to Z_{min}, which means the AUV will now move towards the surface. The temperature and depth values arriving from the CTD sensor are used to determine when the vertical gradient exceeds the new thermocline threshold, Thr_tc. This will change de state machine into the TC2TOP state, signaling the *lower limit* of the thermocline. In order to find the *upper limit*, the algorithm will proceed in much the same way as in the downward motion, but with a natural symmetry: the reference for the vertical controllers will be

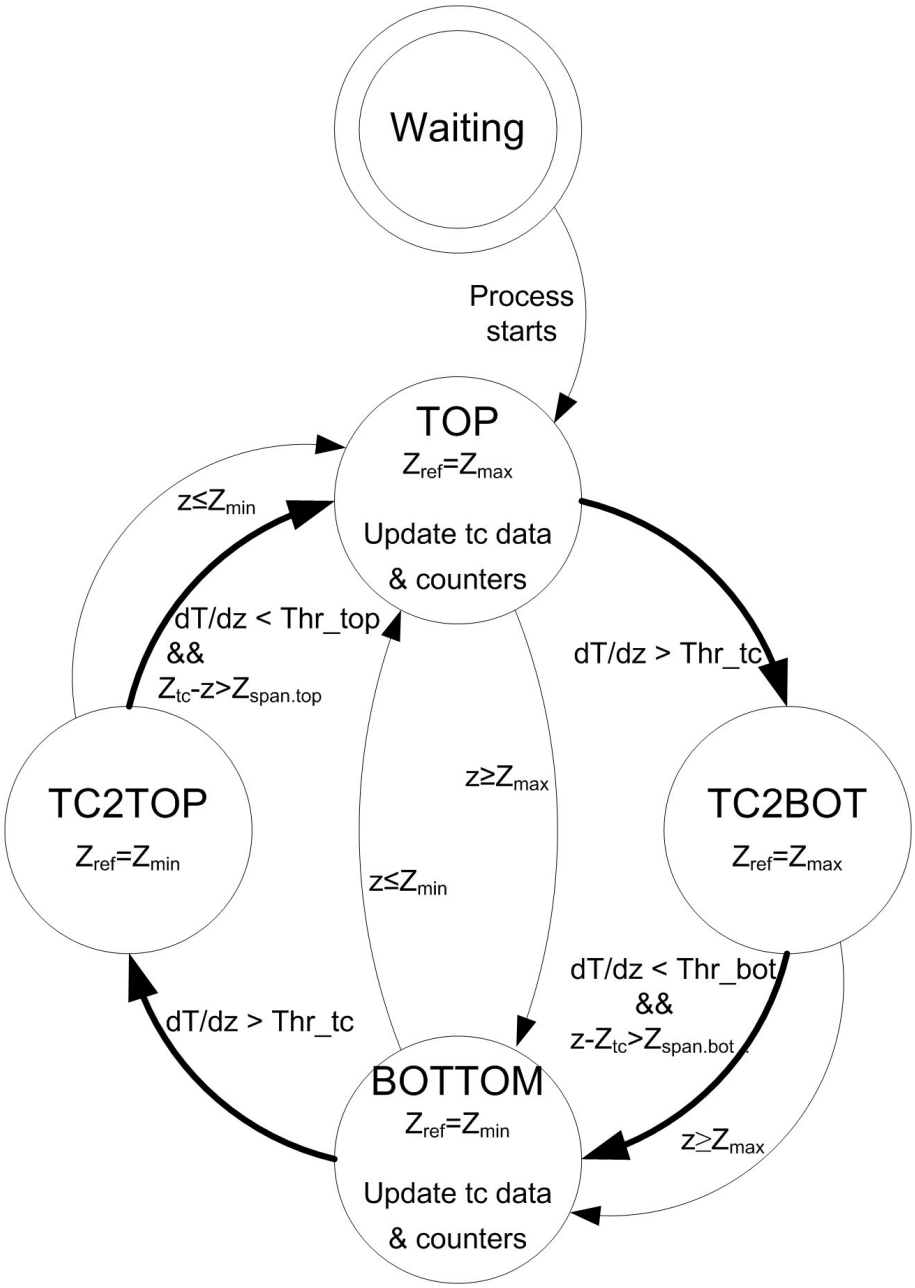

Figure 6.3: State machine and transitions representing the thermocline tracking maneuver. The bold arrows represent the expected cyclic transitions during normal tracking.

maintained at Z_{min} and the gradient search will be done for depths lower than the depth of the maximum gradient. Once again, the TOP state is only confirmed if a minimum vertical span has been covered.

As long as this process is active, the above cycle will be maintained, resulting in a *yo-yo* pattern around the thermocline. In case the thermocline is not detected in one of the vertical profiles, the vehicle will extend the vertical span up to Z_{min} or Z_{max}. It should be noted than on the very first time the algorithm runs (usually during the first descend), it is possible either to use *a priori* data to define the detection thresholds, or to use no information at all and let the AUV acquire a full vertical profile to determine those values.

6.2.2 Practical Implementation Issues

The size of the depth bins is an important design parameter for the algorithm, since it acts as a low pass filter which may affect the ability to detect gradients. If the bins are too small, only few data points will fall into that bin, resulting in large errors in gradient estimation. If the bins are too large, then they will smooth the temperature variations and the algorithm will have difficulty in separating significant variations. After several tests with both real and simulated vertical temperature profiles, we've found that we should have at least 5 to 8 bins spanning the depths of the thermocline to have significant changes in the gradients. Currently, the bin size is a fixed number chosen when the algorithm runs, so, as a rule of thumb, we usually set this value so that the first estimated thermocline spans about 10 bins.

During normal tracking, the transitions between states are triggered by the detection of temperature gradients above or below specific thresholds. These thresholds are updated for each new profile, to allow for temporal and spatial variations of the thermocline parameters, but this choice may have a strong impact on the algorithm performance. In our case, we define the threshold for the thermocline of a new profile (Thr_tc) to be 50% of the maximum gradient found in the previous profile. Typical temperature profiles exhibit more variation towards the surface than towards the bottom and therefore we set Thr_top$= 1/2\times$Thr_tc and Thr_bot$= 1/4\times$Thr_tc.

As described earlier, the estimation of the derivative based on finite differences yields some *noisy* measurements, even with the clustering of data into bins. In order to avoid false triggering of thresholds, we've considered a minimum number of 3 consecutive detections to confirm that the gradient thresholds have been passed. We've also implemented a mechanism of validating a bin, depending on the quantity of data points used. For our experiments, we've considered a minimum number of 5 data points in a bin for its data to be used for gradient detection.

6.2.3 Real Time Performance Evaluation

In order to evaluate the performance of the algorithm, a simple mechanism is to maintain 3 different counters that are increased depending on the state transitions that lead to the reversal of the profiles (TOP and BOTTOM states). The first counter, **full_track**, is increased when the vehicle detects both the beginning and the end of the thermocline, *i.e.* reaches the TOP or BOTTOM

states through one of the dark arrows of the state machine represented in figure 6.3; the second, **begin_only**, is increased when the vehicle enters a transition state (TC2TOP or TC2BOT) and reaches one of the vertical limits before detecting the end of the thermocline. Finally, a third counter, **fail**, is increased if there is a direct transition from the TOP to the BOTTOM limits, or vice-versa, before detecting any significant gradient.

During a tracking maneuver, these counters are permanently evaluated and a set of decisions can be taken depending on their values. For example, the adaptive sampling mission may be aborted if the number or percentage of **full_track** is too small (or **fail** is too large), or the vertical limits may be extended if the counter **begin_only** becomes significant.

6.2.4 Additional Features

During the thermocline tracking maneuver, the model parameters can be passed on to other AUV processes, if necessary, in the same way as the references are passed on to the controllers. This allows, for example, the AUV to switch on any special sensor or to trigger an underwater sampler at the right instant, in order to capture a relevant sample of water for later laboratory analysis, such as suggested in Zhang et al. (2009) to capture a water sample at the estimated peak of the gradient. Additionally, the vertical span of the AUV motion may be extended with respect to the thermocline layer, in order to gather additional data. For example, it is known that phytoplankton often accumulates below the thermocline (Derenbach et al. (1979)), therefore we can switch on a Chlorophyll sensor when the AUV is below the thermocline, and increase the parameter $Z_{span.bot}$ to ensure that the vehicle samples the phytoplankton layer. This may contribute to a better understanding of the correlation between the thermocline characteristics and the phytoplankton layer. This ability to stay very close to a dynamic phenomenon is only possible with a real time, on-board processing of information and it allows the vehicle to capture very small scale variations, hence contributing to a significant increase in the efficiency of the sampling process.

6.2.5 Field Tests and Results

In order to test the thermocline tracking algorithm described in this work, we chose a dam reservoir in the Douro river, about 20 km east of Porto, Portugal. This is a location that we've used extensively for testing multiple aquatic equipment, since we have access to a small support boat and there is a quiet place where we can install a control station. This place (approximate location 41.0604ºN, 8.4544ºW) overlooks a relatively straight stretch of the river, about 1000 meters long by 300 meters wide. The river bed has a "'U"' shape, with depth between 2 and 15 meters, and the currents are usually small, typically less than 50 cm/s.

This location was selected both to facilitate logistics and also because it is known to develop a seasonal thermocline from late spring to early autumn. As an example, figure 6.4 shows a vertical temperature profile acquired by the MARES AUV in July 2008. Comparing this profile with a typical ocean profile (see for example, fig. 2.1), it is clear that the reservoir thermocline has much more small-scale variations, particularly in the mixed layer, above the thermocline. For the

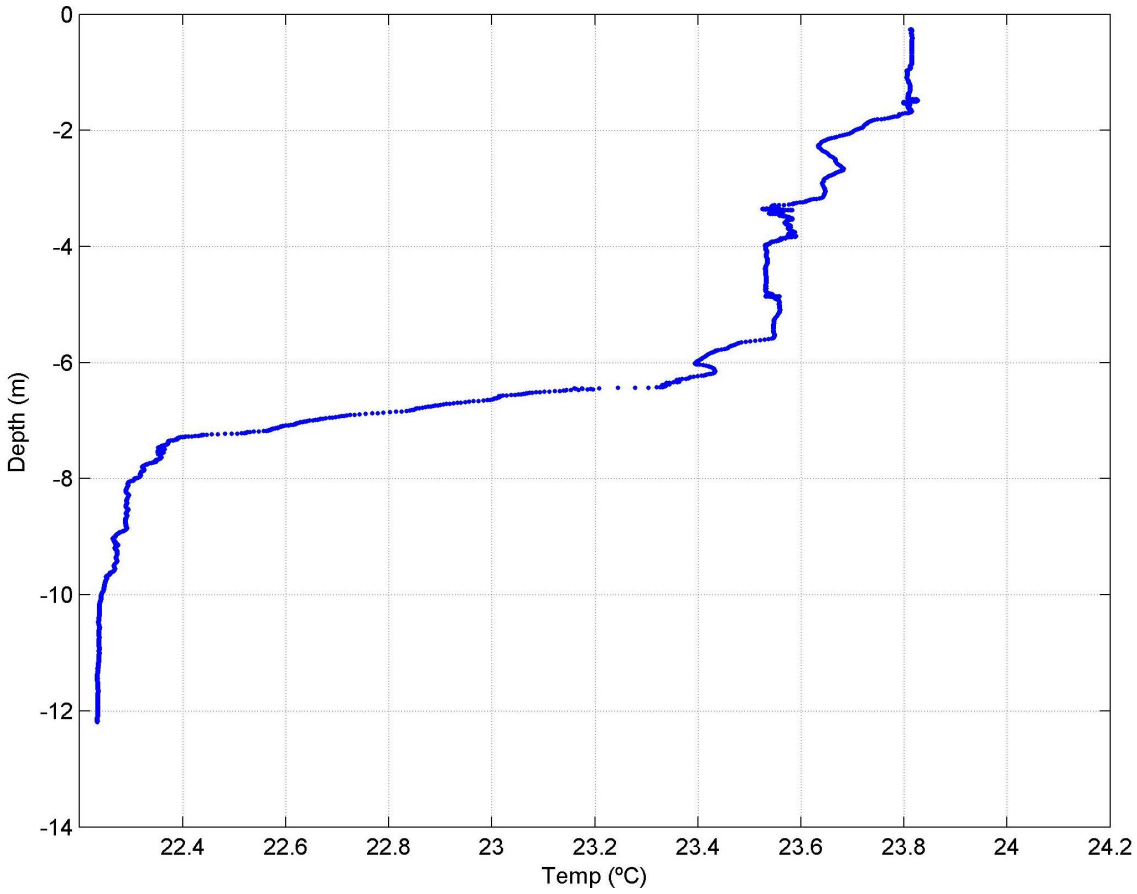

Figure 6.4: Temperature profile measured by the MARES AUV in the Crestuma reservoir, July 2008. Note the small scale variations above the thermocline.

thermocline tracking algorithm, this provides a much harder scenario than a smooth variation and, therefore, it is a good way of demonstrating its effectiveness.

The MARES AUV was configured with a *SBE 49 FastCAT* CTD sensor from Seabird Electronics mounted outside hull, with a similar configuration as in figure 4.10. From the vertical profile, we estimate a maximum temperature gradient in the order of 1°C/m, with a very thin thermocline at around 7 meters of depth. As described earlier, taking these numbers, we chose a bin size of 12cm so that we would have a thermocline spanning around 10 bins. For a vertical velocity of about 10cm/s and a 16Hz sampling rate of the CTD sensor, this results in about 18 samples per bin.

Mission #1 - July 2008

For the first mission, the MARES AUV was programmed to perform a *yo-yo* pattern between a minimum depth of 2 meters and a maximum depth of 12 meters, while the thermocline tracking algorithm was running in a parallel process. This process was called whenever there was a new sample from the CTD sensor, at a rate of 16Hz. The vertical velocity was set to around 0.1 m/s,

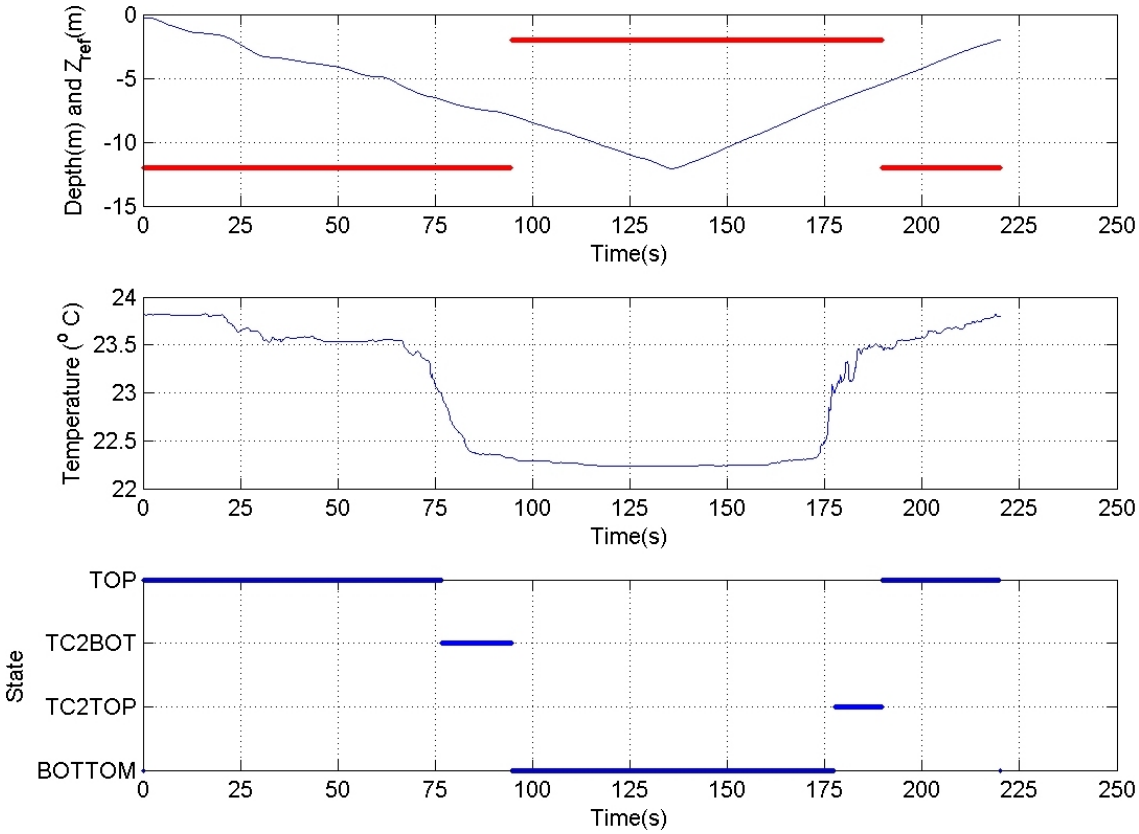

Figure 6.5: *Yo-yo* profile by the MARES AUV detecting the thermocline in the Crestuma reservoir, July 2008. Plots in bold show the outputs of the thermocline tracking algorithm, indicating a thermocline between 5.5 and 7.9 meters of depth.

which resulted in about 160 samples ever meter. Note that at this time the algorithm was being tested in real time but it was not being used to control de vehicle, as the AUV references were being provided by the standard controllers. Figure 6.5 shows the details of the depth during the *yo-yo* motion, the temperature readings and the corresponding state of the algorithm state machine, as described earlier: TOP, TC2BOT, BOTTOM, and TC2TOP.

Note in the first graph the solid red line indicating the depth reference suggested by the thermocline tracking algorithm. When the dive begun, this reference was 12 meters, as the vehicle was trying to find the thermocline on its downward motion. The algorithm detected a consistently high gradient at $t = 77$ seconds and changed the state to TC2BOT. However, the depth reference was maintained at 12 meters, since the vehicle had not yet crossed the thermocline. This only happened at $t = 95$ seconds, when the gradient got back to a low level and the algorithm indicated that the vehicle entered state BOT. It was only at this stage (when the vehicle was at 7.9 meters of depth) that the reference was changed to 2 meters, suggesting an inversion in the direction of the vertical motion, as there would be no need to proceed further deep. Naturally, since the references actually provided to the controllers were the ones from the original *yo-yo*, the vehicle kept diving until the expected depth of 12 meters, reached at $t = 135$ seconds. Note that the thermocline track-

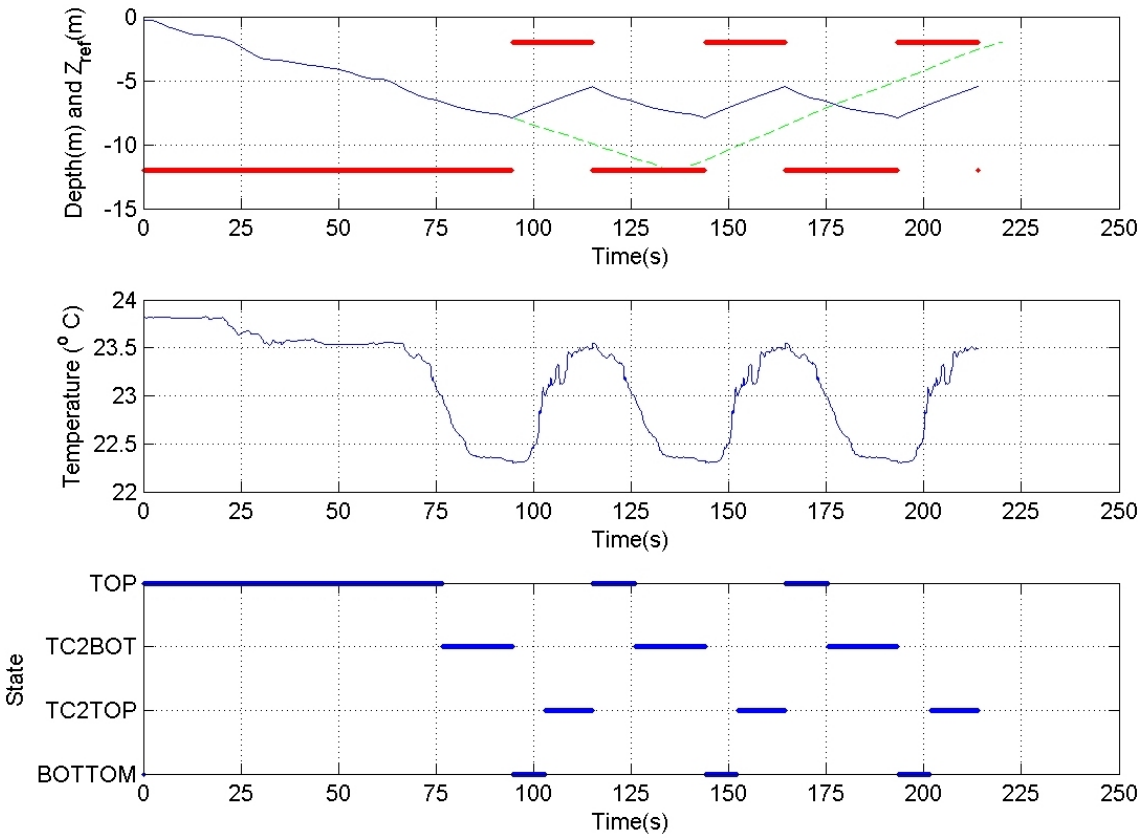

Figure 6.6: Simulation of a *yo-yo* profile using the thermocline tracking maneuver for the same data set shown in fig. 6.5. Note the differences between the new profiles (shown in blue on the first plot) with the original (in light green).

ing algorithm was already trying to detect the thermocline, since $t = 95$ seconds, but the vehicle was still in depths of very little gradients, as indicated in the temperature plot. During the upward motion, the algorithm detected the thermocline at $t = 178$ seconds (changing the state to TC2TOP) and indicated the *upper limit* of the thermocline to be around 5.5 meters of depth.

Although the AUV was not directly controlled by the thermocline tracking algorithm, it is possible to simulate the behavior of the vehicle if the depth reference suggested by the algorithm were transmitted to the vehicle controllers. We assume a simple kinematic model for the vehicle, which is a reasonable assumption since the vertical velocity is very slow. We also assume that the temperature profile is constant, which is also reasonable for such a short duration. Figure 6.6 shows the resulting profile if the vehicle were to use the information provided by the algorithm, superimposed to the original *yo-yo*. With the new algorithm, the initial 10 meters of vertical span are reduced to about 2.5 meters, resulting in a corresponding 4-fold increase in the sampling frequency of the thermocline (from the original 200 seconds period of the *yo-yo* down to 50 seconds). It is obvious that this increase can be much more significant when the ratio between the full water depth and the thickness of the thermocline layer increases, such as the case of deeper water scenarios.

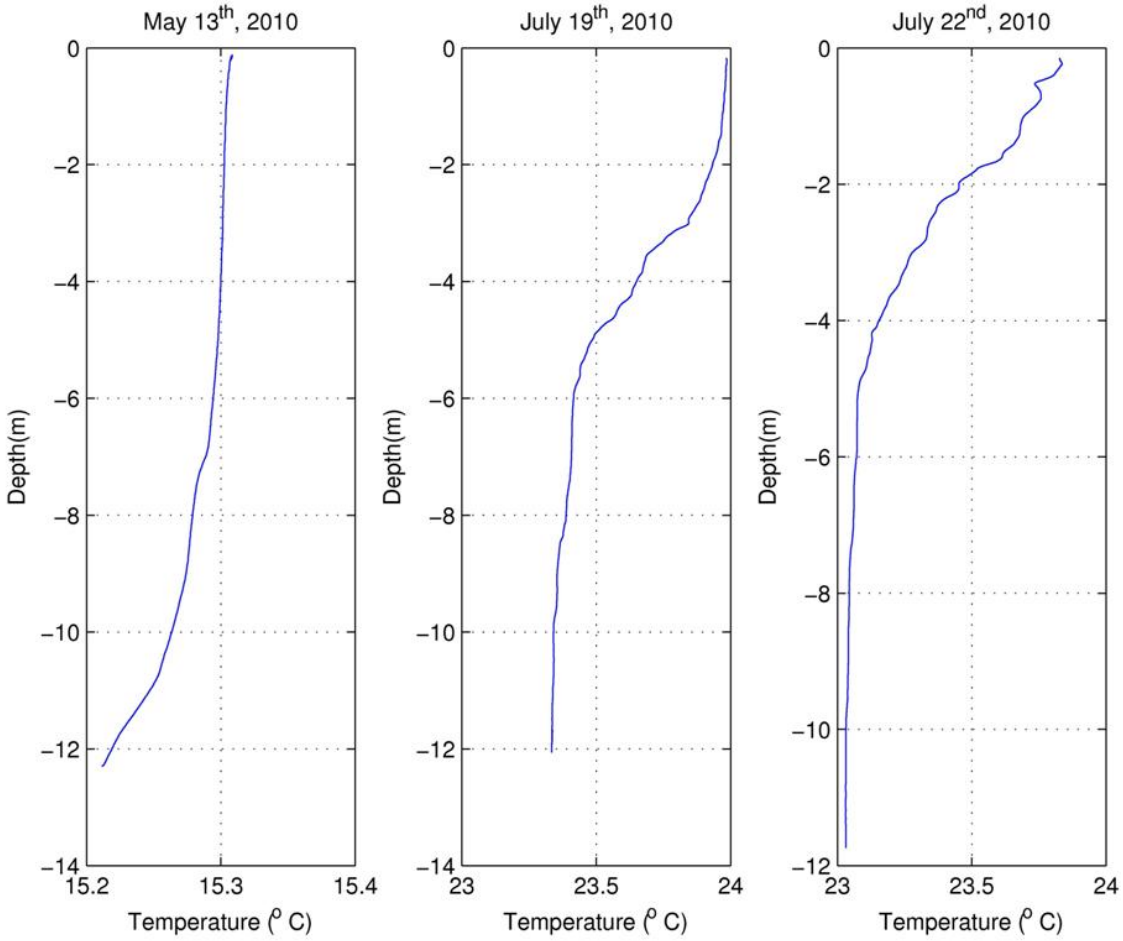

Figure 6.7: Temperature profiles measured at different times of the year by the MARES AUV, at approximately the same location of the Crestuma reservoir. The thermocline is visible with different characteristics in the summer profiles, reaching the surface in the last plot.

Mission #2 - August 2010

After demonstrating the capability of tracking the thermocline by simulation, and testing the algorithm with many different temperature profiles obtained with the MARES AUV, we returned to the same dam reservoir in the summer of 2010, to validate the effectiveness of the algorithm to guide the vehicle in real time. By returning multiple times to the same location, we've confirmed the dynamics of the reservoir thermoclines, as can be seen in the examples of figure 6.7. This variability stresses the need to implement adaptive sampling mechanisms.

The initial tests in the summer of 2008 were performed with very limited horizontal range and the performance was very dependent on the location of the AUV, since in some regions of the dam there was an almost linear variation of temperature from the surface to the bottom. We then changed the mission plan, so that the AUV was programmed to follow a *lat-lon* trajectory, diagonally in the river, trying to capture the characteristics of the thermocline along that direction. We've used a small support boat to deploy 2 buoys with acoustic beacons, located 350m apart,

which provided a baseline for acoustic navigation of the AUV and tracked the vehicle position in real time. Given the shallowness of the river (10–15 meters in the operation area), we've set the upper and lower limits to 0.4 and 10 meters, respectively. Note that at this time we did not have any altimeter on board, otherwise we could have set the lower limit to be an offset above the bottom.

Regarding the initial parameters for the algorithm, we deliberately set a very high threshold for the thermocline gradient. This intentionally forced the vehicle to make a full profile, up to the maximum depth of 10 meters, since it did not detect the thermocline. At the end of this profile, the algorithm automatically analyzed the temperature data and provided some data for the next (upward) profile.

Figure 6.8 shows the details of data logged during one of the missions, in which the MARES AUV performed a total of 10 profiles in about 300 seconds (and roughly 300 meters of horizontal range). Note in the top-most plot the depth reading during the *yo-yo* motion and the solid red line indicating the depth reference provided by the thermocline tracking algorithm. This reference was actually sent to the vertical controllers of the AUV, resulting in the inflections of the profiles. Such inflections have small delays with respect to the reference changes, due to the vehicle dynamics, and these delays are longer close to the surface since the vehicle was slightly buoyant. It is clear from the analysis of this plot that the thermocline was very close to the surface, as the vehicle repeatedly reaches the upper limit of the *yo-yo*. The second plot displays the temperature readings from the CTD sensor, and confirms the difficulty in the detection during the ascending motion, as compared to the descending profiles. Note that the temperature measurements always exhibit a small slope when the vehicle switches from descending to ascending mode. The states of the algorithm state machine are represented in the third plot, and it is possible to see the algorithm cycling through the states TOP-> TC2BOT-> BOTTOM-> TC2TOP-> TOP. It is interesting to note that the AUV spends much more time in TC2BOT than in TC2TOP. This indicates that the thermocline has a much sharper transition close to the surface than towards the bottom. The last plot shows the evolution of the thermocline thresholds as the new profiles were being completed, with values ranging from 0.16°C/m to 0.31°C/m.

In terms of quantitative results, we have summarized the most relevant data in table 6.1. The performance counters ended up this trajectory with: **fail**=2, **beg_only**=3, and **full_track**=5. If we take out the first dive (used to provide the algorithm with initial data), this means that in 8 out of the other 9 profiles, the vehicle was able to detect the thermocline. In the descending profiles, the AUV successfully detected both the beginning and the end of the thermocline layer. However, in the ascending profiles, the algorithm failed to detect the end of the thermocline layer, since it was too close to the surface and, therefore, the upper limit of the *yo-yo* was reached before the gradient decreased below detection threshold. The vehicle failed to detect the thermocline during profile number 8, mainly because the temperature readings showed a lot of small scale variations. At the same time, the thermocline layer was very thin, preventing the algorithm to find a consecutive number of high gradients. Note that the highest gradient detected (0.32°C/m) was in fact above the threshold (0.26°C/m), but the algorithm needs a consecutive number of detections to change

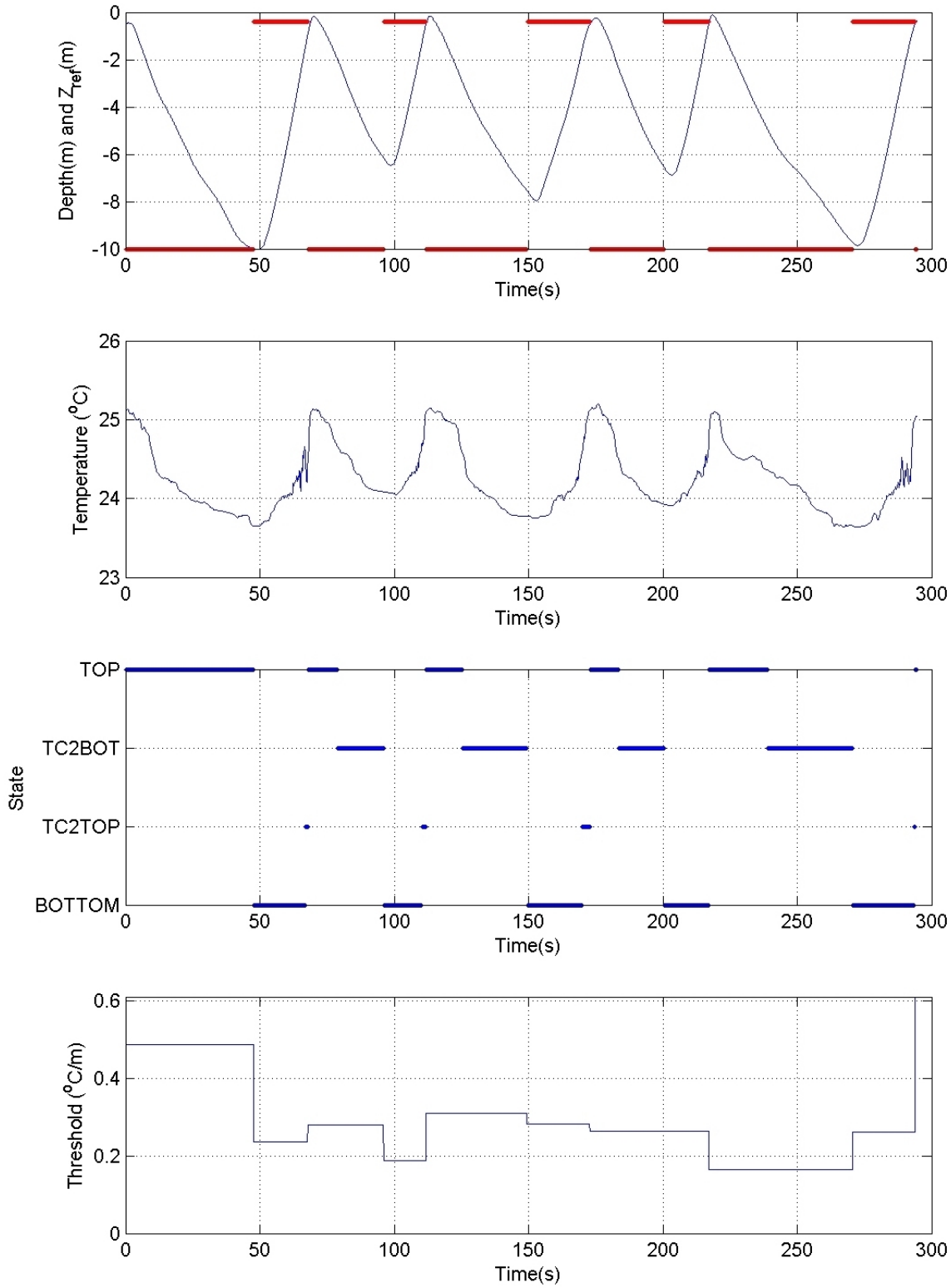

Figure 6.8: MARES AUV data while tracking a thermocline in the Crestuma reservoir, August 2010. The first plot shows the depth of the vehicle in blue and the depth reference in bold-red, during 10 profiles of thermocline tracking, starting with no a-priori information. The states of the third plot indicate the cycling through the state machine presented in figure 6.3.

Profile # Dir.	Time (s)	Depth (m)	Temp. (°C)	Thr_tc (°C/m)	Max dT/dz (°C/m)	Detection
1 ↓	0–48	0.4–10	23.7–25.1	0.50	0.48	fail
2 ↑	48–68	0.9–10.0	23.6–24.7	0.24	0.56	full_track
3 ↓	68–96	0.2–6.1	24.1–25.1	0.28	0.38	full_track
4 ↑	96–112	0.5–6.5	24.1–25.1	0.19	0.62	beg_only
5 ↓	112–149	0.1–7.5	23.8–25.2	0.31	0.56	full_track
6 ↑	149–173	0.5–8.0	23.7–25.1	0.28	0.52	beg_only
7 ↓	173–200	0.2–6.5	23.9–25.2	0.26	0.52	full_track
8 ↑	200–217	0.5–6.9	23.9–24.8	0.26	0.32	fail
9 ↓	217–271	0.1–9.7	23.6–25.1	0.16	0.52	full_track
10 ↑	271–294	0.5–9.9	23.6–25.0	0.26	1.22	beg_only

Table 6.1: Summary of quantitative data of the profiles presented in figure 6.8

the state. A stronger turbulence also affected profiles number 2 and number 10, but in these cases, the thermocline layer was thick enough to allow detection.

The plots of figure 6.9 show the Temperature-Depth profiles captured by the MARES AUV during this mission and they stress the difficulty in tracking, since the thermoclines extend almost to the surface and show very low gradients and many small scale variations. In particular, profiles number 2 and number 10 exhibit strong turbulence between 1 and 3 meters of depth. These plots also highlight that during the ascending profiles (even numbered), the vehicle only reversed the direction when the upper limit of the *yo-yo* was reached, at 0.4m, with a single exception of profile number 2, in which the AUV reversed direction at approximately 1 meter of depth. The case of

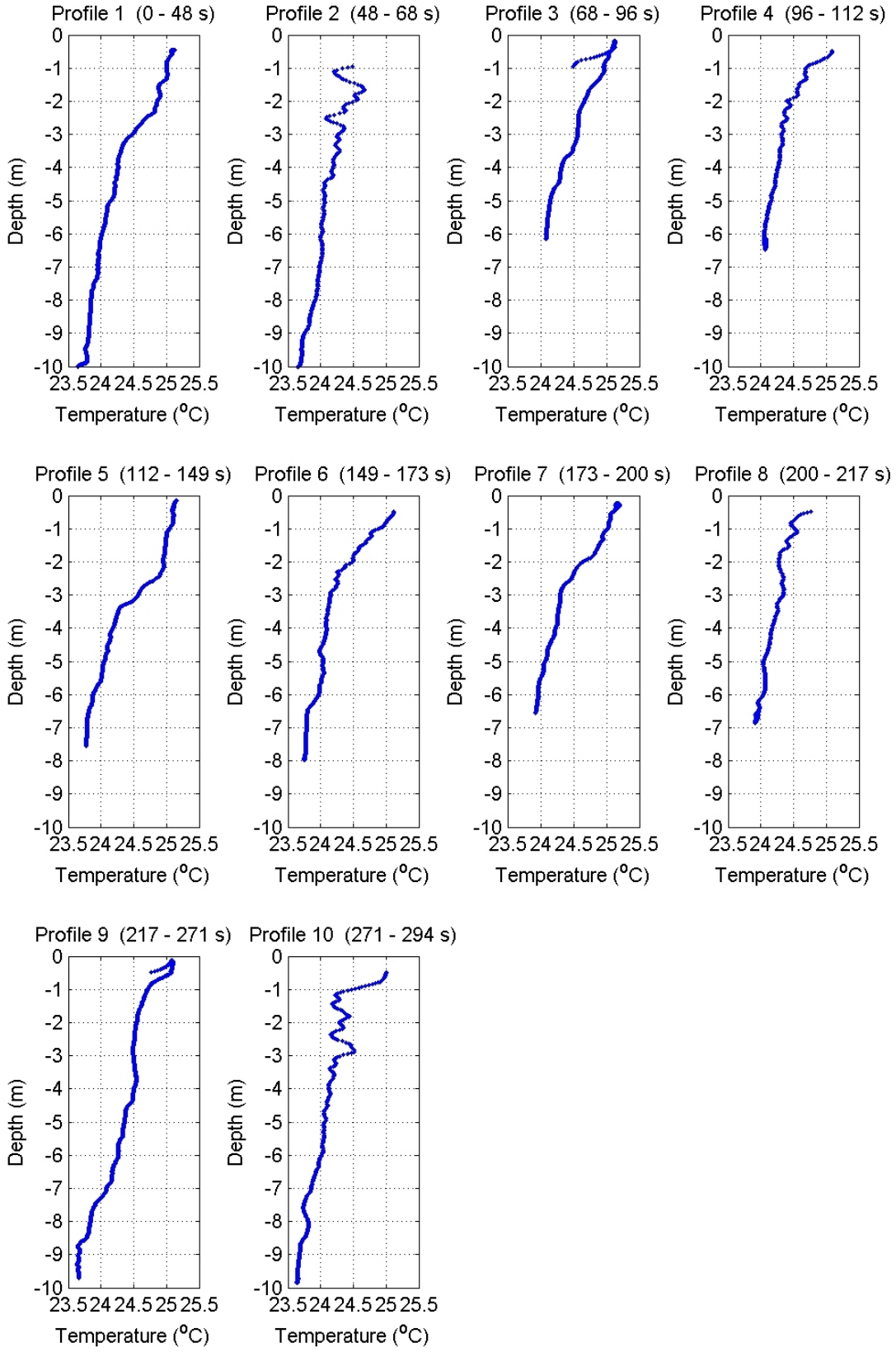

Figure 6.9: Temperature-Depth profiles tracked by the MARES AUV during a thermocline tracking mission.

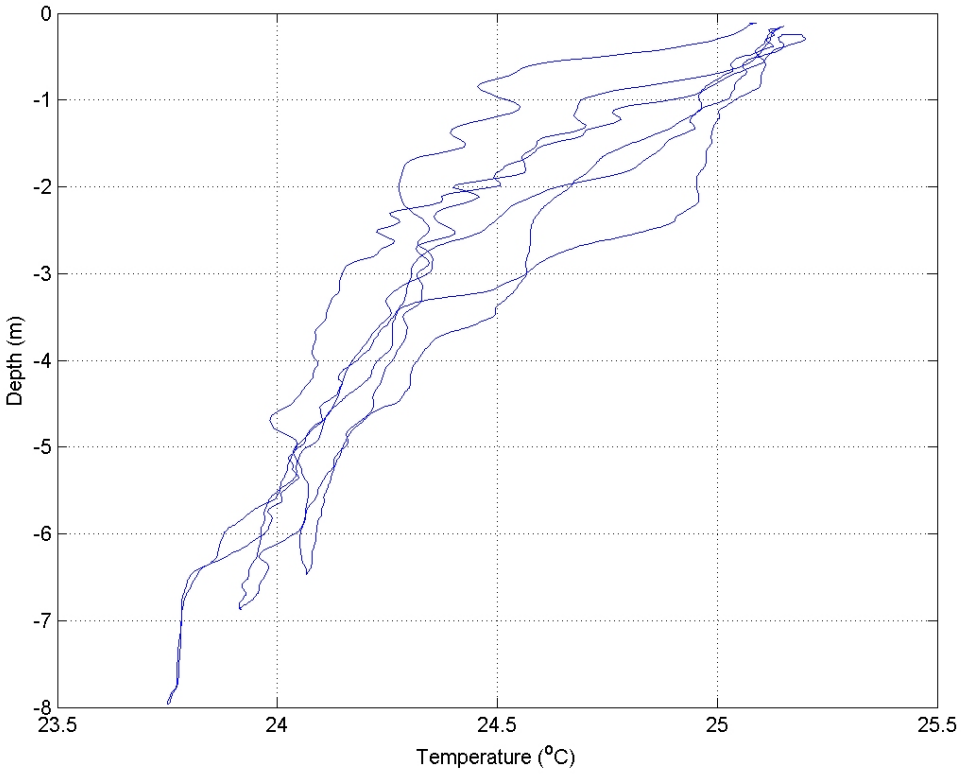

Figure 6.10: Variation of the Temperature-Depth profiles tracked during the demonstration mission, taken during the interval 70–220 s.

the detection failure in profile number 8 can also be understood, given the smooth variation of the temperature data. In all these cases where the thermocline could not be fully identified, it is important to stress that the algorithm proceeded according to the plan, reverting to the default *yo-yo*.

In order to better understand the usefulness of the this thermocline tracking algorithm, we aggregate, in figure 6.10, the temperature-depth plots corresponding to profiles 3–8 in a single plot. This demonstrates the ability to capture the dynamics of the temperature field, as it shows the variations measured by the MARES AUV in only 150 seconds (from 70 to 220 seconds into the mission), corresponding to, roughly, 150 meters. This plot highlights the fact that the variations are much stronger in the water column than at the surface.

6.3 Tracking a Horizontal Boundary

In this section, we expand the adaptive sampling strategy to two dimensions and show how it can be applied to the efficient characterization and tracking of a horizontal boundary for a specific scalar field $\Phi(x,t)$, or Φ for simplicity. Once again, we assume that the scalar field Φ has a transition

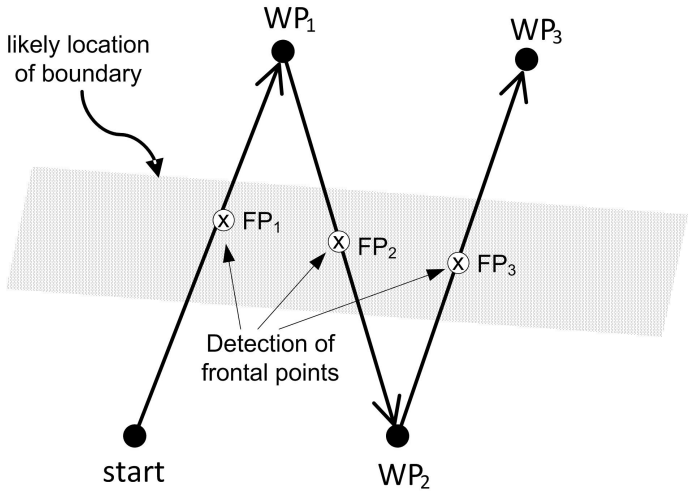

Figure 6.11: Initial phase of the boundary tracking mission, finding the first frontal points. WP_1–WP_3 are programmed based on *a priori* knowledge about feature, so that the likely location of the boundary is crossed three times. For each crossing, a frontal point, FP, should be detected.

zone with a higher gradient than in the rest of the area, which is a typical characteristic of many oceanographic phenomena, like fronts or plume boundaries. In this case, we are only concerned with the horizontal plane, therefore we are assuming that the vehicle will find the transition while navigating at a constant depth and following a specific direction. We assume that the vehicle can take only local measurements of Φ, therefore in order to find the maximum horizontal gradient, the vehicle needs to cross the transition zone, moving from the region where the scalar field has *high* values (the HIGH region) to the region with *low* values (the LOW region), and vice-versa, following the simplified view of figure 6.1, in the beginning of the chapter.

In our approach, the successful tracking of a horizontal gradient results in a combination of a main direction of travel (aligned with the horizontal location of the boundary), together with a *zig-zag* around that direction. Note that neither the evolution of the boundary line, nor the amplitude of the *zig-zag* are known at the beginning of the mission. However, as indicated earlier in our general assumptions for feature tracking, we assume that there is some *a priori* information about the phenomena being studied, such that we can start the mission close to the *likely* location of the boundary. Our strategy for implementing this tracking in the horizontal plane develops in two phases, as follows.

Phase I – Finding the Boundary

For simplicity, let's assume that the mission starts in the LOW part of the scalar field. We then define three initial waypoints WP_1–WP_3, so that the first three trajectories cross the likely location of the boundary, as represented in figure 6.11.

For each of these trajectories we need to acquire a full profile with a shape similar to figure 6.1, and find the location of each frontal point. This can be done using an online method such as the

one described in section 6.1.1. At the end of this first stage, there should be the first three points of maximum gradient (or frontal points FP_1–FP_3), so that the strategy can proceed to phase II. Depending on the application scenario, this first processing can be made online, taking advantage of the availability of the full profile, or it can be done offline by an operator, particularly if the temporal variations of the scalar field are slow. Note also that the trajectory represented in figure 6.11 can be replaced by a different sampling pattern (for example, a spiral), just to ensure that we find the first three frontal points FP_1–FP_3.

Phase II – Tracking the Boundary

As soon as the vehicle gets to WP_3, it enters a fully autonomous mode, in which all processing is done online to keep tracking of the boundary. This requires two algorithms:

1. Automatic generation of new waypoints;
2. Real time, online detection of the maximum gradient along a trajectory.

In order to track the boundary, the vehicle uses algorithm #1 to generate WP_4, *i.e* it projects a new heading (extending to waypoint WP_4) that will ensure an additional crossing of the boundary and, at the same time, some progress along the same boundary, as shown in a simplified version in figure 6.12. As soon as the vehicle starts this new transect, it also starts algorithm #2, processing the samples of the scalar field as soon as they are available and trying to detect the new frontal point FP_4. If algorithm #2 is successful, FP_4 is detected before the vehicle reaches WP_4, so that WP_5 can be generated and the algorithms continue iteratively. WP_4 can then be seen as the maximum excursion that the vehicle will travel if algorithm #2 fails, when the vehicle is moving away from WP_3.

6.3.1 Automatic Generation of New Waypoints

The simplified mechanism shown in figure 6.12 only works well for the generation of waypoints when the boundary follows a line. In fact, if the boundary follows a relatively straight line, there is no need for three frontal points, as only two would be enough to define such line. However, if there is some curvature in the boundary, we need to know (at least) the last three crossings in order to estimate the local curvature and generate the following waypoint.

The proposed algorithm to adapt the crossings with the local curvature is illustrated in figure 6.13. In this figure, WP_i represent the waypoints and FP_i represent the points of maximum gradient, or frontal points. Note that a certain FP_i is detected when the vehicle is moving towards WP_i, but, ideally, before actually getting there. We identify the points DP_i as the places where those detections are made.

Consider that the vehicle has crossed the gradient and has just found front point FP_n (this happens when the vehicle is located at DP_n). The algorithm to generate the next waypoint, WP_{n+1}, is:

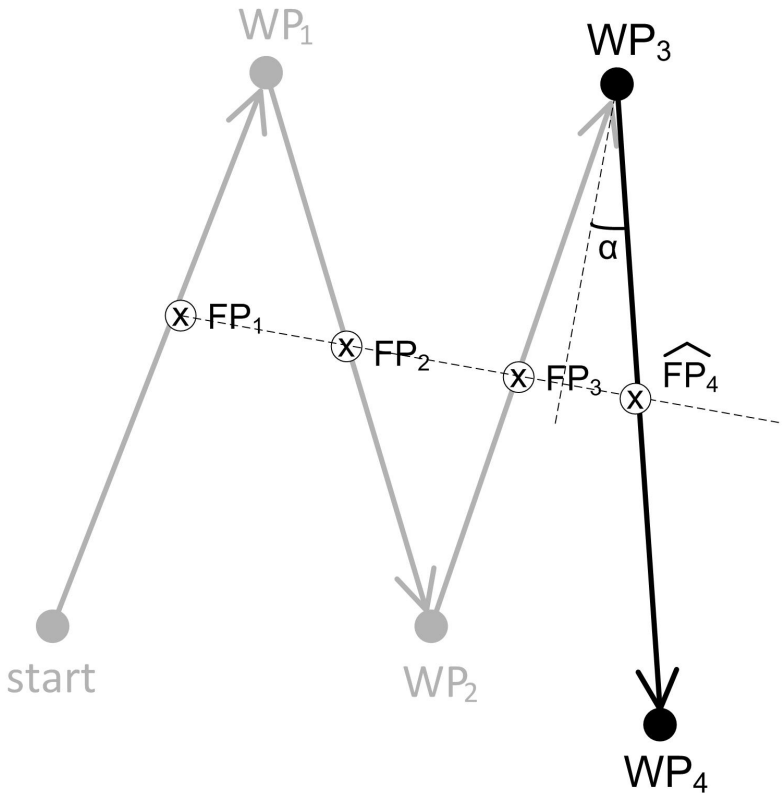

Figure 6.12: Beginning of fully autonomous mode, tracking the boundary. WP_4 is calculated when the vehicle is at WP_3, in such a way as to ensure some progress along the boundary, given by parameter α, so that the boundary is expected to be crossed close to $\widehat{FP_4}$.

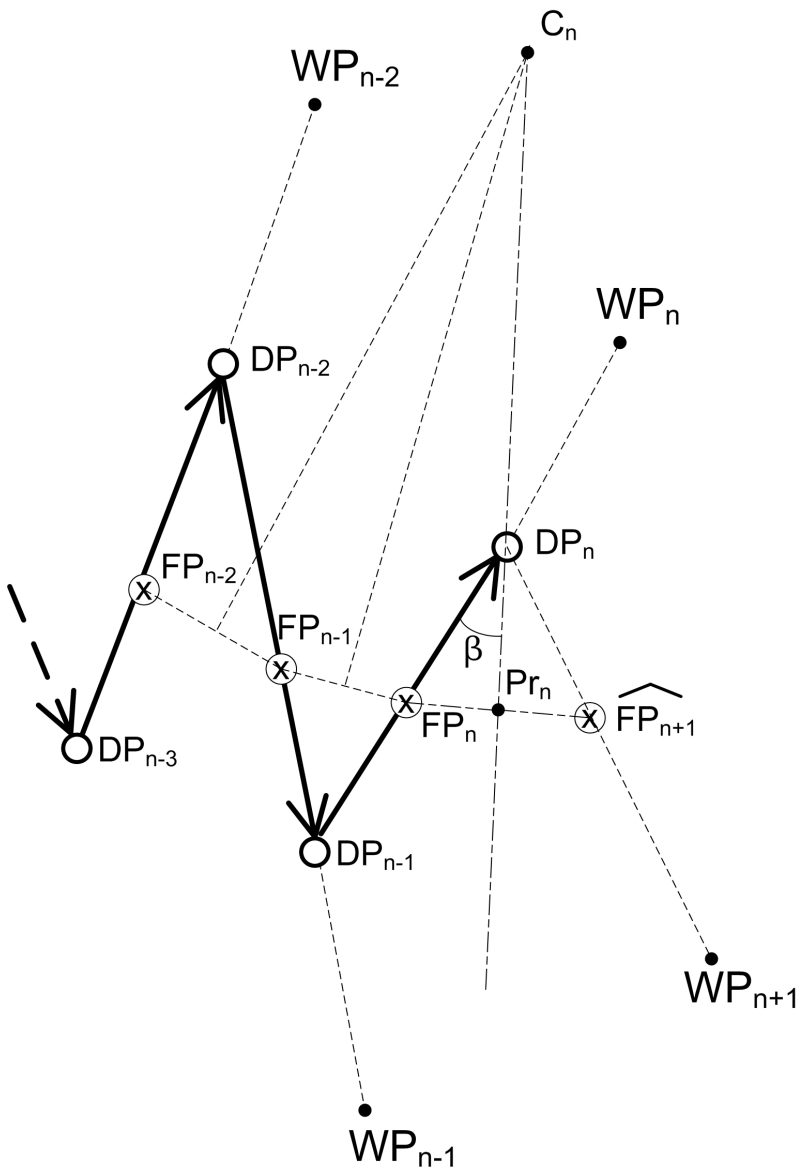

Figure 6.13: Generation of a new waypoint WP_{n+1}, based on detections of previous frontal points $\{\mathrm{FP}_{n-2},\ \mathrm{FP}_{n-1},\ \mathrm{FP}_n\}$ and the curvature they define. The location of the new frontal point is expected at $\widehat{\mathrm{FP}_{n+1}}$.

1. Compute C_n, the center of the circumference defined by the last three frontal points, {FP_{n-2}, FP_{n-1}, FP_n}, by intersecting the bisector of $\overline{FP_{n-2}FP_{n-1}}$ with the bisector of $\overline{FP_{n-1}FP_n}$. This circumference represents the local curvature of the boundary.
2. Connect C_n with DP_n to define an axis of symmetry.
3. Project the last frontal point, FP_n to the other side of this axis to get the next estimated frontal point, $\widehat{FP_{n+1}}$.
4. Determine the new waypoint WP_{n+1}, extending the line connecting DP_n with $\widehat{FP_{n+1}}$, up to a *reasonable* distance.

This algorithm ensures that each "V" shape of a *zig-zag* is oriented towards the center of the local curvature, therefore adapting the crossing angles to ensure future detections of FP's. In terms of practical implementation, however, the uncertainty in the determination of FP_n may result in an incorrect estimate of C_n. This, in turn, can yield a projection $\widehat{FP_{n+1}}$ either *backwards* or too far from FP_n. For this reason, we limit the rate of advance along the boundary within a preset interval, and we assess the direction of motion, verifying that

$$\overrightarrow{FP_{n-1}FP_n} \,.\, \overrightarrow{FP_n\widehat{FP_{n+1}}} > 0$$

As an illustrative example, we've synthesized a scalar field representing a contour (for example, a plume), and used this algorithm to produce new waypoints. Figure 6.14 demonstrates the ability to track the curvature of the boundary. Figure 6.15 details some of the simulated trajectories, where the adaptation of the crossing angles is clear.

6.3.2 Online Detection of the Maximum Gradient

Once again, in order to solve this problem and estimate the gradient of the scalar field, we follow a similar approach to the one employed for tracking the thermocline, described in the previous section. This time, we cluster data points into bins of distance traveled and take the differences of the averaged values. The size of the bins depends on the estimated slope that we intend to track and the amount of data available (which is a function of the sampling rate of the sensor and vehicle velocity). This size acts as a low pass filter which may affect the ability to detect gradients. Smaller bins result in large variations in gradient estimation, while larger bins smooth the variations but hinder the separation of gradients.

As an example, consider the bathymetry map of the slope of a navigation channel, represented in figure 6.16, acquired by the Zarco ASV in July 2014, at Base Naval do Alfeite. Note that in this case, the channel wall drops from roughly 3.5m to roughly 5.5m in less than 5m, and this can be seen as an example where the maximum gradient can be detected, so that an autonomous vehicle can follow the line of maximum gradient.

Although the map seems to be relatively smooth, if we analyze the raw altimeter measurements taken during the bathymetry mission, we can verify that they are relatively noisy, as can be seen

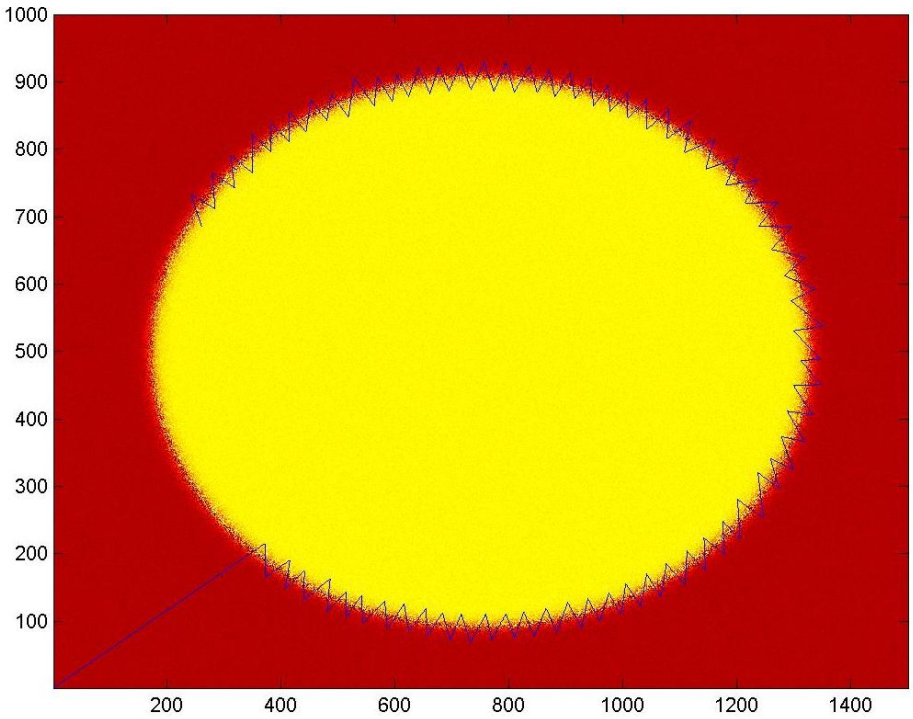

Figure 6.14: Demonstration of the ability to follow a curved horizontal boundary, with the waypoint generation mechanism illustrated in figure 6.13. Note the *zig-zag*'s orientation towards the center of the ellipse.

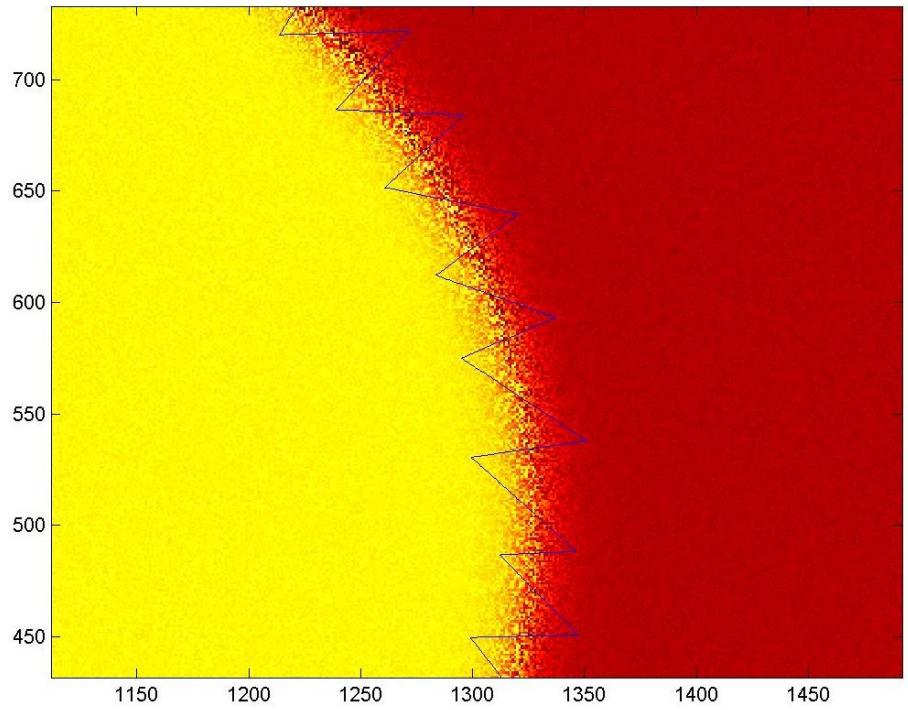

Figure 6.15: Detail of figure 6.14, highlighting the vehicle guidance mechanims to track a horizontal boundary.

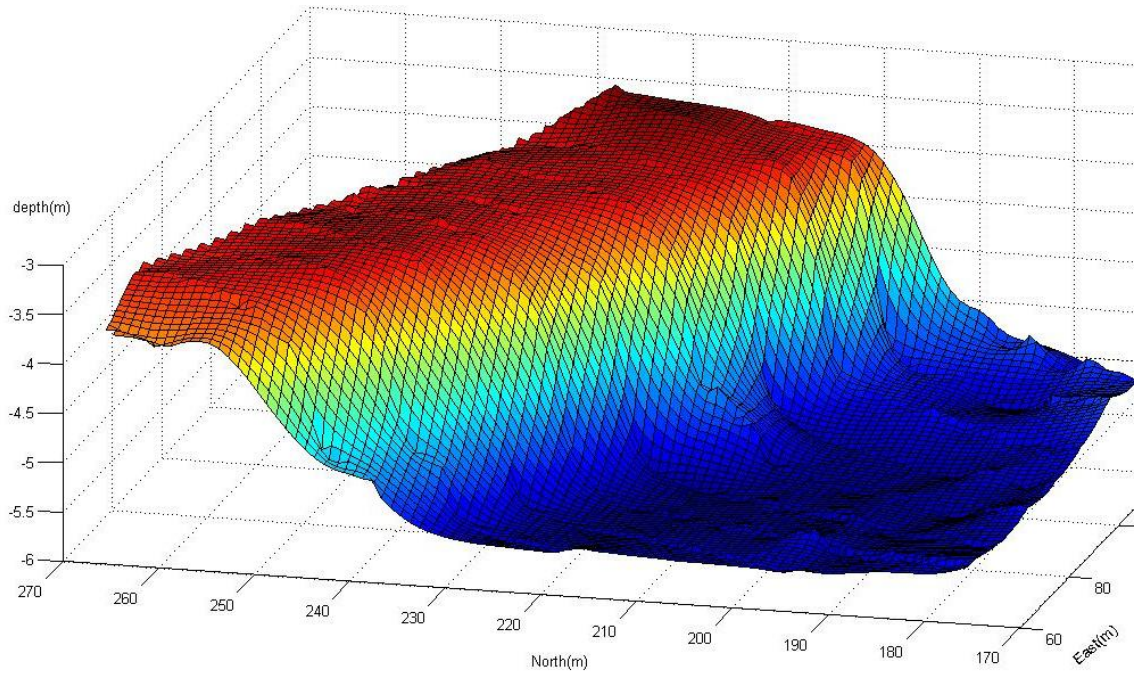

Figure 6.16: Example of a bathymetry map of the slope of a navigation channel, acquired by the Zarco ASV in July 2014, at Base Naval do Alfeite, Portugal.

in the example of a profile shown in figure 6.17 (the topmost left plot). It is also quite difficult to quantify the variations of the gradient along track when we compute them using central finite differences (in the topmost right plot). However, in the other plots of figure 6.17 we show the result of aggregating the measurements into bins of increasing size. The smoothness of the data points is obvious, as well as the increasing evidence of the maximum gradient (around 0.5 m/m), but the location of such maximum gradient is still somewhat ambiguous.

One important aspect to mention is that the vehicle is typically crossing the front at an angle β, as pictured in figure 6.13. This means that the *true* maximum gradient (mg_t) should be computed as the projection of the detected along-track gradient (mg), that is: $mg_t = \frac{mg}{\cos(\beta)}$.

The full algorithm developed for online gradient tracking can be described by the state machine represented in fig. 6.3, where the dark arrows represent the transitions that are expected during a successful tracking. These transitions will cycle the state machine through the most relevant states:

- HIGH - The vehicle is located at the higher part of the scalar field.
- HIGH2LOW - The vehicle is descending the gradient, towards the lower part of the scalar field.
- LOW - The vehicle is located at the lower part of the scalar field.
- LOW2HIGH - The vehicle is climbing the gradient, towards the higher part of the scalar field.

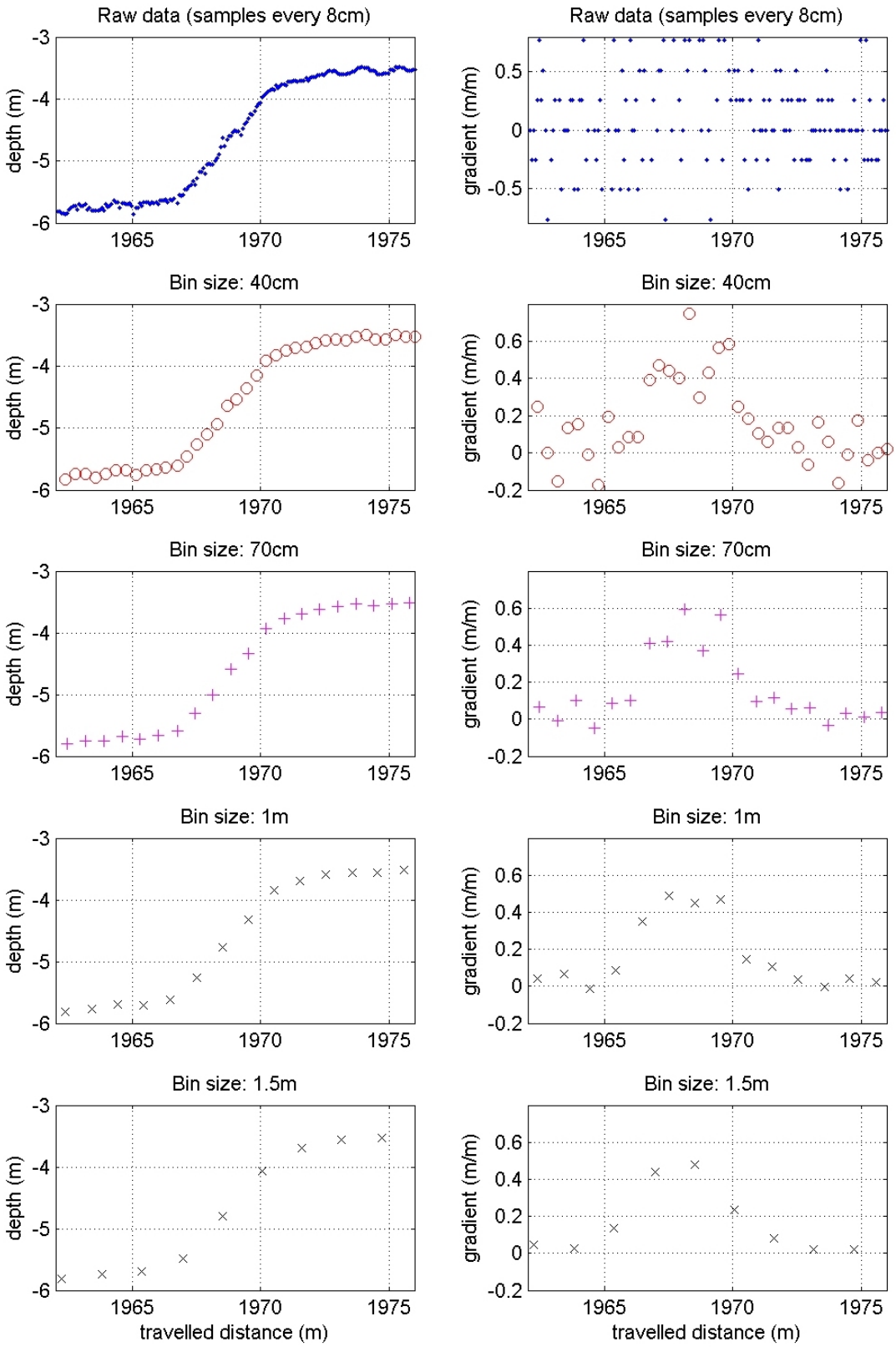

Figure 6.17: Example of altimeter samples collected across the slope of the map shown in figure 6.16 (left-side plots) and gradient estimated from differences (right-side plots). As the samples are aggregated into larger bins (top to bottom), both the profile and the gradient gets smoother.

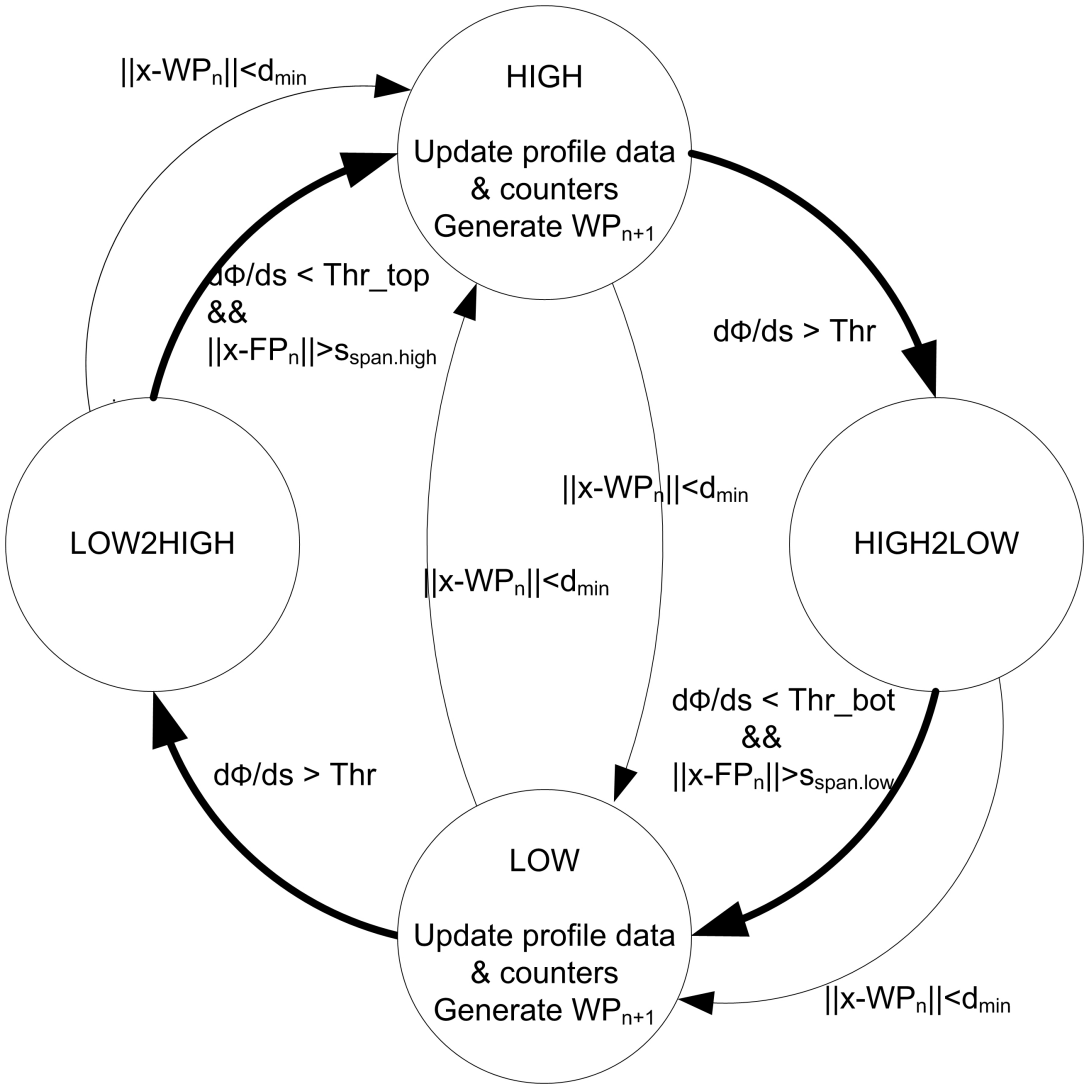

Figure 6.18: State machine and transitions representing the gradient tracking maneuver. The bold arrows represent the expected cyclic transitions during normal tracking.

Suppose for simplicity that the vehicle is in the HIGH part of the scalar field, moving towards a given waypoint. During the trajectory, the vehicle will evaluate the gradient of the scalar field and compare it with a given threshold, **Thr**. When this threshold is exceeded, it will assume it has started descending the gradient towards the lower part of the scalar field, entering the HIGH2LOW state. The vehicle will proceed towards the same waypoint until it detects a reduction in the gradient to a level below **Thr_bot**. In order to confirm the *lower limit* of the gradient and avoid (early) false detections, an additional test is performed, verifying that the vehicle has moved a minimum distance away from the frontal point, FP_n, *i.e.* if $||x - FP_n|| > s_{span.low}$, where x is the current position, FP_n is the position of the frontal point detected, and $s_{span.low}$ is a parameter set by the user to allow further excursion into the LOW part of the scalar field (for example to capture complementary data). When both these conditions are met, the vehicle enters the BOTTOM state.

Note from the state machine of fig. 6.3 that the LOW state is also reached if $||x - WP_N|| < d_{min}$, which is a safety mechanism to ensure that the trajectory is limited to reaching the waypoint, even if the algorithm is not able to positively detect the *upper limit* or the *lower limit* of the gradient. If this happens, then the next waypoint is calculated following the algorithm described in section 6.3.1, using the previously computed center of local curvature. When the vehicle enters the LOW state, the characteristics of the gradient are extracted from the previous profile (in particular, the maximum gradient and the limits of the regions) and this information is used to adapt the thresholds for the gradient detection during the next trajectory. The new waypoint is then generated with the algorithm described before, and passed on to the on-board navigation system. As long as this process is active, the above cycle will be maintained, resulting in a *zig-zag* pattern around the boundary.

In order to evaluate the performance of the algorithm, a simple mechanism is to maintain 3 different counters that are incremented depending on the state transitions that lead to the reversal of the profiles (HIGH and LOW states). The first counter, **full_track**, is increased when the vehicle detects both the beginning and the end of the gradient, *i.e.* reaches the HIGH or LOW states through a dark arrow; the second, **begin_only**, is increased when the vehicle enters a transition state (HIGH2LOW or LOW2HIGH) but does not detect the end of the gradient, *i.e.* it changes trajectory because it reaches the waypoint. Finally, a third counter, **fail**, is increased if there is a direct transition from the HIGH state to LOW, or vice-versa. Naturally, the information provided by these counters can be used individually or in combination (for example, abort the mission if **fail** > 3 or if **fail/full_track** > 0.1).

Figure 6.19 shows 12 profiles acquired with the Zarco ASV across the navigation channel of figure 6.16 and the result of the application of the gradient detection algorithm described in section 6.1.1. Table 6.2 presents a summary of the qualitative data regarding these slopes.

6.4 Discussion

In this chapter, we have described the implementation of a new approach to AUV surveys that replaces the standard predefined *mission* by an adaptive sampling strategy. Such an approach exploits the on-board computational power to infer some characteristics of the oceanographic environment and react to this environment by making decisions about the best sampling strategy to use. By continuously interpreting collected data, this decision can be made in real time so that the vehicle can use most of the available resources (mainly power) in sampling the ocean in regions of interest. Naturally, this contributes to an increase in the details that are captured about a given oceanographic process, resulting in more efficient surveys.

The MARES on-board software architecture was adapted to incorporate this capability of real time adaptive sampling, providing a framework to implement innovative guidance algorithms based on the interpretation of incoming sensor data. Such framework has been demonstrated to track a space- and time-varying thermocline, capturing its main characteristics in a very difficult scenario, with significant small-scale variations, very low separation between surface and bottom

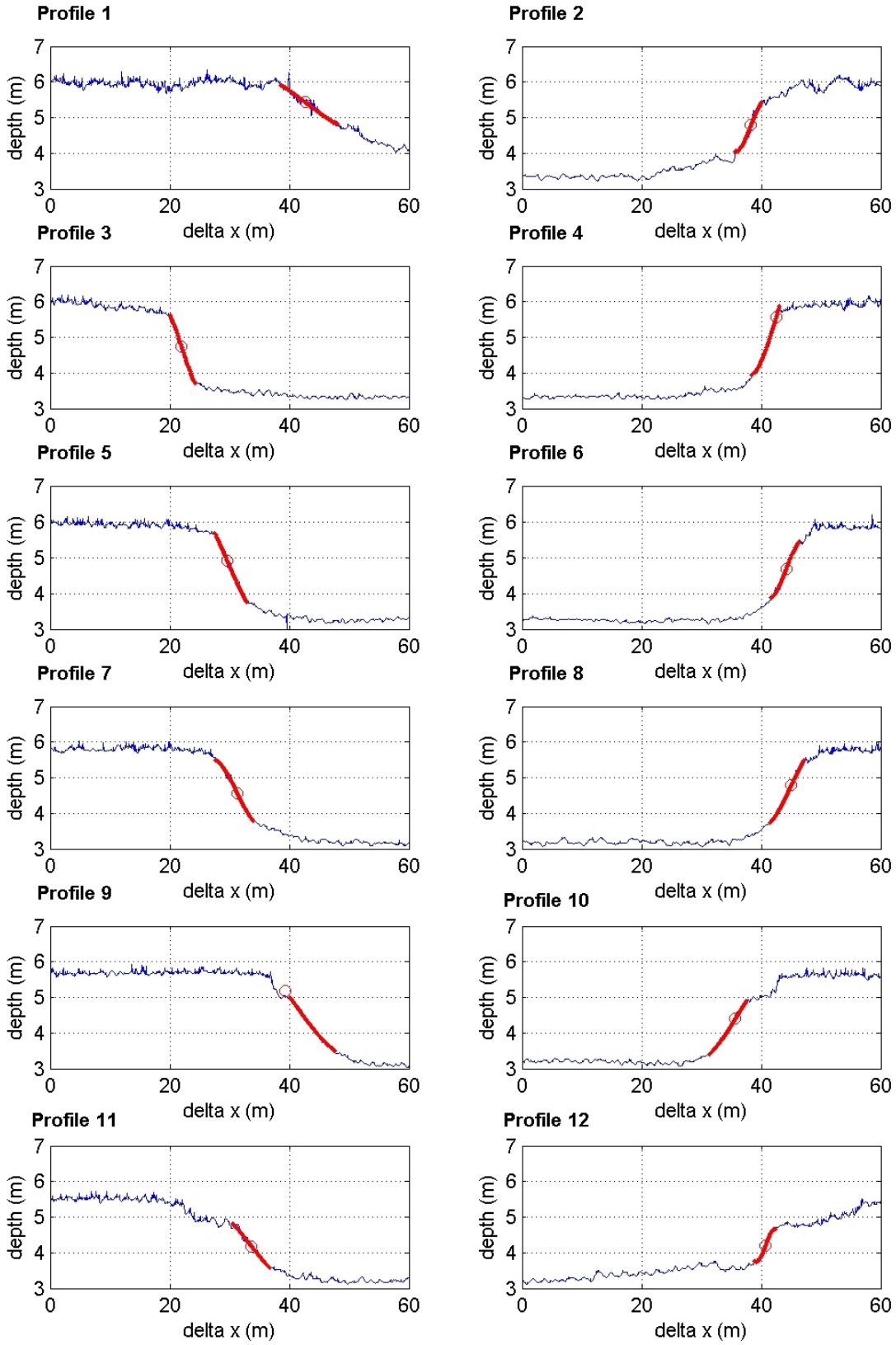

Figure 6.19: Maximum gradient detected in the slopes of the navigation channel.

Profile # Dir.	Max dh/ds (m/m)	Position of Max dh/ds (m)	Depth of Max dh/ds (m)
1 ↓	-0.13	42.6	5.4
2 ↑	0.43	38.3	4.8
3 ↓	-0.51	22.0	4.7
4 ↑	0.55	42.5	5.6
5 ↓	-0.38	29.6	4.9
6 ↑	0.44	44.2	4.7
7 ↓	-0.34	31.3	4.6
8 ↑	0.36	45.0	4.8
9 ↓	-0.24	39.4	5.2
10 ↑	0.27	35.7	4.4
11 ↓	-0.21	33.7	4.2
12 ↑	0.45	40.7	4.2

Table 6.2: Summary of quantitative data of the profiles presented in figure 6.19

temperatures (about 1^oC) and maximum gradients as low as 0.2–0.3^oC/m. In our implementation, we assume that the thermocline can be coarsely approximated by a very simple model with time varying parameters. We've described how a small size AUV can change the sampling pattern in order to maintain tracking of the thermocline, using a very low complexity algorithm that may be implemented in real time with minor impact on CPU load and memory usage. Using this maneuver, the AUV gathers much more information about the thermocline than a standard *yo-yo*. This improvement may be accentuated in scenarios with a thin thermocline layer, particularly in deeper waters, where the ratio between the thickness of the thermocline and the water depth is greatly reduced.

The results demonstrated an excellent tracking performance and even though the acquired data affects the vehicle motion pattern, the algorithm was implemented on the MARES AUV in such a way as to ensure safety of operation – in the cases the algorithm was not able to positively detect the thermocline, then the AUV reverted to a standard *yo-yo* pattern. To our knowledge, it was the first time that an AUV had successfully tracked a thermocline in real time, and the initial algorithms and results have been published in Cruz and Matos (2010a) and Cruz and Matos (2010b). At almost the same time, similar efforts were being carried out using different approaches, particularly the work described in Zhang et al. (2010) and Petillo et al. (2010), and our own performance has been praised and used as a benchmark, as described in many comparison analysis, such as Zhang et al. (2012a); Mora et al. (2013); Woithe and Kremer (2015); Petillo (2015). In the particular case of Woithe and Kremer (2015), the authors employ our algorithms to achieve significant improvements in efficiency when using underwater gliders for thermocline tracking. In another example (Gottlieb et al. (2012)) a similar method to ours has been used to track a front.

The one-dimensional detection of the maximum gradient, used for thermocline tracking, has been extended to the horizontal plane, in order to find and track a horizontal boundary with an autonomous marine vehicle. These algorithms produce geographic waypoints or directions that the vehicle has to follow, therefore they can can be implemented on virtually any ASV or AUV that is able to move at a constant depth. The vehicle can be commanded to cross the transition zone in constant *zig-zag*'s, while advancing along the boundary. On each crossing, the maximum gradient is detected and its position is used to generate a new waypoint, taking into account the local curvature of the boundary. The concept has been demonstrated using data from multiple crossings of a navigation channel with an ASV carrying an altimeter, and successfully detecting the point of the steepest depth gradient in each crossing. These results have been published in Cruz and Matos (2014).

The real time performance of the algorithms can be evaluated by a set of counters that are maintained during the tracking phase, so that appropriate decisions can be made in case of poor performance. The parameters of the transition zone (location and gradient) can be passed on to other processes, for example to switch any special sensor, to guide another vehicle with complementary sensors, or to trigger an underwater sampler to capture a relevant sample of water for lab analysis, like the work described in Zhang et al. (2009) or in Woithe and Kremer (2015).

As for future developments, we plan to improve the real time filtering of the parameters of the thermocline tracking algorithm, so that the tracking mechanism may benefit more from the results of previous profiles, such as thermocline depth limits, detection thresholds, and temperature levels both above and below the thermocline. We also plan to address the detection of multiple thermoclines that sometimes are present in a single vertical profile. Similarly, there is some room for improvement in terms of filtering data regarding the horizontal tracking, for example the positions of the local center of curvature to reduce sensitivity to turbulent boundaries.

Given the interest of the scientific community in studying the relationship between the characteristics of the thermocline and the vertical distribution of phytoplankton, we plan to complement the thermocline tracking maneuver with data from the optical sensors, in order to evaluate the correlation between thermocline characteristics and chlorophyll concentration. If required, the algorithm may be adapted for different sampling requirements, for example, the AUV may extend the bottommost part of the *yo-yo* to evaluate a phytoplankton layer trapped below the thermocline.

There are many examples of scalar fields where the horizontal tracking algorithm can be employed and we intend to validate them in challenging boundaries, both with ASVs and AUVs. This horizontal tracking can be combined with the vertical tracking demonstrated for thermocline sampling, resulting in a 3D adaptive sampling mechanism, that can be used to map the space and time evolution of pollution plumes.

Apart from the direct improvements over the proposed algorithms, the architecture of the implementation allows for an easy testing of other algorithms. A software routine is called upon the reception of every new data point (from any sensor) and just needs to produce new references for the vehicle controllers. It is therefore a very convenient way to evaluate the performance of other adaptive sampling mechanisms.

Finally, the availability of heterogeneous robotic vehicles for marine operations opens up he possibility of cooperative sampling. This can be done with multiple AUVs, or with a suitable combination of ASVs and AUVs, in a pragmatic example of implementation of an AOSN. In order to prepare for this longer term goal, we have already started addressing the possibilities of cooperative motion (Ferreira et al. (2013); Cruz et al. (2013b)), and doing experimentation with communication networks that will be required to support such operations (Cruz et al. (2012, 2013a)).

Chapter 7

Conclusion

Science never solves a problem without creating ten more.

— George Bernard Shaw (1856–1950)

The development of this work followed a systematic approach, starting from the identification of a class of ocean processes for which the available sampling tools are not adequate. It also included an analysis of the state of the art with respect to available technology to collect ocean data. With this analysis, we've identified some challenges for the ocean robotics community and we've tackled some of these challenges to develop innovative sampling tools. These tools include a family of modular robotic vehicles for operation in the marine environment and also some methods to take advantage of their potential capabilities in order to increase the efficiency in the sampling process. This chapter provides an overview of the work conveyed in the preceding chapters, including a highlight of the main contributions, and some topics for future research and development.

7.1 Contributions of this Thesis

This thesis addressed the development of efficient tools to collect ocean data. In particular, it addressed the development of modular robotic systems for the marine environment and their use in the observation of dynamic oceanographic processes. We believe that our contributions include three main aspects. First, our integrated approach to problem solving by carefully taking into account the overall requirements and the limitations of available solutions to identify the main challenges to fulfill such requirements; second, the design and development of a family of modular ASVs and a family of modular AUVs; finally, the design and implementation of algorithms to provide these vehicles with an increased level of *autonomy*.

7.1.1 A Systematic Approach to Ocean Sampling

Although a tremendous effort has been dedicated to the development of marine robotic technology, it seems that most of this effort has been put in designing different versions of similar solutions. In fact, there is such a lack of ocean data that simply collecting measurements with a *standard* AUV in a simple lawnmower pattern is already a huge leap. However, as we could describe earlier, there are many scenarios where the requirements are more demanding and this mainstream solution may not be the most effective or the most efficient. In other situations, the challenges are even greater and cannot be addressed by the available solutions. In all of these, the robotics community may have an important role, following a systematic approach that starts with a thorough analysis of the requirements and a deep understanding of the capabilities and limitations of the available systems.

In the case of our own problem, the most visible side of this approach was the identification, in chapter 3, of the open challenges that need to be addressed to allow a more widespread and efficient utilization or robotic platforms in the ocean. Some of these challenges were tackled in the remaining chapters of this thesis, but all of them will stay open in the coming years. In our approach, we designed and implemented modular robotic systems that can easily be reconfigured for specific missions and we have implemented new algorithms that take advantage of the available computational power to endow these vehicles with higher levels of *autonomy*.

7.1.2 Robotic Systems

We believe that our families of modular AUVs and modular ASVs are important contributions of this thesis. Our AUV building blocks includes both physical parts and also software and control systems. These modules can be rearranged, replaced or individually redesigned to yield a great variety of AUV configurations in a relatively short time. Using a set of modular building blocks, we have built the MARES AUV in 2007, a hovering vehicle that has been used in operational scenarios and that has also supported the demonstration of many research developments. In particular, the MARES AUV easily supports all the adaptive sampling mechanisms that we have developed in this work, and will surely support many more. Taking advantage of the system modularity, we have already designed many new modules, and redesigned others, with a minimum impact on system availability. To our knowledge, MARES was the first man-portable hovering AUV and also the first truly modular vehicle of its class.

The same building blocks were reassembled in 2011, together with newly designed modules, to develop the TriMARES AUV, a 3-body hybrid AUV/ROV with 75kg, that includes high quality video, multiple sonars, and water quality sensors. This vehicle was developed in little over 6 months, and exported to Brazil to be used in a large dam in Tocantins, both for wall inspection (as an ROV connected with a thin fiber optic cable) and also for monitoring the quality of the water reservoir (as an AUV).

Even without any other advertisement, apart from the scientific publications, we have received another order from Brazil in 2012. This time, a vehicle similar to MARES was shipped in 2013, to

support research and development activities in underwater robotics. Although the commercialization of these vehicles was not an objective when we started the program, these successful examples serve to demonstrate the usefulness of our solutions.

As far as ASVs are concerned, they have their own potential as preferred tools for sampling the marine environment in certain scenarios, but they are particularly relevant to support an integrated program of robotic solutions for marine operations. Not only they can be used to complement the sampling patterns of underwater vehicles, they can also be effective tools to demonstrate specific systems and techniques in two dimensions before being transposed to AUVs. Contrary to AUV development, the availability of high-bandwidth, real time communications accelerates the development and testing phases dramatically.

Similarly to the case of AUV design, our effort has been focused on the development of modular building blocks to foster reconfigurability and versatility. In this case, we use a very simple architecture to yield extremely versatile platforms that have already accumulated hundreds of hours of operation in reservoirs and coastal waters. The largest components can be disassembled and reassembled very rapidly, with a minimum set of tools, which means that the vehicles can be transported in separate blocks that are reassembled at the operation site in just a few minutes. During operations, for example, a depleted battery module can be swapped by a charged one in a few minutes from a pontoon, without the vehicle leaving the water. The modularity of the vehicles also extends to the on-board software and control systems. In fact, many of the device drivers are exactly the same as in the AUVs, and the controllers are developed using similar hydrodynamic equations, with the relevant changes in parameters and degrees of freedom.

Two of these vehicles have supported an ongoing program of vehicle cooperation, not only with ASVs, but also in networks of heterogeneous vehicles (ASVs and AUVs) for specific applications. They have been used in a variety of scenarios, both in Portugal and abroad, and they have been paramount to provide field data to validate scientific developments in many areas of marine research. This has been translated into tens of manuscripts, including scientific papers, thesis, and technical reports, corroborating their value as an effective tool for marine sampling.

7.1.3 Adaptive Sampling with Marine Robotic Vehicles

In this work, we have proposed and implemented algorithms for adaptive sampling of dynamic ocean processes using autonomous marine vehicles. Our algorithms can be applied to processes where there is a sharp transition, for example thermoclines, fronts and plumes. The algorithms exploit the on-board computational power to infer some characteristics of the oceanographic process, and generate guidance references so that the vehicle maintains tracking of the feature. This ensures that measurements are made close to the feature, contributing to an increase in the details that are captured about a given oceanographic process, therefore resulting in more efficient surveys.

The software architecture of the MARES AUV supports this capability of real time adaptive sampling, and the vehicle was used to demonstrate tracking of a space- and time-varying thermocline. In our implementation, we assume that the thermocline can be coarsely approximated by a very simple model with time varying parameters. We've described how a small size AUV can change the sampling pattern in order to maintain tracking of the thermocline, using a very low complexity algorithm that may be implemented in real time with minor impact on CPU load and memory usage. This means that the same algorithm may be used in virtually any other AUV that accepts depth references in real time. During a field trial in a river, the MARES AUV tracked the thermocline even with very small-scale variations, very low separation between surface and bottom temperatures (about 1^{o}C) and maximum gradients as low as 0.2–0.3^{o}C/m. The results demonstrated an excellent tracking performance and that the safety mechanisms were also effective. When the algorithm was not able to positively detect the thermocline, the AUV reverted to a standard *yo-yo* pattern. To our knowledge, it was the first time that an AUV had successfully tracked a thermocline in real time, and the published algorithms and results have been praised in citing works.

We have also extended the one-dimensional detection of the maximum gradient to the horizontal plane, describing the algorithms required to find and track a horizontal boundary with an autonomous marine vehicle. These algorithms interpret the samples from the scalar field in real time, and produce geographic waypoints or directions that the vehicle has to follow, therefore they can can be implemented on virtually any ASV or any AUV that is able to move at a constant depth. The vehicle can be commanded to cross the transition zone in constant *zig-zag*'s, while advancing along the boundary. On each crossing, the maximum gradient is detected and its position is used to generate a new waypoint, taking into account the local curvature of the boundary. We have provided evidence of the efficacy of these algorithms, using data from multiple crossings of a navigation channel with an ASV carrying an altimeter, and successfully detecting the point of the steepest depth gradient in each crossing. These results have been published in Cruz and Matos (2014).

During the tracking phase, a set of counters is maintained to assess the performance of the algorithms and make appropriate decisions in case of poor performance. The parameters of the transition zone (location and gradient) can be passed on to other processes, for example to switch any special sensor, to guide another vehicle with complementary sensors, or to trigger an underwater sampler to capture a relevant sample of water for lab analysis, like the work described in Zhang et al. (2009) or in Woithe and Kremer (2015).

7.1.4 Publications

A substantial part of the work developed for this thesis has already been published, and a significant fraction of it has been presented and discussed in top conferences, namely the MTS/IEEE Oceans Conference. Next, we summarize the contributions of the the most relevant papers that resulted from this work, aggregated by similar topics.

- Cruz et al. (2007) described the development of the Zarco ASV, including the main features and the results of the first trials. Later, the control of the vehicle position was refined in Matos and Cruz (2008). Cruz et al. (2015) describes the integration of a wing sail to provide wind propulsion.

- Cruz and Matos (2008) introduced the MARES AUV, together with the mission support system and the preliminary results of an environmental monitoring mission of the Portuguese coast, sampling the plume from a sewage outfall. The MARES navigation and control system was further detailed in Matos and Cruz (2009); Ferreira et al. (2010, 2012a). Cruz et al. (2011) introduced the TriMARES hybrid AUV/ROV, based on the same building blocks as the MARES AUV, and the control of the vehicle was analysed in Ferreira et al. (2012b). Finally, Cruz et al. (2013c) described the development of the modular building blocks used for AUV construction.

- Almeida et al. (2010) described the upgrade of our navigation buoys to support synchronized emissions for one way travel time navigation of underwater vehicles. This work was a follow up of a long series of previous developments in acoustic navigation systems, described in Matos et al. (1999); Cruz et al. (2001); Matos and Cruz (2004, 2005, 2007). In Aparicio et al. (2015), the same acoustic boards have been used to support experiments in the identification of the characteristics of the acoustic channel.

- Cruz and Matos (2010a) and Cruz and Matos (2010b) presented the main thermocline tracking algorithm, first with simulated data from previous missions and then with data from an adaptive sampling mission. They have been cited by other authors and used as a benchmark, as described in many comparison analysis, such as Zhang et al. (2012a); Mora et al. (2013); Woithe and Kremer (2015); Petillo (2015). In the particular case of Woithe and Kremer (2015), the authors employ our algorithms to achieve significant improvements in efficiency when using underwater gliders for thermocline tracking. In another example (Gottlieb et al. (2012)) a similar method to ours has been used to track an oceanographic front.

- Cruz et al. (2013a), Cruz et al. (2013b) and Ferreira et al. (2013) reported the experimental work conducted with the coordinated operation of our heterogeneous vehicles (ASVs and AUVs). These experiments proved that our vehicles are privileged assets to demonstrate innovative concepts and, at the same time, can be successfully used in practical networked operations.

- Cruz and Matos (2014) presented the algorithm used to track a two-dimensional boundary in the horizontal plane. The boundary was represented by the steepest gradient of a bathymetry map, as measured with an echosounder installed in the Zarco ASV.

7.2 Future Work

There are many stimulating research directions related to the work described in this thesis. Chapter 3 described some of the challenges for efficient ocean sampling and some of them were tackled throughout this work. Naturally, some were also addressed by other researchers in parallel efforts around the world, but certainly many remain unexplored. At the same time, some new avenues were open as we and others proceeded our investigations. In this section, we will provide some pointers to both.

7.2.1 Robotic Systems

Robotic marine platforms have had an extraordinary evolution in the past years, but there are still many subsystems that may be improved. Part of our work may contribute to this development and we think that our modular design can be a privileged means to support it. One of the most obvious directions is the development of new modules for new scenarios of application, for example to have both fins and vertical/lateral thrusters in AUVs, or to install buoyancy engines to complement the modes of operation. An important improvement can also be the redesign of the dry compartment of the AUVs to withstand very high pressures, so that a small AUV similar to MARES may be used in deep water surveys. This has never been done before and is just a small step ahead.

Extending the duration of AUV missions is another natural evolution and there are a few ways to achieve it, either by replacing the batteries as new technologies mature, but mainly by devising docking stations where vehicles can refill their batteries and proceed their operations without recovery. Our modular design facilitates the development of a specific module for docking, while the hovering capability of a vehicle like MARES will allow a slow approximation to the docking station and minimize the risk of damage due to collision.

With the advancement of underwater communications, the concept of a Wireless ROV may also be explored. For this purpose, a vehicle like TriMARES is an ideal platform, since it already acts like an ROV with the thin fiber optic umbilical, and has its own batteries that can support wireless operations.

There are many opportunities to be explored with the operation of networked devices. Again, our vehicles can easily support this effort, and we will proceed the preliminary testing we had done in this direction. We anticipate many different roles for the AUVs and ASVs, from survey platforms to data mules, network access points, gateways or proxies. With our modular blocks, many different configurations are easily assembled and deployed. Moreover, communicating vehicles will be paramount to the implementation of adaptive sampling strategies based on multiple platforms, that we surely want to explore.

Navigation systems have long been a challenge in underwater robotics, and we have been developing our own solutions based on acoustics. For most application scenarios, current accuracies are sufficient, but soon the requirements will become more demanding. Some preliminary work in collaboration with partner institutions for the identification of the acoustic channel has had some promising results. Our acoustic modules can be upgraded to increase accuracy and to provide

complementary functions, such as simultaneous communications and navigation. Naturally, our vehicles can easily continue to support the field trials of such systems.

Another topic that will surely advance in the coming years is vehicle perception of the environment. This includes, for example, short range visual perception of distances and relative position of targets, using stereo cameras with integrated processing. Such an improvement, together with increased navigation accuracy, will enable the implementation of small intervention capabilities in our vehicles. Naturally, such operations will generate some new challenges in control that will need to be thoroughly investigated.

Autonomous Surface Vehicles will certainly maintain their role as testbeds for marine sensors, subsystems, and algorithms, either for their own operation, or for validation before implementation in AUVs. Given the availability of real time communications, they can easily be used to demonstrate the implementation of COLREGS in autonomous vehicles, a step that will certainly be required for the joint operations of manned and unmanned systems in the same area. They will also be fundamental assets for the investigation of energy harvesting solutions, fostering a long-sought permanent presence in the ocean. Concepts like the integration of wind propulsion have already been tested and will lead the way into more environmental friendly operations at sea. Once again, the modularity of our systems may surely be explored to implement various equipment and strategies for power management.

7.2.2 Adaptive Sampling with Marine Robotic Vehicles

The implementation of adaptive sampling strategies in the marine environment is still at its infancy, so the possibilities for the future are immense. Regarding our own algorithms, an obvious evolution is to integrate the advantages of the methods proposed by other authors, in order to increase the efficiency and robustness, at least for some specific scenarios. In the case of thermocline tracking, we plan to address the detection of multiple thermoclines that sometimes are present in a single vertical profile. Similarly, there is some room for improvement in terms of filtering data regarding the horizontal tracking, for example the positions of the local center of curvature to reduce sensitivity to turbulent boundaries or other short scale variations.

Apart from the direct improvements over the proposed algorithms, the architecture of the implementation allows for an easy testing of other algorithms, therefore we can use our vehicles to compare different proposals from different researchers. A software routine is called upon the reception of every new data point (from any sensor) and just needs to produce new references for the vehicle controllers. It is therefore a very convenient way to evaluate the performance of other adaptive sampling mechanisms in the field, fully supported by our robotic platforms.

There is a great interest of the scientific community in studying the relationship between the characteristics of the thermocline and the vertical distribution of phytoplankton. We plan to complement the thermocline tracking maneuver with data from the optical sensors, in order to evaluate the correlation between thermocline characteristics and chlorophyll concentration. Such a

correlation may open up the possibility of using chlorophyll data to guide the vehicle, instead of temperature.

Regarding the horizontal tracking algorithms, there are many examples of scalar fields where they can be employed and we intend to validate them in challenging boundaries, both with ASVs and AUVs. At a later stage, we intend to combine this horizontal tracking with the vertical tracking demonstrated for thermocline sampling, resulting in a 3D adaptive sampling mechanism, that can be used to map the space and time evolution of pollution plumes with an AUV.

As far as new algorithms are concerned, there are other fields of knowledge where we can get both inspiration and new methods to interpret data in real time. These include, for example, geometric methods from computer vision, bio mimetic motion from biology, and information extraction from machine learning and information theory.

Finally, the availability of heterogeneous robotic vehicles for marine operations opens up he possibility of cooperative sampling. This can be done with multiple AUVs, or with a suitable combination of ASVs and AUVs, in a pragmatic example of implementation of an AOSN. In order to prepare for this longer term goal, we have already started addressing the possibilities of cooperative motion, and doing experimentation with communication networks that will be required to support such operations.

Appendix A

Enabling Technology

The best way to predict your future is to create it.
— Abraham Lincoln (1809–1865)

Throughout the development of the main tasks of the thesis, several other pieces of technology were developed in parallel. They were left aside from the main document, not only because they are not the core of the work, but also because they do not convey very relevant research results and, in some cases, the developments are still at an early stage. However, some of them were required for the experimental validation of the proposed work and most may provide significant building blocks for future AOSN implementations. In this chapter, we provide some information about these devices and methods.

A.1 Underwater Acoustics for Navigation

The development of acoustic navigation systems has been a topic of our own research for many years. At the heart of these systems are separate boards for transmission and reception of underwater acoustic signals, as well as a controller board. With these modules, it is possible to assemble different acoustic stacks either to integrate in beacons or in vehicles.

A.1.1 Acoustic Modules

The acoustic modules are independent, so that they can be arranged differently, depending on whether they are used for beacons, for vehicle systems, or for listening devices. All our current systems use frequency ranges in the order of 20–30kHz.

Acoustic Transmission

On the transmitter board, the waveforms are synthetically generated on a microcontroller and then amplified to provide up to 198dB re 1V/μPa of transmitted power into an acoustic transducer. The waveforms may be selected by switches or by an external input.

Acoustic Reception

The reception of acoustic pings is done through a receiver board, where a set of analog filters are tuned to 8 different frequencies allowing for the parallel detection and time-stamping of 8 incoming signals. The detection of each channel is activated whenever the respective filter exceeds a given threshold. All these thresholds can be changed by software, depending on the environmental acoustic noise and the expected range. Alternatively, an FPGA based system has also been tested successfully to perform a matched filter.

Interfacing and Control

A controller board serves as the interface between the acoustic stack and the system where it is integrated. It interfaces with all the filters to adjust the detection thresholds and it keeps a counter to timestamp all events (transmissions and receptions).

A.1.2 Navigation Beacons

Navigation and Instrumentation Buoys (NIBs) are moored floating platforms with on-board electronics and energy management system (figure A.1). The basic configuration includes rechargeable batteries, a compact GPS receiver and a low-power radio modem. NIBs can carry a great variety of sensors and transmit data in real time using the radio link. During an AUV mission, they can also work as portable observatories, getting relevant information about the environment (such as current profiles, ambient noise, or reference sensor data, for example), to allow for post-mission data processing and interpretation. Figure A.2 provides an overview of the main components of a NIB.

NIBs are specially dedicated to work as acoustic navigation beacons for AUVs. They have one acoustic stack with one transmitter, one receiver and one controller board. Each beacon has a response map, that maintains the correspondence between an incoming signal and the expected reply. As soon as the receiver board detects an incoming signal at a specific frequency, the controller board sends a command to the transmitter board to reply with the corresponding signal stored in the response map. The map can be changed by radio, but has to be matched with the information stored on board the AUV. All detections and replies are stored on-board and also sent by radio to a control station to monitor the behavior of the acoustic network.

The GPS location of the NIBs is also monitored and logged throughout the mission, to allow for post-mission corrections of sensor data location, since there may be significant changes of buoy position due to wind and/or currents.

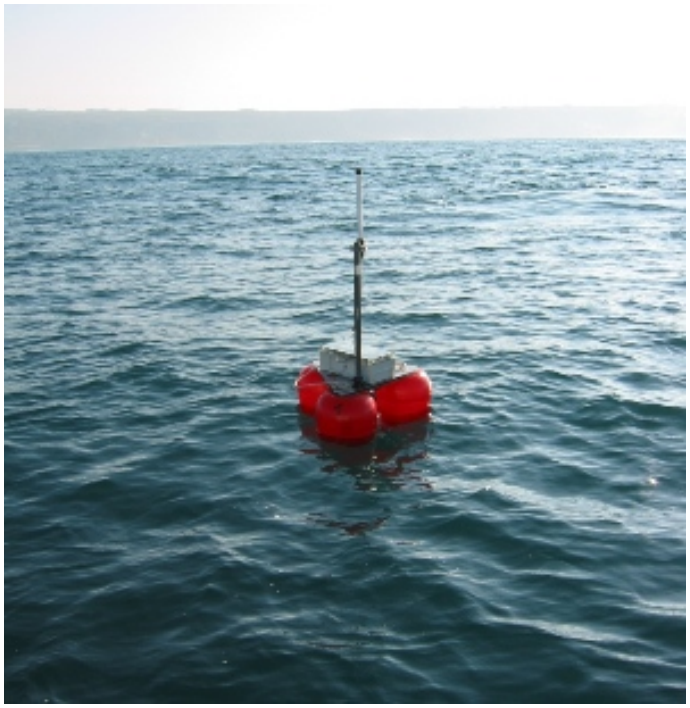

Figure A.1: An example of a Navigation and Instrumentation Buoy (NIB) used to provide acoustic ranges to AUVs.

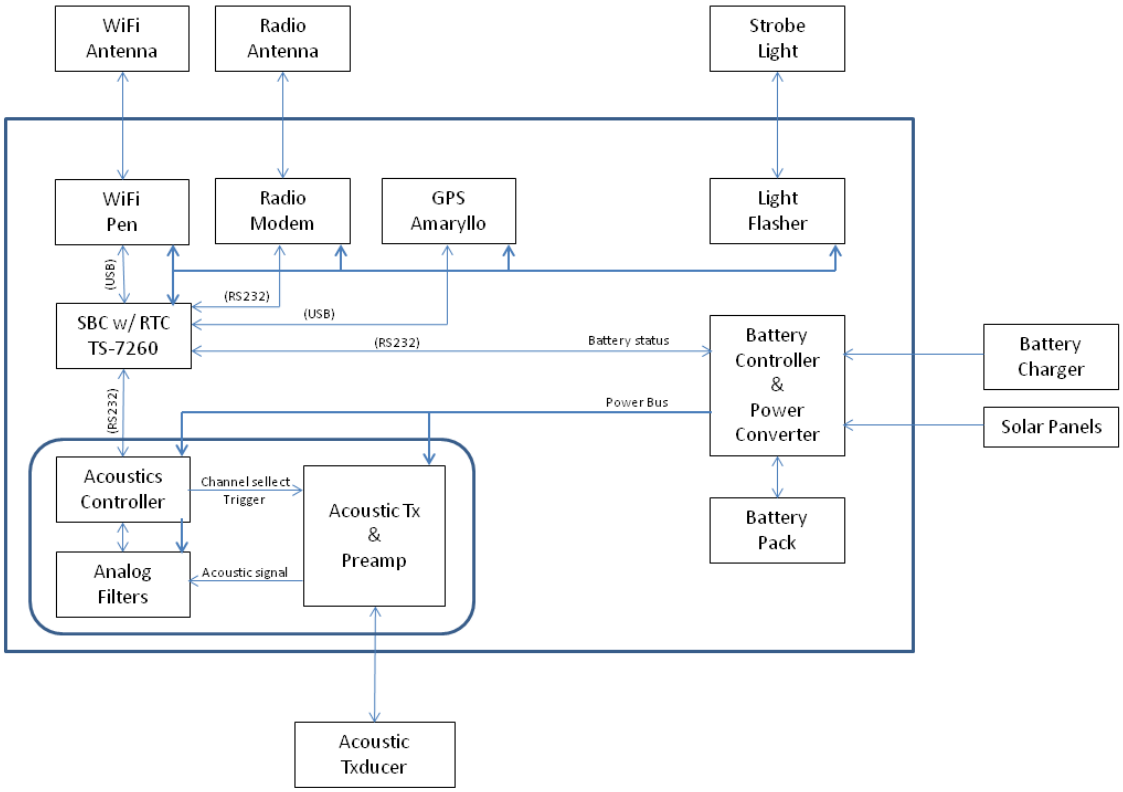

Figure A.2: Block diagram of the components of a NIB.

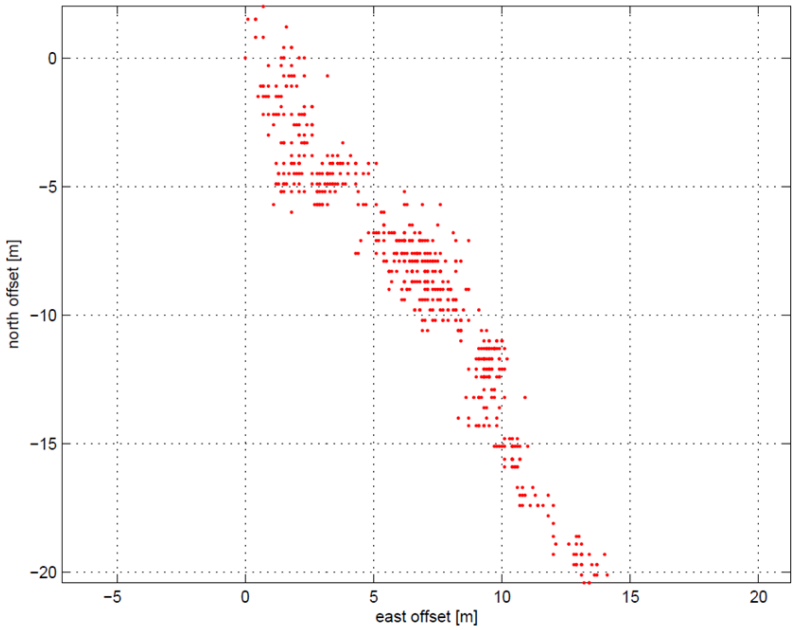

Figure A.3: NIB GPS log showing the motion relative to the initial position.

Fig. A.3 shows the position variation of one of NIBs during a 3 hr operation at sea, with about 30 meters of offset.

A.1.3 Vehicle System

Each vehicle that needs to navigate using acoustics needs to integrate an acoustic stack, with the same modules as the beacon (transmitter, receiver, and control) but wired differently. In the case of the vehicles navigating in LBL, they initiate the trilateration scheme by choosing a beacon to ping to. The transmitter board sends the ping and the receiver board will detect the reply from the corresponding beacon. The controller board detects both events in the same clock, therefore it can compute distance. The process will continue to the other(s) beacon(s). In the case of the vehicles the receiver board also serves to detect *reserved* channels, for example indicating to abort the mission. Each vehicle also has a response map, that maintains the correspondence between an incoming signal and the expected reply. Although the vehicles are seldom needed to reply to a signal, such feature may be used to range the vehicle in case of any malfunctioning. Figure 4.23 shows the acoustic stack installed in TriMARES.

A.2 Innovative Navigation Algorithms

Having the ability to make changes to the basic building blocks of acoustic transmission and reception, allows us to implement and test multiple navigation algorithms, either of our own design, or adapted from literature proposals.

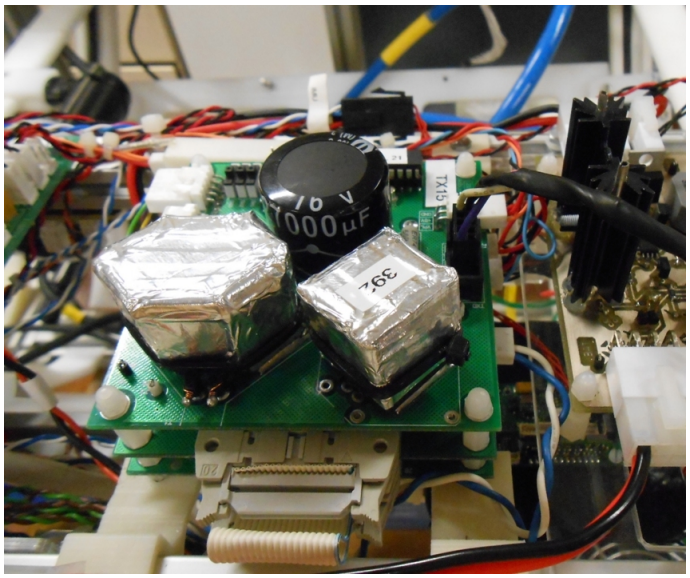

Figure A.4: Acoustic stack installed in the TriMARES hybrid AUV/ROV.

A.2.1 Integrated Navigation and Tracking

The ability to track, in real-time, an autonomous underwater vehicle is a major safety issue, particularly in the case of adaptive sampling, in which the vehicle trajectory is not defined *a-priori*. Although it is possible to encompass safety measures in the on-board software (like obstacle avoidance and virtual walls, for example), it is much safer to be able to tell the vehicles' position in real-time and to interfere with the actual mission in case the vehicle trajectory does not seem to be correct.

We have designed and implemented an LBL navigation system that ensures that, while the vehicle is navigating, a receiving device can track the vehicle position just by listening to the acoustic signals exchanged underwater, without any further signals being transmitted. This algorithm was first described in Cruz et al. (2001).

A.2.2 Navigation using One Way Travel Time

A standard LBL navigation scheme requires the vehicle to ping and wait for a reply, in order to compute the distance to a beacon. For trilateration, other ranges are required to other beacons. When the distance between the vehicle and the beacons increase more than a few hundred meters, such turnaround time may take a few seconds. Furthermore, given the limitations of the bandwidth of the acoustic transducers and the underwater channel, it is not feasible to use such a scheme for multiple vehicles. Instead, we've proposed an alternative approach, where both the vehicle's and the beacon clocks are synchronized, and the beacons transmit pings at predefined instants/intervals. This scheme opens up the possibility of navigation of a large number of vehicles in the same acoustic network. Moreover, since the vehicles will be mostly listening, their power consumption will be reduced. This work was published in Almeida et al. (2010).

A.2.3 Navigation in a Moving Network of Transponders

The maximum practical range of our beacons is around 2–3km, which limits the operation area where a vehicle can safely navigate. However, in many situations, a longer mission may be required and it may not be possible or convenient to change the moorings of the beacons. Moreover, for operations in deep water, mooring the beacons can be a very difficult task. We have developed the concept of a moving network, where the beacons can be installed on moving platforms, like ASVs, so that they act as virtual moorings. This work has been published in Matos and Cruz (2005).

A.3 Acoustic Networking

In order to support the operation of multiple cooperating platforms, they may need to exchange information. We have addressed many problems of communication between heterogeneous platforms, with a particular interest in networking, such as described in Cruz et al. (2012, 2013a,b).

References

Nuno Abreu, Aníbal Matos, Patrícia Ramos, and Nuno Cruz. Automatic interface for AUV mission planning and supervision. In *Proc. MTS/IEEE Int. Conf. Oceans'10*, Seattle, WA, USA, Sept. 2010.

Jaime Abril, Jaime Salom, and Oscar Calvo. Fuzzy control of a sailboat. *International Journal of Approximate Reasoning*, 16(3–4):359–375, 1997.

Rui Almeida, Nuno Cruz, and Aníbal Matos. Synchronized intelligent buoy network for underwater positioning. In *Proc. IEEE Int. Conf. Oceans'10*, Sydney, Australia, May 2010.

Thomas W. Altshuler, Thomas W. Vaneck, and James G. Bellingham. Odyssey IIb – towards commercialization of AUVs. *Sea Tech.*, pages 15–19, Dec. 1995.

Bob Anderson and Jon Crowell. Workhorse auv – a cost-sensible new autonomous underwater vehicle for surveys/ soundings, search & rescue, and research. In *Proc. MTS/IEEE Int. Conf. Oceans'05*, Washington, D.C., USA, Sep. 2005.

J. H. Anton, E. T. Tse, and C. H. Wells. Parameter identification criteria for salt brine dispersion from desalination plant ocean outfalls. In *Proc. IEEE Int. Conf. Oceans'71*, San Diego, CA, USA, Sep. 1971.

Joaquín Aparicio, Ana Jiménez, Fernando J. Álvarez, Jesús Ureña, Carlos De Marziani, Daniel de Diego, Nuno Cruz, and Helder Campos. Accurate detection of spread-spectrum modulated signals in reverberant underwater environments. *Applied Acoustics*, 88:57–65, 2015.

The Ashburton Guardian. A boat with fins, Aug. 30th 1897.

Marcel Babin, Collin S. Roesler, and John J. Cullen, editors. *Real-time Coastal Observing Systems for Marine Ecosystem Dynamics and Harmful Algal Blooms: theory, instrumentation and modelling*. Monographs on oceanographic methodology. UNESCO, 2008.

Vladan Babovic and Hong Zhang. Modeling of vertical thermal structure using genetic programming. In *Proc. 7th OMISAR Workshop on Ocean Models*, Singapore, Sep. 2002.

Ralf Bachmayer and Naomi Ehrich Leonard. Vehicle networks for gradient descent in a sampled environment. In *Proc. IEEE Conf. Decision and Control CDC'02*, Las Vegas, NV, USA, Dec. 2002.

Robert D. Ballard. Notes on a major oceanographic find. *Oceanus*, 20(3):35–44, Summer 1977.

Christian Barat and Maria João Rendas. Benthic boundary tracking using a profiler sonar: A mixture model approach. In *Proc. MTS/IEEE Int. Conf. Oceans'03*, pages 1409–1416, San Diego, CA, USA, Sep. 2003.

William Beebe. *Half Mile Down*. Harcourt, Brace and Co., New York, 1934.

J. H. Belanger and M. A. Willis. Biologically-inspired search algorithms for locating unseen odor sources. In *Proc. IEEE Int. Symp. Intelligent Control ISIC'98*, pages 265–270, Gaithersburg, MD, USA, 1998.

J. G. Bellingham, C. A. Goudey, T. R. Consi, J. W. Bales, D. K. Atwood, J. J. Leonard, and C. Chryssostomidis. A second generation survey AUV. In *Proc. IEEE Symp. Autonomous Underwater Vehicle Tech. AUV'94*, pages 148–155, Cambridge, MA, USA, Jul. 1994.

James G. Bellingham. New oceanographic uses of autonomous underwater vehicles. *Mar. Tech. Soc. J.*, 31(3):34–47, Fall 1997.

James G. Bellingham, Thomas R. Consi, Robert M. Beaton, and William Hall. Keeping layered control simple. In *Proc. IEEE Symp. Autonomous Underwater Vehicle Tech. AUV'90*, pages 3–8, Washington, DC, USA, Jun. 1990.

James G. Bellingham, Thomas R. Consi, Usha Tedrow, and Diane Di Massa. Hyperbolic acoustic navigation for underwater vehicles: Implementation and demonstration. In *Proc. IEEE Symp. Autonomous Underwater Vehicle Tech. AUV'92*, Washington DC, USA, Jun. 1992.

James G. Bellingham, Bradley A. Moran, Yanwu Zhang, J. Scott Willcox, Nuno Cruz, Robert Grieve, John J. Leonard, and James W. Bales. Haro strait experiment 1996: MIT Sea Grant component. Technical report, Massachusetts Institute of Technology, Sea Grant College Program, Cambridge, MA, USA, 1996. Internal Report.

Andrew A. Bennett and John J. Leonard. A behavior-based approach to adaptive feature detection and following with autonomous underwater vehicles. *IEEE J. Oceanic. Eng.*, 25(2):213–226, Apr. 2000.

Deepak Bhadauria, Volkan Isler, Andrew Studenski, and Pratap Tokekar. A robotic sensor network for monitoring carp in Minnesota lakes. In *Proc. IEEE Int. Conf. Robotics and Automation (ICRA)*, pages 3837–3842, Anchorage, AK, USA, May 2010.

Brian Steven Bingham. Navigating autonomous underwater vehicles. In Alexander V. Inzartsev, editor, *Underwater Vehicles*, chapter 3, pages 33–50. InTech, Vienna, Austria, Dec. 2009.

Anders Bjerrum. Future requirements for coastal environmental surveying. In *Proc. 1st Workshop on AUVs*, Porto, Portugal, Sept. 1993.

Giulio Boccaletti, Ronald C. Pacanowski, S. George Philander, and Alexey V. Fedorov. The thermal structure of the upper ocean. *J. Phys. Oceanogr.*, 34(4):888–902, Apr. 2004.

Albert M. Bradley, Michael D. Feezor, Hanumant Singh, and F. Yates Sorrell. Power systems for autonomous underwater vehicles. *IEEE J. Oceanic. Eng.*, 26(4):526–538, Oct. 2001.

Mark Brown, Mike Kelley, and Paul McGill. MBARI vertical profiler. In *Proc. MTS/IEEE Int. Conf. Oceans'01*, pages 2482–2485, Honolulu, HI, USA, Nov. 2001.

Erik Burian, Dana Yoerger, Albert Bradley, and Hanumant Singh. Gradient search with autonomous underwater vehicles using scalar measurements. In *Proc. IEEE Symp. Autonomous Underwater Vehicle Tech. AUV'96*, pages 86–98, Monterey, CA, USA, Jun. 1996.

Massimo Caccia. Autonomous surface craft: prototypes and basic research issues. In *Proc. 14th Mediterrenean Conf. on Control and Automation, MED'06*, Ancona, Italy, June 2006.

Massimo Caccia, Marco Bibuli, Gabriele Bruzzone, Vladimir Djapic, Stefano Fioravanti, and Alberto Grati. Modular usv and payload design for advanced capabilities in marine security applications. In *Proc. 19th Mediterranean Conf. on Control and Automation*, Corfu, Greece, June 2011.

A. Caffaz, A. Caiti, G. Casalino, and A. Turetta. The hybrid glider/AUV Folaga. *Robotics Automation Magazine, IEEE*, 17(1):31–44, Mar. 2010.

Richard Camilli, Christopher M. Reddy, Dana R. Yoerger, Benjamin A. S. van Mooy, Michael V. Jakuba, James C. Kinsey, Cameron P. McIntyre, Sean P. Sylva, and James V. Maloney. Tracking hydrocarbon plume transport and biodegradation at Deepwater Horizon. *Science*, 330:201–204, Oct. 2010.

Christopher J. Cannell, Aditya S. Gadre, and Daniel J. Stilwell. Boundary tracking and rapid mapping of a thermal plume using an autonomous vehicle. In *Proc. MTS/IEEE Int. Conf. Oceans'06*, pages 1–6, Boston, MA, USA, Sept. 2006.

François Cazenave, Yanwu Zhang, Erika McPhee-Shaw, James G. Bellingham, and Timothy P. Stanton. High-resolution surveys of internal tidal waves in Monterey Bay, California, using an autonomous underwater vehicle. *Limnol. Oceanogr. Methods*, 9:571–581, Dec. 2011.

R. L. Chase, J. R. Delaney, H. P. Johnson, S. K. Juniper, J. L. Karsten, J. E. Lupton, S. D. Scott, and V. Tunnicliffe. Hydrothermal vents and sulfide deposites, axial seamount, Juan de Fuca ridge. In *Proc. MTS/IEEE Int. Conf. Oceans'83*, pages 801–801, San Francisco, CA, USA, Aug. 1983.

Peter C. Chu, Charles R. Fralick Jr., Steven D. Haeger, and Michael J. Carron. A parametric model for the Yellow Sea thermal variability. *J. Geophys. Res.*, 102(C5):10499–10507, May 1997.

Peter C. Chu, Qianqian Wang, and Robert H. Bourke. A geometric model for the Beaufort/Chukchi Sea thermohaline structure. *J. Atmos. Oceanic Technol.*, 16(6):613–632, Jun. 1999.

Peter C. Chu, Chenwu Fan, and W. Timothy Liu. Determination of vertical thermal structure from sea surface temperature. *J. Atmos. Oceanic Technol.*, 17(7):971–979, Jul. 2000.

T. R. Consi, J Atema, C. A. Goudey, J. Cho, and C. Chryssostomidis. AUV guidance with chemical signals. In *Proc. IEEE Symp. Autonomous Underwater Vehicle Tech. AUV'94*, pages 450–453, Cambridge, MA, USA, Jul. 1994.

Jon Crowell. Small AUV for hydrographic applications. In *Proc. MTS/IEEE Int. Conf. Oceans'06*, Boston, MA, USA, Sept. 2006.

Jon Crowell. Design challenges of a next generation small auv. In *Oceans - San Diego, 2013*, pages 1–5, San Diego, CA, USA, Sept. 2013.

Nuno Cruz, Aníbal Matos, Alfredo Martins, Jorge Silva, Domingos Santos, Dmitri Boutov, Diogo Ferreira, and Fernando Lobo Pereira. Estuarine environment studies with Isurus, a REMUS class AUV. In *Proc. MTS/IEEE Int. Conf. Oceans'99*, Seattle, WA, USA, Sep. 1999.

Nuno Cruz, Luís Madureira, Aníbal Matos, and Fernando Lobo Pereira. A versatile acoustic beacon for navigation and remote tracking of multiple underwater vehicles. In *Proc. MTS/IEEE Int. Conf. Oceans'01*, pages 1829–1834, Honolulu, HI, USA, Nov. 2001.

Nuno Cruz, Aníbal Matos, Sérgio Cunha, and Sérgio Silva. Zarco – an autonomous craft for underwater surveys. In *Proc. 7th Geomatic Week*, Barcelona, Spain, Feb. 2007.

Nuno A. Cruz and José C. Alves. Autonomous sailboats: an emerging technology for ocean sampling and surveillance. In *Proc. MTS/IEEE Int. Conf. Oceans'08*, Quebec, Canada, Sept. 2008.

Nuno A. Cruz and Aníbal C. Matos. The MARES AUV, a modular autonomous robot for environment sampling. In *Proc. MTS/IEEE Int. Conf. Oceans'08*, Quebec, Canada, Sept. 2008.

Nuno A. Cruz and Aníbal C. Matos. Reactive AUV motion for thermocline tracking. In *Proc. IEEE Int. Conf. Oceans'10*, Sydney, Australia, May 2010a.

Nuno A. Cruz and Aníbal C. Matos. Adaptive sampling of thermoclines with autonomous underwater vehicles. In *Proc. MTS/IEEE Int. Conf. Oceans'10*, Seattle, WA, USA, Sept. 2010b.

Nuno A. Cruz and Aníbal C. Matos. Autonomous tracking of a horizontal boundary. In *Proc. MTS/IEEE Int. Conf. Oceans'14*, St. John's, NFL, Canada, Sep. 2014.

Nuno A. Cruz, Aníbal C. Matos, Rui M. Almeida, Bruno M. Ferreira, and Nuno Abreu. TriMARES - a hybrid AUV/ROV for dam inspection. In *Proc. MTS/IEEE Int. Conf. Oceans'11*, Kona, HI, USA, Sep. 2011.

Nuno A. Cruz, Bruno M. Ferreira, Aníbal C. Matos, Chiara Petrioli, Roberto Petroccia, and Daniele Spaccini. Implementation of an acoustic network using multiple heterogeneous vehicles. In *Proc. MTS/IEEE Int. Conf. Oceans'12*, Hampton Roads, VA, USA, Oct. 2012.

Nuno A. Cruz, Bruno M. Ferreira, Oleksiy Kebkal, Aníbal C. Matos, Chiara Petrioli, Roberto Petroccia, and Daniele Spaccini. Investigation of underwater acoustic networking enabling the cooperative operation of multiple heterogeneous vehicles. *Mar. Tech. Soc. J.*, 47(2):43–58, Mar./Apr. 2013a.

Nuno A. Cruz, Bruno M. Ferreira, and Aníbal C. Matos. Ocean observation with coordinated robotic platforms. *Sea Tech.*, 54(5):37–40, May 2013b.

Nuno A. Cruz, Aníbal C. Matos, and Bruno M. Ferreira. Modular building blocks for the development of AUVs – from MARES to TriMARES. In *Proc. Int. Symp. Underwater Tech. UT'13*, Tokyo, Japan, Mar. 2013c.

Nuno A. Cruz, José C. Alves, Tiago Guedes, Rômulo Rodrigues, Vitor Pinto, Daniel Campos, and Duarte Silva. Integration of wind propulsion in an electric asv. In Anna Friebe and Florian Haug, editors, *Proc. 8th Int. Robotic Sailing Conf.*, pages 15–27. Springer International Publishing, Mariehamn, Finland, Aug. 2015. ISBN 978-3-319-23334-5.

G. T. Csanady. On the equilibrium shape of the thermocline in a shore zone. *J. Phys. Oceanogr.*, 1(4):263–270, Oct. 1971.

Joseph Curcio, John Leonard, and Andrew Patrikalakis. Scout – a low cost autonomous surface platform for research in cooperative autonomy. In *Proc. MTS/IEEE Int. Conf. Oceans'05*, Washington, D.C., USA, Sept. 2005.

Tom Curtin, James Bellingham, Josko Catapovic, and Doug Webb. Autonomous oceanographic sampling networks. *Oceanography*, 6(3):86–94, 1993.

R.E. Davis, D. C. Webb, L. A. Regier, and J. Dufour. The autonomous lagrangian circulation explorer (ALACE). *J. Atmos. Oceanic Technol.*, 9(3):264–285, June 1992.

R.E. Davis, J. T. Sherman, and J. Dufour. Profiling ALACEs and other advances in autonomous subsurface floats. *J. Atmos. Oceanic Technol.*, 18(6):982–993, June 2001.

C. E. J. de Ronde, S. L. Walker, F. Caratori Tontini, E. T. Baker, R. W. Embley, and D. Yoerger. Application of AUVs in the Exploration for and Characterization of Arc Volcano Seafloor Hydrothermal Systems. *AGU Fall Meeting Abstracts*, page C1050, December 2014.

Max Deffenbaugh, Henrik Schmidt, and James G. Bellingham. Acoustic navigation for arctic under-ice AUV missions. In *Proc. MTS/IEEE Int. Conf. Oceans'93*, pages I–204–I–209, Victoria, BC, Canada, Oct. 1993.

J. B. Derenbach, H. Astheimer, H. P. Hansen, and H. Leach. Vertical microscale distribution of phytoplankton in relation to the thermocline. *Mar. Ecol. Prog. Ser.*, 1:187–193, 1979.

Mari Carmen Domingo. An overview of the internet of underwater things. *J. Network and Computer Applications*, 35(6):1879–1890, 2012.

Robert L. Doneker and Gerhard H. Jirka. Expert systems for mixing-zone analysis and design of pollutant discharges. *J. Water Resour. Plann. Manage.*, 117(6):679–697, Nov./Dec. 1991.

Daniel Doolittle. The payoff is in the payload: Using AUVs in scientific research. *Underwater Magazine*, Mar./Apr. 2003. http://www.diveweb.com/uw/.

Matthew Dunbabin and Lino Marques. Robotics for environmental monitoring. *IEEE Robotics and Automation Magazine*, 19(1):24–39, Mar. 2012.

Phil Dyke. *Modelling Marine Processes*. Prentice Hall, 1996.

Donald P. Eickstedt, Michael R. Benjamin, Ding Wang, Joseph Curcio, and Henrik Schmidt. Behavior based adaptive control for autonomous oceanographic sampling. In *Proc. Int. Conf. Robot. Autom*, Rome, Italy, Apr. 2007.

Charles C. Eriksen, T. James Osse, Russell D. Light, Timothy Wen, Thomas W. Lehman, Peter L. Sabin, John W. Ballard, and Andrew M Chiodi. Seaglider: A long-range autonomous underwater vehicle for oceanographic research. *IEEE J. Oceanic. Eng.*, 26(4):424–436, Oct. 2001.

Maurice F. Fallon, Georgios Papadopoulos, and John J. Leonard. Cooperative AUV navigation using a single surface craft. In *Proc. 7th Int. Conf. Field and Service Robots (FSR 2009)*, Cambridge, MA, USA, July 2009.

O. Faltinsen. *Hydrodynamics of high-speed marine vehicles*. Cambridge University Press, 2005.

David M. Farmer, Eric A. D'Asaro, Mark V. Trevorrow, and Geoffry T. Dairiki. Three-dimensional structure in a tidal convergence front. *Cont. Shelf Res.*, 15(13):1649–1673, Nov. 1995.

Jay A. Farrell, Wei Li, Shuo Pang, and Richard Arrieta. Chemical plume tracing experimental results with a REMUS AUV. In *Proc. MTS/IEEE Int. Conf. Oceans'03*, pages 962–968, San Diego, CA, USA, Sep. 2003.

M.D. Feezor, F.Yates Sorrell, P.R. Blankinship, and J.G. Bellingham. Autonomous underwater vehicle homing/docking via electromagnetic guidance. *IEEE J. Oceanic. Eng.*, 26(4):515–521, Oct 2001.

Bruno Ferreira, Aníbal Matos, Nuno Cruz, and Miguel Pinto. Modeling and control of the MARES autonomous underwater vehicle. *Mar. Tech. Soc. J.*, 44(2), Mar./Apr. 2010.

Bruno Ferreira, Aníbal Matos, and Nuno Cruz. Automatic reconfiguration and control of the MARES AUV in the presence of a thruster fault. In *Proc. IEEE Int. Conf. Oceans'11*, Santander, Spain, June 2011.

Bruno M. Ferreira. *Control and Cooperation of Marine Vehicles*. PhD thesis, Faculty of Engineering, University of Porto, Feb. 2014.

Bruno M. Ferreira, Jerome Jouffroy, Aníbal C. Matos, and Nuno A. Cruz. Control and guidance of a hovering AUV pitching up or down. In *Proc. MTS/IEEE Int. Conf. Oceans'12*, Hampton Roads, VA, USA, Oct. 2012a.

Bruno M. Ferreira, Aníbal C. Matos, and Nuno A. Cruz. Modeling and control of TriMARES AUV. In E. Bicho, F. Ribeiro, and L. Louro, editors, *Proc. 12th Int. Conf. on Autonomous Robot Systems and Competitions, Robotica 2012*, pages 57–62, Guimarães, Portugal, 2012b.

Bruno M. Ferreira, Aníbal C. Matos, Nuno A. Cruz, and Rui M. Almeida. Towards cooperative localization of an acoustic pinger. In *Proc. MTS/IEEE Int. Conf. Oceans'12*, Hampton Roads, VA, USA, Oct. 2012c.

Bruno M. Ferreira, Aníbal C. Matos, and Nuno A. Cruz. Optimal positioning of autonomous marine vehicles for underwater acoustic source localization using TOA measurements. In *Proc. Int. Symp. Underwater Tech. UT'13*, Tokyo, Japan, Mar. 2013.

Edward Fiorelli, Naomi Ehrich Leonard, Pradeep Bhatta, Derek A. Paley, Ralf Bachmayer, and David M. Fratantoni. Multi-auv control and adaptive sampling in monterey bay. *IEEE J. Ocean Eng.*, 31:935–948, Oct 2006.

Barbara Fletcher. New roles for UUVs in intelligence, surveillance, and reconnaissance. In *Proc. 9th Pacific Congr. Marine Science and Technology*, Honolulu, HI, USA, Jun. 2000.

Thor I. Fossen. *Guidance and Control of Ocean Vehicles*. John Wiley & Sons, UK, 1995.

Richard W. Garvine. Dynamics of small-scale oceanic fronts. *J. Phys. Oceanogr.*, 4:557–569, Oct. 1974.

Arthur Gelb, editor. *Applied Optimal Estimation*. The MIT Press, Cambridge, MA, USA, 1996.

C. R. German, T. M. Shank, M. D. Lilley, J. E. Lupton, D. K. Blackman, K. M. Brown, T. Baumberger, G. Früh-Green, R. Greene, M. A. Saito, S. Sylva, K. Nakamura, J. Stanway, D. R. Yoerger, L. A. Levin, A. R. Thurber, J. Sellanes, M. Mella, J. Muñoz, J. L. Diaz-Naveas, and Inspire Science Team. Hydrothermal Exploration at the Chile Triple Junction - ABE's last adventure? *AGU Fall Meeting Abstracts*, page D6, Dec. 2010.

Fritz Gessner. The vertical distribution of phytoplankton and the thermocline. *Ecology*, 29(3): 386–389, July 1948.

Jeremy Gottlieb, Rishi Graham, Thom Maughan, Frédéric Py, Gabriel Elkaim, and Kanna Rajan. An experimental momentum-based front detection method for autonomous underwater vehicles. In *Proc. Int. Conf. on Robotics and Automation, ICRA 2012*, Saint Paul, MN, USA, May 2012.

C. Gugliandolo, F. Italiano, T. L. Maugeri, S. Inguaggiato, D. Caccamo, and J. P. Amend. Submarine hydrothermal vents of the Aeolian Islands: Relationship between microbial communities and thermal fluids. *Geomicrobiology J.*, 16(1):105–117, Jan. 1999.

Steven D. Haeger. Vertical representation of ocean temperature profiles with a gradient feature model. In *Proc. MTS/IEEE Int. Conf. Oceans'95*, pages 579–585, San Diego, CA, USA, Oct. 1995.

Bing Han, Hai feng Jiu, Shuo Pang, and Jin long Li. Hydrothermal plume simulation for autonomous hydrothermal vent discovery. In *Proc. MTS/IEEE Int. Conf. Oceans'2012*, pages 1–7, Yeosu, Korea, May 2012.

D. J. Harvey, Tien-Fu Lu, and M. A. Keller. Comparing insect-inspired chemical plume tracking algorithms using a mobile robot. *IEEE T. Robotics*, 24(2):307–317, April 2008.

E. Hayashi, H. Kimura, C. Tam, J. Ferguson, J. Laframboise, G. Miller, C. Kaminski, and A. Johnson. Customizing an autonomous underwater vehicle and developing a launch and recovery system. In *Proc. Int. Symp. Underwater Tech. UT'13*, pages 1–7, Tokyo, Japan, Mar. 2013.

William L. High. Submersibles for marine biological research. In *Proc. IEEE'71 Eng. in the Ocean Environment Conf.*, pages 37–40, San Diego, CA, USA, Sep. 1971.

Thomas Hiller, Arnar Steingrimsson, and Robert Melvin. Expanding the small auv mission envelope; longer, deeper & more accurate. In *Proc. IEEE/OES Conf. Autonomous Underwater Vehicles AUV 2012*, Southampton, UK, Sept. 2012.

Roger Hine and Philip A. McGillivary. Wave-powered autonomous surface vessels as components of ocean observing systems. In *Proc. PACON 2007*, Honolulu, HI, USA, June 2007.

Eric Hirst. Buoyant jets with three-dimensional trajectories. *J. Hydr. Div.*, HY11(HY11):1999–2014, Nov. 1972.

Jeff C. Ho and Anna M. Michalak. Challenges in tracking harmful algal blooms: A synthesis of evidence from Lake Erie. *J. Great Lakes Research*, 41(2):317–325, June 2015.

B. Hobson, M. Kemp, and A. Leonessa. Integration of a hovering module with the morpheus auv: application to mcm missions. In *Proc. MTS/IEEE Int. Conf. Oceans'02*, volume 1, pages 207–209, Biloxi, MI, USA, Oct. 2002.

Brett W. Hobson, James G. Bellingham, Brian Kieft, Rob McEwen, Michael Godin, and Yanwu Zhang. Tethys-class long range AUVs - extending the endurance of propeller-driven cruising AUVs from days to weeks. In *Proc. IEEE/OES Conf. Autonomous Underwater Vehicles AUV 2012*, Southampton, UK, Sept. 2012.

Sighard F. Hoerner. *Fluid-Dynamic Drag*. Published by author, 1965.

Brett M. Johnson, Laurel Saito, Mark A. Anderson, Paul Weiss, Mary Andre, and Darrell G. Fontane. Effects of climate and dam operations on reservoir thermal structure. *J. Water Resour. Plann. Manage.*, 130(2):112–122, Mar./Apr. 2004.

Jérôme Jouffroy and Johann Reger. An algebraic perspective to single-transponder underwater navigation. In *Proc. IEEE Int. Conf. on Control Applications (CCA 2006)*, Munich, Germany, Oct. 2006.

Hassan K. Khalil. *Nonlinear Systems*. Prentice Hall, Upper Saddle River, NJ, USA, 2nd edition, 1996.

J.C. Kinsey, D.R. Yoerger, M.V. Jakuba, Rich Camilli, Charles R. Fisher, and C.R. German. Assessing the Deepwater Horizon oil spill with the sentry autonomous underwater vehicle. In *Proc. Int. conf. Intelligent Robots and Systems (IROS)*, pages 261–267, San Francisco, CA, USA, Sept. 2011.

Holger Klinck, Selene Fregosi, Haru Matsumoto, Alex Turpin, David K. Mellinger, Anatoli Erofeev, John A. Barth, R. Kipp Shearman, Karim Jafarmadar, and Roland Stelzer. Mobile autonomous platforms for passive-acoustic monitoring of high-frequency cetaceans. In Anna Friebe and Florian Haug, editors, *Proc. 8th Int. Robotic Sailing Conf.*, pages 29–37. Springer International Publishing, Mariehamn, Finland, Aug. 2015. ISBN 978-3-319-23334-5.

K. Komaki, M. Hatta, K. Okamura, and T. Noguchi. Development and application of chemical sensors mounting on underwater vehicles to detect hydrothermal plumes. In *Proc. IEEE Int. Symp. Underwater Tech. UT 2015*, pages 1–3, Feb 2015.

Hayato Kondo, Soncheol Yu, and Tamaki Ura. Object observation in detail by the AUV "Tri-Dog 1" with laser pointers. In *Proc. MTS/IEEE Int. Conf. Oceans'01*, Honolulu, HI, USA, Nov. 2001.

John L. Largier. Tidal intrusion fronts. *Estuaries*, 15(1):26–39, Mar. 1992.

Joseph H. W. Lee and Peter Neville-Jones. Initial dilution of horizontal jet in crossflow. *J. Hydr. Engrg.*, 113(5):615–629, May 1987.

M. Lindemuth, R. Murphy, E. Steimle, W. Armitage, K. Dreger, T. Elliot, M. Hall, D. Kalyadin, J. Kramer, M. Palankar, K. Pratt, and C. Griffin. Sea robot-assisted inspection. *Robotics Automation Magazine, IEEE*, 18(2):96–107, June 2011.

Lonny Lippsett. R.I.P. ABE. *Oceanus*, 48(1), June 2010.

Lonny Lippsett. At 50, alvin gets an extreme makeover. *Oceanus*, 51(1), Summer 2014.

John E. Lupton, Edward T. Baker, Newell Garfield, Gary J. Massoth, Richard A. Feely, James P. Cowen, Ronald R. Greene, and Thomas A. Rago. Tracking the evolution of a hydrothermal event plume with a RAFOS neutrally buoyant drifter. *Science*, 280(5366):1052–1055, May 1998.

J.E. Manley. Development of the autonomous surface craft ACES. In *OCEANS '97. MTS/IEEE Conference Proceedings*, volume 2, pages 827–832 vol.2, Halifax, NS, Canada, Oct 1997.

Justin E. Manley. Unmanned surface vehicles, 15 years of development. In *Proc. MTS/IEEE Int. Conf. Oceans'08*, Quebec, Canada, Sept. 2008.

George Marmorino, Farid Askari, and Richard Mied. Observations of the creation and evolution of small-scale oceanic frontal cusps and slicks. *J. Mar. Syst.*, 37(1–3):17–29, Nov. 2002.

Mark V. Martin and Kosuke Ishii. Design for variety: Developing standardized and modularized product platform architectures. *Res. Eng. Des.*, 13(3):213–235, 2002.

A. Matos and N. Cruz. Auv navigation and guidance in a moving acoustic network. In *Proc. IEEE Int. Conf. Oceans'05*, volume 1, pages 680–685 Vol. 1, 2005.

A. Matos and N. Cruz. Coordinated operation of autonomous underwater and surface vehicles. In *Proc. MTS/IEEE Int. Conf. Oceans'07*, 2007.

A. Matos and N. Cruz. Positioning control of an underactuated surface vessel. In *Proc. MTS/IEEE Int. Conf. Oceans'08*, Quebec, Canada, Sept. 2008.

Aníbal Matos and Nuno Cruz. MARES – navigation, control and on-board software. In Alexander V. Inzartsev, editor, *Underwater Vehicles*, chapter 17, pages 315–326. In-Tech, Austria, Jan. 2009.

Aníbal Matos and Nuno Cruz. Algorithms for external tracking of an AUV. In *Proc. 5th IFAC Symp. Intelligent Autonomous Vehicles IAV'2004*, Lisbon, Portugal, Jul. 2004.

Aníbal Matos, Nuno Cruz, Alfredo Martins, and Fernando Lobo Pereira. Development and implementation of a low-cost LBL navigation system for an AUV. In *Proc. MTS/IEEE Int. Conf. Oceans'99*, Seattle, WA, USA, Sep. 1999.

Aníbal Matos, Nuno Cruz, and Fernando L. Pereira. Post mission trajectory smoothing for the Isurus AUV. In *Proc. MTS/IEEE Int. Conf. Oceans'03*, pages 1234–1238, San Diego, CA, USA, Sep. 2003.

Metcaff & Eddy, Inc. *Wastewater Engineering: Treatment, Disposal, and Reuse*. McGraw-Hill, 3rd edition, 1991.

Vernon W. Miller. Measurements for instrumentation design at high temperature hydrothermal vents. In *Proc. MTS/IEEE Int. Conf. Oceans'89*, pages 26–31, Seattle, WA, USA, Sep. 1989.

David Mindell and Brian Bingham. New archaeological uses of autonomous underwater vehicles. In *Proc. MTS/IEEE Int. Conf. Oceans'01*, pages 555–558, Honolulu, HI, USA, Nov. 2001.

Andres Mora, Colin Ho, and Srikanth Saripalli. Analysis of adaptive sampling techniques for underwater vehicles. *Autonomous Robots*, 35(2-3):111–122, 2013.

Douglas W. Murphy. The transparent hull submersible Makakai. In *Proc. IEEE Int. Conf. Oceans'71*, pages 298–301, San Diego, CA, USA, Sep. 1971.

W. Naeem, R. Sutton, and J. Chudley. Chemical plume tracing and odour source localization by autonomous vehicles. *The Journal of Navigation*, 60(2):173–190, May 2007.

National Research Council, Commission on Geosciences, Environment, and Resources, and Ocean Studies Board. *Illuminating the Hidden Planet: The Future of Seafloor Observatory Science*. National Academy Press, Washington, D.C., USA, 2000.

James O'Donnell. Surface fronts in estuaries: A review. *Estuaries*, 16(1):12–39, Mar. 1993.

Shuo Pang. Plume source localization for auv based autonomous hydrothermal vent discovery. In *Proc. MTS/IEEE Int. Conf. Oceans'10*, pages 1–8, Seattle, WA, USA, Sept. 2010.

Shuo Pang and J. A. Farrell. Chemical plume source localization. *IEEE T. Systems, Man, and Cybernetics, Part B: Cybernetics,*, 36(5):1068–1080, Oct. 2006.

A. Pascoal, P. Oliveira, C. Silvestre, L. Sebastiao, M. Rufino, V. Barroso, J. Gomes, G. Ayela, P. Coince, M. Cardew, A. Ryan, H. Braithwaite, N. Cardew, J. Trepte, N. Seube, J. Champeau, P. Dhaussy, V. Sauce, R. Moitie, R. Santos, F. Cardigos, M. Brussieux, and P. Dando. Robotic ocean vehicles for marine science applications: The european ASIMOV project. In *Proc. MTS/IEEE Int. Conf. Oceans'00*, pages 409–415, Providence, RI, USA , Sep. 2000.

J. Paulos, N. Eckenstein, T. Tosun, J. Seo, J. Davey, J. Greco, V. Kumar, and M. Yim. Automated self-assembly of large maritime structures by a team of robotic boats. *Automation Science and Engineering, IEEE Trans.*, 12(3):958–968, July 2015.

Holly Peterson and Brian Lamb. Comparison of results from a meandering-plume model with measured atmospheric tracer concentration fluctuations. *J. Appl. Meteor.*, 31(6):553–564, June 1992.

Stephanie Petillo, Arjuna Balasuriya, and Henrik Schmidt. Autonomous adaptive environmental assessment and feature tracking via autonomous underwater vehicles. In *Proc. IEEE Int. Conf. Oceans'10*, Sydney, Australia, May 2010.

Stephanie Petillo, Henrik Schmidt, and Arjuna Balasuriya. Constructing a distributed AUV network for underwater plume-tracking operations. *Int. J. Distr. Sensor Networks*, 2012, 2012.

Stephanie M. Petillo and Henrik Schmidt. Autonomous and adaptive underwater plume detection and tracking with AUVs: Concepts, methods, and available technology. In *Proc. 9th IFAC Conf. Maneuvering and Control of Marine Craft, MCMC'2012*, Arenzano, Italy, Sept. 2012.

Stephanie Marie Petillo. *Autonomous and Adaptive Oceanographic Feature Tracking On Board Autonomous Underwater Vehicles*. PhD thesis, Massachusetts Institute of Technology and Woods Hole Oceanographic Institution, 2015.

Anne Alexandra Petrenko. *Detection and Characterization of the Sewage Plume at Sand Island, Hawaii*. PhD thesis, University of South California, Los Angeles, CA, USA, May 1997.

George L. Pickard and William J. Emery. *Descriptive Physical Oceanography – An Introduction*. Pergamon Press, 5th (SI) edition, 1990.

Eduardo Pinto, Francisco Marques, Ricardo Mendonça, André Lourenço, Pedro Santana, and José Barata. An autonomous surface-aerial marsupial robotic team for riverine environmental monitoring: Benefiting from coordinated aerial, underwater, and surface level perception. In *Proc. IEEE Int. Conf. Robotics and Biomimetics (ROBIO)*, pages 443–450, Bali, Indonesia, Dec. 2014.

Miguel Pinto, Bruno Ferreira, Aníbal C. Matos, and Nuno A. Cruz. Side scan sonar image segmentation and feature extraction. In *Proc. MTS/IEEE Int. Conf. Oceans'09*, Biloxi, MI, USA, Oct. 2009.

Miguel Pinto, Bruno Ferreira, Heber Sobreira, Aníbal Matos, and Nuno Cruz. Spline navigation and reactive collision avoidance with colregs for asvs. In *Proc. MTS/IEEE Int. Conf. Oceans'13*, San Diego, CA, USA, Sept. 2013.

R. T. Pollard and L. A. Regier. Vorticity and vertical circulation at an ocean front. *J. Phys. Oceanogr.*, 22(6):609–625, Jun. 1992.

Timothy Prestero. Verification of a six-degree of freedom simulation model for the REMUS autonomous underwater vehicle. Master's thesis, Massachusetts Institute of Technology and Woods Hole Oceanographic Institution, Sep. 2001.

E. Ramirez-Llodra, A. Brandt, R. Danovaro, B. De Mol, E. Escobar, C. R. German, L. A. Levin, P. Martinez Arbizu, L. Menot, P. Buhl-Mortensen, B. E. Narayanaswamy, C. R. Smith, D. P. Tittensor, P. A. Tyler, A. Vanreusel, and M. Vecchione. Deep, diverse and definitely different: unique attributes of the world's largest ecosystem. *Biogeosciences*, 7(9):2851–2899, 2010.

Patrícia Ramos, Nuno Cruz, Aníbal Matos, Mário L. Neves, and Fernando L. Pereira. Monitoring an ocean outfall using an AUV. In *Proc. MTS/IEEE Int. Conf. Oceans'01*, pages 2009–2014, Honolulu, HI, USA, Nov. 2001.

C. G. Rauch, M. J. Purcell, T. Austin, and G. J. Packard. Ship of opportunity launch and recovery system for REMUS 600 AUV's. In *Proc. MTS/IEEE Int. Conf. Oceans'08*, Quebec, Canada, Sept. 2008.

David Ribas, Pere Ridao, Lluís Magí, Narcís Palomeras, and Marc Carreras. The Girona 500, a multipurpose autonomous underwater vehicle. In *Proc. IEEE Int. Conf. Oceans'11*, Santander, Spain, June 2011.

Pere Ridao, Marc Carreras, David Ribas, Pedro J. Sanz, and Gabriel Oliver. Intervention AUVs: The next challenge. In *Proc. 19th IFAC World Congress*, pages 12146–12159, Cape Town, South Africa, Aug. 2014.

Raymond J. Roark and Warren C. Young. *Roark's Formulas for Stress and Strain*. McGraw-Hill, New York, USA, 6th edition, 1989.

Philip J. W. Roberts. Line plume and ocean outfall dispersion. *J. Hydr. Div.*, 105(HY4):313–331, Apr. 1979.

Philip J. W. Roberts. Sea outfalls. In V. P. Singh and W. H. Hager, editors, *Environmental Hydraulics*, chapter 3, pages 63–110. Kluwer Academic Publishers, The Netherlands, 1996.

Dean Roemmich, Gregory C. Johnson, Stephen Riser, Russ Davis, John Gilson, W. Brechner Owens, Silvia L. Garzoli, Claudia Schmid, and Mark Ignaszewski. The argo program – observing the global ocean with profiling floats. *Oceanography*, 22(2):34–43, June 2009.

Patrick F Rynne and Karl D von Ellenrieder. Unmanned autonomous sailing: Current status and future role in sustained ocean observations. *Marine Technology Society Journal*, 43(1):21–30, 2009.

Anatoly M. Sagalevich. Mir-1 and mir-2 submersibles mark 25 years of history. *Sea Tech.*, 53 (12):45–48, Dec. 2012.

Mehul Sangekar, Mandar Chitre, and Teong Beng Koay. Hardware architecture for a modular autonomous underwater vehicle Starfish. In *Proc. MTS/IEEE Int. Conf. Oceans'08*, pages 1–8, Quebec, Canada, Sept. 2008.

Nuno Santos, Aníbal Matos, and Nuno Cruz. Navigation of an autonomous underwater vehicle in a mobile network. In *Proc. MTS/IEEE Int. Conf. Oceans'08*, Quebec, Canada, Sept. 2008.

Henrik Schmidt, James G. Bellingham, Mark Johnson, David Herold, David M. Farmer, and Richard Pawlowicz. Real-time frontal mapping with AUVs in a coastal environment. In *Proc. MTS/IEEE Int. Conf. Oceans'96*, Fort Lauderdale, FL, USA, Sep. 1996.

Toby Schneider and Henrik Schmidt. Model-based adaptive behavior framework for optimal acoustic communication and sensing by marine robots. *IEEE J. Ocean Eng.*, 38(3):522–533, July 2013.

Robert T. Schnoor. Modularized unmanned vehicle packages for the littoral combat ship mine countermeasures missions. In *Proc. MTS/IEEE Int. Conf. Oceans'03*, volume 3, pages 1437–1439, San Diego, CA, USA, Sept 2003.

Oscar Schofield, Trisha Bergman, Paul Bisset, J. Frederick Grassle, Dale B. Haidvogel, Josh Kohut, Mark Molin, and Scott M. Glenn. The long-term ecosystem observatory: An integrated coastal observatory. *IEEE J. Oceanic. Eng.*, 27(2):146–154, Apr. 2002.

Bruno Scrosati and Jürgen Garche. Lithium batteries: Status, prospects and future. *J. Power Sources*, 195(9):2419–2430, 2010.

Paul D. Scully-Power, Paul A. Nysen, Carl S. Nilsson, Paul F. Twitchell, David G. Browning, Richard C. Swenson, John C. Andrews, and Richard W. Bannister. A multisystem technique for the detection and measurement of warm core ocean eddies. In *Proc. MTS/IEEE Int. Conf. Oceans'75*, pages 761–768, San Diego, CA, USA, Sep. 1975.

Arnold G. Sharp. Design curves for oceanographic pressure-resistant housings. Technical Memorandum 3–81, Woods Hole Oceanographic Institution, Woods Hole, MA, USA, Aug 1981.

Jonathan Sharples. Investigating the seasonal vertical structure of phytoplankton in shelf seas. *Mar. Model.*, 1(1–4):3–38, 1999.

David Shea, Christopher Williams, Moqin He, Peter Crocker, Neil Riggs, and Ralf Bachmayer. Design and testing of the Marport SQX-500 twin-pod AUV. In *Proc. IEEE/OES Conf. Autonomous Underwater Vehicles AUV 2010*, Monterey, CA, USA, Sept. 2010.

Jeff Sherman, Russ E. Davis, W. B. Owens, and J. Valdes. The autonomous underwater glider "Spray". *IEEE J. Oceanic. Eng.*, 26(4):437–446, Oct. 2001.

Chao Shuzhe, Hong Geok Soon, Eng You Hong, and Mandar Chitre. Modular modeling of autonomous underwater vehicle. In *Proc. MTS/IEEE Int. Conf. Oceans'11*, pages 1–6, Kona, HI, USA, Sept. 2011.

Martin Siderius, Michael B. Porter, Paul Hursky, and Vincent McDonald. Effects of ocean thermocline variability on noncoherent underwater acoustic communications. *J. Acoustical Society of America*, 121(4):1895–1908, 2007.

António Silva, Aníbal Matos, Cristiano Soares, José Alves, José Valente, Frederich Zabel, Henrique Cabral, Nuno Abreu, Nuno Cruz, Rui Almeida, R. Nunes Ferreira, Salman Ijaz, and Victor Lobo. Measuring underwater noise with high endurance surface and underwater autonomous vehicles. In *Proc. MTS/IEEE Int. Conf. Oceans'13*, San Diego, CA, USA, Sept. 2013.

Sérgio Silva, Sérgio Cunha, Aníbal Matos, and Nuno Cruz. An In-SAS system for shallow water surveying. In *Proc. 7th Geomatic Week*, Barcelona, Spain, Feb. 2007a.

Sérgio Silva, Sérgio Cunha, Aníbal Matos, and Nuno Cruz. An autonomous boat based synthetic aperture sonar. In *Proc. MTS/IEEE Int. Conf. Oceans'07*, pages 1–7, 2007b.

Sérgio R. Silva, Sérgio R. Cunha, Aníbal C. Matos, and Nuno A. Cruz. Shallow water surveying using experimental interferometric synthetic aperture sonar. *Mar. Tech. Soc. J.*, 43(1):50–63, Mar. 2009.

Hanumant Singh. *An Entropic Framework for AUV Sensor Modelling*. PhD thesis, Massachusetts Institute of Technology/Woods Hole Oceanographic Institution Joint Program, 1995.

Hanumant Singh, Josko Catipovic, Robert Eastwood, Lee Freitag, Henrich Henriksen, Franz Hover, and Dana Yoerger. An integrated approach to multiple AUV communications, navigation and docking. In *Proc. MTS/IEEE Int. Conf. Oceans'96*, Fort Lauderdale, FL, USA, Sep. 1996.

Hanumant Singh, James G. Bellingham, Franz Hover, Steven Lerner, Bradley A. Moran, Keith Von der Heydt, and Dana Yoerger. Docking for an autonomous ocean sampling network. *IEEE J. Oceanic. Eng.*, 26(4):498–514, Oct. 2001.

C. Sivapragasam, Nitin Muttil, S. Muthukumar, and V.M. Arun. Prediction of algal blooms using genetic programming. *Marine Pollution Bulletin*, 60(10):1849–1855, Oct. 2010.

Norman H. Sleep and Janet L. Morton. Hydrothermal resources at mid-oceanic ridge axes. In *Proc. MTS/IEEE Int. Conf. Oceans'83*, pages 782–786, San Francisco, CA, USA, Aug. 1983.

Theodore J. Smayda. What is a bloom? a commentary. *Limnology and Oceanography*, 42(5,part 2):1132–1136, 1997.

R. Smith, J. Das, H. Heidarsson, A. Pereira, F. Arrichiello, I. Cetnic, L. Darjany, M.-E. Garneau, M. Howard, C. Oberg, M. Ragan, E. Seubert, E. Smith, B. Stauffer, A. Schnetzer, G. Toro-Farmer, D. Caron, B. Jones, and G. Sukhatme. Usc cinaps builds bridges. *Robotics Automation Magazine, IEEE*, 17(1):20–30, Mar. 2010.

Ryan N. Smith, Philip Cooksey, Frederic Py, Gaurav S. Sukhatme, and Kanna Rajan. Adaptive path planning for tracking ocean fronts with an autonomous underwater vehicle. In *Proc. Int. Symp.on Experimental Robotics ISER 2014*, pages 1–15, Marrakech, Morocco, June 2014.

Samuel M. Smith, P. Edgar An, Ken Holappa, James Whitney, Aaron Burns, Kevin Nelson, Eric Heazig, Olaf Kempfe, David Kronen, Tom Pantelakis, Ed Henderson, Gary Font, Richard Dunn, and Stanley E. Dunn. The Morpheus ultramodular autonomous underwater vehicle. *IEEE J. Oceanic. Eng.*, 26(4):453–465, Oct. 2001.

Nancy N. Soreide, Catherine E. Woody, and Stephen M. Holt. Overview of ocean based buoys and drifters: Present applications and future needs. In *Proc. MTS/IEEE Int. Conf. Oceans'01*, pages 2470–2472, Honolulu, HI, USA, Nov. 2001.

Roland Stelzer and Karim Jafarmadar. The robotic sailing boat ASV Roboat as a maritime research platform. In *Proc. 22nd Int. HISWA Symp.*, Amsterdam, The Netherlands, Nov. 2012.

Roger Stokey, Thomas Austin, Christopher von Alt, Mike Purcell, Rob Goldsborough, Ned Forrester, and Ben Allen. AUV bloopers or why murphy must have been an optimist: A practical look at achieving mission level reliability in an AUV. In *Proc. Int. Symp. Unmanned Untethered Submersible Tech. UUST'99*, pages 32–40, Durham, NH, USA, Aug. 1999.

Roger Stokey, Ben Allen, Tom Austin, Rob Goldborough, Ned Forrester, Mike Purcell, and Chris Von Alt. Enabling technologies for REMUS docking: An integral component of an autonomous ocean-sampling network. *IEEE J. Oceanic. Eng.*, 26(4):487–497, Oct. 2001a.

Roger Stokey, Tom Austin, Ben Allen, Ned Forrester, Eric Gifford, Rob Goldsborough, Greg Packard, Mike Purcell, and Chris von Alt. Very shallow water mine countermeasures using the REMUS AUV: A practical approach yielding accurate results. In *Proc. MTS/IEEE Int. Conf. Oceans'01*, pages 149–156, Honolulu, HI, USA, Nov. 2001b.

Gaurav S. Sukhatme, Amit Dhariwal, Bin Zhang, Carl Oberg, Beth Stauffer, and David A. Caron. Design and development of a wireless robotic networked aquatic microbial observing system. *Environ. Eng. Sci.*, 24(2):205–215, Mar. 2007.

H. U. Sverdrup, Martin W. Johnson, and Richard H. Fleming. *The Oceans: Their Physics, Chemistry, and General Biology*. Prentice-Hall, New Jersey, USA, 1942.

K. Tamura, Taro Aoki, Toshiaki Nakamura, Satoshi Tsukioka, Takashi Murashima, Hiroshi Ochi, Hidehiko Nakajoh, Tadahiko Ida, and Tadahiro Hyakudome. The development of the AUV-Urashima. In *Proc. MTS/IEEE Int. Conf. Oceans'00*, pages 139–146, Providence, RI, USA, Sep. 2000.

Hwee-Pink Tan, Roee Diamant, Winston K. G. Seah, and Marc Waldmeyer. A survey of techniques and challenges in underwater localization. *Ocean Eng.*, 38(14–15):1663–1676, 2011.

Dan Ling Tang, BaoPing Di, Guifeng Wei, I-Hsun Ni, Im Oh, and SuFen Wang. Spatial, seasonal and species variations of harmful algal blooms in the South Yellow Sea and East China Sea. *Hydrobiologia*, 568(1):245–253, Sep. 2006.

V.G. Tarasov, A.V. Gebruk, A.N. Mironov, and L.I. Moskalev. Deep-sea and shallow-water hydrothermal vent communities: Two different phenomena? *Chemical Geology*, 224(1–3):5–39, 2005. SHALLOW-WATER {HYDROTHERMAL} {VENTING}.

Mikell Taylor and Andy Wilby. Design considerations and operational advantages of a modular AUV with synthetic aperture sonar. In *Proc. MTS/IEEE Int. Conf. Oceans'11*, pages 1–6, Kona, HI, USA, Sept. 2011.

William J. Teague, Michael J. Carron, and Patrick J. Hogan. A comparison between the generalized digital environmental model and Levitus climatologies. *J. Geophys. Res.*, 95(C5):7167–7183, May 1990.

Roy M. Turner, Elise H. Turner, and D. Richard Blidberg. Organization and reorganization of autonomous oceanographic sampling networks. In *Proc. IEEE Symp. Autonomous Underwater Vehicle Tech. AUV'96*, Monterey, CA, USA, Jun. 1996.

Karl Ulrich. The role of product architecture in the manufacturing firm. *Res. Policy*, 24(3):419–440, May 1995.

United States Navy. The Navy unmanned surface vehicle (USV) master plan. Technical report, United States Navy, 2007.

Robert J. Urick. *Principles of Underwater Sound*. Peninsula Publishing, Los Altos, CA, USA, 3rd. edition, 1983.

U.S.E.P.A. Aquatox for windows: A modular fate and effects model for aquatic ecosystems, release 1 - volume 3: Model validation reports. Technical report, U.S.E.P.A., Sept. 2000.

Jerome Vaganay, John J. Leonard, and James G. Bellingham. Outlier rejection for autonomous acoustic navigation. In *Proc. IEEE Int. Conf. Robotics and Automation ICRA'96*, pages 2174–2181, Minneapolis, MI, USA, Apr. 1996.

Eric van Hooydonk. The law of unmanned merchant shipping: an exploration. *J. Int. Maritime Law*, (20):403–423, 2014.

Thomas W. Vaneck, Claudia D. Rodriguez-Ortiz, Mads C. Schmidt, and Justin E. Manley. Automated bathymetry using an autonomous surface craft. *Navigation*, 43(4):407–419, Winter 1996.

Chris von Alt, Ben Allen, Thomas Austin, and Roger Stokey. Remote environmental measuring units. In *Proc. IEEE Symp. Autonomous Underwater Vehicle Tech. AUV'94*, Cambridge, MA, USA, Jul. 1994.

R. Vuillemin, D. Le Roux, P. Dorval, K. Bucas, J.P. Sudreau, M. Hamon, C. Le Gall, and P.M. Sarradin. CHEMINI: A new in situ CHEmical MINIaturized analyzer. *Deep Sea Research Part I: Oceanographic Research Papers*, 56(8):1391–1399, Aug. 2009.

Thomas Waldmann, Marcel Wilka, Michael Kasper, Meike Fleischhammer, and Margret Wohlfahrt-Mehrens. Temperature dependent ageing mechanisms in lithium-ion batteries – a post-mortem study. *J. Power Sources*, 262:129–135, Sept. 2014.

Ding Wang, Pierre F.J. Lermusiaux, Patrick J. Haley, Donald Eickstedt, Wayne G. Leslie, and Henrik Schmidt. Acoustically focused adaptive sampling and on-board routing for marine rapid environmental assessment. *J. Marine Systems*, 78, Supplement:S393 – S407, 2009. Coastal Processes: Challenges for Monitoring and Prediction.

Douglas C. Webb, Paul J. Simonetti, and Clayton P. Jones. SLOCUM: An underwater glider propelled by environmental energy. *IEEE J. Oceanic. Eng.*, 26(4):447–452, Oct. 2001.

R. Wernli. AUVs–the maturity of the technology. In *Proc. MTS/IEEE Int. Conf. Oceans'99*, volume 1, pages 189–195, Seattle, WA, USA, Sept. 1999.

Robert L. Wernli. AUV commercialization – who's leading the pack? In *Proc. MTS/IEEE Int. Conf. Oceans'00*, Providence, RI, USA, Sep. 2000.

Peter Whaite and Frank P. Ferrie. Autonomous exploration: Driven by uncertainty. *IEEE T. Pattern. Anal.*, 19(3):193–205, Mar. 1997.

Frank M. White. *Fuid Mechanics*. McGraw-Hill, 4th edition, 2002.

William S.D. Wilcock and Peter C. Kauffman. Development of a seawater battery for deep-water applications. *J. Power Sources*, 66(1–2):71–75, May–June 1997.

J. Scott Willcox, James G. Bellingham, Yanwu Zhang, and Arthur B. Baggeroer. Performance metrics for oceanographic surveys with autonomous underwater vehicles. *IEEE J. Oceanic. Eng.*, 26(4):711–725, Oct. 2001.

Hans Christian Woithe and Ulrich Kremer. A programming architecture for smart autonomous underwater vehicles. In *Proc. IEEE/RSJ Int. Conf. Intelligent Robots and Systems IROS'09*, St. Louis, MO, USA, Oct. 2009.

Hans Christian Woithe and Ulrich Kremer. Feature based adaptive energy management of sensors on autonomous underwater vehicles. *Ocean Engineering*, 97(0):21 – 29, 2015.

Ken T.M. Wong, Joseph H.W. Lee, and I.J. Hodgkiss. A simple model for forecast of coastal algal blooms. *Estuarine, Coastal and Shelf Science*, 74(1–2):175–196, Aug. 2007.

Steven J. Wright. Mean behavior of buoyant jets in a crossflow. *J. Hydr. Div.*, 103(HY5):499–513, Nov. 1977.

Carl Wunsch. What is the thermohaline circulation? *Science*, 298(5596):1179–1181, Nov. 2002.

D. R. Yoerger, A. M. Bradley, S. C. Martin, and L. L. Whitcomb. The Sentry Autonomous Underwater Vehicle: Field Trial Results and Future Capabilities. *AGU Fall Meeting Abstracts*, page A1674, December 2006.

Dana R. Yoerger, Albert M. Bradley, and Barrie B. Walden. The autonomous benthic explorer (ABE): An AUV optimized for deep seafloor studies. In *Proc. 7th Int. Symp. on Unmanned Untethered Submersible Technology*, pages 60–70, Durham, NH, USA, 1991.

Dana R. Yoerger, Albert M. Bradley, Barrie B. Walden, Michael V. Jakuba, Rodney Catanach, Alan Duester, and Andrew Billings. Exploring the mid ocean ridge and seamounts with the autonomous benthic explorer, 1995-2008. In *Proc. Int. Symp. Unmanned Untethered Submersible Tech. UUST09*, Lee, NH, USA, Aug. 2009.

J. Yuh. Design and control of autonomous underwater robots: A survey. *Autonomous Robots*, 8 (1):7–24, Jan. 2000.

Bin Zhang and G. Sukhatme. Adaptive sampling for estimating a scalar field using a robotic boat and a sensor network. In *Proc. IEEE Int. Conf. Robotics and Automation, ICRA 2007*, pages 3673–3680, Rome, Itally, Apr. 2007.

Yanwu Zhang, Arthur B. Baggeroer, and James G. Bellingham. Spectral-feature classification of oceanographic processes using an autonomous underwater vehicle. *IEEE J. Oceanic. Eng.*, 26 (4):726–741, Oct. 2001.

Yanwu Zhang, Robert S. McEwen, John P. Ryan, and James G. Bellingham. An adaptive triggering method for capturing peak samples in a thin phytoplankton layer by an autonomous underwater vehicle. In *Proc. MTS/IEEE Int. Conf. Oceans'09*, Biloxi, MI, USA, Oct. 2009.

Yanwu Zhang, James G. Bellingham, Michael Godin, John P. Ryan, Robert S. McEwen, Brian Kieft, Brett Hobson, and Thomas Hoover. Thermocline tracking based on peak-gradient detection by an autonomous underwater vehicle. In *Proc. MTS/IEEE Int. Conf. Oceans'10*, Seattle, WA, USA, Sept. 2010.

Yanwu Zhang, James G. Bellingham, Michael A. Godin, and John P. Ryan. Using an autonomous underwater vehicle to track the thermocline based on peak-gradient detection. *IEEE J. Oceanic. Eng.*, 37(3):544–553, July 2012a.

Yanwu Zhang, Michael A. Godin, James G. Bellingham, and John P. Ryan. Using an autonomous underwater vehicle to track a coastal upwelling front. *IEEE J. Oceanic. Eng.*, 37(3):338–347, July 2012b.

Yanwu Zhang, James G. Bellingham, John P. Ryan, Brian Kieft, and Michael J. Stanway. Two-dimensional mapping and tracking of a coastal upwelling front by an autonomous underwater vehicle. In *Proc. MTS/IEEE Int. Conf. Oceans'13*, San Diego, CA, USA, Sept. 2013.